Fall 2010

Effect of structure and plasticizer on the glass transition of adsorbed polymer

Boonta Hetayothin

Department: Chemistry

EFFECT OF STRUCTURE AND PLASTICIZER ON THE GLASS TRANSITION OF ADSORBED POLYMER

by

BOONTA HETAYOTHIN

A DISSERTATION

Presented to the Faculty of the Graduate School of the

MISSOURI UNIVERSITY OF SCIENCE AND TECHNOLOGY

In Partial Fulfillment of the Requirements for the Degree

DOCTOR OF PHILOSOPHY

in

CHEMISTRY

2010

Approved by

Frank D. Blum, Advisor
Michael Van De Mark
Jay A. Switzer
Prakash Reddy
Douglas Ludlow

PUBLICATION DISSERTATION OPTION

The papers included in this dissertation have been prepared in the style of the journal, Macromolecules. Paper I (pages 29-47), Paper II (pages 48-64), Paper III (pages 65-88) and Paper IV (pages 89-111). The Paper V (pages 112-119) has been published by Polymer Preprints and added as the supporting document for Paper I and II. Appendices have been added to include additional characterization and simulation information.

ABSTRACT

The effect of molecular mass on adsorbed poly(methyl methacrylate) (PMMA) on silica was determined using temperature-modulated differential scanning calorimetry (TMDSC). A two-component model, based on loosely-bound polymer (glass transition temperature, T_g, similar to that of bulk) and tightly-bound polymer (T_g higher than that of bulk) was used to interpret the thermograms. Similar amounts of tightly-bound polymer were found for 450 and 85 kDa PMMA (0.78 mg/m^2), while the 32 kDa sample had a smaller amount (0.48mg/m^2). A comparison of adsorbed PMMA, poly(vinyl acetate) (PVAc), and poly(methyl acrylate) (PMA) on silica was made using the same technique. The amounts of tightly-bound PMMA (0.78 mg/m^2), PVAc (0.78 mg/m^2), and PMA (0.72 mg/m^2), adsorbed on silica surfaces did not differ much. The ratios of heat capacity increments of the loosely- and tightly-bound components ($\Delta C_{pA}/\Delta C_{pB}$) at T_g, indicating the relative mobility of the two components, were also estimated to be about 1.8.

The dynamics of the phenyl-deuterated plasticizer di(propylene glycol) dibenzoate in bulk and adsorbed PVAc on silica were probed using solid-state ^{2}H NMR. The dynamics of this plasticizer in the plasticized-bulk polymer system were found to be heterogeneous. For adsorbed PVAc on silica, the dynamics of the plasticizer was found to be even more motionally heterogeneous than that observed in bulk samples. The NMR results provided solid evidence that, when there is only a small amount of adsorbed polymer (i.e., 0.8 mg/m^2), the plasticizer has very little or almost no effect on the dynamics of that polymer. The plasticizer was observed to be effective at higher adsorbed amounts.

ACKNOWLEDGMENTS

I would like to thank Dr. Frank D. Blum for all of his patience, forgiveness, and advising during my graduate career at Missouri S&T. I thank my committee members, Dr. Michael Van De Mark and Dr. Prakash Reddy for being encouraging and advising me, and Dr. Jay A. Switzer and Dr. Douglas Ludlow for their thoughtful comments and suggestions.

I thank the both present and past members of the Blum research group, Dr. Manikantan Nair, Dr. Piyawan Krisanangkura, Dr. Zhefei Li, Krunal Waghela, Xiaoming Cheng, Tan Zhang, Jong-Sik Moon and summer students Mark Hickle and Adam Daily. I also thank Dr. Robert O' Connor for his useful discussion on NMR project.

I thank Ms. Barbara Harris for all of her assistance with editing. I also thank Raymond Kendrick and Joe Council for technical support with NMR and TMDSC projects. I thank my great collaborator Roy Cabaniss from the Computer Science Department for his assistance with the NMR simulation program. I thank Dr. Cyriac Kandoth and Waraporn Viyanon for their help on Fortran programming. I also thank Dr. Tadashi Tokuhiro, Dr. Terry Bone, Dr. Pericles Stavropoulos, Dr. Woelk Klaus, Dr. Jeff Winiarz and staff members of Chemistry Department; Dean Lenz, Mike Myers, Dave Satterfield, Kathy Eudaly, Donna Riggs, Carol Rodman and Dr. Eric Bohannan at Materials Research Center. I thank Jeanine Bruening at the Writing Center and Dr. Neil Book at Chemical & Biological Engineering Department.

I acknowledge the Chemistry Department, the Materials Research Center of Missouri University of Science and Technology and the National Science Foundation (NSF) for financial support of this research. I also acknowledge the ACS South Central Missouri Local Section for the travel grant to the ACS national meeting.

Finally, I thank my husband Floyd, my parents and siblings in Thailand, my parents in law Elaine & Floyd, my friends Rolla and Sierra for being tremendous supportive throughout my graduate career and to make this work is possible.

TABLE OF CONTENTS

Page

PUBLICATION DISSERTATION OPTION iii

ABSTRACT iv

ACKNOWLEDGMENTS v

LIST OF ILLUSTRATIONS x

LIST OF TABLES xiv

NOMENCLATURE xv

SECTION

1. INTRODUCTION 1

REFERENCES 3

2. BACKGROUND 4

2.1. ADSORPTION 4

2.1.1. Polymer Conformations in Solution. 4

2.1.2. Thermodynamics of Polymer Solution 5

2.1.3. Surface Tension of Polymer Solutions, γ. 7

2.1.4. Polymers at Interfaces. 8

2.1.5. Important Features of Interfacial Polymers (Adsorbed Amounts and Interfacial Structures). 10

2.2. GLASS TRANSITION TEMPERATURE, T_g 10

2.2.1. Free Volume Theories on T_g. 11

2.2.2. Factors That Affect The T_g. 11

2.3. CHARACTERIZATION TECHNIQUES FOR POLYMERIC MATERIALS 14

2.3.1. Differential Scanning Calorimetry (DSC) 16

2.3.2. Temperature Modulated Differential Scanning Calorimetry (TMDSC) 18

2.3.3. Solid State Deuterium (^{2}H) NMR 20

2.4. REFERENCES 26

PAPER

1. THERMAL ANALYSIS OF ADSORBED POLY(METHYL METHACRYLATE) ON SILICA: EFFECT OF MOLECULAR MASS 29

ABSTRACT 29

1. INTRODUCTION 30

2. EXPERIMENTAL 32

2.1. Model 34

3. RESULTS 35

4. DISCUSSION 39

5. CONCLUSIONS 44

6. ACKNOWLEDGEMENTS 45

7. REFERENCES 45

2. COMPARISON OF HYDROGEN-BONDED POLYMERS ON SILICA USING TEMPERATURE-MODULATED DIFFERENTIAL SCANNING CALORIMETRY 48

ABSTRACT 48

1. INTRODUCTION 49

2. EXPERIMENTAL 51

2.1. Model 53

3. RESULTS 54

4. DISCUSSION 59

5. CONCLUSIONS 62

6. ACKNOWLEDGEMENTS 62

7. REFERENCES 63

3. DYNAMICS OF DI(PROPYLENE GLYCOL) DIBENZOATE-d_{10} IN POLY(VINYL ACETATE) BY SOLID-STATE ^{2}H NMR 65

ABSTRACT 65

1. INTRODUCTION 66

1.1. NMR Theoretical Background 67

2. EXPERIMENTAL 71

3. RESULTS 72
4. DISCUSSION 82
5. CONCLUSIONS 85
6. ACKNOWLEDGEMENTS 85
7. REFERENCES 86

4. DYNAMICS OF DI(PROPYLENE GLYCOL) DIBENZOATE-d_{10} IN ADSORBED POLY(VINYL ACETATE) BY SOLID-STATE ^{2}H NMR 89

ABSTRACT 89
1. INTRODUCTION 90
2. EXPERIMENTAL 91
3. RESULTS 95
4. DISCUSSION 104
5. CONCLUSIONS 107
6. ACKNOWLEDGEMENTS 108
7. REFERENCES 108

5. QUANTITATIVE ANALYSIS OF THERMOGRAMS FOR ADSORBED POLYMERS ON SILICA 112

1. INTRODUCTION 112
2. EXPERIMENTAL 113
2.1. Model 113
3. RESULTS AND DISCUSSION 114
4. CONCLUSIONS 119
5. ACKNOWLEDGEMENTS 119
6. REFERENCES 119

APPENDICES

A. TEMPERATURE-MODULATED DIFFERENTIAL SCANNING CALORIMETRY (TMDSC) THERMOGRAMS FOR ADSORBED POLYMERS ON SILICA 120

B. THERMAL DEGRADATION OF ADSORBED PMMA ON AMORPHOUS FUMED SILICA (CAB-O-SIL M5) 134

C. ^{1}H NMR AND FTIR SPECTRA OF DEUTERATED PLASTICIZER, DI(PROPYLENE GLYCOL) DIBENZOATE (DPGDB-D10)…….. 143

D. SOLID STATE ^{2}H NMR SPECTRA OF THE PLASTICIZER DI(PROPYLENE GLYCOL) DIBENZOATE-d10 IN BULK AND ADSORBED POLY(VINYL ACETATE)……..146

E. SIMULATIONS AND FITTINGS FOR SOLID STATE ^{2}H NMR SPECTRA……....155

VITA……...170

LIST OF ILLUSTRATIONS

Figure Page

SECTION

2.1. The conformations of polymers at the interface. 10

2.2. Heat flux differential scanning calorimeter 17

2.3. The derivatives of total heat flow (a red dashed line), nonreversing heat flow (a blue dash dotted line), and reversing heat flow (a green solid line) of bulk PMMA. 19

2.4. Energy level diagram of the Zeeman and quadrupolar interactions for a single crystal deuteron (absence of motion). The corresponding spectrum is shown at the bottom for each transition. The magnitude and direction of the quadrupolar perturbation depends upon the orientation of the electric field gradient with respect to the external magnetic field; ω_0 is the Larmor frequency and $\delta = 3e^2qQ/8h$ where e^2qQ/h is a quadrupole coupling constant. 20

2.5. The deuterium NMR powder line shape and how it arises. a) A sphere divided into latitudes of equal frequency (orientation possibilities); 0 is the orientation when the C-D bond is parallel to the external magnetic field (β_0) and $\pi/2$ is the perpendicular orientation. b) Combination of all orientations of the C-D bonds with respect to the magnetic field; 0º is the least intense while 90º ($\pi/2$) has the largest intensity. c) A smoother version of b) for both transitions (m = - 1) <-> (m = 0) and (m = 0) <-> (m = 1), $\Delta\nu_q$ is the doublet spacing [44]. 23

2.6. The quadrupole echo pulse sequence in solid-state deuterium NMR. (a) The hatched areas after the pulses represent the receiver dead time. (b) The time where is data acquisition begins at the top of the echo. 26

PAPER 1

1. A motional gradient of the surfaced-bound polymer. 31

2. TMDSC thermograms of bulk PMMA for three different molecular masses (450 kDa, 85 kDa, and 32 kDa)……..35

3. TMDSC thermograms of various adsorbed amounts of high molecular mass PMMA (450 kDa) on silica…… 36

4. TMDSC thermograms of various adsorbed amounts of medium molecular mass PMMA (85 kDa) on silica…….. 40

5. TMDSC thermograms of various adsorbed amounts of low molecular mass PMMA (32 kDa) on silica..... 38

6. The ratio (r) of the areas under the transitions A and B as a function of the adsorbed amounts (mg polymer/m^2 silica) for three different molecular masses of PMMA..... 39

7. Bound fractions of PMMA on silica as a function of adsorbed amount from TMDSC for the 450 (squares), 85 (triangles), and 32 kDa (circles) and FTIR experiments plotted from ref. 13. The smooth curves are based on a model with a fixed amount of bound material. 43

PAPER 2

1. Simplified configurations of a surface-bound polymer. 50
2. TMDSC of bulk PMMA, PVAc, and PMA. 54
3. TMDSC thermograms of various adsorbed amounts of PMMA on silica. 55
4. TMDSC thermograms of various adsorbed amounts of PVAc on silica. 56
5. TMDSC thermograms of various adsorbed amounts of PMA on silica. 57
6. Plots of ratios (r) of the areas under the A and B transitions, as a function of the adsorbed amounts (mg polymer/m^2 silica) for PMMA, PVAc, and PMA 61
7. Bound fractions of PMMA, PVAc and PMA on silica as a function of the adsorbed amounts. The smooth curves are based on a constant M_B for each polymer. 60

PAPER 3

1. ^{2}H NMR of 180º aromatic ring flip. 68
2. Synthesis of deuterated benzoyl chloride-d_5. 69
3. Synthesis of deuterated di(propylene glycol) dibenzoate-d_{10} 70
4. Thermogravimetric (TGA) analysis of: (A) 0%, (B) 10%, (C) 22%, (D) 27%, and (E) 37% DPGDP-d_{10} in PVAc. 72
5. ^{2}H NMR spectra for pure plasticizer DPGDB-d_{10} 73
6. Experimental (black) and simulated (grey) ^{2}H NMR spectra for a 10% DPGDB-d_{10}/PVAc sample. 74
7. Experimental (black) and simulated (grey) ^{2}H NMR spectra for a 22% DPGDB-d_{10}/PVAc sample. 75
8. Experimental (black) and simulated (grey) ^{2}H NMR spectra for a 27% DPGDB-d_{10}/PVAc sample. 76
9. Experimental (black) and simulated (grey) ^{2}H NMR spectra for a 37% DPGDB-d_{10}/PVAc sample. 77
10. The log average jump rates values, $\langle \log k \rangle$, for DPGDB-d_{10} as a function of temperature for the different plasticizer contents (10, 22, 27, and 37%). 84
11. Average of the log jump rates values, $\langle \log k \rangle$, for DPGDB-d_{10} as a function of temperature for the different plasticizer contents (10, 22, 27, and 37%). 85

12. TMDSC derivative reversing heat flow curves for: (A) 0%, (B) 10%, (C) 22%, (D) 27%, and (E) 37% plasticized-d_{10} PVAc. The maximum of the derivative curve is taken as the T_g (TMDSC). 81

13. Glass-transition temperatures (T_g's) as a function of plasticizer content of deuterated polymer (PVAc-d_3) [36] and deuterated plasticizer in PVAc (PVAC/ DPGDB-d_{10}) from both TMDSC and NMR. 84

PAPER 4

1. Synthesis of deuterated benzoyl chloride-d_5. 92

2. Synthesis of deuterated di(propylene glycol) dibenzoate-d_{10}. 93

3. Thermogravimetric analysis (TGA) plot of 37% plasticized-adsorbed PVAc on silica. (A) Smaller adsorbed-amount sample with 2.60 mg/m^2 and (B) larger adsorbed amount sample with 0.76 mg/m^2 PVAc on silica. 96

4. The ^{2}H NMR spectra of deuterated plasticizer di(propylene glycol) dibenzoate-d_{10}. 97

5. Experimental (black) and simulated (grey) ^{2}H NMR spectra for 37% plasticizer (DPGDB-d_{10}) with PVAc for the larger adsorbed-amount (2.60 mg/m^2) sample. 98

6. Experimental (black) and simulated (grey) ^{2}H NMR spectra for 37% plasticizer (DPGDB-d_{10}) with PVAc for the smaller adsorbed-amount (0.76 mg/m^2). 99

7. A comparison of the ^{2}H NMR spectra of the plasticizer DPGDB-d_{10} at a temperature of 24 ºC: A) pure plasticizer, B) 37% plasticizer in bulk sample, and 37% plasticizer in adsorbed samples with C) 2.60 mg/m^2 PVAc and D) 0.76 mg/m^2 PVAc. 101

8. The log average jump rates values, log $\langle k \rangle$ for DPGDB-d_{10}, as a function of temperature for 37% plasticized-adsorbed sample, 2.60 mg/m^2. 102

9. Average of the log jump rates values, $\langle \log k \rangle$ for DPGDB-d_{10}, as a function of temperature for 37% plasticized-adsorbed sample, 2.60 mg/m^2. 103

10. TMDSC derivative reversing heat flow rate curves of 37% plasticized-bulk PVAc (r.h. scale), 37% plasticized-adsorbed PVAc on silica for the larger (2.60 mg/m^2) and smaller (0.76 mg/m^2) adsorbed-amount samples. The bulk intensity has been normalized by arbitrary number to fit this overlay figure. 104

PAPER 5

1. Derivative thermogram of adsorbed PMMA on silica showing the sigmoidal baseline applied for each transition in the earlier method. 115

2. Derivative thermogram of adsorbed PMMA on silica showing the perpendicular drop method. 115

3. Derivative thermogram of adsorbed PMMA on silica showing the intercept of the tangent lines that determine the starting and end points for the area under the transition. 116

4. Ratio (r) of the areas of the A and B thermal transitions of adsorbed PMMA as a function of the relative amount of polymer (m'_p), using the sigmoidal baseline method for area integration. 117

5. Ratio (r) of the areas of the A and B thermal transitions of adsorbed PMMA on silica as a function of the relative amount of polymer (m'_p), using the perpendicular drop method with linear baseline for area integration. 117

6. Failure of the sigmoidal baseline application in the second thermal transition (tightly-bound) of adsorbed PVAc on silica. 118

7. Failure of the sigmoidal baseline application in the second thermal transition (tightly-bound) of adsorbed PMA on silica. 118

LIST OF TABLES

Table Page

SECTION

2.1. Comparison of Various Characterization Techniques for Multi-Component Polymeric Materials 16

PAPER 1

1. Glass Transition Temperature (Tg) of Different Molecular Mass PMMA for Bulk and Surface Adsorbed PMMA on Silica 38

2. Ratios of Heat Capacity Changes at T_g ($\Delta C_{pA}/\Delta C_{pB}$), Tightly Bound Amount (M_b) and Corresponding Thickness for PMMAs Adsorbed on Silica 41

PAPER 2

1. Comparison of T_gs of PMMA, PVAc, and PMA for Bulk and Adsorbed Polymers on Silica 57

2. Values of the Heat Capacity Ratio ($\Delta C_{pA}/ \Delta C_{pB}$), Tightly Bound Amount (M_B) and Effective Thickness for PMMA, PVAc, and PMA Adsorbed on Silica 60

PAPER 3

1. ^{2}H NMR Glass Transition Temperature Ranges[a] for DPGDB-d10/PVAc at Various Plasticizer Contents. 77

2. Motional Components Used to Simulate Experimental Line Shapes[a,b] 79

3. TMDSC Glass Transition Temperature for DPGDB-d_{10}/PVAc at Various Plasticizer Contents. 82

PAPER 4

1. NMR and TMDSC Glass Transition Temperature Ranges[a,b] for Pure Plasticizer and 37% Plasticized Samples 100

NOMENCLATURE

Symbol	Description
ΔG_m	Free Energy of Mixing
ΔH_m	Enthalpy of Mixing
ΔS_m	Entropy of Mixing
ϕ_s , ϕ_p	Volume Fraction of Solvent and Polymer, respectively.
χ	Interaction Parameter
γ	Surface Tension
ω_0	Larmor Frequency
γ	Magnetogyric Ratio
B_0	Applied Magnetic Field
η	Asymmetry Parameter
θ	Polar Angle
φ	Spherical Polar Angle
ΔQ	Heat Flow Change
ΔC_p	The Change in Heat Capacity
f_B	Bound Fraction

1. INTRODUCTION

Polymers are part of our everyday lives and can be found everywhere from household items such as drinking bottles, milk cartons, food containers, and grocery bags, to technological applications such as coatings, radar cable insulation, optics, lenses, electronic devices, artificial organs (heart or legs), etc. For several applications, polymers have replaced other important materials such as metal, glass, and ceramics due to their light weight, flexibility, chemical inertness, durability, and inexpensive cost.

Polymers are used in different forms such as in bulk and also in composites. A bulk polymer is defined as a system containing only a single polymeric component, such as a homopolymer. On the other hand, a polymer composite is generally a phase separated multi-component material such as a polymer blend, structured latex, and adsorbed polymer. Polymer composites have become very important due to needs for specific uses and superior performance, as compared to that available through the use of bulk polymers. The structural and functional properties of polymer composites depend upon the properties and interactions of their components, especially at interfaces where the different components of multi phases come into contact. An understanding of the behavior of polymers at interfaces is essential and beneficial for improving their properties or for developing novel materials for specific uses.

Among polymer composites, adsorbed polymers are often part of the materials used. Interactions between polymers adsorbed onto surfaces are important in many systems. The importance of these interactions ranges in applications all the way from adhesion, lubrication, surface protection, stabilization, and controlled flocculation of colloidal dispersion to biological processes of membrane-polymer interactions and medicinal applications [1-8]. The physical properties of adsorbed polymers are, as expected, more complex than those of bulk polymers since they involve multi-components, polymers and interfaces.

Plasticized polymers are also commonly used as they offer desirable properties such as flexibility, softness, reduced stiffness, shock resistance, pliability and workability [9-10]. Plasticizers reduce the glass transition temperatures (T_g) polymers via a process

called “plasticization” which can be described by the free volume theory. According to this theory, the small molecules of a plasticizer occupy the space between polymeric chains resulting in a free-volume expansion in a polymer matrix, thereby causing the longer-range segmental motions to occur at lower temperatures [9, 10].

Interfacial properties have a significant impact on the properties of composite materials. Therefore, the improvement or development of existing or novel polymeric materials depends on the ability to manipulate and characterize polymeric materials on an interfacial scale, in the range of a nanometer, or so. In this work, we have probed molecular motional properties, such as glass transition temperature (T_g), which are related to the heat capacity of adsorbed polymers using temperature-modulated differential scanning calorimetry (TMDSC). A two-component model, based on loosely-bound polymer (with a T_g similar to that of bulk) and more tightly-bound polymer (with a T_g higher than that of loosely bound) was used to interpret the thermograms. Molecular motion at the interface can be linked to molecular surface structures, where many of the chemical and mechanical properties such as adhesion, lubricity, wearability, wettability, dispersibility, and biocompatibility, are determined [11-12].

In addition to studies of the T_g from calorimetry, understanding the dynamics of plasticized polymers is also important. This is because molecular motions are related to many properties found in polymeric materials including processability, material deformation, and the diffusion of plasticizer [13]. The dynamics of plasticized polymers are more complex than those of (non-plasticized) homopolymers since they generally involve the physical characteristics of the two components. Here, we probed the dynamics of the plasticizer in a polymer-plasticizer system and at the interfaces in a silica-polymer-plasticizer system using solid-state deuterium NMR. In this work, the dynamics of plasticizer in plasticized poly(vinyl acetate) was probed. Another part of the dynamics study was done on a silica-polymer-plasticizer system. The study was built on the previous study from our group [14]. In that work, it was found that samples with small amounts of adsorbed polymer show little, or no, effect of plasticizer on the dynamics of the adsorbed polymer. Our goal here is to understand what causes this minimal effect of plasticizer through the probing of plasticizer itself.

REFERENCES

1. Feast W. J.; Munro, H. S., *Polymer Surfaces and Interfaces*; Wiley, NY, 1987.
2. Wicks, Z. W.; Jones, F. N.; Pappas, S. P.; Wicks, D. A. *Organics Coatings Science and Technology 3rd edn*; Wiley Interscience, New Jersey, 2007.
3. Reiter, G. *Macromolecules* **1994**, *27*, 3046.
4. Moddel, M.; Bachmann, M.; Janke, W. *J. Phys. Chem. B*, **2009**, *113*, 3314.
5. Kajiyama, T., Tanaka, K., Takahara, A. *Macromolecules* **1997**, *30*, 280.
6. Soga, I, *J. Coat. Technol.* **2003**, *75* (938), 53.
7. Dan, N. *Langmuir* **2000,** *16,* 4045.
8. Fleer, G. J.; Cohen Stuart, M. A.; Scheutjens, J. M. H. M.; Cosgrove, T.; Vincent, B. *Polymers at Interfaces*; Chapman and Hall: London, U.K., 1993.
9. Nambiar, R.; Blum, F. *Macromolecules* **2008**, *41*, 9837.
10. Gould, R. *Plasticization and Plasticizer Processes*, American Chemical Society, Washington, D.C, 1965.
11. Wang, J.; Chen, C.; Buck, S. M.; Chen, Z. *J. Phys. Chem. B* **2001,** *105,* 12118.
12. Wang, J.; Clarke, M. L.; Chen, X.; Even, M. A.; Johnson, W. C.; Chen, Z. *Surf. Sci.* **2005**, *587(1-2)*, 1-11.
13. Bingemann, D.; Wirth, N.; Gmeiner, J.; Rossler, E. A. *Macromolecules* 2007, *40*, 5379.
14. Nambiar, R.; Blum, F. D. *Macromolecules* **2009**, *42*, 8998.

2. BACKGROUND

2.1. ADSORPTION

Studies of polymer adsorption are usually done with the polymers adsorbed from solution. Adsorption of polymers, when polymers attach onto the substrate, can involve the formation of a covalent or ionic bonds called chemisorption. On the other hand, when only physical interactions (such as a weak van der Waals force or hydrogen bonding) play a role, such an adsorption is called physisorption. Several important aspects of adsorption include the adsorbed amount, layer thickness, coverage, and interfacial structure. Many factors affect the adsorption process, including structures and properties of polymers, surfaces, and solvents.

2.1.1. Polymer Conformations in Solution. In a dilute polymer solution, individual polymer molecules are surrounded by solvent and are, on average, far enough apart that their mutual interactions become negligible. Flexible polymers have large internal degrees of freedom and their rotation around for example, single bonds in a polymer backbone, lead to a variety of conformations. A primary structure of a flexible polymer is a "linear" chain of atoms connected by chemical bonding with some pendant groups or atoms. When the rotation around a single bond of a backbone chain is hindered by bulky pendant groups, then the interaction between neighboring groups can lead to preferred sequences of bond rotations, some of which are found in secondary structures like helices or folded sheets. Polymers are considered to be flexible if their thermal motion overcomes the energy barriers involved in backbone rotations. Flexible, non-crystalline polymers have a tertiary structure, a so-called random coil, which is randomly distributed along a chain in three dimensions and is described statistically by averaging the individual conformations allowed [2].

The analysis of the conformations and configurations of a chain molecule often starts with a freely jointed chain. Kuhn [3] first applied the universal two-dimensional random walk model to describe the conformational properties of long flexible chains. A chain is considered to be a sequence of N links of length, l, randomly oriented. Links have negligible volume and possibly cross each other, or occupy the same space. The

distribution of end-to-end distance, r, is often modeled as a Gaussian distribution function which can be related to free energy and the entropy. The chain is often folded on itself in a conformation called "coiled". In this model, we can obtain the mean squared end-to-end distance $\langle r^2 \rangle$ that is proportional to N, therefore,

$$\langle r^2 \rangle = Nl^2 \tag{1}$$

and the radius of gyration R_g is the root-mean-square (rms) distance of the segments from the center of the mass, which is given by

$$R^2_g = (1/6)Nl^2 \tag{2}$$

However, unperturbed real chains have fixed valence angles between the bonds, and rotation about the bonds is not entirely free. Therefore the mean square end-to-end distance of an unperturbed real chain is

$$\langle r^2 \rangle = C_\infty Nl^2 \tag{3}$$

where C_∞ is called a characteristic ratio (a rigidity constant which depends on the architecture of the chain and the molecular mass). The values of r and R_g increase as the chain becomes more and more rigid.

In a dilute polymer solution with a good solvent, excluded volume refers to the part of a polymer chain cannot occupy space that is already occupied by another part of the same chain. The excluded volume effect decreases the number of equilibrium conformations of the polymer coil, and causes the ends of a polymer chain (on average, a measure of the size of the polymer coil) to be farther apart than they would be in a non-excluded volume situation, thereby increasing the average coil size. The radius of gyration in this case is proportional to

$$R_g = N^\nu \tag{4}$$

where ν ranges from 0.5 for a polymer in a theta solvent to 0.6 for a polymer in a thermodynamically good solvent. In addition, the radius of gyration R_g can also be written in terms of the molecular mass (proportional to N) as:

$$R_g = aM^\nu \tag{5}$$

where M is the molecular mass, a and ν are constants.

2.1.2. Thermodynamics of Polymer Solution. At equilibrium where the polymer solution is a mixture of polymer and solvent, the free energy change must be negative for

mixing to occur spontaneously from the two separate species ($\Delta Gm < 0$). It is known that the free energy change, upon mixing at a given temperature, is related to the enthalpy and entropy change by

$$\Delta G_m = \Delta H_m - T\Delta S_m \quad (6)$$

in which the enthalpy of mixing, ΔH_m, and entropy of mixing, ΔS_m, is related to interaction, arrangement and packing of molecules in the solution. Lattice theory has been used to account for the number of configurations (entropic part) of the system using a lattice model [4]. However, the problem with this theory is the influence of molecular interactions on arrangements in which similar types of molecules tend to stick together. Subsequently, a mean field approximation was used to account for the effects of the energy of interaction [4]. This approximation assumes that the energy of interaction experienced by any one molecule is an average of all possible configurations. With this assumption, the entropic and enthalpic parts can be treated separately. However, these two parts alone do not account for polymer solutions properly. Flory [5] and Huggins [6-8] later developed a thermodynamic theory for polymer solutions using many assumptions of the regular solution theory. The Flory-Huggins equation for the free energy of polymer solutions is expressed as equation x.

$$\Delta G_m/RT = n_s \ln \phi_s + n_p \ln \phi_p + n_s \ln \phi_p\chi \quad (7)$$

where R is a gas constant, n_s and n_p are the number of moles of solvent and polymer, ϕ_s and ϕ_p are the volume fractions of the solvent and polymer. χ is the interaction parameter between components describing the change in energy of solvent-solvent and polymer-polymer contacts, replaced by solvent-polymer interactions.

To derive a change in the entropy of mixing for polymer solutions, Flory and Huggins assumed that a polymer was a chain of segments and each of these segments was equal in size to a solvent molecule and the combinatorial entropic part, as shown in equation 8 was given as:

$$\Delta S_m/R = n_s \ln \phi_s + n_p \ln \phi_p \quad (8)$$

where the volume fraction of solvent ϕ_s and polymer ϕ_p are given, respectively by:

$$\phi_s = n_sV_s/(n_sV_s + n_pMV_s) = n_s/(n_s + n_pM) \quad (9)$$

$$\phi_p = n_pMV_s/(n_pMV_s + n_sV_s) = n_pM/(n_pM + n_s) \quad (10)$$

where n_p is the number of polymer molecules, M is the number of segments in each polymer chain, and V_s is the volume of each segment. An interesting piece of information from this entropic expression regarding the adsorption process is that the longer chain (higher molecular mass) lowers the entropy change in mixing. Therefore, high molecular mass polymers, not only usually have larger adsorbed amounts, but they also adsorb preferentially over lower mass polymers.

The Flory-Huggins theory described the enthalpy of mixing using the χ parameter. This parameter accounts for the temperature-normalized interactions between pairs which, in this case, the pair is a solvent and a segment of polymer chain. The interactions between pairs of solvent-solvent, polymer-polymer, and solvent-polymer are represented by the energy parameters ω_{ss}, ω_{pp}, and ω_{sp}, respectively. The change in energy described the formation of a single solvent-polymer contact, $\Delta\omega_{sp}$ is:

$$\Delta\omega_{sp} = \Delta\omega_{sp} - \tfrac{1}{2}(\omega_{ss} + \omega_{pp}) \tag{11}$$

Flory further suggested that the number of solvent-polymer contacts was approximately equal to $zn_s\phi_p$, where z was the coordination number of the lattice therefore

$$\Delta H_m = zn_s\phi_p \Delta\omega_{sp} \tag{12}$$

The χ parameter was introduced as

$$\chi = z\Delta\omega_{sp}/kT \tag{13}$$

As a result, the enthalpy change in mixing is

$$\Delta H_m = \chi n_s\phi_p kT \tag{14}$$

In addition, χ_{sp} (that given by the solubility parameter) is given as:

$$\chi_{sp} = 0.34 + V_r/RT (\delta_s - \delta_p)^2 \tag{15}$$

where V_r is a molar volume of polymer which is equal to that of the solvent in the case of polymer solutions; δ_s and δ_p are the solubility parameters of solvent and polymer, respectively.

2.1.3. Surface Tension of Polymer Solutions, γ. Polymeric liquids or polymer solutions are usually denser than typical organic solvents. The surface tension of polymeric liquids or polymer solutions is usually higher than those of common solvents. Adsorption of polymers onto solid surfaces is preferential when the polymer in solution has a lower liquid-air as well as liquid-solid interfacial tensions than that of the solvent [9]. A large amount of adsorption of the polymer on the surface occurs at a low

concentrations (monolayer coverage), followed by little change in the concentration. Szleifer and Widom [10] developed a lattice model of diluted phase-separated polymer solutions which allowed the expression for the liquid-air surface tension to be related to χ. It was found that stronger interaction between polymer and solvent leads to larger liquid-air surface tension of polymer solutions.

It is known that the adsorption of polymers is molecular mass dependent [11-15]. It is also interesting to understand how the surface tension depends on the molecular mass. According to a scaling analysis [10, 16, 17, 18], the surface tension is both temperature and molecular mass dependent, as shown in equation 16. The surface tension decreases as molecular mass increases, which leads to a larger adsorption of polymers or

$$\gamma = N^{-1} f[1/2 * \sqrt{N} * (1-T/T_c)] \quad (16)$$

where N is the number of repeating units, T is the temperature and T_c is the critical temperature where the surface tension go as to zero.

2.1.4. Polymers at Interfaces. Adsorption of polymers onto surfaces affects various interfacial properties such as adhesion, friction, lubrication, surface tension or colloidal dispersion ability [14]. For a polymer solution, the properties of a liquid near an interface can be different from its bulk properties. The most important effect found in the adsorption process is a change in composition near the interface [2]. Factors that affect the adsorption of polymers onto surfaces include molecular mass, polydispersity, concentration, solvency, surfaces, and temperature.

The amount of adsorption of polymers has been found to increase with increasing molecular mass for randomly adsorbing polymers. However, as the molecular mass becomes larger, the adsorbed amount tends to become less dependent on the size of the polymer [12]. The molecular mass dependence on an adsorbed amount has been shown to be proportional to M^x, where M is the molecular mass and x is a constant value of 0.3-0.5 for an unperturbed chain. This molecular mass dependence is more pronounced in a thermodynamically poor solvent and at lower polymer concentrations [14]. As the solution concentration increases, the molecular mass dependence decreases.

After discovering that the adsorption process was molecular mass dependent, the effect of polydispersity then was subsequentially investigated for randomly adsorbing polymers [2, 13, 15, 19, 20]. It was found that, at equilibrium, high molecular mass

polymers not only had larger adsorbed amounts, but they also adsorbed preferentially over lower mass polymers. Although adsorption sites on the surface were almost equally covered by polymer with different chain lengths, the entropy of mixing in the solution decreased significantly as chain length increased (see eqn. 6). Hence, adsorption is favored preferentially by the longer polymer chains. As with molecular mass dependence, this polydispersity effect also depends on concentration of the solution. This effect is more pronounced in a dilute solution. This is because at equilibrium the amount of polymer adsorbed per unit of surface rapidly increases as the polymer concentration increases. It eventually reaches a plateau value where the adsorption is no longer dependent on bulk concentration. This effect can be easily observed on the adsorption isotherm plot.

A number of studies have reported that the adsorbed amount of polymer is larger when a thermodynamically poor, rather than a good solvent is used. The adsorbed amount of polymer decreases progressively with increased solvent power, the interpretation of which was more straightforward for non-polar hydrocarbon polymers adsorbed on non-porous, non-polar Graphon surfaces [14, 21-22]. However, when the polymer and the surface contained polar groups, the effect of changing the solvents was much more complex. This is because a change in the solvent affects both the polymer-solvent interaction (χ) and the polymer-surface energy interaction (χ_s).

A change in substrate also affects the polymer-surface energy interaction, χ_s. For the same polymer, different surfaces result in different surface affinity [2]. For instance, the adsorption of polymers with carbonyl groups on the surface of silica occurred via hydrogen bonding between the carbonyl and silanol groups [23-24]. For non-polar polymers, such as polystyrene, a rather weaker van der Waals interaction plays a role. The strength of the interaction was different when the silica surfaces were treated [25]. For example, treating the surface silanols with a silane coupling agent would alter the polarity. The surface of the silica could be made less polar, or even non polar, which preferentially favors the non-polar interaction between the polymers surfaces [25].

Finally, the temperature dependence of adsorption is small [14]. There is no generalization for this effect. Both positive and negative changes in adsorption were found at an elevated temperature.

2.1.5. Important Features of Interfacial Polymers (Adsorbed Amounts and Interfacial Structures). The important quantitative and qualitative features of interfacial polymers include adsorbed amount and interfacial structures. For adsorption from dilute solution, the adsorbed amount can be described as the amount of polymer in the interfacial region in excess of the bulk solution concentration, or the total amount of polymer in contact with the surface. The width of the interfacial region of adsorbed polymers can extend up to distances on the order of the coil radius as often expressed in R_g. An adsorption isotherm, a plot of the total adsorbed amount, as a function of the equilibrium concentration of bulk polymer at a given temperature, is commonly used to characterize the amount of adsorption.

In the adsorption process, polymer chains are forced to change their shapes due to the interface, e.g., from spherical or coil to more planar. The conformations of polymer at the interface were proposed by Jenkel and Rumbach [26] as being composed of three types of sub-chains, the so-called trains, loops, and tails shown in Figure 2.1.

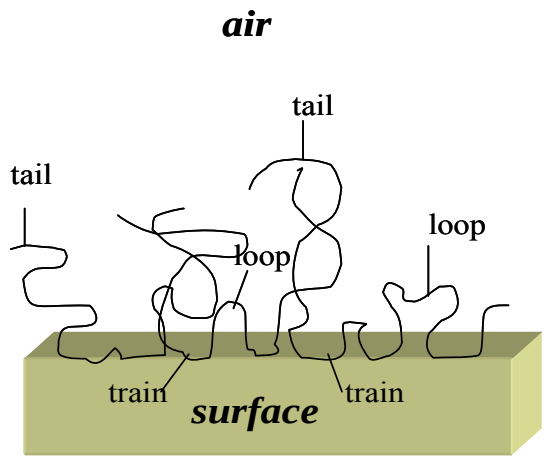

Figure 2.1. The conformations of polymers at the interface.

2.2. GLASS TRANSITION TEMPERATURE, T_g

A glass transition is a reversible change in an amorphous material or, in amorphous regions of a partially crystalline material, at which the material changes from

one without significant molecular mobility to one with mobility. For polymers, this change is typically from a hard brittle solid to a viscous or rubbery plastic, or vice versa [27]. The approximate midpoint of the temperature range over which the glass transition occurs is called the "glass transition temperature" (T_g). Amorphous materials are solid (glassy) below the T_g, and are more liquid-like state when above the T_g. A glassy state has no long-range order and any long-range transitional molecular motions are essentially frozen, although some motions, such as vibration or other types of local motions can exist. An amorphous polymer exhibits a glass transition, as evidenced by the continuous change in the slope of thermodynamic properties, such as volume (V), enthalpy (H), and entropy (S), or by a broad discontinuity in heat capacity (C_p), thermal expansion (α), and compressibility (κ) with temperature [4, 27].

2.2.1. Free Volume Theories on Tg. The concept of free volume has been used to account for the Tg, which is related to mechanical and rheological properties of materials [4, 28]. The oscillations from thermal motions of molecules create some free volume over and above the empty or unoccupied space. As temperature increases, the amplitude of the oscillations increases resulting in an increase in free volume, and is related to the thermal expansion coefficient. The free volume fluctuates; allowing motions as a result of random oscillation and collisions that occur between the molecules. The temperature where there is sufficient free volume to allow molecules to change their positions is the glass transition temperature. The free volume is related to segmental mobility in which bond rotations cause a change in conformations. Since segments of polymers are composed of several bonds, a rotation about a single bond could result in a huge displacement that would be forbidden by the packing of the chains. However, various kinds of coupled rotations of adjacent or neighboring bonds have been proposed that would allow only a small displacement of segments without a gigantic displacement of much of the chain.

2.2.2. Factors That Affect The Tg. Several factors affect the Tg including molecular mass, chemical structure, cross- linking, crystallization, and the presence of diluents. In the low molecular mass range with relatively short chains, the Tg increases with increasing molecular mass and then levels off, reaching a limiting value. As mentioned, the free volume is associated with the cooperative motions. Since the chain

ends have more freedom than the central segments and low molecular mass polymers have more chain ends than those of longer chains, the result is a lower T_g. Fox and Flory [29-30] expressed the molecular mass dependence of T_g using a free volume approach as:

$$T_g = T_g^{\infty} - K/M_n \quad (17)$$

where T_g^{∞} is the glass transition temperature of an infinite molecular weight polymer, K is a constant related to the parameter describing the free volume.

The effect of chemical structure on the T_g is also known. Polymers with a bulky group, such as benzene ring, or bulky pendant groups tend to have a relatively higher T_gs due to a steric hindrance of the bulky groups that cause a high energy barrier to rotation. Therefore, significant amounts of segmental mobility occur only at high temperatures. However, there is a limit to the increase in the T_g when the pendant groups become larger and are further away from the backbone; i.e., they no longer restrict bond rotations. On the other hand, attaching a long flexible linker as a side chain to the polymer backbone can result in a reduction of T_g. This is because these side chains increase the free volume, via their effect on the chain packing and their motions about their side-chains. By increasing the length of the side chain, the T_g can be decreased. Structure modification such as cross-linking or the existence of crystallinity also affect the T_g. Cross-linking decreases free volume since parts of the chain are tied closer together. Crystallinity limits the mobility of the chains in amorphous regions. Hence, increasing the cross-linking and crystallinity increases the T_g [4].

The presence of the diluents such as solvent or plasticizer can cause a change in T_g. Plasticizers are compounds that provide desired properties, such as flexibility, softness, reduced stiffness, shock resistance, pliability, and workability [31-32]. Plasticizers alter the thermal and mechanical properties of a polymer by lowering its T_g via a process called plasticization. Plasticizers can be categorized into two main groups as internal and external. Internal plasticizers are a part of polymer molecules, e.g., a copolymer of vinyl chloride and vinyl acetate (85:15) in which the T_g of the poly(vinyl chloride) is about 85 ºC and the T_g of the poly(vinyl acetate) is 30 ºC. The T_g of this vinyl chloride-vinyl acetate copolymer is 63 ºC; therefore, a vinyl acetate monomer whose polymer has a lower T_g is considered to be an internal plasticizer in this system. Copolymerization also often results in a less ordered structure. As a consequence, more

free volume is created from loose packing, which lowers the T_g. Another type of internal plasticizer is through the introducion of side chains, such as these found in polyacrylates and polymethacrylates, or alkylation of polyamides. External plasticizers are generally low vapor pressure compounds added in the polymers. In general, they are more widely used because they allow the manufacturer more flexibility in their formulations than an internal plasticizer does, and sometimes provide more satisfactory combinations of properties.

The choice of a plasticizer involves several important criteria, including: 1) The plasticizer should have a high degree of compatability with the polymer, with the ability to penetrate both crystalline and amorphous regions. Plasticizers used as the softeners should only penetrate the amorphous regions, but not the crystalline regions. 2) The plasticizer should be compatible with the polymer system for the processing in the entire temperature range of applications. In addition, the exposure of plasticized polymers to moisture, air, or sunlight should not disrupt the compatibility. Polymer-plasticizer compatibility, however, is affected by the molecular mass of the plasticizer and its chemical structure including polarity, shape, and size. 3) The plasticizer's efficiency should be considered; however, this has no absolute value but depends upon desirable polymer properties. For instance, the efficiency may be expressed in terms of the T_g depression, stiffness reduction or etc. Plasticizer efficiency is governed by chemical structure, molecular mass, and rate of diffusion of the plasticizer in the polymer matrix. Generally, the higher the diffusion rate, the greater plasticizer efficiency. However, fast diffusion rates are found in small molecules and the smaller molecules tend to have higher vapor pressures. Therefore, the rate of evaporation of plasticizer also increases. 4) The plasticizers should be permanent. The permanence of a plasticizer is its tendency to remain in the plasticized polymers. The larger the plasticizer, the lower its vapor pressure and, thus, the greater the permanence; however, the diffusion rate may also be decreased [32].

It is somewhat difficult to absolutely characterize the behavior of a plasticizer because it is intimately tied up with the polymer matrix. In addition, the behavior of a polymer highly depends on its previous history. For instance, different film processing

can result in different crystallinity and the effect of the plasticizer will, therefore, be quite different.

Plasticizers increase the free volume of the system, thereby lowering the T_g. The relationship between the free volume of a mixture and the free volume of the pure components was assumed (for example) to be additive; therefore, the T_g of the mixture can sometimes be related to that of its pure components, using Fox equation [33], or:

$$1/T_g = w_1/T_{g1} + w_2/T_{g2} \quad (18)$$

where T_{g1} and T_{g2} are the T_g's of the pure components in Kelvin and w_1 and w_2 are the respective weight fractions present in the mixture. This equation was first derived to describe the T_g of random copolymers.

For plasticized polymers, equations have been proposed relating the T_g depression due to the plasticizer content [32].

$$T_{g,mix} = T_{g1} - kw_2 \quad (19)$$

where $T_{g,mix}$ and T_{g1} are the respective T_g of plasticized and pure polymers, w_2 is the weight fraction of the plasticizer, and coefficient, k, varies from 200 to 500 K. This equation is valid only at relatively low dilution. A parabolic function has been shown to account for the deviation from linearity at higher dilutions, or:

$$T_{g,mix} = T_{g1}w_1 + T_{g2}w_2 + bw_1w_2(T_{g1} - T_{g2}) \quad (20)$$

where T_{g1} and T_{g2} are the respective Tg's of pure polymer and plasticizer and b is a constant that depends on the polymer-plasticizer system [31, 34-35].

As mentioned above, both composition and molecular mass affect the T_g. As a result, the T_gs of multi-component materials are often different from each individual pure component. Polymer solutions including the ones with low molecular mass components as plasticizers exhibit relatively broad glass transitions. A macroscopically phase-separated system, such as adsorbed polymer, may have more than one glass transition and these are usually quite broad.

2.3. CHARACTERIZATION TECHNIQUES FOR POLYMERIC MATERIALS

Polymers are used for applications in both bulk and also composite forms. A bulk polymer is defined as a system containing only a single polymeric component, such as a homopolymer. On the other hand, a polymer composite is generally multi-component material such as a polymer blend, structured latex, interpenetrating polymer network

(IPNs), or adsorbed polymer. The characterization of polymeric materials, especially for those with multi-components, has been vigorously pursued in recent years. However, exploring better techniques of characterization has been challenging and remains so even now. Morphology affects mechanical properties in these materials; therefore, information about morphological parameters, such as the thickness, weight (volume) fraction of interfaces, composition distribution in the phase, phase size/shape, and T_gs is clearly important. Since interfacial properties have a significant impact on the properties of composite materials, an understanding of the interfacial characteristics of these materials and the ability to optimize its properties are necessary for the improvement and development of polymeric materials.

Many techniques have been used to characterize the morphology of multi-component polymeric materials [36]. Scattering and microscope techniques have been used to study the shape and size of the domain, and the interface content. For instance, small-angle X-ray (SAXS) and neutron scattering (SANS) have yielded information about interfacial thickness and domain size [37-38]. Transmission electron microscopy (TEM) is a technique that has provided both interfacial thicknesses and information on composition gradients across an interface [37]. It has been used to determine the miscibility, size and shape of domains and their distribution in polymer blends, or phase segregation of IPNs. However, sample preparations can sometimes be difficult due to the need for ultra thin sections. In addition, electron beams can sometimes cause artifacts and damage to a sample [39, 40].

Thermal analysis techniques, such as differential scanning calorimetry (DSC), and dynamic mechanical thermal analysis (DMTA), are suitable for T_g measurement. DSC has been widely used to determine some thermal properties of materials, such as T_g and heat capacity, due to its fairly rapid analysis, simple operation, and easy sample preparations. However, the DSC's sensitivity and resolution are not good, which sometimes results in an overlap of thermal events. DMTA has been used to observe transitions in complex phase structures such as IPNs, but also suffers from potential difficulty in the association of the measured event with a molecular process.

The dynamics of multi-component polymeric materials are more complex than those of a single component as they depend upon the dynamics of each component.

Interfacial diffusion and dynamics of polymeric composite materials, for example plasticized-adsorbed polymer [31, 41], have been studied using solid-state NMR spectroscopy.

A listing of some of the characterization techniques for multi-component polymeric materials is shown in Table 2.1. However, there is no technique that can provide all the information desired. Therefore, it is very desirable to explore and develop widely applicable techniques for characterizing multi-component polymeric materials that can overcome the disadvantages of available techniques.

Table 2.1. Comparison of Various Characterization Techniques for Multi-Component Polymeric Materials [35].

	DSC	**SAXS**	**SANS**	**DMTA**	**SEM**	**TEM**	**NMR**
Resolution (nm)	20	2	1	15	20	1	1
Sample Preparation	Easy	Easy	Difficult	Easy	Easy	Difficult	Easy
T_g	Quant	No	No	Quant	No	No	Qual*
Multi-phase information	Yes	Yes	Yes	Yes	Yes	Yes	Yes
Interfacial information	Yes*	Yes	Yes	Yes*	No	Yes*	Yes
Interfacial thickness	No	Quant	Quant	No	No	Qual	No
Weight fraction	Qual	No	No	No	No	No	Yes*
Domain size	No	Yes	Yes	No	Yes	Yes	No

Qual = qualitative; Quant = quantitative

*Not always possible

In this work, we used the temperature modulated scanning calorimetry (TMDSC) technique, an advanced version of standard DSC, for the characterization of plasticized polymers for both bulk and adsorbed samples. In addition, the dynamics of plasticizer in bulk and adsorbed polymers were probed using the deuterium (^{2}H) NMR technique.

2.3.1. Differential Scanning Calorimetry (DSC). Differential Scanning Calorimetry, DSC, is a technique which combines the quantitative features of calorimetry with measurement during heating and cooling cycles. In DSC, the temperature is measured continuously and the difference in heat flow between a sample and a reference

is measured as a function of time and temperature under controlled conditions (time, temperature, and pressure). The most common design of DSC instruments is the heat flux calorimeter, as shown in Figure 2.2 In this design, a metallic disc (constantan) is used to transfer heat between a sample and a reference. A sample is packed in a metal pan such as aluminum, and an empty pan is used as a reference. Those two pans are placed on the raised platform of the metallic disc. When heat is transferred to the disc, the differential heat flow to the sample and to the reference is measured by a thermocouple, which is connected to chromel pieces beneath the metallic disc. An inert gas such as nitrogen, helium, or argon is used for purging to ensure a uniform, stable thermal environment which results in a better baseline and better sensitivity (signal-to-noise). The purge gas enters the sample chamber through an orifice in the heating block.

The differential heat flow is measured by thermocouples with $dQ/dt = \Delta T/R_D$, where dQ/dt is heat flow, T is the temperature difference between the reference and sample, and R_D is the thermal resistance of the metallic disc.

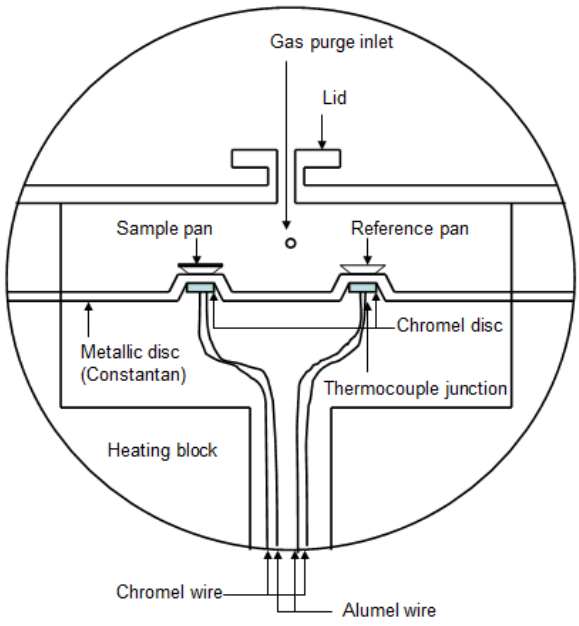

Figure 2.2. Heat flux differential scanning calorimeter

DSC is a thermal analysis technique used to measure the temperature and heat flow involved in the transition of materials, as a function of time and temperature. It provides quantitative and qualitative analysis information about the physical and chemical changes associated with endothermic and exothermic processes, or changes in heat capacity. DSC is applicable to several kinds of materials, such as polymers, organic and inorganic compounds. Among thermal analysis techniques, DSC is most widely used because of the reasonable time required for analysis, simple preparation of samples in both liquids and solids, and the wide range of temperatures involved. However, there are some limitations to the use of DSC, including; 1) The improper analysis of the complex transitions because DSC only measures the sum of thermal events in a sample. When there are many transitions in the same range of temperature, results can be confusing and misinterpreted. For instance, the magnitude of enthalpy relaxation, an endothermic process, can be different depending on the thermal history of the materials. 2) The sensitivity required to detect weak transitions is limited since it depends on both noise and baseline. However, the primary limitation to detecting weak transitions is variation in the shape of the baseline (baseline drift from linearity). Noise can be reduced by signal averaging. 3) The resolution of DSC comes at the expense of the sensitivity, or vice versa. Small sample size and a low heating rate are required for high resolution to separate transitions that are only a few degrees apart. However, a reduction in sample size and heating rate also decreases the heat flow signal. 4) Complex experiments, such as heat capacity and thermal conductivity, require multiple experiments or modifications to the standard DSC cell which can be time consuming and more prone to introduce error.

2.3.2. Temperature Modulated Differential Scanning Calorimetry (TMDSC). Temperature modulated differential scanning calorimetry (TMDSC) is an improved version of the standard DSC, which has overcome most of its previous limitations. TMDSC offers the same information as conventional DSC, with the addition of other unique information that one might not be able to obtain due to limitations in conventional DSC [42]. TMDSC also measures the difference in heat flow between a sample and an inert reference, as a function of time and temperature. The major difference between standard DSC and TMDSC is the application of a sinusoidal modulation (oscillation) imposed on the conventional linear heating or cooling ramp to yield a different

temperature profile, since the average temperature of a sample changes with time, in a non-linear fashion. One can simply picture the two experiments being run simultaneously on a sample as a conventional linear (average) heating rate and a sinusoidal (instantaneous) heating rate. The actual rates for these depend on the heating rate, period of modulation, and the temperature amplitude of modulation. The general equation which describes the resulting heat flow for a DSC or a MDSC experiment is

$$dQ/dT = Cp\beta + f(T,t) \quad (21)$$

where dQ/dT is total heat flow, Cp is heat capacity, β is heating rate and f(T,t) is kinetic heat flow (absolute temperature and time dependent) processes.

Conventional DSC only measures the total heat flow, dQ/dT, whereas TMDSC provides those two individual heat flows, Cpβ, (reversing heat flow) and kinetic component, f(T,t), (nonreversing heat flow), as well as the total heat flow (the sum). In TMDSC, the average heating rate provides total heat flow information, while the sinusoidal heating rate yields heat capacity information from the heat flow that responds to a change in heating rate. The nonreversing heat flow is the difference between the total heat flow and the reversing heat flow. As shown in Figure 2.3, weak or overlapping transitions, such as the glass transition of polymers (which involves enthalpy relaxation), can be accurately obtained from the reversing heat flow component.

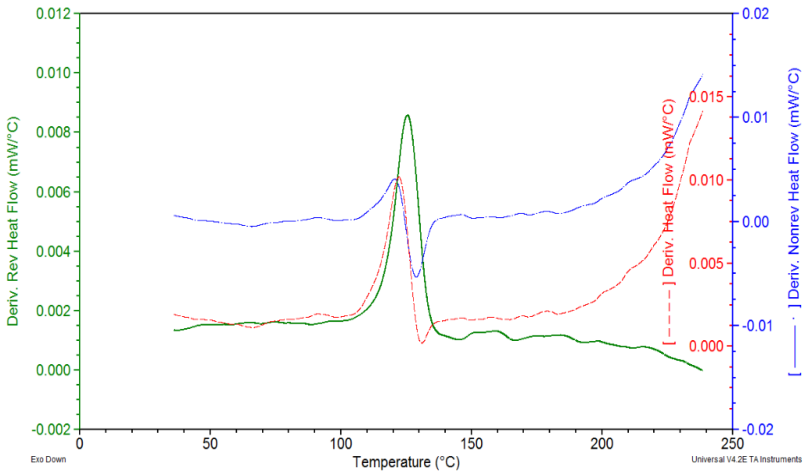

Figure 2.3. The derivatives of total heat flow (a red dashed line), nonreversing heat flow (a blue dash dotted line), and reversing heat flow (a green solid line) of bulk PMMA.

2.3.3. Solid State Deuterium (2H) NMR. The deuterium nucleus (^{2}H) has a spin of I = 1 so that, in the presence of the magnetic field, three quantized energy levels corresponding to m_z = 1, 0, -1 are found. These represent the quantization of magnetic moments along the magnetic field direction as identified with quantum number, m_z. The energy level diagram for the combined Zeeman and quadrupolar interactions for a spin 1 nucleus is shown in Figure 2.4. A doublet with peak separations for a spin 1 nucleus, interacting with an axially symmetric field gradient, is the result of two allowed transitions (m_z = -1) <-> (m_z = 0) and (m_z = 0) <-> (m_z = 1). When there is no molecular motion, in the presence of a magnetic field, the doublet spacing depends on the angle between the C-D bond and the direction of the external magnetic field. In the presence of molecular motion, doublet spacing depends on the motion and on the orientation of the deuteron with respect to the molecular symmetry axis and magnetic field.

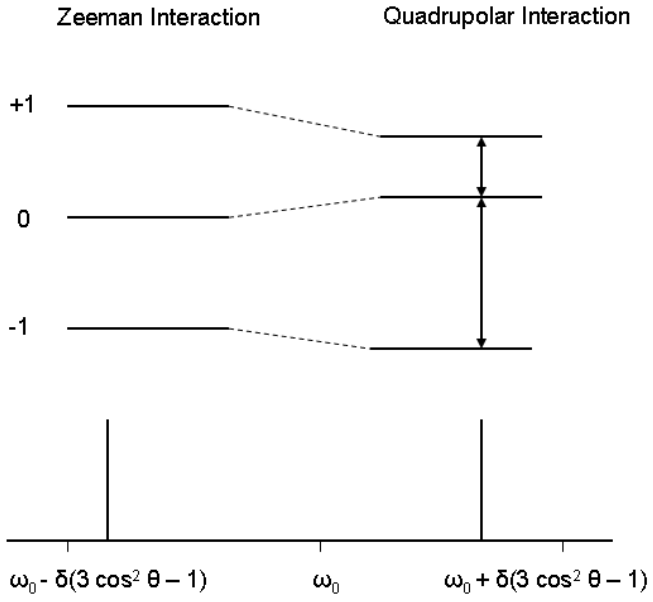

Figure 2.4. Energy level diagram of the Zeeman and quadrupolar interactions for a single crystal deuteron (absence of motion). The corresponding spectrum is shown at the bottom for each transition. The magnitude and direction of the quadrupolar perturbation depends upon the orientation of the electric field gradient with respect to the external magnetic field; ω_0 is the Larmor frequency and $\delta = 3e^2qQ/8h$ where e^2qQ/h is a quadrupole coupling constant.

In the absence of motion, with the presence of an external magnetic field, the total Hamiltonian of the deuterium nucleus can be described by: [43-48]

$$H_T = H_Z + H_Q + H_D + H_{CS} + H_J \quad (22)$$

where H_Z represents the Hamiltonian for the Zeeman interaction (the interaction of the nuclei with the external magnetic field), H_Q is quadrupolar interaction, H_D is dipole-dipole interaction with other nuclei, H_{CS} is the chemical shift as a result of magnetic shielding by the surrounding electrons, and H_J is the scalar coupling interaction between the nuclei. However, for solids, the two dominant terms are from the Zeeman and quadrupolar interactions. In deuterium (spin I = 1), the interaction of the quadrupole moment with the electric field gradient at the nucleus substantially perturbs the Zeeman splitting. Other interactions, such as dipole-dipole, chemical shift, and scalar coupling are small and may be neglected. Thus, the reduced form of the Hamiltonian equation of deuterium nucleus can also be written as

$$H = H_Z + H_Q \quad (23)$$

The interaction of the magnetic moment of the deuterium nucleus with the external magnetic field gives rise to precession, as described by the Larmor equation with frequency, ω_0. For a deuterium nucleus, this frequency is 61.39 MHz at 9.4 T. The Zeeman energy level can be described as: [43-48].

$$E(m_Z) = -\omega_0 m_Z \hbar \quad \text{with } \omega_0 = \gamma B_0 \quad (24)$$

where γ is the magnetogyric ratio, indicating the magnitude of the magnetic moment of the nucleus, m_Z is a quantum number (m_Z= -1, 0, 1 for deuterium nucleus), and B_0 is the external magnetic field strength.

The quadrupole Hamiltonian H_Q arises from an electrostatic interaction of the nuclear quadrupole moment (Q) with an electric field gradient (eq) at the position of nucleus. The quadrupole Hamiltonian can be described by following equation: [43-48].

$$\omega = \omega_0 +/- \delta(3\cos^2\theta - 1 - \eta \sin^2\theta \cos^2\phi) \quad (25)$$

$\delta = 3e^2qQ/8h$, where e^2qQ/h is the quadrupole coupling constant and ω_0 is the Zeeman frequency. The polar angle θ is the angle between the principle component that the electric field gradient tensor makes with the magnetic field β_0 (for instance, in the case of icy D_2O will be the O-D vector, whereas in our polymers, the vector will be a C-D bond). The spherical polar angle, ϕ, also specifies the azimuthal orientation of the principle axis

system of the electric field gradient tensor with respect to the external magnetic field. The quantity η is the asymmetry parameter and is usually zero for aliphatic C-D bonds, indicating that the electric field gradient tensor is axially symmetric. However, for aromatic C-D bonds, the motionally averaged field gradient tensor is not axially symmetric [44]. If $\eta = 0$, as in the case of the aliphatic C-D bonds, the NMR frequencies of the two transitions are [43-48].

$$\omega = \omega_0 +/- \delta(3 \cos^2 \theta - 1) \quad (26)$$

Thus, the resonance frequency depends on the angle θ that a C-D bond makes with the external magnetic field. In the absence of motion, a single crystal, that has only one type of C-D bond angle with respect to the external magnetic field, yields a doublet spectrum. In an amorphous polymer, where many C-D bond orientations exist, the intensity of each orientation can be pictured as a sphere divided into latitudes of equal frequency. The polar angle of $\theta = 90$ is where the C-D bond is perpendicular to the external magnetic field would have the highest intensity while $\theta = 0$ for which C-D bond is parallel to the external magnetic field where it would have the least intensity. Distributions for other orientations are shown in Figure 2.5.

The Pake powder pattern is composed of the spectra from the two transitions which contain all available C-D bond orientations with respect to the external magnetic field. The splitting between the doublets of the powder pattern is given as [43-48].

$$\Delta v_q = ¾ (e^2qQ/h)(3\cos^2 \theta(t) -1- \eta\sin^2 \theta(t) \cos^2\phi) \quad (27)$$

where e^2qQ/h is a quadrupole coupling constant, t is time, θ and ϕ are the spherical polar angles that specify the orientation of the principle axis system of the electric field gradient tensor with respect to the external magnetic field. In polymers with the absence of motion, the quadrupole coupling constant for a static C-D (aliphatic deuteron) is about 160-170 kHz. The splitting between the doublets is about 120-128 kHz, or three fourths of the quadrupole coupling constant.

Glassy polymers have complex distributions of thermally activated molecular motions, including longer range, larger scale displacements and torsional oscillations of a local nature. NMR spin interactions are intrinsically short range, meaning they are local in character; however, they can be sensitive to the full range of motional frequencies that occur. As temperature increases, the motional amplitudes and frequencies also increase.

Polymeric structures may have interchain and intrachain interactions which change with conformation.

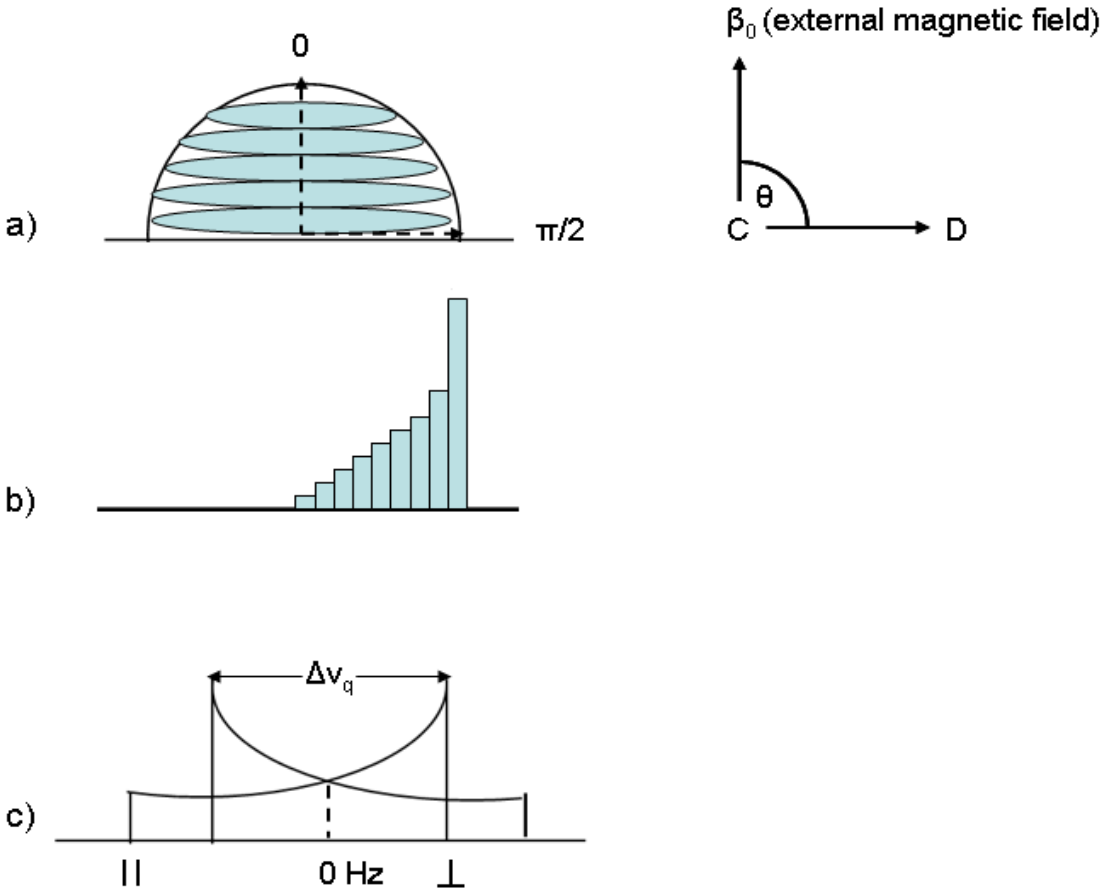

Figure 2.5. The deuterium NMR powder line shape and how it arises. a) A sphere divided into latitudes of equal frequency (orientation possibilities); 0 is the orientation when the C-D bond is parallel to the external magnetic field (β_0) and $\pi/2$ is the perpendicular orientation. b) Combination of all orientations of the C-D bonds with respect to the magnetic field; 0º is the least intense while 90º ($\pi/2$) has the largest intensity. c) A smoother version of b) for both transitions (m = - 1) <-> (m = 0) and (m = 0) <-> (m = 1), $\Delta\nu_q$ is the doublet spacing [44].

An NMR study of motion in glassy polymers is more of an extensive investigation than a simple observation of one or two spectra. However, a detailed and often site-specific view of chain motions can be revealed, for instance, the motional

mechanism (jump or diffusion), symmetries, distribution of rates and their character (homogeneous or inhomogeneous), activation energies, and so on. There is no other technique that is capable of probing these motions in such extensive detail. The basic NMR experiments for describing molecular motion can be categorized into those probing line shapes, spin-lattice relaxation, spin alignment, and spin echoes [49].

Line shapes are affected by motions that approximate, or are faster or on the order of the interaction (in terms of frequency) responsible for the line shapes. In the presence of rapid molecular motion on the deuterium NMR time scale (in this case, the effect on the line shape in solids requires motions on the order of the splitting), the orientation of the C-D changes due to molecular motion. The change in NMR line shapes depends upon two factors. One is the motional rate and another is the type of motion. The motional rate is a function of temperature and in some cases, so it the motional mechanism. In glassy polymers, as the motional rate increases, the powder pattern starts collapsing and the splitting becomes narrower as the rates of motion become fast compared to the quadrupole splittings. A single line NMR spectrum is observed when the motion becomes fast and isotropic, as that found in a liquid. Various types of motion that are found in synthetic polymers include static C-Ds (doublet spacing d = 120 - 128 kHz), rotating methyls $–CD_3$ (d = 40-42.5 kHz), two-site hops (d = 0, when the bisector of the hop angle is 54.7, the magic angle.), 180º phenyl ring flips (d = 32 kHz) and free diffusion of phenyl rings (d = 16 kHz) [44].

Many interesting dynamics processes that exist in bulk polymers have correlation times of less than 10^{-7} s (fast motion on the NMR time scale). These include methyl rotations, aromatic ring flips, diffusion of plasticizers, and some side-chain motions. In the fast motion time regime ($<10^{-7}$ s.), the deuterium NMR line shape provides information about the various types, angular ranges or amplitudes of these motions. However, the line shapes give no additional information about the rates of these processes if they are fast. These rates can be obtained through a spin-lattice relaxation experiment (T_1).

The advantages of using deuterium NMR include sensitivity and selectivity to local motions, less interference from unlabeled deuterons due to deuterium's low natural abundance (0.016%), and different types of motion can be identified unambiguously.

However, the primary drawback of deuterium NMR is the need for labeling compounds although labeling does not alter the molecular structure. The second disadvantage is the rather low sensitivity associated with deuterium NMR [50] as compared to that of protons.

Simulations of the deuterium NMR line shapes have been used to understand the motional mechanism (types of motion) and motional rates in different systems in which the change in NMR line shapes is sensitive in the frequency range below 10^7 s^{-1} (Hz). In this study, the experimental NMR line shapes were simulated using a FORTRAN program known as MXQET [47, 51-52]. Our simulation was based on a two-site jump model for two different orientations of a phenyl deuteron that executes a 180º flip. The experimental line shapes were then fitted with a superposition of the simulated spectra by using a mathematical program (MATLAB, the Mathworks, Inc., Natick, MA). The weight fractions of each of the simulated spectra were found by minimizing the differences between the experimental spectra and the sum of the simulated ones. A constrained least-squares fit was applied to find the absolute weight fractions of a series of spectra.

Due to the broad line shape of the powder patterns in deuterium NMR, which can be as large as 250 kHz, a high-powered transmitter pulse is required to ensure an adequate 90º pulse across the entire spectrum with a very short pulse time (pulse width) in order to minimize the loss of signal intensity. A reasonable 90º pulse width is approximately 3 μs, but even at that pulse width, the parallel edges of the sample will still suffer intensity losses. In addition, fast digitization is needed because the free-induction decay (FID) signal dies away very rapidly.

In solid-state deuterium NMR, the decay of the signal after perturbation is rapid (about a few tens of microseconds) so much of the signal is lost during the receiver dead time. The quadrupole-echo pulse sequence gives time for the receiver to recover from the high-power transmitter pulse, as shown in Figure 2.6. Typical times for t_1 and t_2 for our studies were 30 μs and 33 μs (including an extra ring down time), respectively. Prior to Fourier transformation, the data points of the FID signal are usually left shifted so that the transformed FID signal begins at the exact top of the echo maximum [44, 47-48].

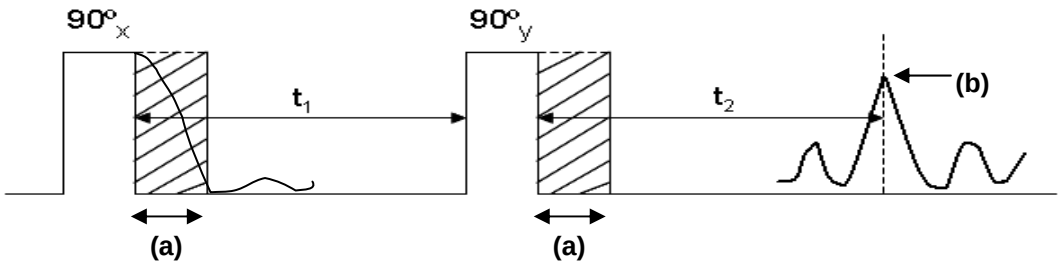

Figure 2.6. The quadrupole echo pulse sequence in solid-state deuterium NMR. (a) The hatched areas after the pulses represent the receiver dead time. (b) The time where is data acquisition begins at the top of the echo.

2.4. REFERENCES

1. Kinloch, A. J. *Adhesion and Adhesives: Science and Technology*, Chapman and Hall, 1987
2. Fleer, G. J.; Cohen Stuart, M. A.; Scheutjens, J. M. H. M.; Cosgrove, T.; Vincent, B. *Polymers at Interfaces*; Chapman and Hall: London, U.K., 1993.
3. Kuhn, W. *Kolloid Z.* **1934**, *68*, 2.
4. Painter, P. C.; Coleman, M. M. *Fundamentals of Polymer Science 2nd ed*; CRC Press: Boca Raton, 1997.
5. Flory, P. J. *Principles of Polymer Chemistry*; Cornell Univ. Press: Ithaca, N.Y., 1953.
6. Huggins, M. *J. Phys. Chem.* **1942**, *46*, 151.
7. Huggins, M. *Ann. NY Acad. Sci.* **1942**, *41*, 1.
8. Huggins, M. *J. Am. Chem. Soc.* **1942**, *64*, 1712.
9. Slow, K. S.; Patterson, D. *J. Phys. Chem.* **1973**, *77(3)*, 356.
10. Szleifer, I.; Widom, B. *J. Chem. Phys.* **1989**, *90*, 7524.
11. White, J. L.; Sadakne, G. S. *J. Appl. Polym. Sci.* **1973**, *17*, 453.
12. Silberberg, A. *J. Chem. Phys.* **1968**, *48*, 2835.
13. Stuart, C. M. A.; Scheutjens, J. M. H. M.; Fleer G. J. *J. Polym. Sci.* **1980**, *18*, 559
14. Roe, R. J. *J. Chem. Phys.* **1974**, *60*, 4192.
15. Linden C. V.; Leemput, R. V. *J. Colloid Interface Sci.* **1978**, *67*, 63.

16. de Gennes, P. G. *Scaling Concepts in Polymer Physics*; Cornell Univ. Press: Ithaca, N.Y., 1979.
17. Xia, K. Q.; Franck, C.; Widom, B. *J. Chem. Phys.* **1992**, *97*, 1446.
18. Adamson, A. W.; Gast, A. P. *Physical Chemistry of Surfaces 6thed*; John Wiley & Son: N.Y., 1997.
19. Felter, R. E.; Ray, L. N. *J. Colloid Interface Sci.* **1970**, *32*, 349.
20. Roe, R. J. *Adhesion and Adsorption of Polymers, Polymer Science and Technology, part 12B, ed. Lee, L. H.*; Plenum, N.Y., 1980, p. 629.
21. Kolthoff, I. M.; Gutmacher, R. E.; Kahn, A. *J. Phys. Chem.* **1951**, *55*, 1240.
22. Schick, M. J.; Harvey, E. N. *Preprints, ACS Div. Org. Coatings Plast. Chem.* **1967**, *27*, 47.
23. Kulkeratiyut, S.; Kulkeratiyut, S.; Blum F. D. *J. Polym. Sci Part B.* **2006**, 44, 2071.
24. Blum, F. D.; Young, E. Y.; Smith, G.; Sitton O. C. *Langmuir* **2006**, 22, 4741.
25. Kabomo, M. T; Blum, F. D.; Kulkeratiyut, S.; Kulkeratiyut, S.; Krisanangkura, P. *J. Polym. Sci: Part B*, **2008**, *46*, 649.
26. Jenkel, E.; Rumbach, B. *Z.Elektrochem.* **1951**, 55, 612.
27. Seyler, R. J. *Assignment of the Glass Transition*; ASTM: Philadelphia, P.A., 1994.
28. McKenna, G. B. *"Glass Formation and Glassy Behavior" in Comprehensive Polymer Sci. Vol. 2. Polymer Props,* Booth, C.; Price, C., Eds.; Pergamon Press: Oxford, England, 1989; Vol.2.
29. Fox, T. G.; Flory, P. J. *J. Appl. Phys.* **1950**, 21, 581.
30. Fox, T. G.; Flory, P. J. *J. Polym. Sci.* **1954**, 14, 315.
31. Nambair, R.; Blum, F. *Macromolecules* **2008**, *41*, 9837.
32. Gould, R. *Plasticization and Plasticizer Processes*, American Chemical Society, Washington, D.C, 1965.
33. Fox, T. G. *Bull. Am. Phys. Soc.* **1956**, *1*, 123.
34. Jenckel, E.; Heusch, R. *Kolloid-Zeitschrift*, **1953**, *130*, 89.
35. Dubault, A.; Bokobza, L.; Gandin, E.; Halary, J. L. *Polym. Int.* **2003**, *52*, 1108.
36. Reading, M.; Hourston, D. J. *Modulated Temperature Differential Scanning Calorimetry, Theoretical and Practical Applications in polymer Characterisation*. Springer: Dordrecht. The Netherlands, 2006.

37. Annighofer, F.; Gronski, W. *Makromol. Chem.* **1984**, *185*, 2231.
38. Roe, R. J. *J. Appl. Crystallogr.* 1982, *15*, 18.
39. Vesely, D. *In Polymer Blends and Alloys,* Folkes, M. J.; Hope, P. S., Eds.; Blackie Academic & Professional: London 1993.
40. Thomas, D. A. *In advances in Preparation and characterization of Multi-polymer Systems*, Ambrose, R. J.; Aggarwal, S. L., Eds.; John Wiley and Sons: N.Y. 1978.
41. Bingemann, D.; Wirth, N.; Gmeiner, J.; Rossler, E. A. *Macromolecules* **2007**, *40*, 5379.
42. TA Instruments. *Modulated DSC Compendium, Basic Theory & Experimental Considerations*.
43. Fyfe, C. A. *Solid State NMR for Chemists*.; C.F.C. Press: Ontario, Canada. 1983.
44. Jelinski, L. W. *"Deuterium NMR of Solid Polymers", High-Resolution NMR Spectroscopy of Synthetic Polymers in Bulk*, Komoroski Ed.; VCH Publishers, Inc. 1986.
45. Higinbotham, J.; Marshall, I. in *Annual Reports on NMR Spectroscopy*, Webb, G. A., Ed.; Academic, San Diego, **2001**, vol. 43, p. 59.
46. Ulrich, A. S., Grage, S. L., in *Solid State NMR of Polymers*, Ando, I. Asakura, Elsevier, 1998, p 190.
47. Metin, B. **2006**. *Segmental Dynamics in Poly(Methyl Acrylate) through the Glass Transition Region. Dissertation(Ph.D.)*. University of Missouri-Rolla.
48. Lin, W. Y. **1997**. *Segmental Dynamics in Bulk and Adsorbed Poly(Methyl Acrylate)-d_3 by Deuterium NMR.* University of Missouri-Rolla.
49. McBrierty, V. J. *Nuclear Magnetic Resonance in Solid Polymers*; Cambridge University Press: Cambridge, Great Britain 1993.
50. Seelig, *J. Quarterly Reviews of Biophysics 10*, **1977**, *3*, 353.
51. Greenfield, M. S; Ronemus, A. D.; Vold, R. L.; Vold, R. R.; Ellis, P. D.; Raidy, T. E.; *J. Magn. Reson.* **1987**, 72, 89.
52. Vold, R. R.; Vold, R. L. *Adv. Magn. Opt. Reson.* **1991**, 16, 85.

PAPER

1. THERMAL ANALYSIS OF ADSORBED POLY(METHYL METHACRYLATE) ON SILICA: EFFECT OF MOLECULAR MASS

Boonta Hetayothin[1], Suriyaphongse Kulkeratiyut[2], Suntree Kulkeratiyut[2], and Frank D. Blum[1, 3]*

1. Department of Chemistry and Materials Research Center, Missouri University of Science and Technology, Rolla, Missouri 65409-0010
2. Department of Transfusion Medicine, Faculty of Allied Health Sciences, Chulalongkorn University, Bangkok 10330, Thailand
3. Department of Chemistry, Oklahoma State University, Stillwater, Oklahoma74078

ABSTRACT

The effect of molecular mass on the adsorption of poly(methyl methacrylate) (PMMA) on a silica surface was made using temperature-modulated differential scanning calorimetry (TMDSC). A two-component model based on loosely-bound polymer (with a glass transition temperature, Tg similar to that of bulk) and more tightly-bound polymer (with a Tg higher than that of the loosely bound polymer) was used to interpret the thermograms. PMMA (with high and medium molecular mass of 450 kDa and 85 kDa, respectively) had similar amounts of tightly-bound polymer (approximately 0.78 +/- 0.25 and 0.78 +/- 0.17 mg/m2). The low molecular mass, 32 kDa PMMA, had a smaller amount of tightly-bound polymer (about 0.48 +/- 0.09 mg/m2). The ratio of heat capacity increment for the loosely-bound and tightly-bound (ΔCpA/ΔCpB) at the Tg indicated the relative mobility of the two components. For the low molecular mass PMMA, this ratio was about 1, whereas in medium molecular mass and high molecular mass PMMA, the ratios of ΔCpA/ΔCpB were about 1.2 and 1.7, respectively.

* Author to whom correspondence should be addressed: Frank D. Blum (fblum@okstate.edu)

1. INTRODUCTION

Thin polymeric films that range in thickness from a few to several hundred nanometers are of technological interest for the development of electronic and optical devices [1-2]. Because such thin layers of polymeric films may not survive on their own as free-standing films, a supporting surface is often needed. Accordingly, the physical properties of thin polymeric films become rather complicated since they involve both polymers and surfaces. An understanding of the behavior of adsorbed polymers on a surface is essential for improving properties for specific uses.

Studies of polymer adsorption have been approached in several ways [3-7]. In general, adsorption can be described as the attachment of species (in this case for polymers) to the substrate. Studies of polymer adsorption are usually made from polymers adsorbed from solution. Polymer adsorption is often a relatively irreversible process, as suggested by the small amounts of desorption observed upon dilution with a solvent [8]. In the dilute solution, where the adsorption is typically of single molecules, monolayer adsorption occurs. Polymers segments randomly adsorbing on the surface, typically do so as alternating three-dimensional loops and two-dimensional surface-contained trains [7, 9].

One interesting aspect of polymer adsorption that has been extensively investigated is the dependence of the adsorbed amount on molecular mass. It is known that for randomly adsorbing high molecular mass polymers not only yield larger adsorbed amounts, but they also adsorb preferentially over the lower mass polymers [6-10]. The molecular mass dependence of an adsorbed amount has been shown to be proportional to M^x, where M is the molecular mass and x is a constant of about 0.3-0.5 for an unperturbed chain [7]. In the higher range of molecular mass range, x tends to be independent of molecular mass. This molecular mass dependence is also more pronounced in a poor solvent ($\chi >= 0.5$) than that in a good solvent ($\chi << 0.5$) [7].

It is well known that the structures and properties of polymers are time and temperature dependent [11], most polymer solids are unlikely to achieve true equilibrium because of their relatively large sizes and high molecular masses. Solid polymers often

exhibit a range of relaxation times and properties in response to their environment. Their dynamic behavior allows the polymers to restructure or reorient in response to environmental changes to minimize free energy. In different systems, such as bulk and adsorbed polymers, the behavior of these polymers may or may not be the same. Although they have common characteristics, a number of studies have reported that, in some ways, adsorbed polymers behave differently from their bulk counterparts. For instance, the restricted motion of an adsorbed polymer on an attractive surface (as shown in Figure 1) results in higher and broader of $T_g s$ than those found in bulk polymers. The T_g is a good indication of the mobility of these adsorbed polymers [12-14].

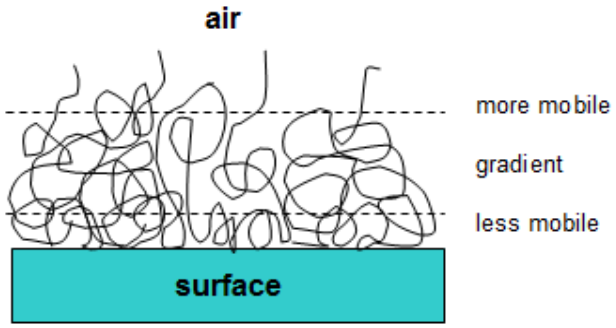

Figure 1. A motional gradient of the surfaced-bound polymer.

Several techniques have been used to probe the molecular motions of adsorbed polymers, including NMR [15-17], ESR [18], contact angle measurements [19], force modulation scanning force microscopy (force modulation SFM) [20-22], lateral force microscopic (LFM) [22-23], and thermal analysis [12, 14]. Among these, thermal analysis is perhaps the most common and widely used technique for obtaining information on thermodynamic properties, such as the T_g and heat capacity. The heat capacity is primarily based on molecular motions and has been used to evaluate conformational energies of organic molecules [24]. In bulk polymers, when there are no specific attractions such as hydrogen bonding, ionic bonding (ionomers) or others, the change in heat capacity at the Tg is primarily determined by the change in conformational

structures [25-26]. Below the T_g, large-scale conformational motions of the polymers are virtually nonexistent, while at higher temperatures, they are common. In adsorbed polymers, the changes in molecular motion at the glass transition are different from bulk polymers. In the present case, this motion is significantly affected by a specific interaction, namely hydrogen bonding between the carbonyls of PMMA and the surface silanols on the silica.

A study of adsorbed PMMA on silica using temperature modulated differential scanning calorimetry (TMDSC) has been reported [14] and a relatively narrow, single glass transition for bulk PMMA, plus broader two-component transitions were found for the adsorbed polymer. A two-state model, based on loosely-bound polymer (T_g similar to bulk) and more tightly-bound polymer (T_g higher than bulk) was used to interpret the thermograms. Based on that work, the ratio of the change in heat capacities for the tightly-bound and the loosely-bound polymer at the T_g, and the amount of tightly bound polymer were estimated. In the present work, we have used the same technique based on this two-state model to study the effect of molecular mass on the adsorption of PMMA on silica.

2. EXPERIMENTAL

PMMA with molecular masses, M_w, of 32, 85, and 450 kDa with polydispersities of 1.5, 1.6 and 2.6, respectively, were used as received (Aldrich Chemical Co., Milwaukee, WI). The molecular masses were determined by using gel permeation chromatography with a Dawn EOS laser light scattering instrument (LLS) and an Optilab refractive index detector (Wyatt Technology, Santa Barbara, CA). The tacticities of these samples have been reported as percentage of triads as: isotactic triads (mm), atactic triads (rm), and syndiotactic triads (rr). The tacticities were 10.0 (mm), 35.5 (rm), 54.5 (rr) for the 450 kDa sample, 27.7 (mm), 37.6 (rm), 34.7 (rr) for the 85 kDa sample, and 13.1 (mm), 36.4 (rm), 50.5 (rr) for the 32 kDa sample [13]. Cab-O-Sil M-5P silica, with a

specific surface area of 200 m^2/g (Cabot Corporation, Tuscola, IL), was used as the substrate.

The silica was dried in an oven at 400 ºC for 24 hour before use. Various concentrations of PMMA solutions of 5, 10, 20, 40, 80 mg/mL in toluene (10 mL) were prepared. 300 mg of silica were added to the PMMA solution. The test tubes containing mixtures of silica and the PMMA solutions were put in a mechanical shaker for 48 h and then centrifuged at 2500 rpm for 1 h. The supernatant liquids were removed, and the adsorbed polymers were washed three times with toluene (7 mL) to remove the excess polymer. The toluene from the last wash was not decanted; instead, it was removed by passing air (using a glass pipette at a low flow rate) through the adsorbed polymer-silica mixture, as it was being agitated. Then, the absorbed samples were dried in a vacuum oven under 30 mm Hg at 60 ºC for 24 h.

Thermogravimetric analysis (TGA) measurements were made using a Hi-Res TGA-2950 (TA Instruments, New Castle, DE) to determine the amount of absorbed polymer at the surface of the silica. Samples of approximately 8-12 mg were placed in a platinum pan and heated from 25 to 750 ºC, with a heating rate of 20 ºC/min in air. The mass loss was followed as a function of time (temperature) up to roughly about 300-450 ºC.

The thermal behavior in the glass transition region was measured with a TA Instruments model 2920 MDSC (TA Instruments, New Castle, DE). The samples were referenced against the empty pans and the cell purged with nitrogen gas at a flow rate of 50 mL/ min. The samples were held at 0 ºC for 5 min, heated to 280 ºC at a rate of 2.5 ºC/min with a modulation amplitude of +/- 1.0 ºC, and a period of 60 s, held for 3 min, cooled to 0 ºC at the same rate and then held at 0 ºC for 3 min in order to minimize the effects of previous thermal history. After the first heating and cooling scan, the second heating scan was done with the same conditions as the first heating scan. The T_g was determined based on the second heating scan. The results are shown as differential reversing heat flow rate (dQ_{rev}/dT) vs temperature. A 15 ºC smoothing was applied to the thermograms to reduce the high-frequency noise and highlight the broad transitions.

A perpendicular drop method (TA Universal Analysis V4.2E software) was used to estimate the area under the transitions in the ($dQ_{reversing}/dT$) plots. In this method, a

straight baseline was chosen over a range of two transition temperatures. The two overlapping transitions were separated by a vertical line that was perpendicular to the baseline at the temperature where the first transition (loosely bound) ended and the second transition (tightly bound) began. The areas under those two transitions were integrated. The T_g of each transition was taken at the peak of the derivative curve [27].

2.1. Model.

A two-state model was previously applied to the thermal analysis of adsorbed polymers [14]. The model will be briefly outlined here. The model was based on loosely-bound polymer (with a T_g similar to, but not necessarily equal to that of bulk) and tightly-bound polymer (with a T_g higher than that of the loosely bound polymer).

A normalized polymer mass, m'_p, was defined as the total mass of adsorbed polymer (from TGA) divided by the mass of silica used, which is the sum of the masses for the two components, or

$$m'_p = m'_{pA} + m'_{pB} \quad (1)$$

where m'_{pA} is the normalized mass of loosely-bound polymer and m'_{pB} is the normalized mass of tightly-bound polymer.

The ratio of the heat flow changes of components, A (loosely bound) and B (tightly bound), given by r, is related to the ratios of the heat capacities of the components, or:

$$r = \Delta Q_A / \Delta Q_B = m'_{pA} \Delta C_{pA} / (m'_{pB} \Delta C_{pB}) \quad (2)$$

where the ΔQs represent the heat flows and the ΔC_ps represent the changes in heat capacity in the glass transition region.

In effect, the ratio, r, is the ratio of the area under the two transitions in the thermograms. From equations (1) and (2), a linear equation can be made, or

$$r = (m'_p - m'_{pB}) \Delta C_{pA} / (m'_{pB} \Delta C_{pB})$$

$$= [\Delta C_{pA} / (m'_{pB} \Delta C_{pB})] m'_p - \Delta C_{pA} / \Delta C_{pB} \quad (3)$$

This equation suggests that r should be linear function of m'_p (which is known and related to the adsorbed amount). As noted above, m'_p, was defined as the total mass of adsorbed polymer (from TGA), divided by the mass of silica used. Therefore, one can calculate the adsorbed amount of the polymer on the silica from m'_p, based on the specific surface area of the silica.

The bound fraction, f_B, was the ratio of the mass of tightly-bound polymer at the interface to the total amount of polymer. This can be expressed as a function of the experimental observable, r, as

$$f_B = m'_{pB}/m'_p = m_{pB}/m_p = 1/(1+ r\Delta C_{pB}/\Delta C_{pA}) \quad (4)$$

The fraction of bound polymer, f_B, and the ratios of the ΔCp's can be estimated from the model, using the value of m'_{pB} obtained from the intercept, divided by the slope from the linear regression.

3. RESULTS

The bulk T_gs of the three different molecular mass PMMA (450 kDa, 85 kDa, and 32 kDa) are shown in Figure 2. The T_g of 450 kDa PMMA is of about 123 ºC while the T_gs of 85 kDa and 32 kDa PMMA are 108 ºC and 109 ºC, respectively.

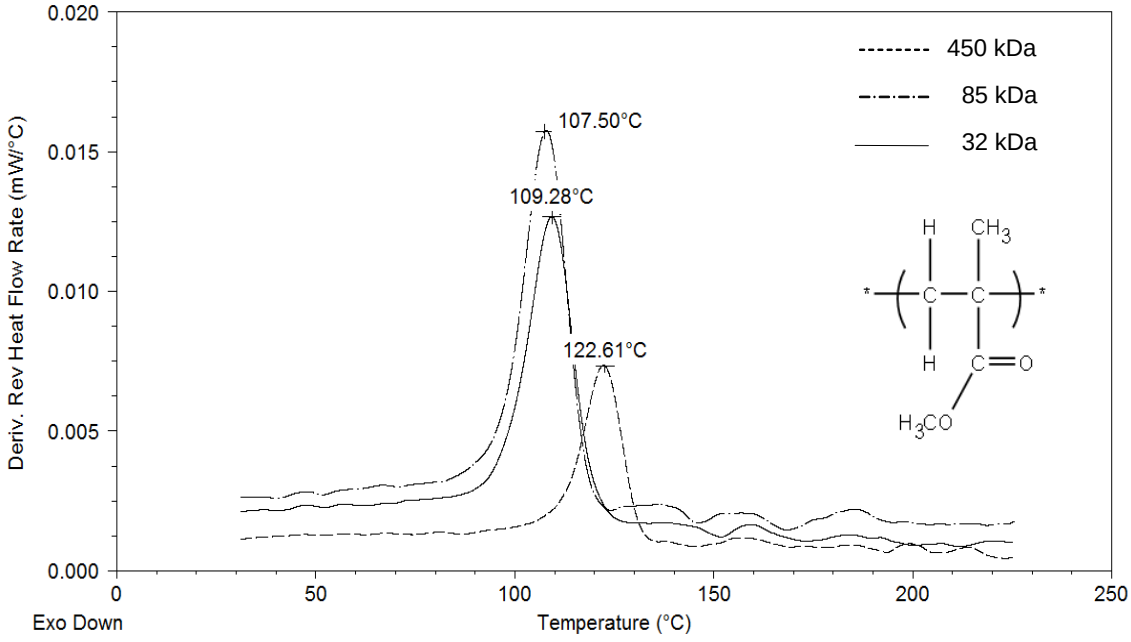

Figure 2. TMDSC thermograms of bulk PMMA for three different molecular masses (450 kDa, 85 kDa, and 32 kDa).

The thermograms of the high molecular mass PMMA (450 kDa) adsorbed on silica for different absorbed amounts are shown in Figure 3 The vertical scale in the thermograms was shifted to allow comparisons between thermograms. The T_g of the high molecular mass PMMA was about 123 ºC for the bulk polymer (from the derivative heat flow at 2.5 ºC/min). The thermograms for the adsorbed polymers showed two distinct peaks which we refer to as the A component (loosely bound, T_g similar to bulk) and the B component (tightly bound, T_g higher than bulk). As the adsorbed amount increased, the area under transition A increased, whereas that of transition B remained roughly constant. For this high molecular mass PMMA, the peak of the transition for the A component was shifted to slightly higher temperature than that in the bulk. The average of the temperature of the peak for the A component was 130 +/- 3 ºC (SD), and that of the B component was about 156 +/- 2 ºC (SD). The standard deviation (SD) was calculated from all the adsorbed 450 kDa PMMA samples with different adsorbed amounts. Thus, the T_g of the B-component was about 33 °C higher than that of the bulk polymer.

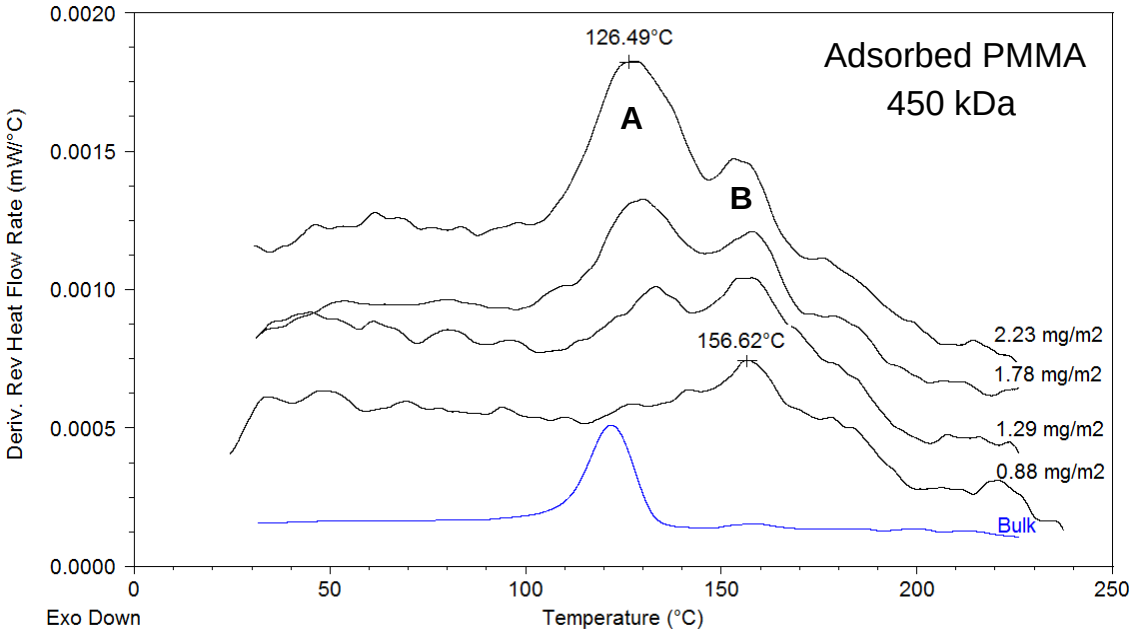

Figure 3. TMDSC thermograms of various adsorbed amounts of high molecular mass PMMA (450 kDa) on silica.

The thermograms of different amounts of the medium molecular mass PMMA (85 kDa) adsorbed on silica are shown in Figure 4. The bulk T_g for this polymer was about 108 ºC. The peak of the transition for the A component increased from that in bulk to 117 +/- 1 ºC (SD), and the position of the B component was about 140 +/- 3 ºC (SD). The T_g for the B-component was about 32 °C above that for the bulk polymer.

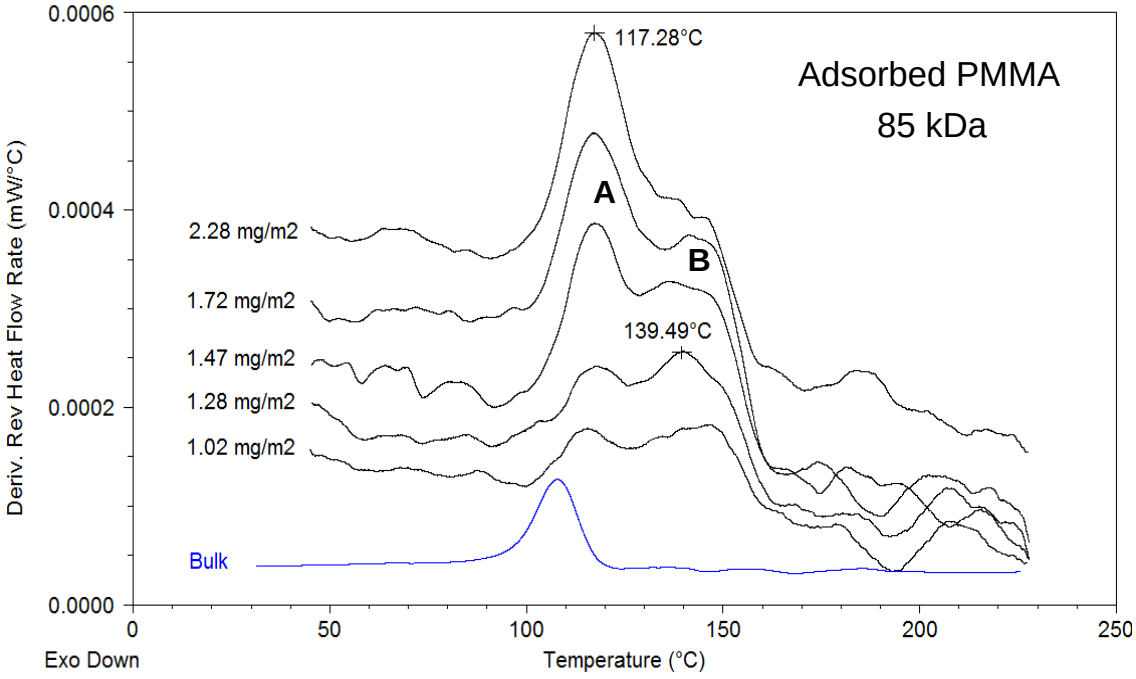

Figure 4. TMDSC thermograms of various adsorbed amounts of medium molecular mass PMMA (85 kDa) on silica.

Thermograms of different amounts of low molecular mass PMMA (32 kDa) adsorbed on silica are shown in Figure 5. The bulk T_g was about 109 ºC. The peak of the transition for the A component increased from that in bulk to 129 +/- 6 ºC (SD) and the position of the B component was about 154 +/- 4 ºC (SD). The T_g for the B-component was 45 °C above that of the bulk polymer. A summary of T_gs for bulk PMMA and absorbed PMMA (including both loosely- and tightly-bound polymers) is shown in Table 1.

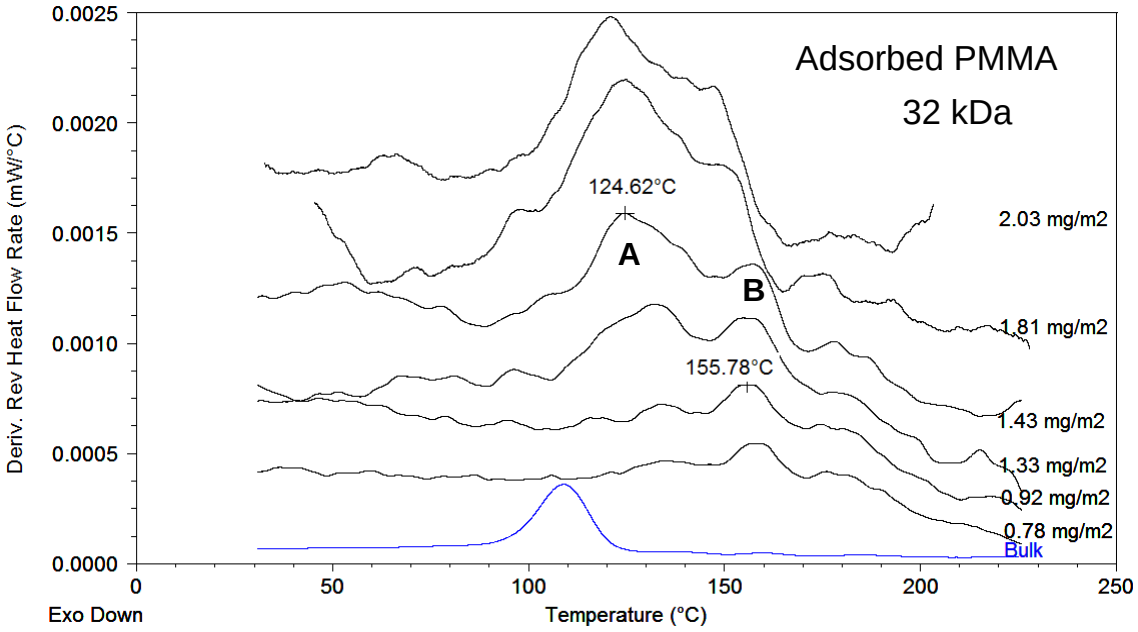

Figure 5. TMDSC thermograms of various adsorbed amounts of low molecular mass PMMA (32 kDa) on silica.

Table 1. Glass Transition Temperature (T_g) of Different Molecular Mass PMMA for Bulk and Surface Adsorbed PMMA on Silica

Molecular Mass (kDa)	Polydispersity	Bulk T_g (ºC)	Adsorbed T_g (ºC) +/- (SD[a])	
			Loosely Bound	Tightly Bound
450	2.6	123	130 +/- 3	156 +/- 2
85	1.6	108	117 +/- 1	140 +/- 3
32	1.5	109	129 +/- 6	154 +/- 4

[a] SD is the standard deviation from all the different adsorbed amounts for each molecular mass.

A plot of the ratio, r, for the areas of the A and B components in the derivative thermograms, was a linear function of the total relative mass of polymer (m'_p), or adsorbed amounts (mg polymer/m^2 silica), as shown in Figure 6. Our studies focused on the region through which the intensities of the two components of the adsorbed polymers

had similar intensities. According to eq. 3, the intercept of the line yields the negative value of the changes in heat capacity ratio, $\Delta C_{pA}/\Delta C_{pB}$, around the T_g and the slope yields $\Delta C_{pA}/(m'_{pB}\ \Delta C_{pB})$. The data were linear with positive slopes. The extrapolation of the linear plot was valid as a negative value since the intercept was negative. Below the critical value of M_b, r was roughly equal to zero, because there was little of component A (loosely bound) in those samples.

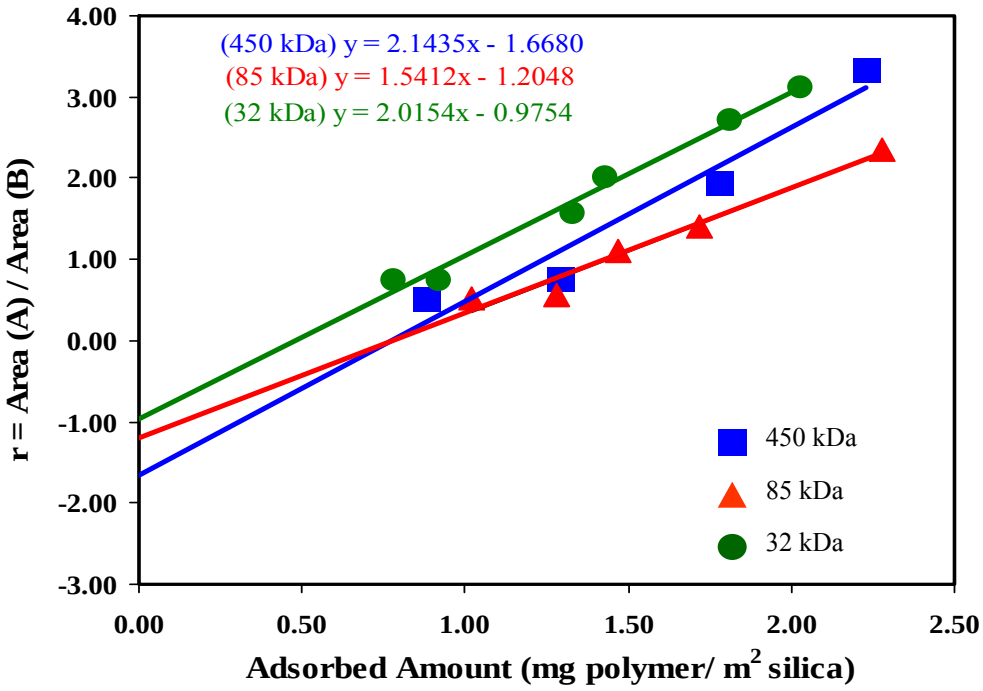

Figure 6. The ratio (r) of the areas under the transitions A and B as a function of the adsorbed amounts (mg polymer/m^2 silica) for three different molecular masses of PMMA.

4. DISCUSSION

High molecular mass PMMA (450 kDa) has a higher T_g for both the bulk (123 ºC) and bulk-like region (loosely bound polymer) (130 ºC) of the adsorbed polymers, as

compared with that of the lower molecular mass polymers. This difference can be explained based on a free volume approach [28]. Low molecular mass polymers have more chain ends per unit volume than the long chains in a high molecular mass. The chain ends have more mobility than the other segments in the chain do, and thus have more free volume. T_g is roughly an inverse of the fraction of the free volume. The more the free volume, the lower the T_g, or vice versa. With this free volume approach, Fox and Flory [29-30] developed an equation to express the relationship between T_g and molecular mass. However, in this molecular mass series, a deviation from the trend arose for the T_g of the medium mass (85 kDa) polymer. Its behavior is comparable with that of the low mass (32 kDa) polymer as shown in Figure 2. In this case, the tacticity may account for this deviation. The low molecular mass polymer had a higher percentage of the syndiotactic segments than that of the medium mass polymer, resulting in a higher T_g for this polymer. For PMMA, the syndiotactic segments pack better than the isotactic ones, creating less free volume and, thereby, increases the T_g [31].

It was also observed that the tightly-bound polymers have a higher T_g than that found in bulk and the loosely-bound region of the same polymer. It should also be noted that in spite of the differences in T_g of the bulk polymers for the 450 and 85 kDa samples, likely due to tacticity, the increase in the T_g for the B-components upon adsorption was about the same in both cases, suggesting that the effect of adsorption was similar. The situation for the 32 kDa PMMA was different in that it had a much larger increase in the B-component upon adsorption. This effect for the low molecular mass polymer was previously observed [32]. In essence, the binding of the polymer on the surface mitigates, to some extent, the influence of the chain ends.

As mentioned earlier, the adsorbed polymers have more restricted motions than the bulk polymers, which result in shifts to higher T_gs. This effect was pronounced for our systems because of hydrogen bonding between the polymer carbonyls and substrate silanols [13-14]. In addition, a broader range of T_g was also found for adsorbed samples which can be estimated from the width at half height of the transition A and B. Nevertheless, the transition width of each component can be clearly defined when the two components have roughly equal intensity as can be found in the samples with the adsorbed amounts roughly about 1.0-1.3 mg/m^2. For bulk, the range of T_g was roughly

about 15 ºC while those of adsorbed sample were 22 ºC for the loosely bound, and 26 ºC for the tightly bound. The broadening of the T_gs for adsorbed samples was due to a loss in the cooperative large-amplitude motions. These motions resulted in an endothermic contribution to the heat capacity [33]. The broadening of the T_g is an important characteristic of a multi-component material, such as an adsorbed polymer.

The amount of the tightly-bound polymer (M_b) and the corresponding effective thicknesses of three different molecular mass PMMA adsorbed on silica are shown in Table 2. PMMA, with a high and medium molecular mass of 450 kDa and 85 kDa, respectively, showed a larger amount of tightly-bound polymer (0.78 mg/ m^2) than that in the 32 kDa (0.48 mg/ m^2) polymer. The corresponding effective thicknesses of 6.5 Å and 4.0 Å, respectively, were calculated using a PMMA bulk density of 1.2 g/cm^3. The thickness of the tightly bound polymer for the high molecular mass PMMA (450 kDa) appeared to be thinner than that previously reported [14]. This discrepancy is due to the different quantitative analysis method used in the choice of assigning baseline which affects the integrated area under the transitions [27]. Nevertheless, our current results do correlate well with the thermograms, as seen in Figure 3-5. When the amount of tightly bound polymer is greater than the M_B, 0.78 mg/m^2 (450 and 85 kDa) and 0.48 mg/m^2 (32 kDa), a transition for loosely bound region is then observed.

Table 2. Ratios of Heat Capacity Changes at T_g ($\Delta C_{pA}/\Delta C_{pB}$), Tightly Bound Amount (M_b) and Corresponding Thickness for PMMAs Adsorbed on Silica

Molecular mass (kDa)	($\Delta C_{pA}/\Delta C_{pB}$) +/- 1 S.D.	Tightly bound amount (M_b) mg PMMA/ m^2 silica +/-1 S.D.[a]	Tightly bound thickness (Å)
450	1.67 +/- 0.49	0.78 +/- 0.25	6.50 +/- 2.08
85	1.20 +/- 0.23	0.78 +/- 0.17	6.50 +/- 1.41
32	0.98 +/- 0.16	0.48 +/- 0.09	4.00 +/- 0.75

[a] SD is the standard deviation from the uncertainties in the slope and intercept.

The bound fractions, based on the ratios of the integrals of the different peaks was calculated from eq. 4 as a function of the amount of adsorbed polymer. Plots of the bound fraction for various adsorbed amounts of polymer in three different molecular mass PMMAs are shown in Figure 7. As expected, the bound fraction in all three decreased relatively smoothly when the adsorbed amounts increased. The smooth curves are for the model based on fixed values of m_B for each system (also from eq. 4). For low molecular mass PMMA (32 kDa), the bound fractions were smaller than those of the high and medium molecular masses. The amount of tightly bound polymer for the high (450 kDa) and the medium (85 kDa) molecular mass were only slightly different when these two bound fractions were overlaid.

Interestingly, FTIR experiments [13] showed no differences in the amount of tightly bound polymer for all three different molecular masses as shown in Figure 7. In addition, the amounts of polymer that were tightly-bound from FTIR were considerably lower than that of TMDSC experiments. This is because the FTIR technique is only sensitive to segments directly bound to the surface via the carbonyls where as the TMDSC technique accounts for many more segments beyond those directly attached [34].

The molecular mass effect observed presumably involves the effect of polymer end groups--the low molecular mass polymer has more chain ends compared with those of higher mass. These free chain ends are more mobile and apparently not strongly binding on the surface [17, 19]. Metin and Blum [17] studied the ^2H NMR data of adsorbed PMA on silica. For an adsorbed amount of 1.5 mg/m^2, they observed the smallest amount of mobile component (corresponding to the loosely-bound component, transition A at the molecular mass of 77 kDa. When the molecular masses were above or below 77 kDa, higher mobility of polymer segments was found. These results correlate well with our data. As shown in Figure 6, for the same adsorbed amount of 1.5 mg/m^2, the 85 kDa PMMA also has the lowest area ratio (r) of the transitions A and B (or the smallest amount of mobile component) while above and below this molecular mass, the larger amount of mobile component were found in both 450 and 32 kDa, respectively.

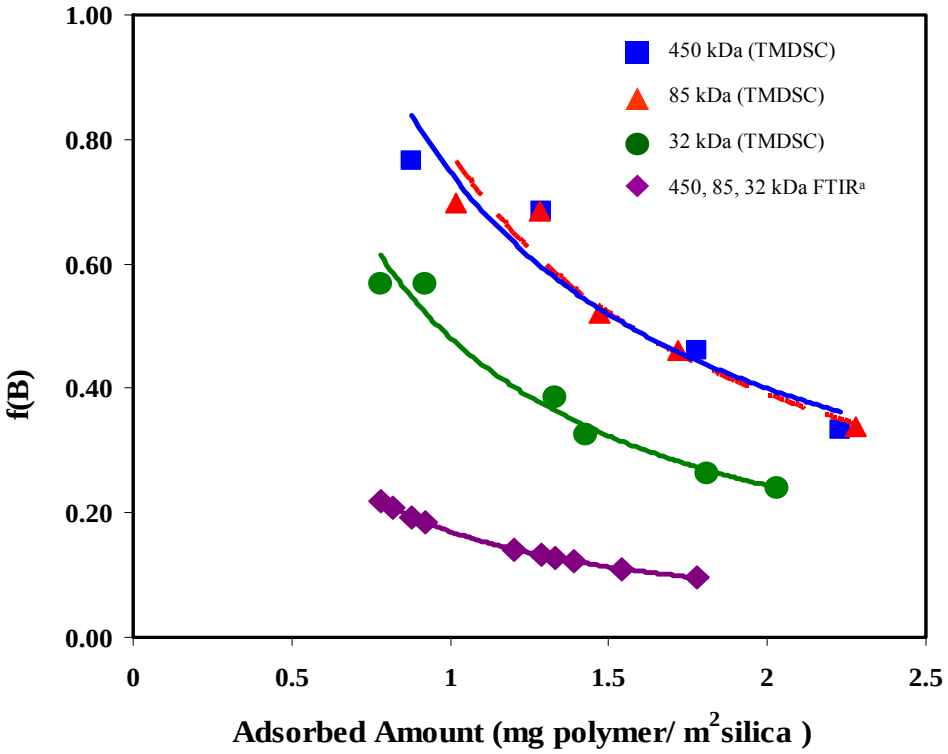

Figure 7. Bound fractions of PMMA on silica as a function of adsorbed amount from TMDSC for the 450 (squares), 85 (triangles), and 32 kDa (circles) and FTIR experiments plotted from ref. 13. The smooth curves are based on a model with a fixed amount of bound material.

Kajiyama *et al.,* who studied surface molecular motion of polystyrene using forced modulation scanning force microscopy (SFM) and lateral force microscopic (LFM). They also observed the molecular mass, M_n, dependence on the adsorption of polystyrene film on a silicon wafer [22]. They reported that, at M_n higher from 40.4 to 1800 kDa, the output voltage was almost constant. Their result indicated that the adsorbed polystyrene on the silicon wafer was molecular mass dependent over a lower range (M_n = 5-26 kDa) and became constant when M_n was greater than 40.4 kDa. There were a few differences such as types of polymer, surfaces and interfacial interactions of the systems; however, the range of molecular mass dependence (M_n for comparison) was agreeable with our data obtained from TMDSC.

To verify the validity of the tightly bound thickness obtained from the TMDSC experiment (based on a two-component model), a comparison was made of the thin layer of a molecular scale with findings from other experiments. Using ellipsometry, Silberzan and L′eger [35] observed approximately 10 Å thick of a molecular precursor-film by spreading poly(dimethylsiloxane) (PDMS) on a silica surface. These two systems are different in some aspects. For instance, different types of polymers with different functional groups were interacting with the surface. One was based on monolayer polymer adsorption from a dilute solution, with hydrogen bonding as a specific interaction between the polymer and the surface. The other was considered to be a multilayer adsorption from polymer melt (no solvent). Nevertheless, a molecular precursor film was in a region of monolayer adsorption, resulting in thickness that appeared to be of the same magnitude as the tightly bound polymers. This comparison revealed the existence of a molecular-scale thin film that was measureable.

On the basis of the model, the change in heat capacity is related to the molecular motion of polymers adsorbed on the surface. The ratios of heat capacity increments $\Delta C_{pA}/\Delta C_{pB}$ at T_g for the three different molecular masses 450, 85 and 32 kDa were roughly about 1.7, 1.2 and 1.0 nm, respectively. These ratios indicated that, at the T_g, the loosely bound polymer had more mobility than the tightly bound polymer (for both the high and the medium molecular mass), whereas there small differences in the mobilities of the loosely and tightly bound polymers were found in the low molecular mass PMMA. This suggests that the heat capacity increment at the T_g depends on the molecular mass.

5. CONCLUSIONS

TMDSC was used to probe the interaction of adsorbed PMMA on the surface of silica. Using a two-component model, with the assumption that the amount bound polymer would remain roughly constant regardless of the amount of polymer adsorbed, the amount of the tightly bound polymer was determined. This amount seemed to be molecular mass dependent. However, the amount of the bound polymer seemed to be

constant when the molecular mass was high. According to our data, the amount of tightly bound PMMA for a high and medium molecular mass of 450 and 85 kDa, respectively, appeared to be the same (about 0.78 mg/ m^2). This amount was larger than that of the lower molecular mass, 32 kDa, which was about 0.48 mg/ m^2. These amounts of tightly bound polymer corresponded to thicknesses of 6.5 Å and 4.0 Å, respectively. The relative mobility between loosely bound and tightly bound polymer was also seen from the ratios of heat capacity increments of $\Delta C_{pA}/\Delta C_{pB}$ at T_g, which were roughly about 1.7, 1.2 and 1.0 for all three different molecular masses of 450, 85 and 32 kDa, respectively. At the T_g, the loosely bound polymer seemed to be somewhat more mobile than the tightly bound polymer of the high and medium molecular masses. For the low molecular mass PMMA, the mobility changes at the T_g, of the loosely-bound and tightly-bound polymers was roughly the same probably due to the effect of the mobile chain ends.

6. ACKNOWLEDGEMENTS

The authors acknowledge the support of the National Science Foundation under grant DMR-01005606, and the Missouri University of Science and Technology for financial support of this research.

7. REFERENCES

1. Reiter, G. *Macromolecules* **1994**, *27*, 3046.
2. Feast W. J.; Munro, H. S., *Polymer Surfaces and Interfaces*; Wiley, NY, 1987.
3. Hobden, J. F.; Jellinek, H. H. G. *J. Polym. Sci* **1953**, 11, 365.
4. Howard, G. J.; McConnell, P. *J. Chem. Phys.* **1967**, 71, 2974.
5. Herd, M. J.; Hopkins, A. J.; Howard, G. J. *J. Polym. Sci* **1971**, 34, 211; *ibid.* **1971** A-2, 9, 841.
6. White, J. L.; Sadakne, G. S. *J. Appl. Polym. Sci.* **1973**, 17, 453.

7. Silberberg, A. *J. Chem. Phys.* **1968**, 48, 2835.
8. Stuart, C. M. A.; Scheutjens, J. M. H. M.; Fleer G. J. *J. Polym. Sci.* **1980**, 18, 559.
9. Roe, R. J. *J. Chem. Phys.* **1974**, 60, 4192.
10. Linden C. V.; Leemput, R. V. *Colloid Interface Sci.* **1978**, 67, 63.
11. Andrade, J. D. *Polymer Surface Dynamics*; Plenum Press: New York, 1988.
12. Porter, C. E.; Blum, F. D. *Macromolecules* **2002**, 35, 7448.
13. Kulkeratiyut, S.; Kulkeratiyut, S.; Blum F. D. *J. Polym. Sci Part B.* **2006**, 44, 2071.
14. Blum, F. D.; Young, E. Y.; Smith, G.; Sitton O. C. *Langmuir* **2006**, 22, 4741.
15. Blum, F. D.; Lin, W. Y.; Porter, C. E. *Colloid Polym. Sci.* **2003**, 281, 197.
16. Lin, W. Y.; Blum, F. D. *Macromolecules* **1997**, 18, 5331.
17. Metin, B.; Blum, F. D. *J. Chem. Phys.* **2006**, 125, 054707/054701-054709.
18. Thambo, G.; Miller, W. G. *Macromolecules* **1990**, 23, 4397.
19. Damme, H. S.; van Hogt, A. H.; Feijen, J. *J. Colloid Interface Sci.* **1985**, 106, 289.
20. Maivald, P.; Butt, H. J.; Gould, S. A. C.; Prater, C. B.; Drake, B.; Gurley, J. A.; Elings, V. B.; Hansma, P. K. *Nanotechnology* **1991**, 2, 103.
21. Overney, R. M.; Meyer, E.; Frommer, J.; Guntherodt, H.-J.; Fujihira, M.; Takano, H.; Gotoh, Y. *Langmuir* **1994**, 10, 1281.
22. Kajiyama, T., Tanaka, K., Takahara, A. *Macromolecules* **1997**, 30, 280.
23. Lee, W. K.; Yoon, J. S.; Tanaka, K.; Satomi, N.; Jiang, X.; Takahara, A.; Ha, C. S.; Kajiyama, T. *Polymer Bulletin* **1997**, 39, 369.
24. O'Reilly, J. M. *J. Appl. Phys.* **1977**, 48, 4043.
25. Pyda, M.; Wunderlich, B. *Macromolecules* **1999**, 32, 2044.
26. Pyda, M. *Macromolecules* **2002**, 35, 4009.
27. Hetayothin, B.; Blum, F. D. *Polymer Preprints,* **2010,** 51(1), 480.
28. Painter, P. C.; Coleman, M. M. *Fundamentals of Polymer Science 2nd ed*; CRC Press: Boca Raton, 1997.
29. Fox, T. G.; Flory, P. J. *J. Appl. Phys.* **1950**, 21, 581.
30. Fox, T. G.; Flory, P. J. *J. Polym. Sci.* **1954**, 14, 315.
31. Grohens, Y.; Carriere, P.; Hamon, L.; Holl, Y.; Schultz, J. *Symposium FF Interfaces, Adhesion and Processing in Polymer Systems MRS Proceedings* **2000,** *629,* FF1.7

32. Kabomo, M. T.; Blum, F. D.; Kulkeratiyut, S.; Kulkeratiyut, S.; Krisanangkura, P. *J. Polym. Sci.: B: Polym. Phys.*, **2008**, *46*, 649.
33. Wunderlich, B. *Thermal analysis of polymeric materials;* Springer: New York, 2005.
34. Blum, F. D.; Krisanangkura, P. *Thermochemica. acta.* ***2009,*** *492*, 55.
35. Silberzan, P.; L′eger, L. *Macromolecules* **1992**, 25, 1267.

2. COMPARISON OF HYDROGEN-BONDED POLYMERS ON SILICA USING TEMPERATURE-MODULATED DIFFERENTIAL SCANNING CALORIMETRY

Boonta Hetayothin, [1] and Frank D. Blum[1,2]*

1. Department of Chemistry and Materials Research Center, Missouri University of Science and Technology, Rolla, Missouri 65409-0010, USA
2. Department of Chemistry, Oklahoma State University, Stillwater, Oklahoma74078, USA

ABSTRACT

The behavior of three amorphous polymers, namely poly(methyl methacrylate) (PMMA), poly(vinyl acetate) (PVAc), and poly(methyl acrylate) (PMA) absorbed (hydrogen bonded) on silica were studied using temperature-modulated differential scanning calorimetry (TMDSC). A two-component model, based on loosely-bound polymer with a glass transition temperature (T_g) similar to that of bulk, and a tightly-bound polymer (with a T_g higher than that of the loosely-bound polymer) was used to interpret the thermograms. Although, the thermograms of similarly structured (PMMA, PVAc, and PMA) were different, the amounts of tightly-bound polymer on silica did not differ much (approximately 0.75 mg/m^2). The ratio of heat capacity increments of loosely-bound and tightly-bound polymer ($\Delta C_{pA}/\Delta C_{pB}$) around the T_g indicated the relative mobility of the two components. These ratios were also found to be similar, approximately 1.8. These results imply that PMMA, PVAc, and PMA behave similarly at the polymer-silica interface.

* Author to whom correspondence should be addressed: Frank D. Blum

(fblum@okstate.edu)

1. INTRODUCTION

The interactions between polymers adsorbed onto surfaces are important in many applications such as adhesion, lubrication, surface protection, stabilization, controlled flocculation of colloidal dispersions, and even in biological processes such as membrane-polymer interactions and medicinal applications [1-8]. The physical properties of adsorbed polymers are typically more complex than those in bulk polymers since they involve multi-components, including the polymers and surfaces. Understanding the behavior of adsorbed polymers on solid substrates is essential for improving their properties in applications, and are beneficial in designing materials for specific uses.

Adsorption of polymers from solution to a surface may occur when there is an attractive polymer-surface interaction that overcomes the entropy loss associated with the adsorption [9]. Hence, variables such as the nature of the polymer, surface, or solvent may affect the adsorption process. For flexible polymers, a wide range of shapes or conformations is a result of a significant internal degree of freedom from rotation about single bonds [8]. However, polymers with bulky pendant groups may hinder the rotation and make some conformations unfavorable. In addition, when polymers are adsorbed on the surface, the adsorption may cause changes in their shapes [10]. Conformations of polymers at an interface, as first proposed by Jenkel and Rumbach, [11] were composed of three types of sub-chains, so-called trains, loops, and tails (shown in Figure 1).

Many of the chemical and mechanical properties of polymers adsorbed on surfaces (e.g., adhesion, lubricity, wearability, wettability, dispersibility, and biocompatibility) are determined by their interfacial structures, such as surface conformation [12-13], orientation of surface functional groups, coverage, and adsorbed amount (or layer thickness) [9, 14]. In several cases, these interfacial structures were revealed through the study of molecular motion at the interface [12, 15]. Several studies found that polymer molecules and segments at surfaces or interfacial regions exhibit motions and relaxations that are not be identical to those observed in bulk [15-16]. Nevertheless, these interfacial polymers have some mobility and can rearrange or reorient at the interfaces in an attempt to minimize the surface free energy with the neighboring

phase [15]. Interfacial molecular motions can be probed by various techniques, including NMR [17-19], ESR [20], Fluorescence [21-23], force modulation scanning force microscopy (force modulation SFM) [24-26], lateral force microscopy (LFM) [26-27], contact angle measurements [28], and thermal analysis [29-30], to name just a few. Among these techniques, thermal analysis is perhaps the quickest and simplest technique for obtaining parameters such as glass transition temperatures (T_g) and heat capacity involving polymer mobility. On the other hand, it gives only very limited information on the molecular nature of the polymer.

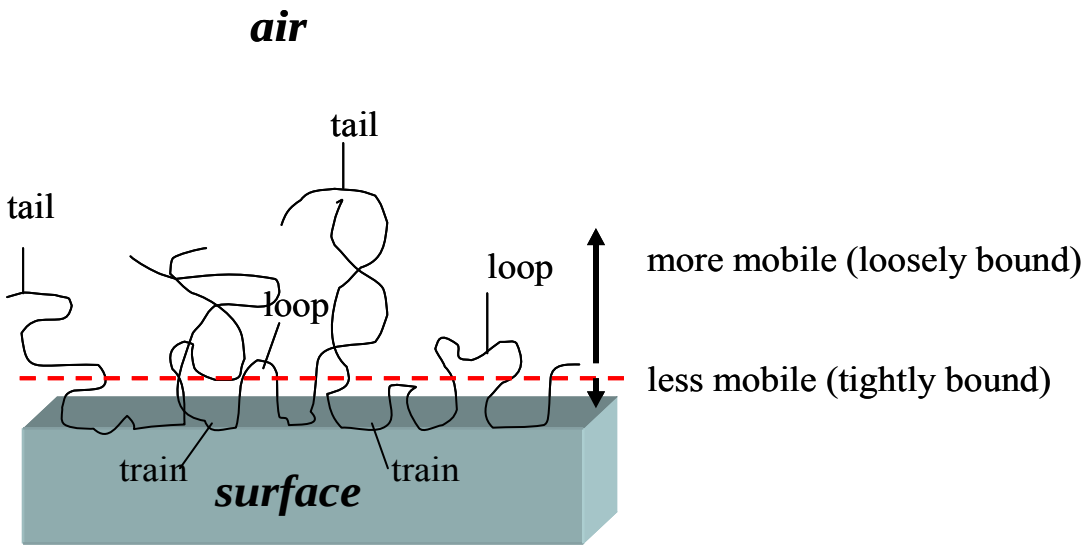

Figure 1. Simplified configurations of a surface-bound polymer.

Homopolymers, such as poly(methyl methacrylate) (PMMA), poly(vinyl acetate) (PVAc), and poly(methyl acrylate) (PMA) have similar structures. PMMA is known for its uses in glass windows and automotive applications; however, it is also widely used in materials for biomedical implants, lenses, fiber optics, micro lithography, barriers and membranes [12]. PVAc and PMA are used in adhesives, paints and coatings [31]. In most of these applications, an understanding the surface structures of these homopolymers is very important. Despite the similarity in their structures, their T_gs are quite different.

PMMA is a hard plastic at room temperature, PVAc is a little softer, and PMA is more rubber-like.

In this paper, we report the use of the temperature-modulated differential scanning calorimetry (TMDSC) to compare the behavior of three polymers. This study builds on previous studies of adsorbed PMMA on silica using the same technique [30, 32]. A two-state model, based on loosely-bound polymer (T_g similar to bulk) and more tightly-bound polymer (T_g higher than bulk) was used to interpret the thermograms (see Figure 1). A direct comparison with consistent data treatment on PMMA, PVAc, and PMA allows addition insight on the generality of the behavior previously reported for PMMA [30, 32].

2. EXPERIMENTAL

PMMA with molecular mass (M_w) of 450 kDa and polydispersity (PD) of 2.6 (Aldrich Chemical Co., Milwaukee, WI) and PVAc with M_w of 240 kDa and PD of 2.0 (Scientific Polymer Products, Inc., Ontario, NY) were used as received. PMA with M_w of 130 kDa and PD of 1.3 was prepared in our laboratory using atom transfer radical polymerization (ATRP). The molecular masses were determined using gel permeation chromatography with a Dawn EOS laser light scattering instrument (LLS) and an Optilab refractive index detector (Wyatt Technology, Santa Barbara, CA). The samples were dried in an oven at 60 ºC for 24 h before use. Cab-O-Sil M-5P silica, with a specific surface area of 200 m^2/g (Cabot Corporation, Tuscola, IL), was used as the substrate. The silica was dried in an oven at 400 ºC for 24 h. before use.

Solutions of various concentrations of PMMA, PVAc, and PMA (in a range of 5-80 mg/mL) in toluene (10 mL) were prepared. 300 mg of silica were added to the polymer solution in test tubes. The test tubes, with mixtures of silica and polymer solutions, were put in a mechanical shaker for 48 h and then centrifuged at 2500 rpm for 1 h. The supernatant liquids were removed, and the adsorbed polymers were washed three times with toluene (7 mL) to remove the excess polymer. The toluene from the last wash was not discarded; instead, it was removed by passing air (using a glass pipette at a

low flow rate) through the adsorbed polymer-silica mixture, as it was being agitated. Then, the absorbed samples were dried in a vacuum oven under 30 mm Hg at 60 ºC for 24 h.

Thermogravimetric analysis (TGA) measurements were made using a Hi-Res TGA-2950 (TA Instruments, New Castle, DE) to determine the amount of absorbed polymer at the surface of the silica. Samples of approximately 8-12 mg were placed in a platinum pan and heated from 25 to 750 ºC, with a heating rate of 20 ºC/min in air. The mass loss was followed as a function of time (temperature). The amount of polymer adsorbed was taken to be the mass loss as the silica was inert at these temperatures.

The thermal behavior in the glass transition region was measured with a TA Instruments model 2920 MDSC (TA Instruments, New Castle, DE). The sample pans were referenced against the empty pans and the cell purged with a nitrogen gas at a flow rate of 50 mL/ min. For PMMA, the samples were held at 0 ºC for 5 min, heated to 280 ºC at a rate of 2.5 ºC/min with a modulation amplitude of +/- 1.0 ºC, and a period of 60 s, held for 3 min, cooled to 0 ºC at the same rate, and then held at 0 ºC for 3 min in order to minimize the effects of previous thermal history. After the first heating and cooling scan, the second heating scan was applied with the same conditions as the first heating scan. For PVAc and PMA, the same procedure was applied with adjustment of the temperature range to -40 to 200 ºC and -40 to 150 ºC, respectively. The T_g was determined using the second heating scan. Results are shown as differential reversing heat flow (dQ_{rev}/dT) vs temperature. A 15 ºC smoothing was applied to the thermograms to reduce the high-frequency noise and highlight the transition, without significantly distorting the thermograms.

A perpendicular drop method (TA Universal Analysis V4.2E software) was used to estimate the area under the transitions in the ($dQ_{reversing}/dT$) plots. In this method, a straight baseline was chosen over a range of two transition temperatures. The two overlapping transitions were separated by a vertical line that was perpendicular to the baseline at the temperature where the first transition (loosely bound) ended, and the second transition (tightly bound) began. The areas under those two transitions were integrated. The T_g of each transition was taken at the peak of the derivative curve [33].

2.1. Model

The two-state model was previously applied to the thermal analysis of adsorbed PMMA [30, 32] and its essence repeated here. The model was based on loosely-bound polymer (component A, T_g similar to, but not necessarily equal to that of bulk) and tightly-bound polymer (component B, T_g higher than that of the loosely-bound polymer).

A normalized polymer mass, m'_p, was defined as the total mass of adsorbed polymer (from TGA) divided by the mass of silica used, which is the sum of the masses for the two components, or

$$m'_p = m'_{pA} + m'_{pB} \quad (1)$$

where m'_{pA} is the normalized mass of loosely-bound polymer and m'_{pB} is the normalized mass of tightly-bound polymer.

The ratio of the heat flow changes of components A and B, given by r, is related to the ratios of the heat capacities of the components, or

$$r = \Delta Q_A / \Delta Q_B = m'_{pA} \Delta C_{pA} / (m'_{pB} \Delta C_{pB}) \quad (2)$$

where the ΔQs represent the heat flows and the ΔC_ps represent the changes in heat capacity in the glass transition region.

In effect, the ratio, r, is the ratio of the area under the two transitions in the thermograms. From equations (1) and (2), a linear equation can be made, or

$$\begin{aligned} r &= (m'_p - m'_{pB}) \Delta C_{pA} / (m'_{pB} \Delta C_{pB}) \\ &= [\Delta C_{pA} / (m'_{pB} \Delta C_{pB})] m'_p - \Delta C_{pA} / \Delta C_{pB} \end{aligned} \quad (3)$$

This equation suggests that r should be linear function m'_p which can also be converted to the adsorbed amount (mg polymer/m^2 silica). As noted above, m'_p, was defined as the total mass of adsorbed polymer (from TGA), divided by the mass of silica used. Therefore, one could calculate the adsorbed amount of the polymer on the silica from m'_p, if the specific surface area of silica was known (in this case, 200 m^2/g). As a result, m'_p could be easily converted to the adsorbed amount.

In a previous study [30, 32], the polymer behavior at the interface was defined in terms of a bound fraction, f_B, which was taken as the ratio of the mass of bound polymer at the interface to the total amount of polymer. This can be expressed as a function of the experimental observable, r, as:

$$f_B = m'_{pB}/m'_p = m_{pB}/m_p = 1/(1 + r\Delta C_{pB}/\Delta C_{pA}) \quad (4)$$

The fraction of bound polymer, f_B, and the ratio of the ΔCp's can be estimated from the model, using the value of m'_{pB} obtained from the intercept, divided by the slope of the linear regression.

3. RESULTS

The bulk T_gs of the PMMA, PVAc, and PMA, were different as shown in Figure 2. Among these three homopolymers, PMA has a lowest T_g of about 19 ºC while PVAc has a higher T_g of about 43 ºC and PMMA has the highest T_g of about 122 ºC.

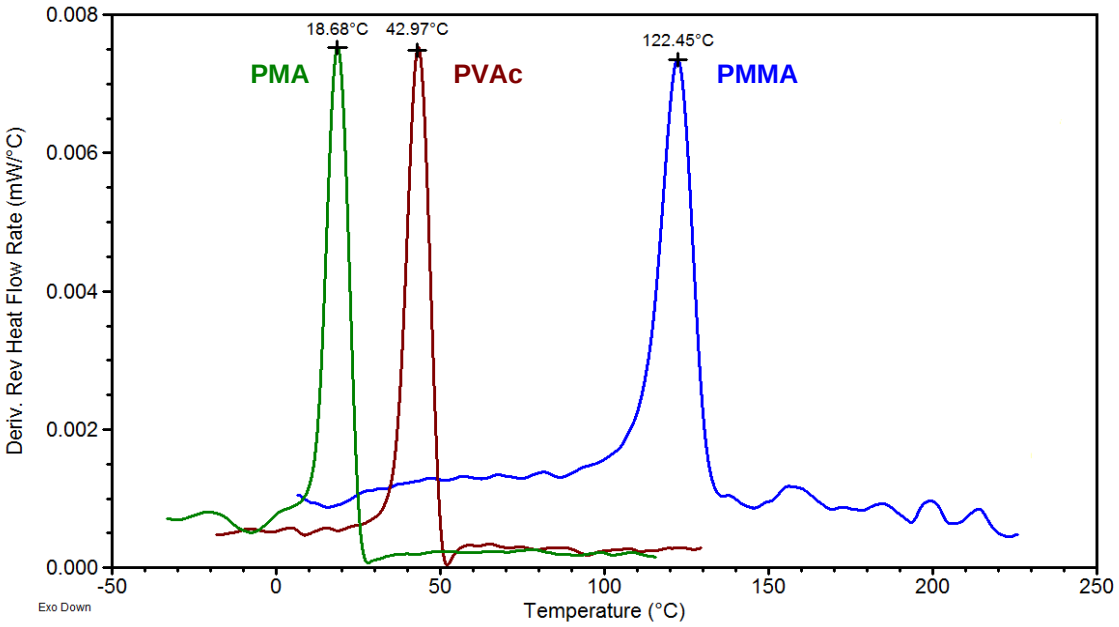

Figure 2. TMDSC of bulk PMMA, PVAc, and PMA.

The thermograms of different amounts of PMMA adsorbed on silica are shown in Figure 3. The vertical scales in the thermograms were shifted for comparison. Bulk

PMMA has a T_g of about 122 ºC (at 2.5 ºC/min). The thermograms of the adsorbed polymers showed two distinct peaks for the loosely-bound component (A) and the tightly-bound component (B). Transition A was shifted slightly to higher temperature than the bulk polymer, to 130 +/- 3 ºC (SD), and the position of the B component was about 156 +/- 2 ºC (SD). The standard deviation was calculated from all the PMMA samples with different adsorbed amounts. The relative area under transition A increased as the adsorbed amount increased, while that of transition B remained roughly constant.

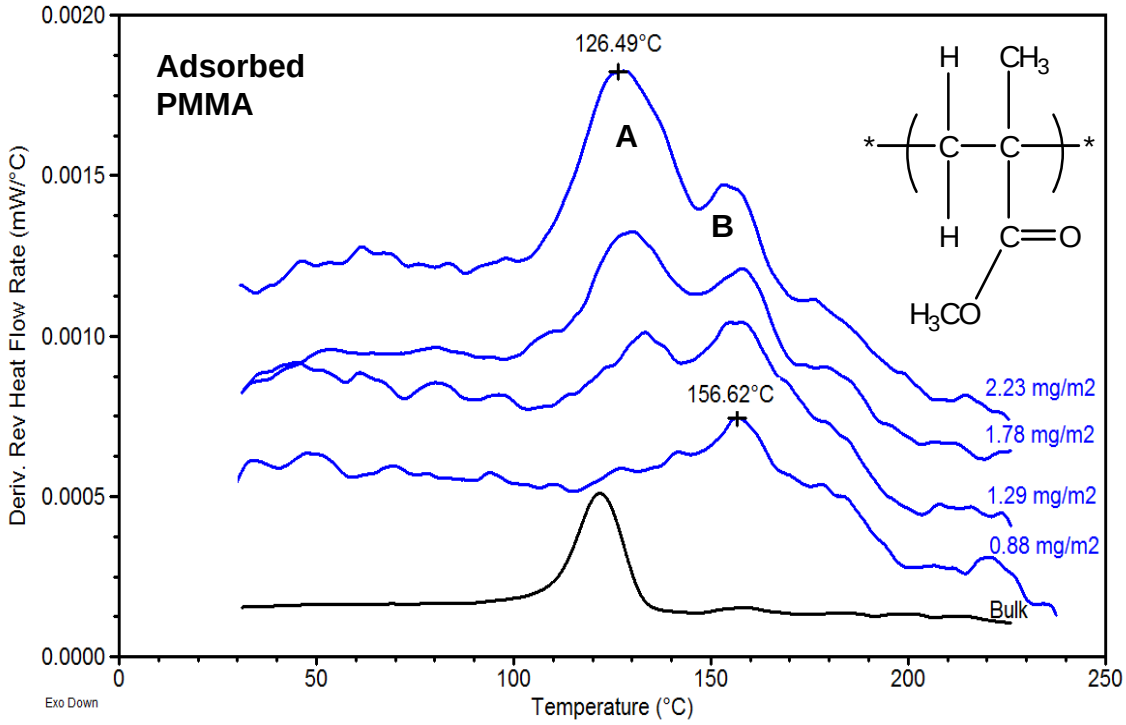

Figure 3. TMDSC thermograms of various adsorbed amounts of PMMA on silica.

Thermograms of different amounts of PVAc adsorbed on silica are shown in Figure 4. The bulk T_g was about 43 ºC (at 2.5 ºC/min). Unlike PMMA, the peak of the transition for the A component of PVAc seemed to be about the same as that of bulk 44 ºC +/- 1 ºC (SD) and the position of the B component shifted to higher temperature than

that of the bulk polymer, about 68 +/- 2 ºC (SD). Similar to PMMA, the intensity of the A component increased while the B component stayed about the same with increasing adsorbed amount. The transitions for absorbed PVAc (A and B) were also not as separated as for adsorbed PMMA.

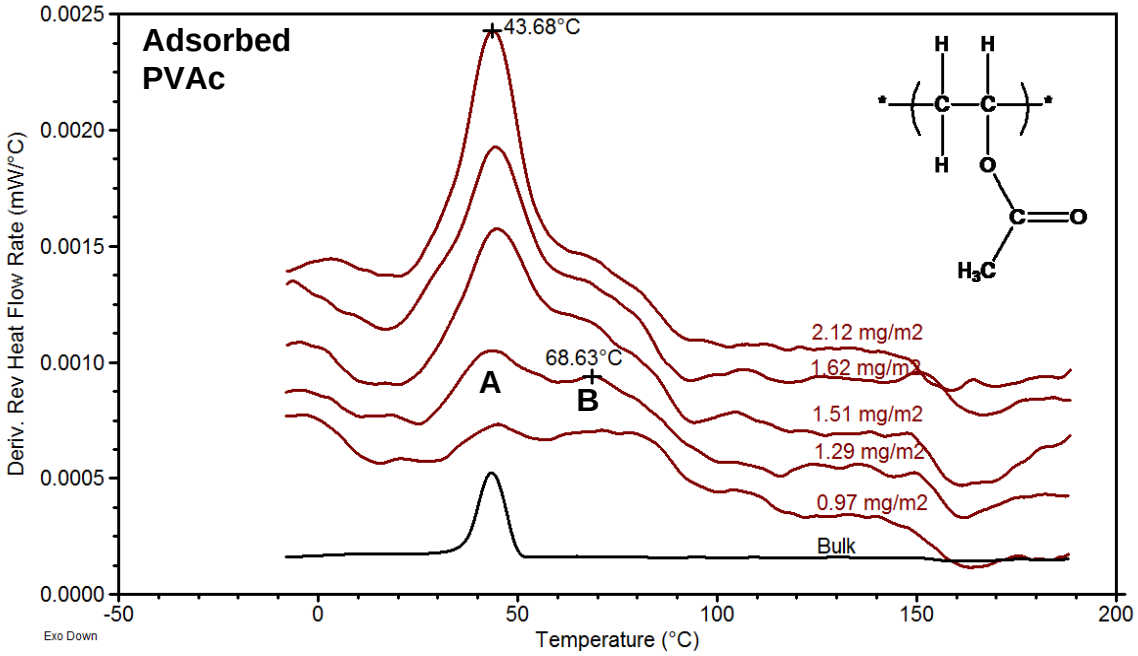

Figure 4. TMDSC thermograms of various adsorbed amounts of PVAc on silica.

Thermograms of different amounts of PMA adsorbed on silica are shown in Figure 5. The bulk T_g was about 19 ºC (at 2.5 ºC/min). The peak of the A transition was close to that of bulk, about 20 +/- 2 ºC (SD), and the position of the B component had shifted to higher temperature than that of bulk; however, an attempt was made in order to identify the T_g of this relatively broad transition of about 55 +/- 2 ºC (SD) ºC. The behavior of PMA was similar to the other polymers except that the two transitions were even less well resolved as previously noted [19]. Summations of T_gs for bulk and adsorbed PMMA, PVAc, and PMA (including both loosely-and tightly-bound polymers) are also shown in Table 1.

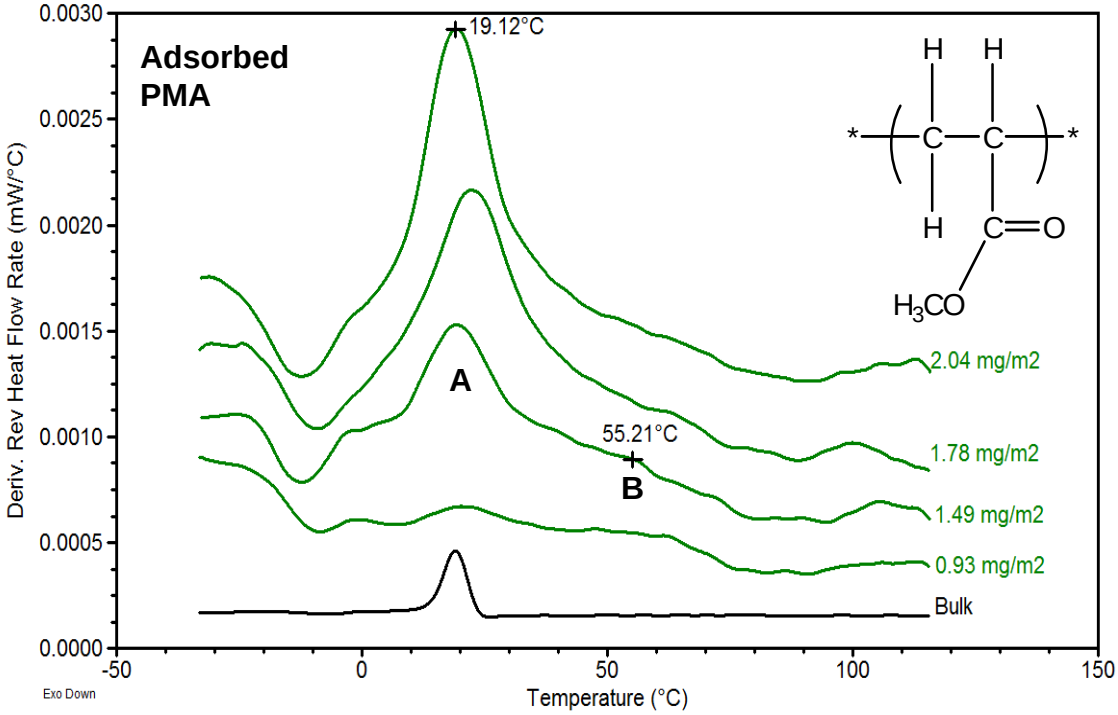

Figure 5. TMDSC thermograms of various adsorbed amounts of PMA on silica.

Table 1. Comparison of T_gs of PMMA, PVAc, and PMA for Bulk and Adsorbed Polymers on Silica

Polymers	Bulk T_g (ºC)	Adsorbed T_g (ºC) +/- (SD)[a]	
		Loosely Bound	Tightly Bound
PMMA	122	130 +/- 3	156 +/- 2
PVAc	43	44 +/- 1	68 +/- 2
PMA	19	20 +/- 2	55 +/- 2

[a] The standard deviations were calculated from all samples with different adsorbed amounts for each polymer.

As shown in Figure 6, a plot of the ratios (r) for the areas under A and B transitions, is a linear function of the total relative mass of polymer (m'_p), or adsorbed amount (mg polymer/ m^2 silica), An adsorbed amount in a range of 0.80-2.40 mg

polymer/m^2 silica was used where the r value varied significantly. The three linear plots for PMMA, PVAc, and PMA overlapped with similar values of the intercepts and slopes. As described in eq. 3, the intercept (negative value) of the line yields the ratio of the heat capacity increments, $\Delta C_{pA}/\Delta C_{pB}$, and the positive slope yields $\Delta C_{pA}/(m'_{pB}\ \Delta C_{pB})$. Therefore, the amount of tightly-bound polymer can be readily obtained from a linear regression. It is difficult to make measurements well below M_B, but consistent with earlier studies [30, 32] the r values approaching M_B appear to go towards zero.

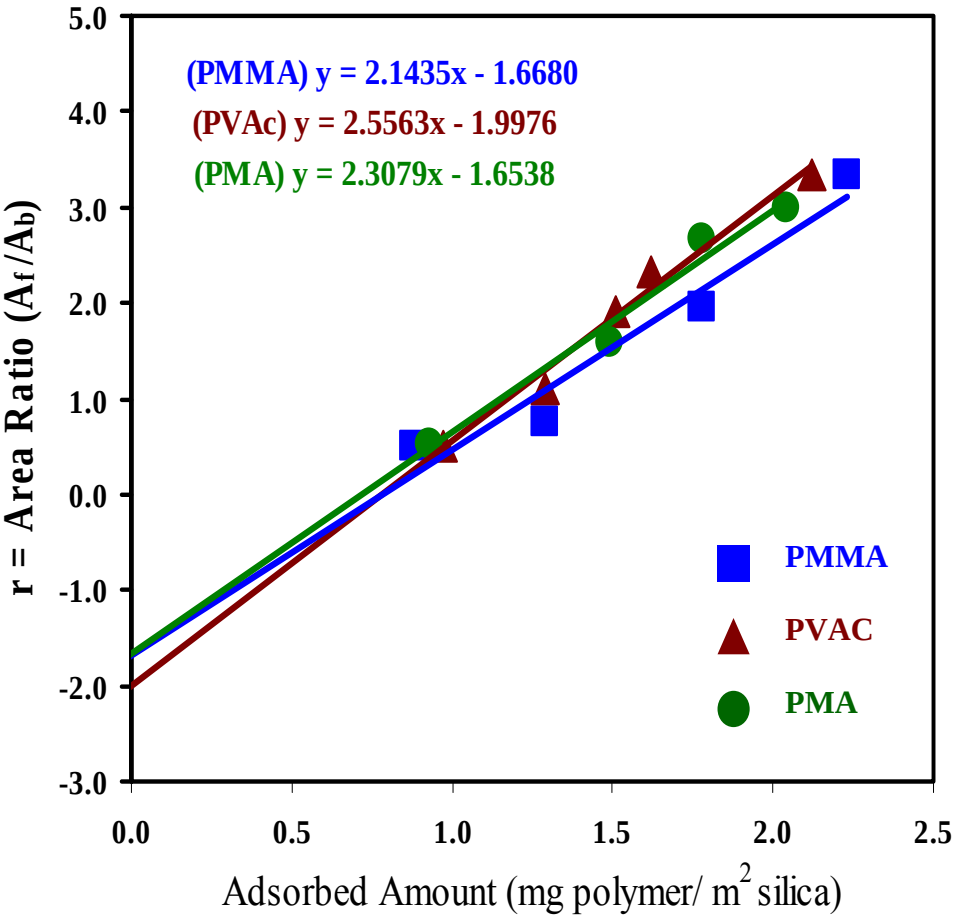

Figure 6. Plots of ratios (r) of the areas under the A and B transitions, as a function of the adsorbed amount (mg polymer/m^2 silica) for PMMA, PVAc, and PMA.

4. DISCUSSION

In these studies, polymers were chosen to be above 100,000 kDa so that the bulk polymers would be in the relatively mass independent regime for the T_gs [34, 35]. The bulk T_gs of the three PMMA, PVAc, and PMA, were different. The different polymers represent rather different behavior for similar structures.

Two thermal transitions of adsorbed PMMA, PVAc, and PMA on silica were observed. The tightly-bound transitions of these adsorbed polymers have higher T_gs than those of bulk. This elevated T_gs has been reported in several studies where the adsorption of polymers onto an attractive substrate resulted in a higher and broader T_g [23, 29, 30, 32]. Such an attraction can come from a specific interaction, such as hydrogen bonding between the polymer and a solid substrate. The broadening of the T_g is an important characteristic of a multi-component material, such as adsorbed polymer, and is due to a loss in the cooperative large-amplitude motions. [36].

The amount of tightly-bound polymer (M_B) and the corresponding thicknesses (using the bulk densities) of these three different polymers adsorbed on silica are calculated as shown in Table 2. Interestingly, the amounts of tightly-bound polymer of these three homopolymers were only slightly different. PMMA and PVAc contained amounts of tightly-bound polymer of about 0.78 +/- 0.25 and 0.78 +/- 0.12 mg/ m^2, respectively. These amounts corresponded to equivalent thicknesses of 6.50 +/- 2.08 Å and 6.50 +/- 1.00 Å, respectively. The amount of tightly-bound polymer for PMA was about 0.72 +/- 0.16 mg/m^2, corresponding to a thickness of 6.00 +/- 1.33 Å.

The bound fractions, based on fixed amounts of bound polymer, were calculated from eq. 4. Plots of the bound fractions for various adsorbed amounts of the three homopolymers are shown in Figure 7. It is apparent that the bound fractions in all three decreased relatively smoothly when the adsorbed amounts increased. For PMMA and PVAc, the bound fractions appeared to be only slightly different when the two fitting curves were compared. In addition, the bound fractions of PMA were only a little smaller than those for PMMA and PVAc. These results support the presumption that adsorption

of similar structures of homopolymers on silica surfaces resulting in similar interfacial structures.

Table 2. Values of the Heat Capacity Ratio ($\Delta C_{pA}/\Delta C_{pB}$), Tightly Bound Amount (M_B) and Effective Thickness for PMMA, PVAc, and PMA Adsorbed on Silica

Adsorbed Polymers	$\Delta C_{pA}/\Delta C_{pB}$ +/-1 S.D.	M_B (mg polymer/m^2 silica) +/-1 S.D.[a]	Effective thickness (Å)
PMMA	1.67 +/- 0.49	0.78 +/- 0.25	6.50 +/- 2.08
PVAc	2.00 +/- 0.27	0.78 +/- 0.12	6.50 +/- 1.00
PMA	1.65 +/- 0.34	0.72+/- 0.16	6.00 +/- 1.33

[a] SD is the standard deviation from the uncertainties in the slope and intercept.

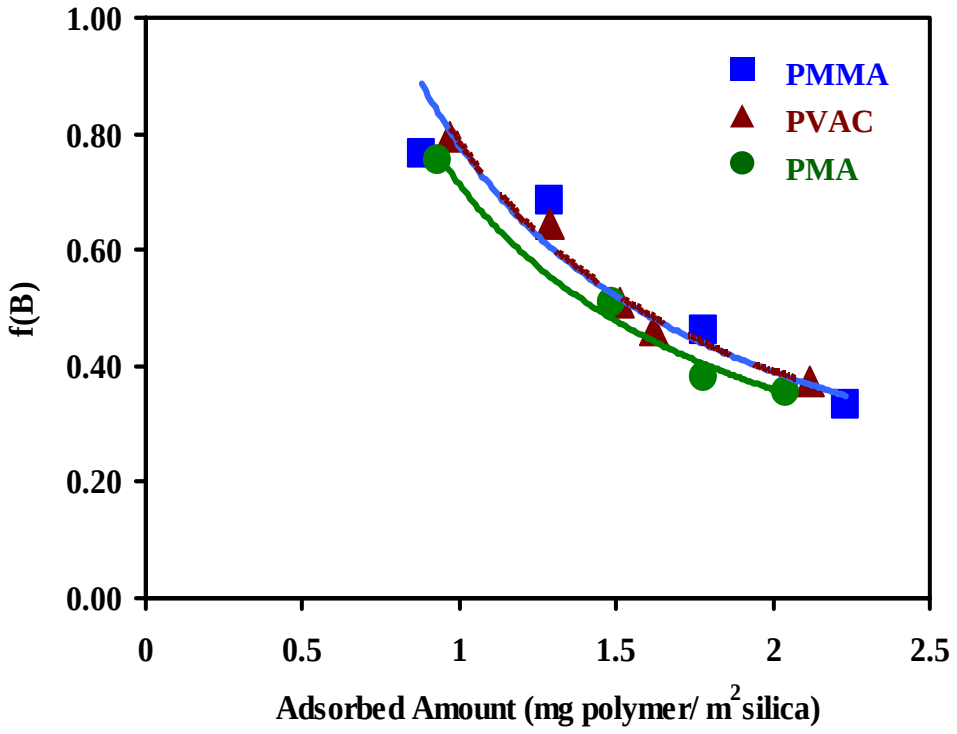

Figure 7. Bound fractions of PMMA, PVAc and PMA on silica as a function of the adsorbed amounts. The smooth curves are based on a constant M_B for each polymer.

A number of studies have compared the adsorption of these homopolymers (PMMA, PVAc, and PMA) on different kinds of surfaces having the common specific interaction via hydrogen bonding. Those observations appear to correlate and agree with our data. Kawaguchi et al. [37] have studied film layers of PMA and PVAc at the air/water interface using ellipsometry. The results from ellipsometric measurements showed that there was no difference between the PMA and PVAc films adsorbed at the air/water interface. Wang and co-workers [12] reported the polymer/air interfacial structure of spin coated PMMA and PMA on fused silica using sum frequency generation (SFG) vibrational spectroscopy. They found that the surface structures of PMMA and PMA are quite similar, with the ester methyl groups dominating on both surfaces.

Backman and Lindberg [38] described the interaction of wood with commercial PVAc glue and PMMA using dynamic mechanical thermal analysis (DMTA). In their work, the authors observed that both PMMA and PVAc have low interaction with wood and concluded that the similar behavior of PMMA and PVAc interaction with wood was a result of their similar chemical structure.

The molecular motion of polymers adsorbed on a surface can be linked to a change in heat capacity (ΔC_p) at T_g [30, 32, 33]. The ratios of the change in heat capacity ($\Delta C_{pA}/\Delta C_{pB}$) at the T_gs (estimated from the negative intercepts for the three homopolymers) were found to be 1.7+/-0.49, 2.0+/-0.27 and 1.7+/-0.34, respectively. Ratios greater than one suggest that the change in C_p at the T_g was greater for the bulk polymer than the adsorbed polymer. Above the T_g, the ΔCp ratio would be dominated by the C_ps of the rubbery polymer. The more limited mobility of the adsorbed segments, has been shown, for example, from NMR studies [17-19].

The ΔC_ps for the bulk polymers were reported in the literature as 0.30, 0.47 and 0.49 J/g·K^{-1} for PMMA, PVAc and PMA, respectively [39]. Wunderlich et al. concluded that the heat capacity change at the T_g was almost constant when the C_p at the T_g was normalized with the bead size (number of beads) for the amorphous polymer chain, regardless of the amorphous polymer types [40-41]. The "bead" here refers to a model of a polymer chain as a string of beads, with a bead being the smallest chain unit that is taken as rigid, but capable of rotation. Roland and co-workers normalized the aforementioned change in the heat capacity of PMMA and PVAc with the number of

beads and found that the normalized heat capacity increments of PMMA and PVAc were very close (about 0.10 and 0.12 $J/g \cdot K^{-1}$, respectively) [39]. PMA was omitted in their study, due to uncertainty regarding the definition of a bead for the acrylate structure. Presumably, the normalized heat capacity increments for the bulk regions of all three homopolymers were similar. Hence, a slight difference in the heat capacity increment ratios implied similar heat capacity increments of the tightly-bound regions of these three homopolymers.

5. CONCLUSIONS

For the three homopolymers studied, TMDSC allowed an estimation of the amount of bound polymer and ratio of heat capacity changes at the T_g for the bound polymers. The amount of tightly-bound polymer was determined by using a two-component model, with the assumption that bound polymer would remain roughly constant regardless of the amount of polymer adsorbed. The similar structures of PMMA, PVAc, and PMA seemed to yield similar amounts of tightly-bound polymer (approximately 0.78-0.72 mg/m^2). The relative mobility between loosely-bound and tightly-bound polymers was also seen from the ratios of heat capacity increments of $\Delta C_{pA}/\Delta C_{pB}$ at T_g, which were roughly about 1.7, 2.0, and 1.7 for PMMA, PVAc, and PMA, respectively. The slight difference in the heat capacity increment ratios indicated similar relative mobility for all three polymers. Regarding the similarity of the amounts of the tightly-bound polymers and that of the heat capacity increment ratios, these results suggested that PMMA, PVAc, and PMA, may have similar interfacial structures at the polymer-silica interface.

6. ACKNOWLEDGEMENTS

The authors acknowledge the support of the National Science Foundation under grant DMR-1005606, and the Missouri University of Science and Technology and the

Oklahoma State University for financial support of this research. The authors thank Dr. Suriyaphongse Kulkeratiyut and Dr. Suntree Kulkeratiyut for PMMA thermograms. The authors thank Dr. Mani Nair and Xiaoming Cheng for their help on ATRP reaction.

7. REFERENCES

1. Feast W. J.; Munro, H. S., *Polymer Surfaces and Interfaces*; Wiley, NY, 1987.
2. Wicks, Z. W.; Jones, F. N.; Pappas, S. P.; Wicks, D. A. *Organics Coatings Science and Technology 3rd edn*; Wiley Interscience, New Jersey, 2007.
3. Reiter, G. *Macromolecules* **1994**, *27*, 3046.
4. Moddel, M.; Bachmann, M.; Janke, W. *J. Phys. Chem. B*, **2009**, *113*, 3314.
5. Kajiyama, T., Tanaka, K., Takahara, A. *Macromolecules* **1997**, *30*, 280.
6. Soga, I, *J. Coat. Technol.* **2003**, *75* (938), 53.
7. Dan, N. *Langmuir* **2000,** *16,* 4045.
8. Fleer, G. J.; Cohen Stuart, M. A.; Scheutjens, J. M. H. M.; Cosgrove, T.; Vincent, B. *Polymers at Interfaces*; Chapman and Hall: London, U.K., 1993.
9. Ka1lrot, N., Linse, P. *Macromolecules* **2007**, *40*, 4669.
10. Gray, J. J. *Curr. Opin. Struct. Biol.* **2004**, *14*, 110.
11. Jenkel, E.; Rumbach, B. *Z.Elektrochem.* **1951**, *55*, 612.
12. Wang, J.; Chen, C.; Buck, S. M.; Chen, Z. *J. Phys. Chem. B* **2001,** *105,* 12118.
13. Wang, J.; Clarke, M. L.; Chen, X.; Even, M. A.; Johnson, W. C.; Chen, Z. *Surf. Sci.* **2005**, *587(1-2)*, 1-11.
14. Rodzivilova, I. S.; Ovchinnikova, G. P.; Artemenko, S. E.; Dmitrienko, T. G. *Fibre Chemistry* **2004**, *36(2)*, 139.
15. Andrade, J. D. *Polymer surface dynamics*; Plenum Press: New York, 1988.
16. Andrade, J. D.; Chen W. Y. *Surf. Intf. Anal.* **2004**, *8(6)*, 253.
17. Blum, F. D.; Lin, W. Y.; Porter, C. E. *Colloid Polym. Sci.* **2003**, *281*, 197.
18. Lin, W. Y.; Blum, F. D. *Macromolecules* **1997**, *18*, 5331.
19. Metin, B.; Blum, F. D. *J. Chem. Phys.* **2006**, *125*, 054707/054701-054709.
20. Thambo, G.; Miller, W. G. *Macromolecules* **1990**, *23*, 4397.
21. Hall, D. B; Torkelson, J. M. *Macromolecules* **1998**, *31*, 8817.

22. Royal, J. S.; Torkelson, J. M. *Macromolecules* **1992**, *25*, 1705.
23. Priestley, R.D.; Ellison, C.J.; Broadbelt, L.J.; Torkelson, J.M. *Science* **2005**, *309*, 456.
24. Maivald, P.; Butt, H. J.; Gould, S. A. C.; Prater, C. B.; Drake, B.; Gurley, J. A.; Elings, V. B.; Hansma, P. K. *Nanotechnology* **1991**, *2*, 103.
25. Overney, R. M.; Meyer, E.; Frommer, J.; Guntherodt, H.-J.; Fujihira, M.; Takano, H.; Gotoh, Y. *Langmuir* **1994**, *10*, 1281.
26. Kajiyama, T., Tanaka, K., Takahara, A. *Macromolecules* **1997**, *30*, 280.
27. Lee, W. K.; Yoon, J. S.; Tanaka, K.; Satomi, N.; Jiang, X.; Takahara, A.; Ha, C. S.; Kajiyama, T. *Polymer Bulletin* **1997**, *39*, 369.
28. Damme, H. S.; van Hogt, A. H.; Feijen, J. *J. Colloid Interface Sci.* **1985**, *106*, 289.
29. Porter, C. E.; Blum, F. D. *Macromolecules* **2002**, *35*, 7448.
30. Blum, F. D.; Young, E. Y.; Smith, G.; Sitton O. C. *Langmuir* **2006**, *22*, 4741.
31. Allcock, H. R.; Lampe, F. W.; Mark, J. E. *Contemporary Polymer Chemistry 3rd edn*; Prentice Hall, New Jersey, 2003.
32. Hetayothin, B.; Kulkeratiyut, S.; Kulkeratiyut, S.; Blum, F. D. "Thermal Analysis of Adsorbed Poly(Methyl methacrylate) on Silica: Effect of Molecular Mass" *To be submitted*.
33. Hetayothin, B.; Blum, F. D. *Polymer Preprints* **2010**, *51(1)*, 480.
34. Fox, T. G.; Flory, P. J. *J. Appl. Phys.* **1950**, *21*, 581.
35. Fox, T. G.; Flory, P. J. *J. Polym. Sci.* **1954**, *14*, 315.
36. Wunderlich, B. *Thermal analysis of polymeric materials;* Springer: New York, 2005.
37. Kawaguchi, M.; Nagata, K. *Langmuir* **1991**, *7*, 1478.
38. Backman, A. C.; Lindberg, K. A. H. *J. Appl. Polym. Sci.*, **2004,** *91*, 3009.
39. Roland, C. M.; Santangelo, P. G.; Ngai, K. L. *J. Chem. Phys.* **1999**, *111(12)*, 5593.
40. Wunderlich, B.; Jones, L. D. *J. Macromol. Sci., Phys.* **1969**, *B3*, 67.
41. Wunderlich, B.; *J. Phys. Chem.* **1960**, *64*, 1052.

3. DYNAMICS OF DI(PROPYLENE GLYCOL) DIBENZOATE-d_{10} IN POLY(VINYL ACETATE) BY SOLID-STATE ^{2}H NMR

Boonta Hetayothin[1], Roy A. Cabaniss[2], and Frank D. Blum[1, 3]*

1. Department of Chemistry and Materials Research Center, Missouri University of Science and Technology, Rolla, Missouri 65409-0010, USA
2. Department of Computer Science, Missouri University of Science and Technology, Rolla, Missouri 65409, USA
3. Department of Chemistry, Oklahoma State University, Stillwater, Oklahoma74078, USA

ABSTRACT

^{2}H solid-state NMR and temperature modulated differential scanning calorimetry were used to probe the dynamics of the plasticizer di(propylene glycol) dibenzoate (DPGDB-d_{10}) in mixtures with poly(vinyl acetate) (PVAc). ^{2}H NMR spectra were obtained from PVAc samples with 10, 22, 27, and 37% deuterated plasticizer content at various temperatures. The dynamics of the plasticizer in a plasticized polymer system was found to be heterogeneous. The experimental ^{2}H NMR line shapes were fitted using a set of simulated spectra obtained from the MXQET program. The simulation were based on the superposition of two types of motion. A two-site jump motion, i.e., 180º ring flips, plus isotropic motions. From both NMR and TMDSC, the reduction in T_g was proportional to the amount of plasticizer added. In addition, the T_gs of DPGDB-d_{10}/PVAc as a function of plasticizer content were found to be similar to those of PVAc-d_3/DPGDB as determined by NMR.

* Author to whom correspondence should be addressed: Frank D. Blum (fblum@okstate.edu)

1. INTRODUCTION

Plasticized polymers are usually binary systems whose physical properties can be adjusted or improved fairly easily with the addition of an external plasticizer. Polymeric materials are often found to contain plasticizers to improve their flexibility, softness, pliability, and processability [1-4]. For instance, poly(vinyl chloride) (PVC) can be used as a plastic or flexible film. Plasticizers reduce the glass transition temperatures (T_g) of polymers via a process called "plasticization" which can be described by, for example, free volume theory. Small molecule plasticizers occupy the space between polymeric chains creating additional free-volume in the polymer matrix, thereby causing the longer-range segmental motions to occur more easily [2, 5, 6].

Understanding the dynamic behavior of these binary glassy systems is quite important. This is because the dynamics are related to many properties found in polymeric materials, including processability, material deformation, and the diffusion of plasticizer [33]. The dynamics of plasticized polymers are more complex than those of (non-plasticized) homopolymers since they generally involve the physical characteristics of the two components which, for example, have different T_gs.

Di(propylene glycol) dibenzoate (DPGDB), is an effective plasticizer for poly(vinyl acetate) (PVAc), a polymer which has been largely used in adhesives, paints, and coatings. Plasticization of PVAc has extended the range of applications of this polymer.

Deuterium (^{2}H) NMR is a powerful technique for probing molecular motion in polymeric systems via changes in line shapes or measurement of the spin-lattice relaxation times [7-11]. The ^{2}H NMR line shapes are not only affected by anisotropic molecular motion with a time scale of about 10^3-10^7 s^{-1}, but also by the type of motion [11-13]. In this work, we have used ^{2}H NMR to probe the dynamics of deuterated plasticizer in polymer matrix via phenyl deuterons. The relationship of the dynamics of plasticizer and the T_gs was also examined. The T_gs of DPGDB-d_{10}/PVAc determined by ^{2}H NMR and temperature-modulated differential scanning calorimetry (TMDSC) were

compared with those of PVAc-d_3/DPGDB where the deuterated polymer was used as the probe [2].

1.1. NMR Theoretical Background

The deuterium NMR spectrum of a static X-D bond is dominated by an electrostatic interaction of the nuclear quadrupole moment (*eQ*) with the electric field gradient (*eq*) at the quadrupolar nucleus. The deuterium NMR transition frequencies are determined by the following factors: 1) the Larmor frequency, ω_0, 2) the quadrupole coupling constant, e^2qQ/h, 3) the asymmetry parameter, η, and 4) the orientation of the electric-field gradient (EFG) and the applied magnetic field, β_0, as shown in equation (1).

$$\omega = \omega_0 +/- \delta(3 \cos^2 \theta - 1 - \eta \sin^2 \theta \cos^2 \varphi) \quad (1)$$

with $\delta = 3e^2qQ/8h$, and e^2qQ/h is the quadrupole coupling constant and the polar angle, θ, is the angle made between the principle axis of the electric field gradient tensor (which in organic compounds, this is primarily along the C-D bond) and the magnetic field, β_0. The spherical polar angle, φ, also specifies the azimuthal orientation of the principle axis system of the electric field gradient tensor with respect to the external magnetic field. The quantity, η, is the asymmetry parameter, which defines the off-axis contribution of the EFG and is usually zero for aliphatic C-D bonds, indicating that the electric field gradient tensor is axially symmetric [11, 14-17]. However, for aromatic C-D bonds, the motionally averaged field gradient tensor is not axially symmetric [18].

The quadrupole coupling constant (qcc) determines the width of the line shape which can be obtained from the superposition of resonance frequencies for two sets of transitions for m_z of +1 -> 0 and 0 -> -1 as a function of the angle θ. The splitting between the two transitions of the line shape can be obtained from equation (2). A typical qcc for a C-D bond is about 160-180 kHz; therefore the splitting (D, for the highest intensity (the "horns" for $\theta = 90$) for a static C-D is ¾ of 160 -180 kHz or 120-135 kHz for an axially symmetric C-D, where the splitting is given by [17, 18]:

$$\Delta\nu = ¾ (e^2qQ/h) (3\cos^2\theta - 1) \quad (2)$$

Both the motional rate (time scale of motion) and the type of motion affect the line shapes [12, 13]. The changes in NMR line shapes are sensitive to the exchange rates of typically about 10^3 to 10^7 Hz. As the motional rates increase, a collapse of a powder

pattern into a narrow line shape is observed. A narrow resonance is a result of an isotropic reorientation of the nuclei.

Phenyl-ring flips are motions that are expected to occur in chemical species with aromatic rings. These have been observed in materials such as synthetic polymers [19-22] or biopolymers [23-24]. In the absence of molecular motion, the ^{2}H NMR line shapes for aromatic rings can result in a rigid lattice with a splitting between the two horns of about D = 120-135 kHz. Continuous rotational diffusion (D/8 = 15-17 kHz) or 180º jumps (D/4 = 30-34 kHz) about the symmetry axis reduce the quadrupole splittings and change the line shapes. A 180º ring flip results in a 120º change in the tensor component that is parallel to the C-D bond, as shown in Figure 1. [14, 24].

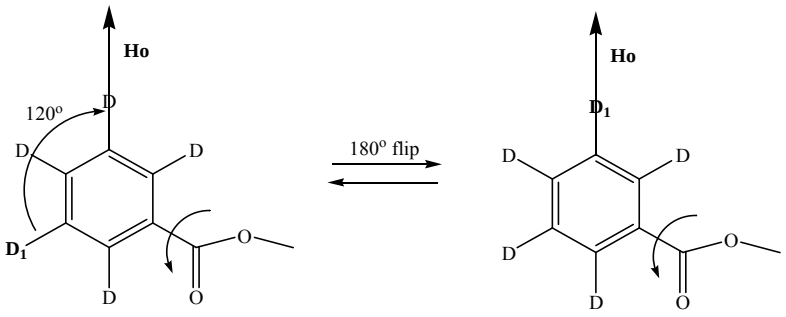

Figure 1. ^{2}H NMR of 180º aromatic ring flip.

2. EXPERIMENTAL

Synthesis of Deuterated Benzoyl Chloride-d_5. Benzoyl chloride-d_5 was prepared from a nucleophilic substitution of benzoic acid-d_5 (Cambridge Isotope laboratories, Inc., Andover, MA) and thionyl chloride (Aldrich, Milwaukee, WI), as shown in Figure 2. Benzoic acid-d_5 (1. 5.017 g 0.0395 mol) was added to a 50 mL two-necked round bottom flask equipped with a drying tube. Thionyl chloride (4.070 g, 0.0560 mol) was then added, dropwise, over 30-40 min [25]. The mixture was stirred under warm conditions about (35-40 °C) and refluxed for about 1-1.5 h until all hydrogen

chloride gas was gone (tested with pH paper). The crude product was distilled twice until it was colorless (or clear pale yellow). The purified yield was 72%.

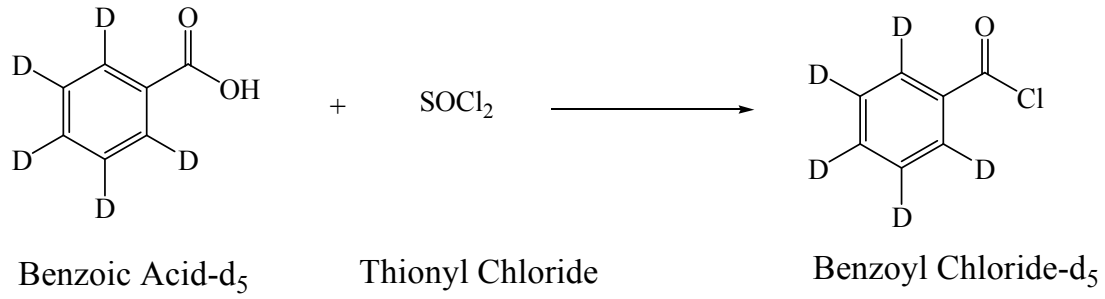

Figure 2. Synthesis of deuterated benzoyl chloride-d_5.

Synthesis of Deuterated Plasticizer, Di(propylene glycol) dibenzoate-d_{10}. A mixture of 4.141 g (0.0284 mol) of prepared benzoyl chloride-d_5 and 1.925 g (0.0142 mol) of di(propylene glycol) (Aldrich, Milwaukee, WI) were added to a 50 mL two-necked round bottom flask equipped with a drying tube [25]. The reaction as shown in Figure 3 was refluxed at 90-110 ºC until the hydrogen chloride gas was expelled. The reaction mixture was allowed to cool to room temperature, and then 20-25 mL of diethyl ether (Aldrich, Milwaukee, WI) was added. The solution was poured into a separatory funnel, and washed with 20 mL of water. The aqueous layer was discarded. The resulting organic layer was washed with a 20 % w/w Na_2CO_3 (Aldrich) solution until it became neutral (tested with pH paper). The Na_2CO_3 solution layer was discarded. The diethyl ether in the organic layer was evaporated, yielding a brownish viscous liquid. The crude product was further purified by re-dissolving it in diethyl ether, and activated charcoal (neutral, Aldrich) was added for decolorizing. The solution mixture was stirred with activated charcoal for 15 min, then the liquid portion was decanted and the diethyl ether was evaporated. The product obtained was a clear viscous liquid with a pale yellow color. ^{1}H NMR (400 MHz, $CDCl_3$) δ 1.34 (m, 6H), 3.66 (m, 4H), 4.27 (m, 1H), 5.30 (m, 1H). There was no visible intensity of the aromatic protons even at very high magnification suggesting a high degree of deuterium incorporation.

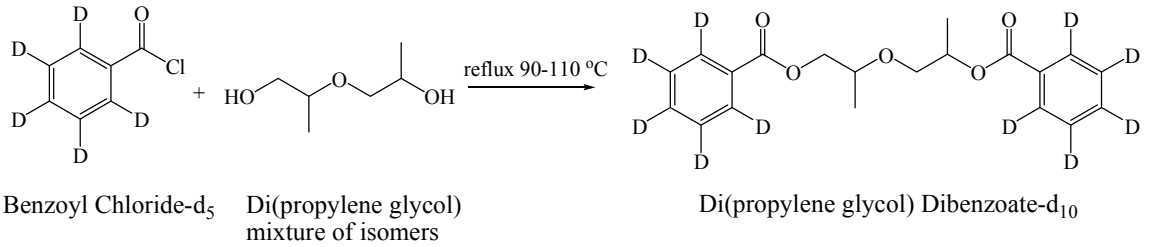

Figure 3. Synthesis of deuterated di(propylene glycol) dibenzoate-d_{10}.

Preparation of Plasticized Polymers. 25% w/w solution of PVAc, M_w = 170 kDa (Scientific Polymer Products, Inc., Ontario, NY) was prepared in a capped test tube using toluene as a solvent. Various amounts of deuterated plasticizer DPGDB-d_{10} were added to make 10, 22, 27, and 37% w/w plasticized polymers. The solutions were shaken using a mechanical shaker for 24 h. The polymer solutions were then cast on glass slides and allowed to dry at ambient temperature for 24 h. The resulting films were colorless and transparent, suggesting there was no phase segregation between the plasticizer and polymers.

Characterization of Plasticized Polymers by TGA and TMDSC. The amounts of polymer and plasticizer contained in the plasticized polymers were analyzed by high resolution thermogravimetric analysis (Hi-Res TGA 2950) (TA Instruments, New Castle, DE). The scans were run at a heating rate of 20 °C/min using high resolution mode from room temperature to 750 ºC in air. The T_g was measured using modulated differential scanning calorimetry (MDSC 2920) (TA Instruments, New Castle, DE). The sample pans were referenced against empty pans and the cell purged with nitrogen gas at a flow rate of 50 mL/ min. The samples were held at -40 ºC for 5 min, heated to 150 ºC at a rate of 2.5 ºC/min with a modulation amplitude of +/- 0.5 ºC, and a period of 60 s, then held for 3 min, cooled to -40 ºC at the same rate, and held for another 3 min. After the first heating and cooling scan, the second heating scan was applied with the same conditions as the first. In order to standardize the effects of previous thermal history, the T_g was determined using this second heating scan. The results are shown as differential reversing heat flow rate (dQ_{rev}/dT) vs temperature. A 10 ºC smoothing was applied to the thermograms to reduce the high-frequency noise and highlight the transition, without

significantly distorting the thermogram. The reported T_g was taken at the peak of the derivative of the reversing heat flow vs. temperature.

Characterization of Plasticized Polymers by Solid-State Deuterium (^{2}H) NMR. The ^{2}H NMR spectra were obtained using a Tecmag Discovery 400 MHz NMR spectrometer equipped with a high-power amplifier, a fast digitizer and an Oxford AS-400 wide bore magnet. A fixed-frequency wide-line probe (Doty Scientific, Columbia, SC) with an 8 mm (diameter) sample coil was used. The quadrupole-echo pulse sequence (delay-90_y-τ-90_x-τ-acquisition) was used with a ^{2}H frequency of 61.48 MHz. The 90° pulse width was 2.8 μs and an echo time (τ) of 30 μs was used. Prior to collecting the data, the probe was tuned at each temperature. The raw data was left shifted so that the Fourier transform was started from the top of the echo. Approximately 4,000 to 70,000 scans were collected, depending on the operating temperature, and no line broadening was used. The spectra were taken at intervals of 5 °C from -30 to 80 °C, depending upon the plasticizer content. The temperature was controlled with the accuracy of +/- 1 ºC. The spectra were processed using the Mestrec software package (Santiago de Compostela University, Spain), and each spectrum shown was scaled to the same height for comparison.

NMR Simulations. The experimental NMR line shapes were simulated using the FORTRAN-based program MXQET [26-28]. Simulations of the deuterium NMR line shapes have been used to model the motional mechanism (types of motion) and motional rates in different systems in which the change of NMR line shapes are sensitive in a frequency range between 10^4-10^8 s^{-1} (Hz). The simulations were based on the phenyl ring motions modeled as 2-site jumps with 180º ring flips, with an asymmetry parameter, η = 0.04. Several authors have reported the asymmetry parameter for phenyl ring in the range of 0.03-0.06 [27, 29-33]. This 180º jump about the C_2 symmetric axis does not result in an isotropic motion, even at fast jump rates, $k > 10^8$ [27-28]. Therefore, the addition of an axial of motion was needed to further average the qcc to obtain an isotropic pattern. For this work, it was sufficient to add a mixed Gaussian/Lorentzian or a Lorentzian single central component to mimic the isotropic resonance, which was not of interest here. The experimental line shapes were then fitted using a mathematical routine (MATLAB, the Mathworks, Inc., Natick, MA). The weight fractions of each of the simulated spectra

were found by minimizing the squares of the differences between the experimental spectra and the sum of the simulated ones, i.e., a constrained least-squares fit.

3. RESULTS

The amount of the plasticizer in the samples was analyzed using thermogravimetric analysis (TGA). The decomposition thermograms for bulk PVAc and plasticized samples are shown in Figure 4. The plasticizer volatilized in the range of 290-325 °C, while decomposition of the polymer occurred at higher temperatures, beyond 325 °C [2]. The amount of plasticizer estimated from the TGA experiments was within 5% of those estimated from the compositions of the original mixtures.

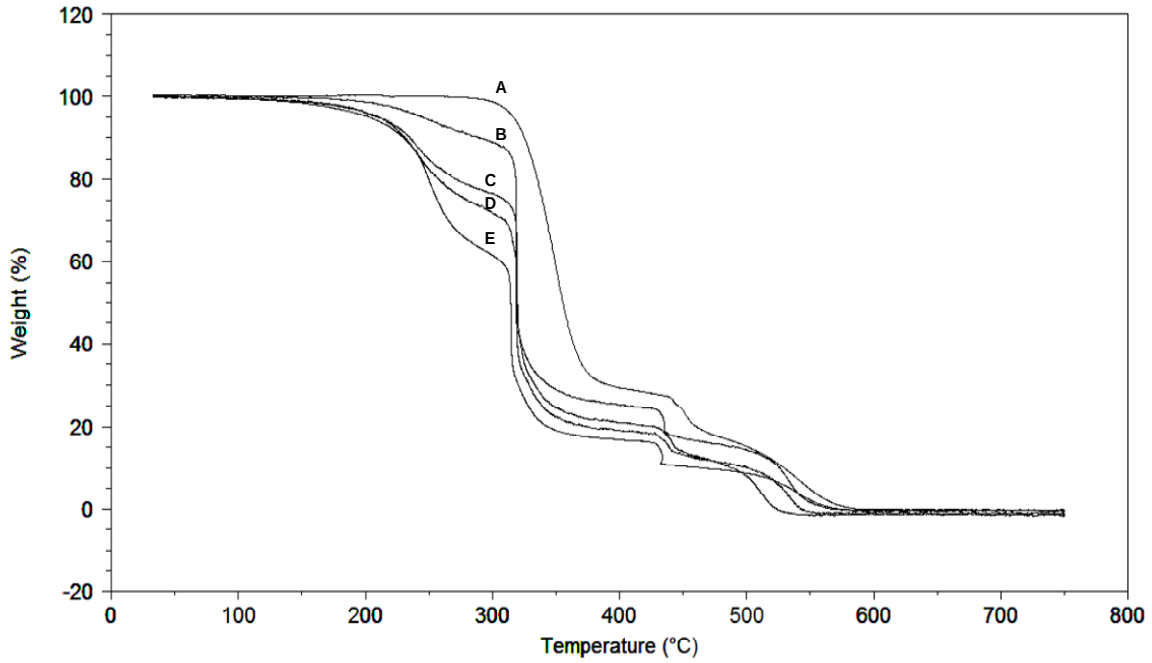

Figure 4. Thermogravimetric (TGA) analysis of: (A) 0%, (B) 10%, (C) 22%, (D) 27%, and (E) 37% DPGDP-d_{10} in PVAc.

The quadrupole echo ^{2}H NMR spectra for the pure plasticizer, DPGDB-d_{10}, were taken at various temperatures ranging from -60 to -20 °C and are shown in Figure 5. The sample became liquid-like at temperatures above -20 °C. Unfortunately, it was not possible to obtain a good spectrum at -25 °C due to very poor S/N. The spectra from -60 to -30 °C were consistent with a rigid powder pattern although the intensity of the spectra was reduced at higher temperatures (reduced S/N). As temperature increased up to -20 ºC, more scans were necessary. As shown in Figure 5.5, there was a very weak intensity for some phenyl rings undergoing 180º flips (inner horns at 29 kHz separation) in this low temperature range. The T_g (NMR) of plasticizer DPGDB-d_{10} was estimated to be about -25 ºC.

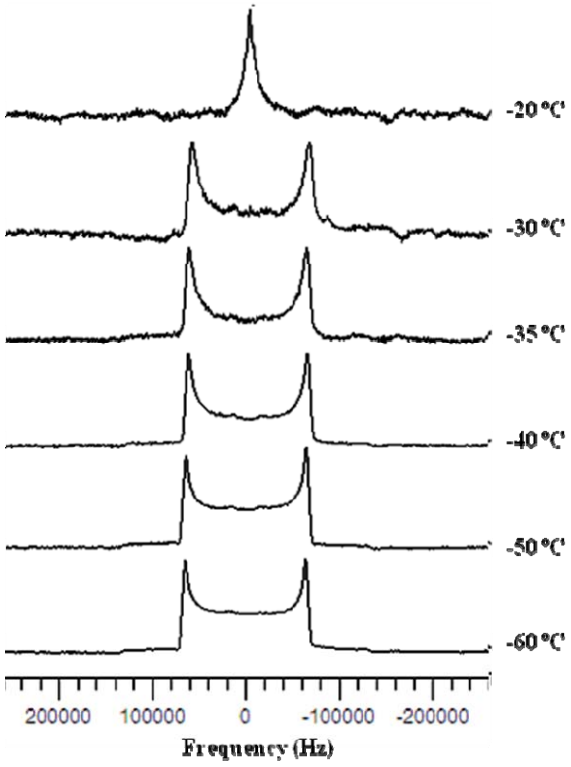

Figure 5. ^{2}H NMR spectra for pure plasticizer DPGDB-d_{10}.

For DPGDB-d_{10} with PVAc, the quadrupole echo ^{2}H NMR spectra were taken as a function of temperature and plasticizer amount. The resulting experimental and

simulated spectra are shown in Figures 6-9. As previously mentioned, the phenyl deuterons appeared to have two motionally-different states. They were rigid C-D bonds, as observed from the splitting of about 125 kHz between the two outer horns, and phenyl rings that execute 180º flips with splitting of about 29 kHz between the two inner horns. At low temperatures, the spectra for the 10% DPGDB-d_{10}/PVAc sample (shown in Figure 6) showed powder patterns from both static rings and those executing 180º ring flips. In the low temperature range of about 24-39 ºC, the line shapes did not seem to change much with temperature. As the temperature increased to 80 °C, the powder pattern collapsed with the rise of a central resonance. The T_g related to plasticizer motion was estimated to be about 59 °C. The central component increased in intensity and smoothed to a single narrower resonance at 80 °C.

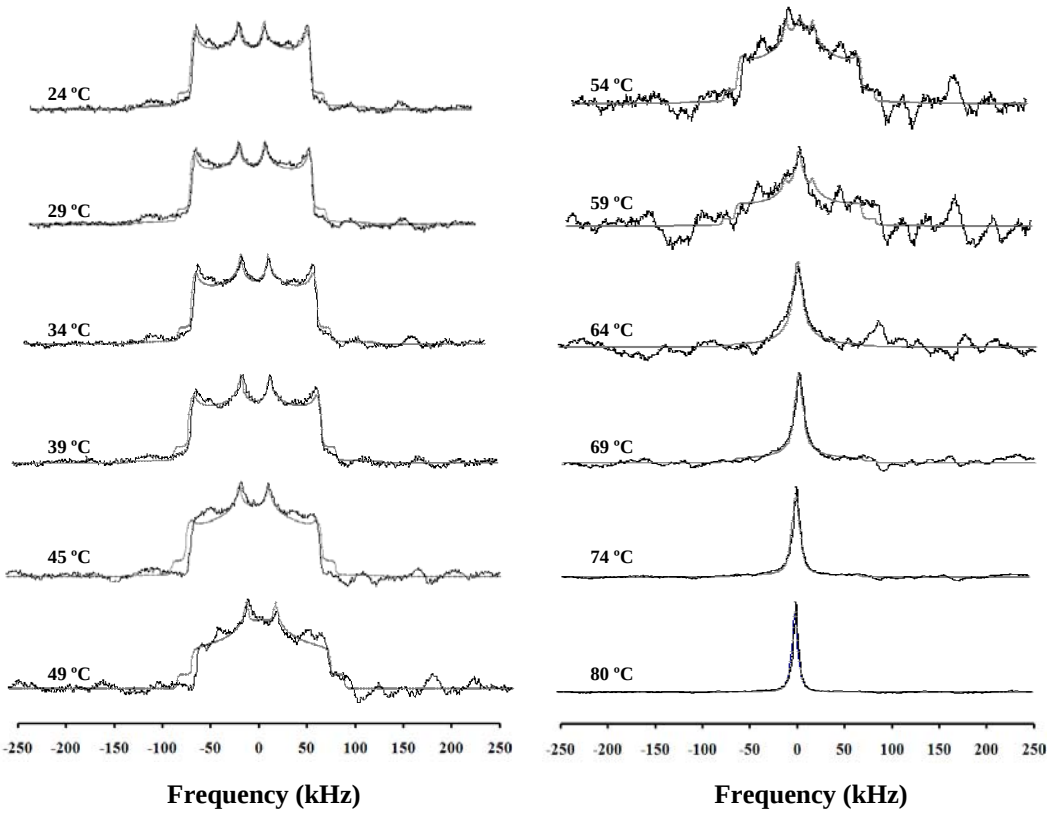

Figure 6. Experimental (black) and simulated (grey) 2H NMR spectra for a 10% DPGDB-d10/PVAc sample.

Although it was easy to observe the spectra going from a Pake pattern (glassy state) to a relatively narrow isotropic resonance (rubbery state) with increasing temperature, assigning a T_g was not necessarily that straightforward. In this work, we have assigned T_gs that are consistent with previous work [34]. Accordingly, the T_g was defined at the temperature where the signal height of the central resonance of the spectrum was about three times (roughly equal intensities) that of the height of the horns. Uncertainties as to these T_g assignments are estimated to be less than +/-5 °C.

The ^{2}H NMR spectra for the 22% DPGDB-d_{10}/PVAc sample are shown in Figure 7 as a function of temperature. The NMR glass transition takes place roughly between 34 and 45 °C and is centered at Tg (NMR) of about 39°C. The line shape of 22% DPGDB-d_{10}/PVAc spectra did not seem to change much at temperatures below the T_g although the contribution from the 180º ring flips increased as the temperature increased.

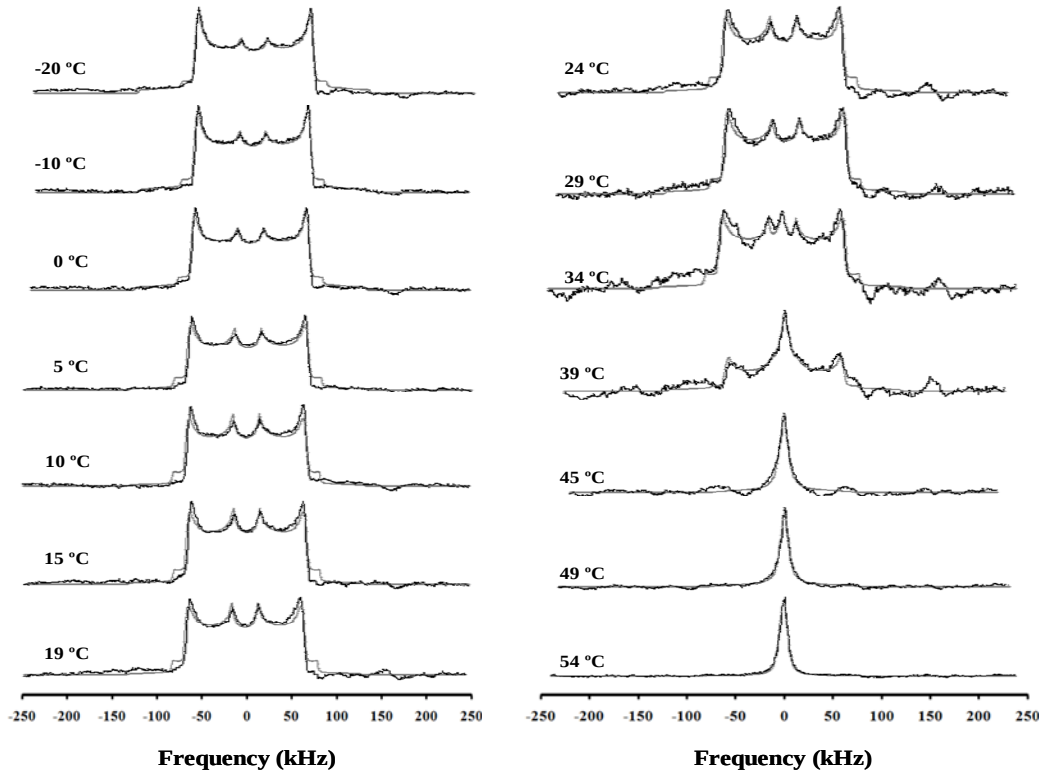

Figure 7. Experimental (black) and simulated (grey) ^{2}H NMR spectra for a 22% DPGDB-d_{10}/PVAc sample.

The spectra for the 27% and 37% plasticized samples are shown in Figures 8 and 9, respectively. These spectra were also similar to those of the 22% DPGDB-d_{10}/PVAc. The collapse of the powder pattern occurred within a range of 29-34 °C or T_g (NMR) of about 32 °C for the 27% plasticized sample. For the 37% DPGDB-d_{10}/PVAc, the powder pattern collapsed between 10 and 19 °C and the T_g (NMR) was assigned as 15 °C. In general, a shift to higher mobility at the same temperatures was also observed as the plasticizer content increased. This effect is consistent with a lowering of the T_g expected with increased amounts of plasticizer. The summary of T_g (NMR) for DPGDB-d_{10}/PVAc at different plasticizer content is shown in Table 1.

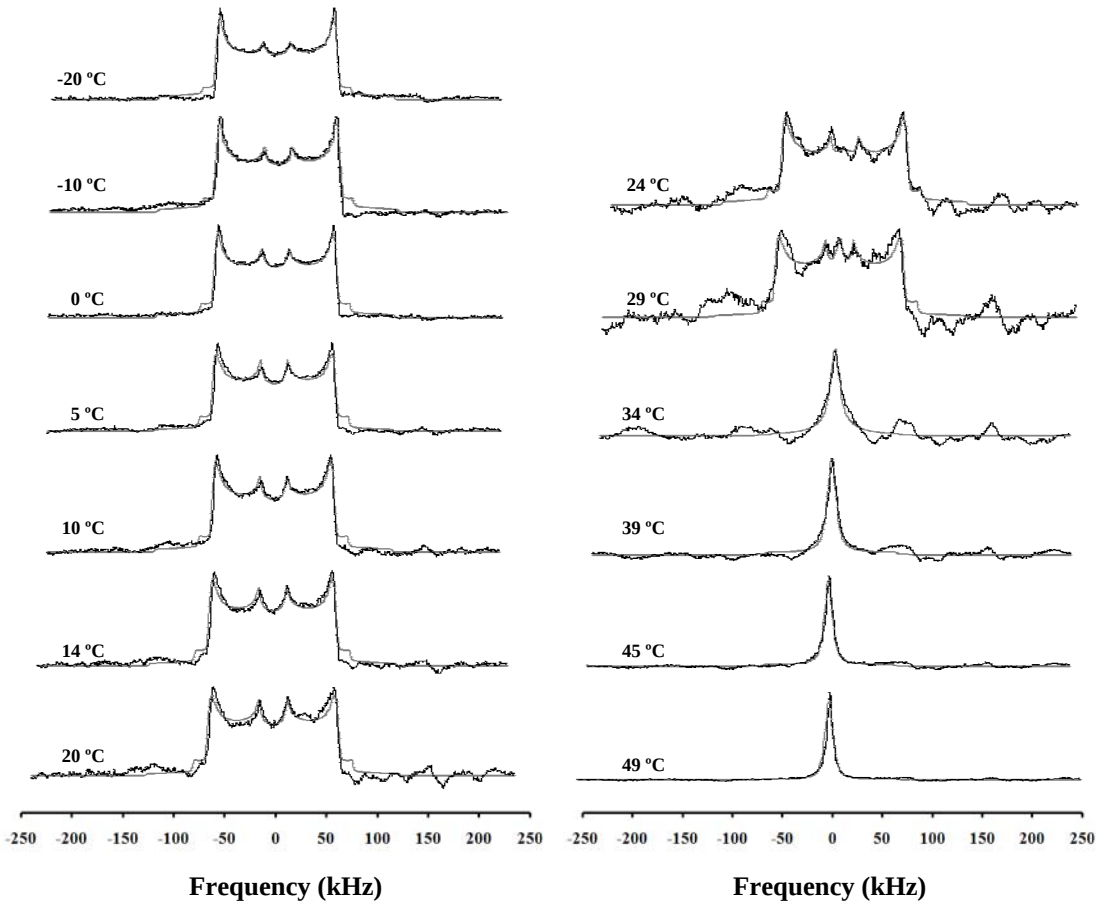

Figure 8. Experimental (black) and simulated (grey) ^{2}H NMR spectra for a 27% DPGDB-d_{10}/PVAc sample.

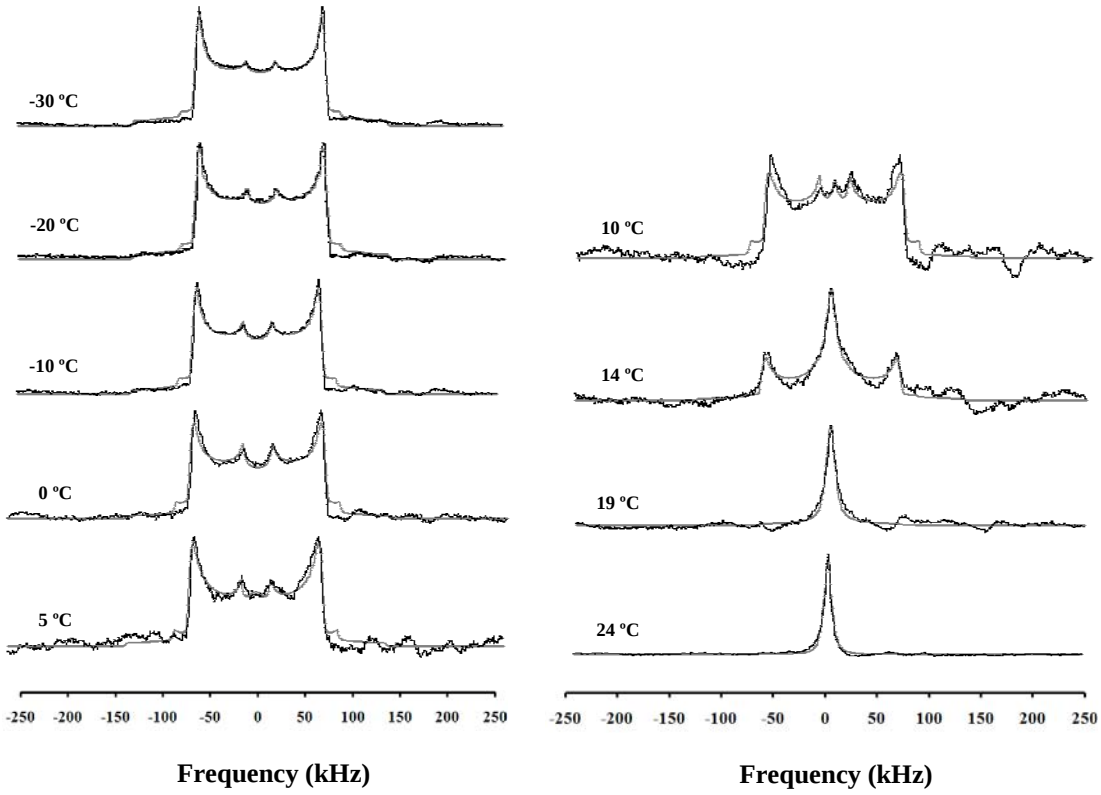

Figure 9. Experimental (black) and simulated (grey) ^{2}H NMR spectra for a 37% DPGDB-d_{10}/PVAc sample.

Table 1. ^{2}H NMR Glass Transition Temperature Ranges[a] for DPGDB-d10/PVAc at Various Plasticizer Contents.[34]

% plasticizer	T_g (NMR)		
	T_{onset} (°C)	T_{mid} (°C)	width (°C)
10	45	59	14
22	24	39	15
27	20	32	12
37	0	15	15
100	-30	-25	5

[a] T_{onset} is where a narrowed component in the spectrum was first observed and T_{mid} is an estimate of the middle of the transition as defined in the text.

The simulations of the experimental ^2H NMR spectra are shown superimposed as lighter lines in Figures 6-9. The fits seemed to be quite good for the rigid and liquid-like ranges, but not as good in the glass transition region where the signal-to-noise ratio of the spectra is poorer. The MXQET program was used to obtain a basic set of spectra with various jump rates ranging from 1 to 1×10^9 Hz.

The simulations were based on a two-site jump model of a phenyl deuteron that executed a 180º ring flip. MATLAB was used to fit the superpositions of simulated spectra to experimental spectra. The slow jump rates are effectively rigid in the NMR simulations. Good fits required a broad distribution of spectra with different jump rates covering from 1 to 1×10^9 Hz. The distributions of (log) jump rates as a function of temperature and plasticizer content are presented using bar graphs and described in the supporting information (appendix E).

For simplicity, the phenyl ring motions were categorized into three groups or regimes as slow, intermediate, and fast with respect to their jump rates, which resulted in different powder pattern intensities. It was observed that a 180º jump about the C_2 symmetric axis would not yield an isotropic motion, even with the fast exchange rate, $k > 10^8$ [24, 27, 28]. Fast isotropic motion, which results a single narrow peak, occurred at the fast exchange rates where the spectrum pattern was no longer sensitive to the jump rate. In a slow regime ($1\text{-}10^4$ Hz), there was no significant intensity loss during a quadrupole echo. However, when the exchange rate becomes faster, at about $10^4\text{-}10^7$ Hz (classified as the intermediate regime), a significant loss of intensity was observed [35]. Only a small amount of intensity loss occurred for the fast regime, $>10^8$ Hz. The motional component fractions used in the fittings at different temperatures are given in Table 2.

The log of the average jump rates (log $\langle k \rangle$) as a function of temperature for different plasticizer contents (10, 22, 27, and 37%) are shown in Figure 10. The average correlation times $\langle t_c \rangle$ that were proportional to the inverse of the jump rates were obtained from these jump rates. The plot of log $\langle k \rangle$ values, as a function of inverse temperature for different plasticizer contents seemed to be linear for low amounts of plasticizer (10-22%). As the amount of plasticizer increased, the deviation from linearity was more pronounced.

Table 2. Motional Components Used to Simulate Experimental Line Shapes[a,b]

	10% plast.				22% plast.				27% plast.				37% plast.			
T(ºC) +/-1	S	I	F	L	S	I	F	L	S	I	F	L	S	I	F	L
-20	-	-	-	-	-	-	-	-	-	-	-	-	26	64	10	0
-10	-	-	-	-	-	-	-	-	46	41	13	0	62	28	10	0
0	-	-	-	-	60	20	20	0	52	29	19	0	36	57	7	0
5	-	-	-	-	31	48	21	0	24	59	17	0	49	38	c	13
10	-	-	-	-	23	49	28	0	47	39	14	0	17	47	18	18
15	-	-	-	-	26	46	28	0	41	40	19	0	20	11	c	69
20	-	-	-	-	22	51	27	0	32	48	20	0	c	c	4	96
25	35	32	33	0	30	46	24	0	52	36	c	12	c	c	c	100
30	33	32	36	0	41	35	24	0	16	46	16	22	-	-	-	-
35	22	38	40	0	16	46	10	28	c	1	4	95	-	-	-	-
40	23	36	41	0	27	10	c	63	2	c	4	94	-	-	-	-
45	16	26	51	7	c	1	4	95	1	c	3	96	-	-	-	-
50	c	30	57	13	c	c	5	95	c	1	c	99	-	-	-	-
55	14	27	29	30	1	c	1	98	-	-	-	-	-	-	-	-
60	3	29	10	58	-	-	-	-	-	-	-	-	-	-	-	-
65	c	3	3	94	-	-	-	-	-	-	-	-	-	-	-	-
70	c	c	12	88	-	-	-	-	-	-	-	-	-	-	-	-
75	3	c	1	96	-	-	-	-	-	-	-	-	-	-	-	-

[a] Components: S, slow ($k <= 1.0 \times 10^4$ Hz); I, intermediate ($1.0 \times 10^4 < k < 1.0 \times 10^8$ Hz); F, fast ($k >= 1.0 \times 10^8$ Hz) where k is the jump rate, and L, liquid which modeled as an isotropic component. [b] Given as the percentages of each component in the simulated spectra. [c] A small (<1%) but non-zero component was required for a good fit.

The activation energies of the 180º ring flip from linear equations of both a 10 and 22% plasticizer content were calculated to be 25 kJ/mol. However, with a broad distribution of jump rates (or correlation times), $\langle t_c \rangle$ was sometimes dominated by longer correlation times. Therefore, the average of the logarithm of the jump rate, $\langle \log k \rangle$ was also calculated for comparison and shown in Figure 11. The $\langle \log k \rangle$ values, as a function of inverse temperature for different plasticizer contents, seemed to fall within the same curve and satisfactorily fit the Arrhenius equation. The calculated activation energy from this $\langle \log k \rangle$ ranged from about 42 to 105 kJ/mol.

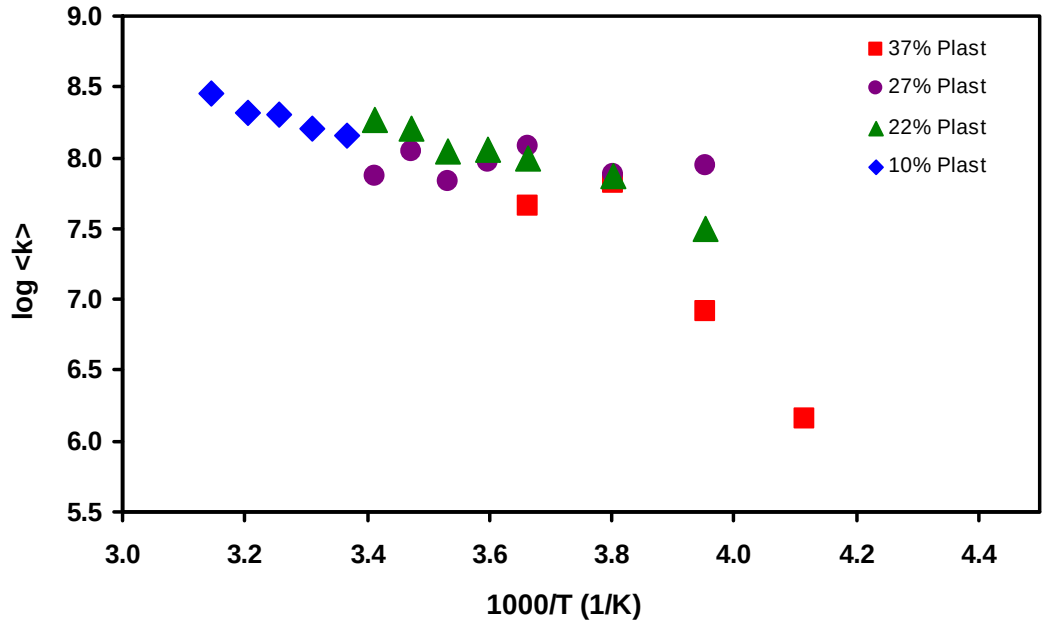

Figure 10. The log average jump rates values, log <*k*>, for DPGDB-d_{10} as a function of temperature for the different plasticizer contents (10, 22, 27, and 37%).

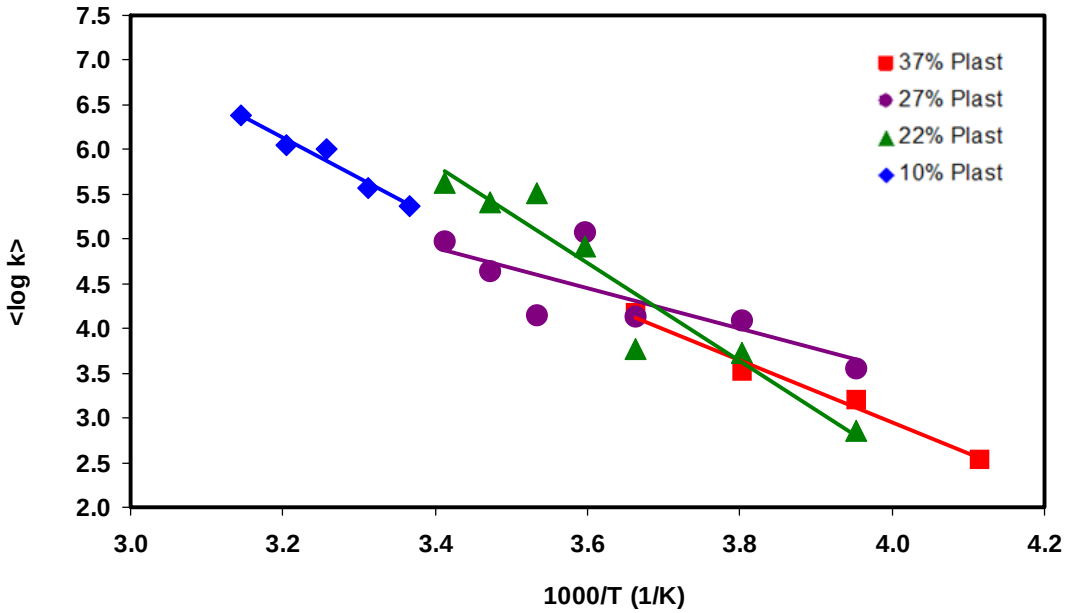

Figure 11. Averages of the log jump rates values, <log *k*>, for DPGDB-d_{10} as a function of temperature for the different plasticizer contents (10, 22, 27, and 37%).

The thermograms for samples containing different amounts of plasticizer were obtained using temperature modulated differential scanning calorimetry (TMDSC) and are shown in Figure 12. The derivatives of the reversible heat flow rates were plotted as a function of temperature for the different DPGDB-d_{10} content in bulk PVAc samples. The T_g (TMDSC) was chosen as the maximum of the derivative reversible heat flow curve. The T_gs (TMDSC) observed for DPGDB-d_{10}/PVAc for a 10%, 22%, 27%, and 37% plasticizer content were 31, 15, 7, and -7 ºC, respectively as shown in Table 3. These T_gs (TMDSC) decreased an average of 7 degrees for every 5% plasticizer added. The reductions of the T_gs (TMDSC) as the amount of plasticizer increased were similar to those in the previous work [2]. The width of the glass-transition obtained from the width at half-height depended upon the amount of plasticizer in the sample. The higher the plasticizer content was, the broader the transition was. A single, relatively narrow transition, observed from the TMDSC experiments, indicated that the polymer-plasticizer system seemed miscible. This seemed to correlate well with observations of the physical appearance of the transparent films, indicating that phase separation had not occurred.

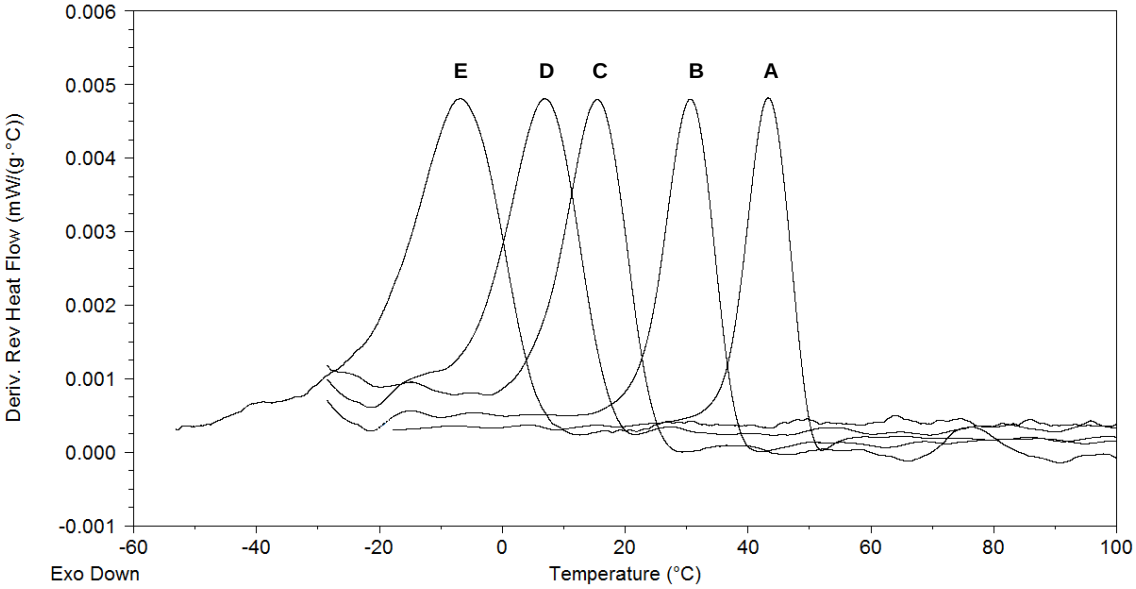

Figure 12. TMDSC derivative reversing heat flow curves for: (A) 0%, (B) 10%, (C) 22%, (D) 27%, and (E) 37% plasticized-d_{10} PVAc. The maximum of the derivative curve is taken as the T_g (TMDSC).

Table 3. TMDSC Glass Transition Temperature for DPGDB-d_{10}/PVAc at Various Plasticizer Contents.

% plasticizer in samples	T_g (TMDSC) (°C)	width (°C)
10	31	10
22	15	12
27	7	14
37	-7	16
100	-53[a]	n/a

[a] from ref. 2

4. DISCUSSION

At temperatures below T_g, all of the DPGDB-d_{10}/PVAc samples exhibited Pake powder patterns with a QCC of 167 kHz, as observed from the splitting of about 125 kHz between the two outer horns. In addition, the splitting of about 29 kHz between the two inner horns indicated that some of the molecules underwent 180º phenyl-ring flip motions. As the temperature increased, reaching the T_g (NMR), the Pake powder patterns (slow motional regime) for DPGDB-d_{10}/PVAc collapsed to motionally narrowed resonances (fast motional regime) due to changes in the mobility of the polymer segments. At a given temperature, the intensity of the central component increased with increases in the plasticizer content, consistent with an increase in the mobility of the segmental polymers. This can be explained based on the free volume theory that plasticizer increases the amount of free volume and allows the long-range segmental motions to occur at reduced temperatures [2, 5, 6]. Increasing the amount of plasticizer provides greater chain mobility. This observation has been previously reported for bulk PVAc-d_3 samples where the mobility of polymer segments increased as the amount of plasticizer increased [2].

A number of NMR studies of plasticized polymers have been conducted [2, 36-41]. It was observed that the Pake powder pattern of polymers and plasticizers collapse to a narrow resonance spectrum at quite different temperatures, indicating the dynamics and

heterogeneities of plasticizer and polymer in the mixture [2, 36]. Our goal here is to probe the dynamics of the plasticizer in a plasticized polymer system. We have found that the dynamics of plasticizer in plasticized polymer were heterogeneous. The appearance of a superposition of rigid and liquid-like patterns (two-phase spectrum) in the plasticized polymers indicated a pronounced motional heterogeneity despite the fact that the mixture is homogeneous and not phase-separated. In contrast to the behavior of the DPGDB-d_{10}, the collapse of the powder pattern for the PVAc-d_3 in the same system passed through a hump-shaped feature [2]. The hump-line shape can be considered as a superposition of residual powder patterns and a liquid-like component. Our data is in agreement with that of Bingemann et al. [36] where it was found that a pure plasticizer was liquid-like at a temperature well below the plasticized PMMA, and the motional heterogeneities of the plasticizer occur even in a rigid polymer matrix.

The distributions of jump rates from the simulations of the ^{2}H spectra also provide information about the homogeneity of the segmental motions in the samples [2, 11]. The line shape sensitive regimes have been divided into three groups: slow, intermediate, and fast. While an isotropic motion with a single narrow peak is no longer sensitive to the jump rate, at a temperature lower than the T_g, the jump rate distributions are quite broad, extending from a rigid to a fast regime. When the temperature of the system approached the T_g, the distribution of jump rates became more homogeneous as a majority of the liquid-like component was found. Although the distribution of jump rates shifted to the fast regime and became more liquid-like at a lower temperature with increasing amounts of plasticizer, the addition of plasticizer did not seem to change the breadth of jump rate distributions.

The changes in rates of ring flips with temperature for the plasticizer can be quantified through averaging. From the simple mean, log <k>, the activation energies for the 180º ring flips were estimated to be about 25 kJ/mol for the 10 and 22% plasticizer content samples. These results correlate with other studies, where the apparent activation energy for the pure 180º ring flip motions was also about 25 kJ/mol [19, 42-43]. However, the log <k> is dominated by the fast k's. Perhaps a more appropriate measure is that from the <log k>, which ranged from about 42 to 105 kJ/mol. Perhaps more importantly, the broad view of the values of <log k> were roughly superimposable in

Figure 11, i.e., the data all fit within a band. This superposition suggests that the different plasticizers have the effect of shifting the temperature of the dynamics rather than changing their nature.

A comparison of the T_g's of plasticized PVAc with different plasticizer contents from different perspectives is in order, i.e, from NMR of PVAc-d_3 or PVAC/DPGDB-d_{10} and from DSC. As mentioned previously, the T_g decreases as the amount of plasticizer increases. From this study, the dependence of T_g on the plasticizer amount is fairly linear; the T_g (NMR) decreased by an average of 8 ºC per 5% increase in plasticizer content, while the T_g (TMDSC) decreased by an average of 7 ºC over the same increment. These results are fairly close to a previous report by Nambiar and Blum [2] who found that the reductions in T_g averaged about 6 ºC and 7 ºC for the NMR and TMDSC experiment, respectively. Moreover, we observed that the NMR T_g was about 25 +/- 3 ºC higher than the TMDSC T_g while the previous work reported about 36 +/- 2 ºC. The difference in T_g for NMR and TMDSC is due to the time scale difference used in the two experiments [2, 44-45].

Although the dynamics of plasticizer and polymer in the plasticized polymer system were different, interestingly, their plasticized polymer NMR T_g's appeared to be similar as shown in Figure 13.

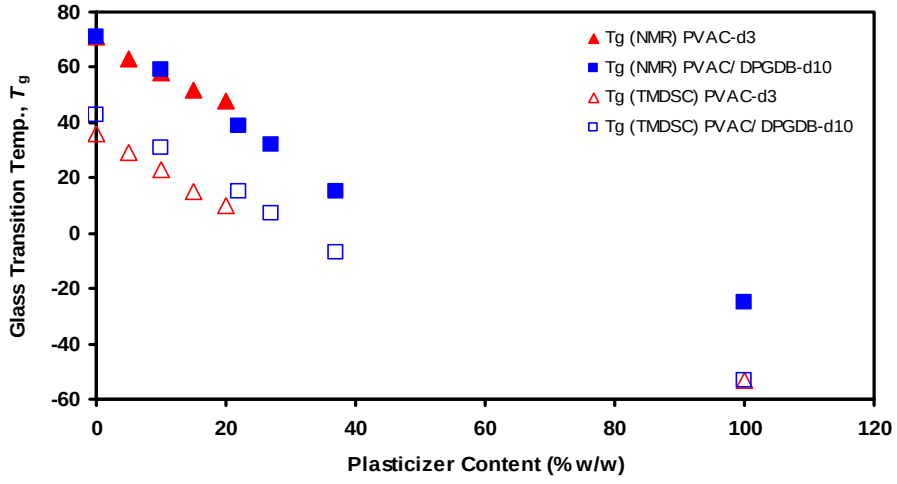

Figure 13. Glass-transition temperatures (T_g's) as a function of plasticizer content of deuterated polymer (PVAc-d_3) [36] and deuterated plasticizer in PVAc (PVAC/ DPGDB-d_{10}) from both TMDSC and NMR.

This might indicate that the behavior of the plasticizer is intimately tied to the polymer matrix [3]. Moreover, it has been reported that, although the addition of plasticizer reduced the correlation time (reduction in T_g), the dynamics of the polymer may remain unchanged [36].

5. CONCLUSIONS

In this work, we have observed the motional heterogeneities of plasticizer in a polymer matrix. The ^{2}H NMR line shapes were fit using a superposition of simulated spectra from the MXQET program, based on a two-site jump model with a 180º ring flip. The distribution of jump rates from the simulations of the ^{2}H spectra also provides information about the homogeneity of segmental motions in the samples. The jump rate distribution is broad (ranging from a rigid to a fast regime at low temperatures) and becomes more homogeneous when the temperature approaches the T_g.

A comparison was made of the T_g's of plasticized PVAc with different amounts of plasticizer content in PVAc-d_3 and PVAC/DPGDB-d_{10}, from both TMDSC and NMR. The reductions in the T_g's, as the amount of plasticizer increased, were found to be slightly different for both probing cases (plasticizer and polymer). Although the dynamics of plasticizer and polymer in the plasticized polymer system were different, their plasticized polymer T_g's (NMR) appeared to be the same.

6. ACKNOWLEDGEMENTS

The authors acknowledge the support of the National Science Foundation under grant DMR-1005606, and the Missouri University of Science and Technology for financial support of this research. The authors gratefully thank Raymond Kendrick for his technical support for some NMR experiments. The authors also thank Dr. Robert

O'Connor for useful discussions and Dr. Cyriac Kandoth and Waraporn Viyanon for their help with Fortran programing.

7. REFERENCES

1. Billmeyer, F. W. *Textbook of Polymer Science*, *3rd ed.;* John Wiley and Sons: New York, **1984.**
2. Nambiar, R.; Blum, F. D. *Macromolecules* **2008**, *41*, 9837.
3. Gould, R. *Plasticization and Plasticizer Processes*, American Chemical Society, Washington, D.C, 1965.
4. Sears, J. K.; Darby, J. R. *The Technology of Plasticizers*; Wiley: New York, 1982.
5. Painter, P. C.; Coleman, M. M. *Fundamentals of Polymer Science 2nd ed*; CRC Press: Boca Raton, 1997.
6. Boyer, R. F. *Transitions and Relaxations in Amorphous and Semicrystalline Organic Polymers and Copolymers*; John Wiley and Sons: New York, 1977.
7. Blum F. D.; Xu, G.; Liang, M.; Wade, C. G. *Macromolecules* **1996**, *29*, 8740.
8. Lin, W. Y.; Blum F. D. *Macromolecules* **1997**, *30*, 5331.
9. Lin, W. Y.; Blum F. D. *Macromolecules* **1998**, *31*, 4135.
10. Lin, W. Y.; Blum F. D. *J. Am. Chem. Soc.* **2001**, *123*, 2032.
11. Metin, B.; Blum, F. D. *J. Chem. Phys.* **2006**, 24, 054908/1-54908/10.
12. Penner, G. H.; Polson, J. M.; Stuart, C.; Ferguson, G.; Kaitner, B. *J. Phys. Chem*. **1992**, *96*, 5121.
13. McBrierty, V. J.; Packer, K. J. *Nuclear Magnetic Resonance in Solid Polymers*, Davis, E. A.; Ward, I. M., Eds.; Cambridge University Press: Cambridge, Britain. 1993.
14. Janusa, M. A.; Wu, X.; Cartledge, F. K.; Butler, L. G. *Environ. Sci. Technol.* **1993**, 27, 1426.
15. Higinbotham, J.; Marshall, I. in *Annual Reports on NMR Spectroscopy*, Webb, G. A., Ed.; Academic, San Diego, **2001**, vol. 43, p. 59.

16. Kemp, W. *NMR in Chemistry-A Multinuclear Introduction*, Macmillan, London, 1986.
17. Schmidt-Rohr, K.; Spiess, H. W. *Multidimensional Solid-State NMR and polymers*, Academic, San Diego, 1994.
18. Jelinski, L. W. *"Deuterium NMR of Solid Polymers", High-Resolution NMR Spectroscopy of Synthetic Polymers in Bulk*, Komoroski Ed.; VCH Publishers, Inc. 1986.
19. Cholli, A. L.; Dumais, J. J.; Engel, A. K.; Jelinski, L. W. *Macromolecules* **1984**, *17*, 2399.
20. Spiess, H. W. *Colloid Polym. Sci.* **1983**, *261*, 193.
21. Inglefield, P. T.; Amici, R. M.; O' Gara, J. F.; Hung, C.-C.; Jones, A. A. Macromolecules **1983**, *16*, 1552.
22. Spiess, H. W. *Annu. Rev. Mater. Sci.* **1991**, *21*, 131.
23. Torchia, D. A. *Ann. Rev. Biophys. Bioeng.* **1984**, *13*, 125
24. Rice, D. M.; Wittebort, R. J.; Griffin, R. G.; Meirovitch, E.; Stimson, E. R.; Meinwald, Y. C.; Freed, J. H.; Scheraga, H. A. *J. Am. Chem. Soc.* **1981**, 103, 7707.
25. Vogel, A. I.; Tatchell, A. R.; Furnis, B. S.; Hannaford, A. J. *Vogel's Textbook of Practical Organic Chemistry 3rd ed.* Pearson Education Limited, England, 1956.
26. Metin, B. **2006**. *Segmental Dynamics in Poly(Methyl Acrylate) through the Glass Transition Region.* Dissertation(Ph.D.). University of Missouri-Rolla.
27. Greenfield, M. S; Ronemus, A. D.; Vold, R. L.; Vold, R. R.; Ellis, P. D.; Raidy, T. E. *J. Magn. Reson.* **1987***, 72,* 89.
28. Vold, R. R.; Vold, R. L. *Adv. Magn. Opt. Reson.* **1991***, 16,* 85.
29. Gall, C. M.; Diverdi, J. A.; Opella, S. J. *J. Am. Chem. Soc.* **1981**, *103*, 5039.
30. Hiraoki, T.; Kogame, A.; Nishi, N.; Tsutsumi, A. *J. Mol. Struct.* **1998**, *441*, 243.
31. Boden, N.; Clark, L. D.; Hanlon, S. M.; Mortimer, M. *Faraday Symp.* **1978**, *13*, 109.
32. Montgomery, C. R.; Bunce, N. J.; Jeffrey, K. R. *J. Phys, Chem.* **1988**, *92*, 3635.
33. Simpson, J. H.; Rice, D. M.; Karasz, F. E. *J. Polym. Sci. A*, **1992**, *30*, 11.
34. Nambiar, R.; Blum, F. D. *Macromolecules* **2009**, *42*, 8998.
35. Abraham, A. *The principles of Nuclear Magnetism*; Clarendon Press: Oxford, U.K., 1961.

36. Bingemann, D.; Wirth, N.; Gmeiner, J.; Rossler, E. A. *Macromolecules* 2007, *40*, 5379.
37. Floudas, G.; Fytas, G.; Fischer, E. W. *Macromolecules*, 1991, 24, 1955.
38. Bergquist, P.; Zhu, Y.; Jones, A. A.; Inglefield, P. T. *Macromolecules* **1999**, *32*, 7925.
39. Parker, A. A.; Hedrick, D. P. Ritchey, W. M. *Macromolecules* **1992**, *25*, 3365.
40. McBrierty, V. J. Farady Discuss. Chem. Soc. **1979**, *68*, 78.
41. Tavares, M. I. B.; Monteiro, E. E. C, Harris, R. K.; Kenwright, A. M. *Eur. Polym. J.* **1994**, *30*, 1089.
42. Hummel, J. P.; Flory, P. J. *Macromolecules* **1980**, *13*, 479
43. Tonelli, A. E. *J. Polym. Sci., Polym. Lett. Ed.* **1973**, *11*, 441.
44. McCall, D. W. *Acc. Chem. Res*. **1971**, 4, 223.
45. Chartoff, R. P.; Weissman, P. T.; Sircar, A. *In Assignment of the Glass Transition*; Seyler, R. J., Ed.; ASTM: Philadelphia, PA, 1994, p. 88.

4. DYNAMICS OF DI(PROPYLENE GLYCOL) DIBENZOATE-d_{10} IN ADSORBED POLY(VINYL ACETATE) BY SOLID-STATE ^{2}H NMR

Boonta Hetayothin[1], Roy A. Cabaniss[2], and Frank D. Blum[1, 3]*

1. Department of Chemistry and Materials Research Center, Missouri University of Science and Technology, Rolla, Missouri 65409-0010, USA
2. Department of Computer Science, Missouri University of Science and Technology, Rolla, Missouri 65409, USA
3. Department of Chemistry, Oklahoma State University, Stillwater, Oklahoma74078, USA

ABSTRACT

The dynamics of the deuterated plasticizer di(propylene glycol) dibenzoate (DPGDB-d_{10}) in conjunction with adsorbed poly(vinyl acetate) (PVAc) were probed using deuterium (^{2}H) solid state NMR and temperature modulated differential scanning calorimetry (TMDSC). PVAc with 37% (w/w) of plasticizer/polymer was adsorbed on silica at adsorbed amounts of 2.60 and 0.76 mg/m^2. The dynamics of the plasticizer in the adsorbed PVAc was found to be more motionally heterogeneous than that observed in bulk samples. The NMR results provided solid evidence that, when there is only a small amount of adsorbed polymer (e.g., only "tightly-bound" polymer, less than 0.8 mg/m^2), the plasticizer is mostly excluded from the polymer chains at the polymer-air interface. When excluded, the plasticizer exists in an environment that is similar to that of pure plasticizer. At higher adsorbed amounts, the plasticizer is effective at lowering the T_g of the adsorbed polymer.

* Author to whom correspondence should be addressed: Frank D. Blum (fblum@okstate.edu)

1. INTRODUCTION

A polymer composite is a multi-component polymeric material such as polymer blend, plasticized polymer, structured latex, or filled system with adsorbed polymer [1]. Polymer composites have attracted interest due to their usefulness and superior performance, as compared to bulk polymers [2, 3]. The structural and functional properties of polymer composites depend upon the properties and interactions of their components, especially at interfaces where the different components of multiple phases come in contact [4-6]. An understanding of the behavior of polymers at interfaces is essential and beneficial for improving their properties or for developing novel materials for specific uses.

Many aspects of the behavior of polymers at interfaces have been studied extensively [5]. Among those studies, the investigations of glass transition temperatures (T_g) and the dynamics of adsorbed polymers are relevant to this work and are, therefore, worth mentioning here. It has been shown that the T_gs of adsorbed polymers can be quite different from those of bulk T_gs [7-10]. Some studies have found increases in the T_gs of polymers adsorbed on an attractive surfaces with specific interactions, such as with hydrogen or covalent bonding [7, 8]. Others have identified a reduction in the T_gs of adsorbed polymers on unattractive surfaces, without any specific interaction between the polymers and the surfaces [9, 10]. Several techniques have been used to study these T_gs, including thermal analysis, [7, 11, 12]; ellipsometry [8, 13]; NMR [4, 14-20]; and ESR [21, 22].

Many factors are known to affect the T_g of a polymer [23], including, the addition of small molecules (known as plasticizers) into the polymeric material [24-26]. Plasticizers increase the total free volume of the system, thereby allowing long-range segmental motion to occur at reduced temperatures [18, 23, 27]. As a result, desired properties can be achieved, such as flexibility, softness, reduced stiffness, shock resistance, ductility, and processability [18, 24-26]. In addition to plasticized bulk polymers, the application of a plasticizer can be expanded to other polymer composites, such as adsorbed polymers that have fillers or fibers [19, 28-31]. The combined effects of

fillers and plasticizers on polymers can produce many interesting properties, such as enhanced conductivity and rigidity in polymer electrolytes [28, 29]. The addition of plasticizer can also facilitate the dispersion of fillers and improve the fluidity of composites [30]. On the other hand, increasing the amount of filler usually reinforces a material with greater storage modulus and a higher T_g [30]. Moreover, filler is sometimes used to reduce the loss of plasticizer in films; for example, through the introduction of chalk into a plasticized poly(vinyl chloride) film [31].

Solid-state NMR is a powerful technique used to probe the molecular motion in polymeric systems [14-19]. In many cases, analysis of NMR line shapes and relaxation times can provide specific information about the rates and types of motion [14-19]. Our research group has focused on using deuterium NMR (^{2}H NMR) to study the dynamics of polymer in bulk and in adsorbed samples [14-19]. In this work, we have used ^{2}H NMR to probe the dynamics of deuterated plasticizer, di(propylene glycol) dibenzoate in adsorbed poly(vinyl acetate) (PVAc) on silica, via the motions of the phenyl ring. This study builds on a previous study of plasticized PVAc-d_3 adsorbed on silica [19]. In that study, it was found that the plasticizer had little or no effect on the dynamics of the adsorbed polymer for samples with very small amounts of adsorbed polymer (i.e., 0.81 mg/m^2). This could be rationalized based on two possible mechanisms. One possibility is that the plasticizer molecules were immobilized in a rigid polymer-silica interfacial layer that did not allow the plasticizer to be effective. Another possibility is the exclusion of the plasticizer from the polymer matrix at the air-polymer interface. Our use of ^{2}H NMR with a deuterated plasticizer, similar to our previous studies on PVAc-d_3 [18-19], allowed us to distinguish between these two possibilities.

2. EXPERIMENTAL

Synthesis of Deuterated Benzoyl Chloride-d_5. Benzoic acid-d_5 (Cambridge Isotope Laboratories, Inc., Andover, MA) was reacted with thionyl chloride (Aldrich, Milwaukee, WI) via the nucleophilic substitution reaction to yield benzoyl chloride-d_5

(Figure 1). In a 50 mL two-necked round bottom flask equipped with a drying tube, a 5.017 g (0.0395 mol) of benzoic acid-d_5 were added, followed by a drop-wise addition of 4.070 g (0.0560 mol) of thionyl chloride [32]. The reaction was stirred using mild heat, refluxed for 1-1.5 h, and pH paper was used to check that all of the hydrogen chloride gas was evaporated. A dark yellow or brownish crude product was found and further purified by distillation until colorless (or clear pale yellow). The yield of this purified product was 72%.

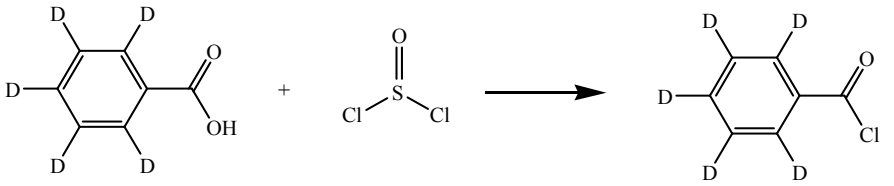

Figure 1. Synthesis of deuterated benzoyl chloride-d_5.

Synthesis of Deuterated Plasticizer, Di(propylene glycol) dibenzoate (DPGDB-d_{10}). The deuterated plasticizer was prepared using an esterification reaction of 4.141 g (0.0284 mol) prepared benzoyl chloride-d_5 and 1.925 g (0.0142 mol) of di(propylene glycol) (Aldrich, Milwaukee, WI) in a 50 mL two-necked round bottom flask equipped with a drying tube [32]. The reaction, Figure 2, was refluxed at 90-110 ºC for 2.5 h or until the hydrogen chloride gas was gone. After the reaction mixture had cooled to room temperature, 20-25 mL of diethyl ether (Aldrich, Milwaukee, WI) were added. The mixture was separated using a separatory funnel and washed with 20 mL of water; the aqueous layer was discarded. A 20% w/w Na_2CO_3 (Aldrich, Milwaukee, WI) solution was used to wash the resulting organic layer until it became neutral (checked with pH paper). After washing, the Na_2CO_3 solution layer was discarded. The organic layer of the diethyl ether was evaporated, resulting in a brownish viscous liquid. The crude product was further purified by dissolving it again in diethyl ether and then adding decolorizing activated charcoal (neutral) (Aldrich, Milwaukee, WI). The solution mixture, with activated charcoal, was stirred for 15 min. The liquid portion was then

decanted and the solvent, diethyl ether, was evaporated. The finished product was a clear pale yellow viscous liquid. ^{1}H NMR (400 MHz, $CDCl_3$) δ 5.30 (m, 1H), 4.27 (m, 1H), 3.66 (m, 4H), 1.34 (m, 6H). Although at high magnification, there was still no visible intensity of the aromatic protons.

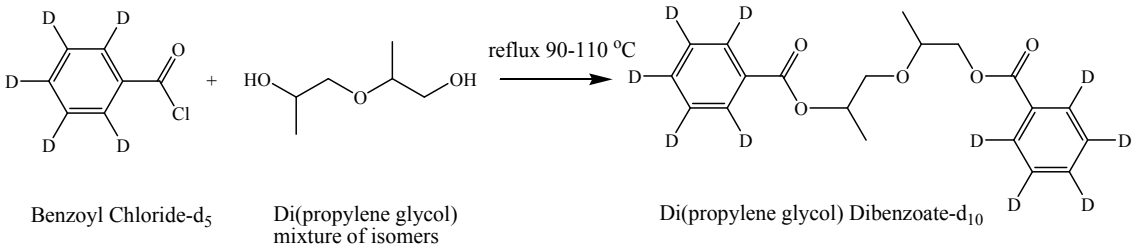

Figure 2. Synthesis of deuterated di(propylene glycol) dibenzoate-d_{10}.

Preparation of Plasticized-Adsorbed Polymers. Solutions of known ratio amounts of PVAc **(**M_w = 170 kDa, Scientific Polymer Products, Inc., Ontario, NY), and plasticizer (as described above) were prepared in test tubes using toluene as the solvent (Aldrich, Milwaukee, WI). These solutions were shaken in a mechanical shaker for 12 h and then 0.3 g of silica (Cab-O-Sil M5, 200 m^2/g) was added. These mixtures were shaken by a mechanical shaker for 72 h at room temperature. The toluene was removed by passing air (using a glass pipette with a low flow rate) through the adsorbed polymer-silica mixtures while they were agitated. The drying of the absorbed samples was completed in a vacuum oven under 30 mm Hg at 60 ºC for 72 h. Two adsorbed samples were prepared at 2.2 mg/m^2, and 0.8 mg/m^2, respectively. These samples will be referred to as those with larger and smaller adsorbed amounts. The use of mg/m^2 refers to the total mass of polymer per square meter of silica surfaces (i.e., the plasticizer is not included in the adsorbed amount reported). The amount of plasticizer in these adsorbed samples was 37% w/w of plasticizer/polymer.

Characterization of the Plasticized-Adsorbed Polymers by TGA and TMDSC. High resolution thermogravimetric analysis (Hi-Res TGA 2950) (TA Instruments, New Castle, DE) was used to quantify the polymer and the plasticizer

content. The scans were run at a heating rate of 20 °C/min in the high-resolution sensitivity mode, beginning at room temperature and progressing to 750 ºC in air. A temperature-modulated differential scanning calorimetry instrument (MDSC 2920) (TA Instruments, New Castle, DE) was used to measure the T_g. The sample pans were referenced against empty pans. Two heating scans and one cooling scan were made using the following procedure: a constant (isothermal) temperature was maintained at -40 ºC for 5 min, and then raised to 150 ºC at a rate of 2.5 ºC/min with a modulation amplitude of +/- 0.5 ºC for a period of 60 s, isothermal for 3 min, cooled to -40 ºC at the same rate, and then isothermal for 3 min. A mass of approximately 7-10 mg of samples was used and the cell was purged with nitrogen gas at 50 mL/min during the scans. After the first heating and cooling scan, the second heating scan was applied under the same conditions as the first heating scan. The T_g was determined based on this second heating scan. Results were depicted as plots of differential reversing heat flow rate (dQ_{rev}/dT) vs. temperature. The peak of the derivative of the reversing heat flow rate versus temperature was assigned as the T_g.

Characterization of the Plasticized-Adsorbed Polymers by Solid State Deuterium (^{2}H) NMR. The ^{2}H NMR spectra were obtained using a Tecmag Discovery 400 MHz NMR spectrometer equipped with a high-power amplifier, a fast digitizer, and an Oxford AS-400 wide bore magnet. A fixed-frequency wide-line probe (Doty Scientific, Columbia, SC) with an 8 mm (diameter) sample coil was used. For surface samples, the 8 mm coil size provides good sample volume for these low concentration samples. The quadrupole-echo pulse sequence (delay-90_y-τ-90_x-τ-acquisition) was used with a ^{2}H frequency at 61.48 MHz. The 90° pulse width was 2.8 μs and an echo time (τ) of 30 μs was used. For each temperature, the probe response was tuned before collecting the spectrum. The raw data was left shifted so that the Fourier transform was started from the top of the echo. Approximately, 20,000 to 110,000 scans were collected for adsorbed samples, depending upon the operational temperature, and no line broadening was used. The spectra were taken from a range of -20 to 40 °C at intervals of 5 °C, depending on the T_g of the samples. Temperature was controlled with an accuracy of +/- 1 ºC. Using the Mestrec software package (Santiago de Compostela University, Spain), the spectra were processed and scaled to the same height for comparison.

NMR Simulations. The experimental NMR line shapes were simulated using a FORTRAN program known as MXQET [33-35]. The information about the motional rates and types of motion was obtained from these simulations. The NMR line shapes were sensitive to changes in the motion that ranged between 10^4 and 10^7 s^{-1}. The ^2H NMR line shapes of aromatic ring motions in a solid can often be the results of a rigid lattice (no motion) with a splitting between the two horns of about 120-135 kHz, 180º jumps (D/4 = 30-34 kHz), and continuous diffusion about their symmetry axes (D/8 = 15-17 kHz) [36]. In this work, the simulations were based on the phenyl ring motion modeling as a 2-site jump, 180º ring flips, with an asymmetry parameter, $\eta = 0.04$. Several authors have reported an asymmetry parameter for phenyl ring in the range of 0.03-0.06. [34, 37-41]. However, even with the fast exchange rate, $k > 10^8$, this 180º jump about the C_2 symmetric axis does not result in the isotropic motion [34-35]. In order to obtain an isotropic spectrum, the addition of isotropic axial of motion was required to further average the quadrupole coupling constant (qcc). For this work, since the isotropic component was not our focus, it was sufficient to add a mixed Gaussian/Lorentzian or a Lorentzian single central component to mimic the isotropic resonance. The experimental line shapes were then fitted with a superposition of the simulated spectra by using the MATLAB mathematical program (The Mathworks, Inc., Natick, MA). The weight fractions of each of the simulated spectra were found by minimizing the differences between the experimental spectra and the sum of the simulated ones. A constrained least-squares fit was applied to find the absolute weight fractions of a series of spectra.

3. RESULTS

Since the signal intensity of NMR depends on the concentrations (or amounts) of a sample held within the coil inside a probe [42], and only a limited amount of adsorbed sample can be packed into a NMR tube that will fit into a coil, the amount of plasticizer in an adsorbed sample may be small. Accordingly, a high ratio of plasticizer to polymer was used to overcome the problems resulting from weak signal intensities. In this work,

the adsorbed polymers contained 37% w/w (plasticizer/PVAc), the approximate amount commonly found in most soft plastic toys and other devices [43]. However, the plasticizer content is not restricted, but can vary between 15 and 60%, depending upon the application [43]. Two samples with different adsorbed amounts (smaller, 0.76 mg/m^2, and larger, 2.60 mg/m^2) were prepared and used throughout this study.

Thermogravimetric analysis (TGA) was used to analyze the amount of plasticizer and polymer in each sample. Figure 3 shows the decomposition thermograms of adsorbed samples containing 37% w/w plasticizer/PVAc for the larger adsorbed amount (2.60 mg/m^2) and 0.76 mg/m^2 for the smaller adsorbed amount sample. The plasticizer volatilized in the range of 290-325 °C for the larger adsorbed quantity and at approximately 270-325 °C for the smaller adsorbed amounts. The polymer started to decompose at a higher temperature of about 350°C [18]. The amount of plasticizer estimated from the TGA experiments was within 5% of those estimated from the compositions of the original mixtures.

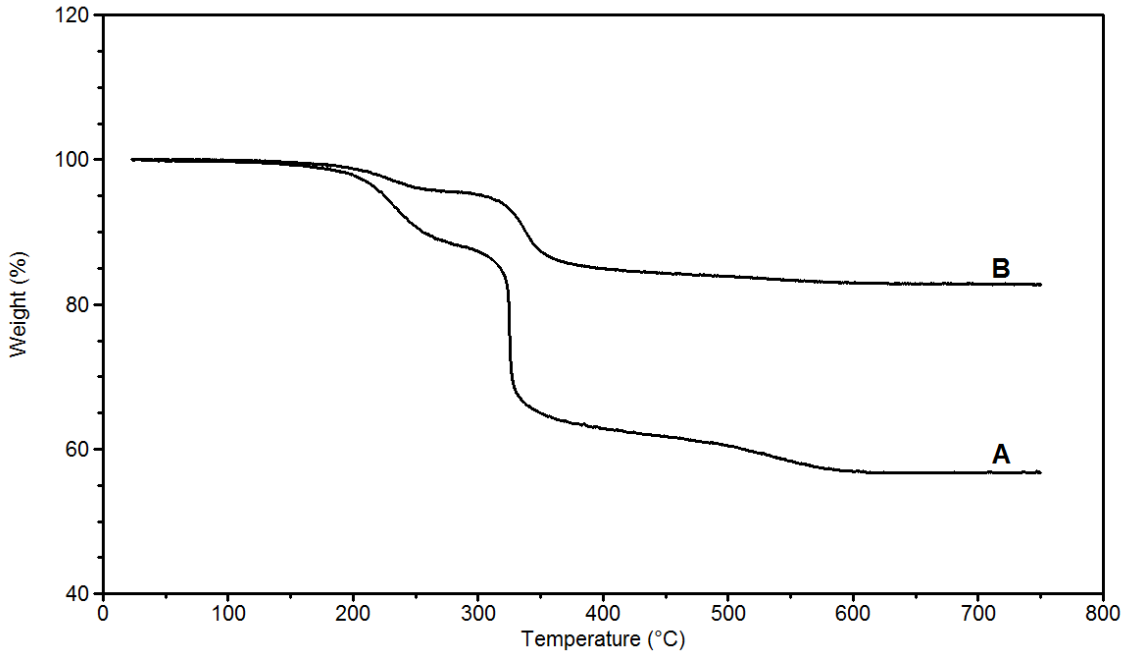

Figure 3. Thermogravimetric analysis (TGA) plot of 37% plasticized-adsorbed PVAc on silica. (A) Smaller adsorbed-amount sample with 2.60 mg/m^2 and (B) larger adsorbed amount sample with 0.76 mg/m^2 PVAc on silica.

The ^{2}H NMR spectra of a pure plasticizer (DPGDB-d_{10}) were taken at various temperatures ranging from -60 to +24 °C. Each spectrum at a different temperature was scaled to the same height for comparison. Low intensities of the 180º ring flip (the two inner horns) were observed at low temperature ranges, as shown in Figure 4. The T_g (NMR) of the plasticizer, DPGDB-d_{10}, was roughly between -30 and -20 °C, and taken to be approximately 25 °C. At -20 ºC, collapse of the Pake powder pattern was almost gone and, instead, appearing as a relatively narrow component at the center. As the temperature increased, the central component gradually smoothed to a very sharp narrow line at 24 ºC, as seen in Figure 4.

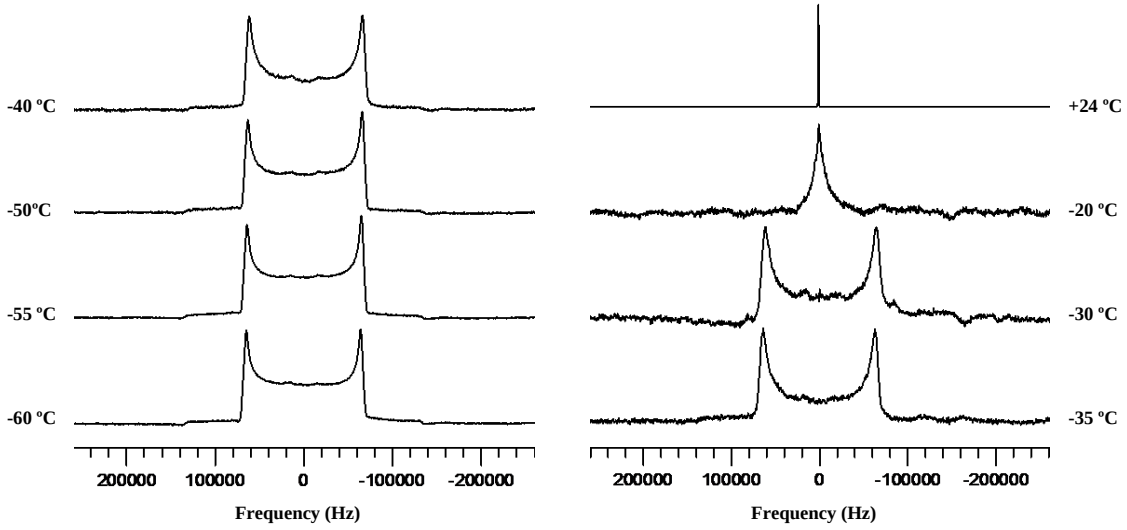

Figure 4. The ^{2}H NMR spectra of deuterated plasticizer di(propylene glycol) dibenzoate-d_{10}.

The quadrupole-echo ^{2}H NMR spectra of a 37% plasticized-adsorbed sample with an adsorbed amount of 2.60 mg/m^2 were taken as a function of temperature and are shown in Figure 5. The spectra showed splitting of about 125 kHz between the two outer horns at lower temperature indicative of a rigid material. The splitting between the two inner horns of about 29 kHz was attributed to the phenyl ring executing a 180º ring flip.

At low temperatures from -20 to 0 ºC, the spectra showed powder patterns for both rigid material and 180º phenyl ring flips. As the temperature increased, however, a narrow central component rose and the Pake powder pattern eventually collapsed. The plasticizer T_g of a 37% plasticized-adsorbed sample at 2.60 mg/m^2 was assigned as 24 ºC. The determinations of the plasticizer T_gs were consistent with those reported in previous work [19, 44] that defined T_g for heterogeneous line shapes as the temperature at which the signal height of the narrow resonance of a spectrum is approximately three times that of the height of the horns. The estimation uncertainties of these plasticizer T_g assignments less than +/-5 °C.

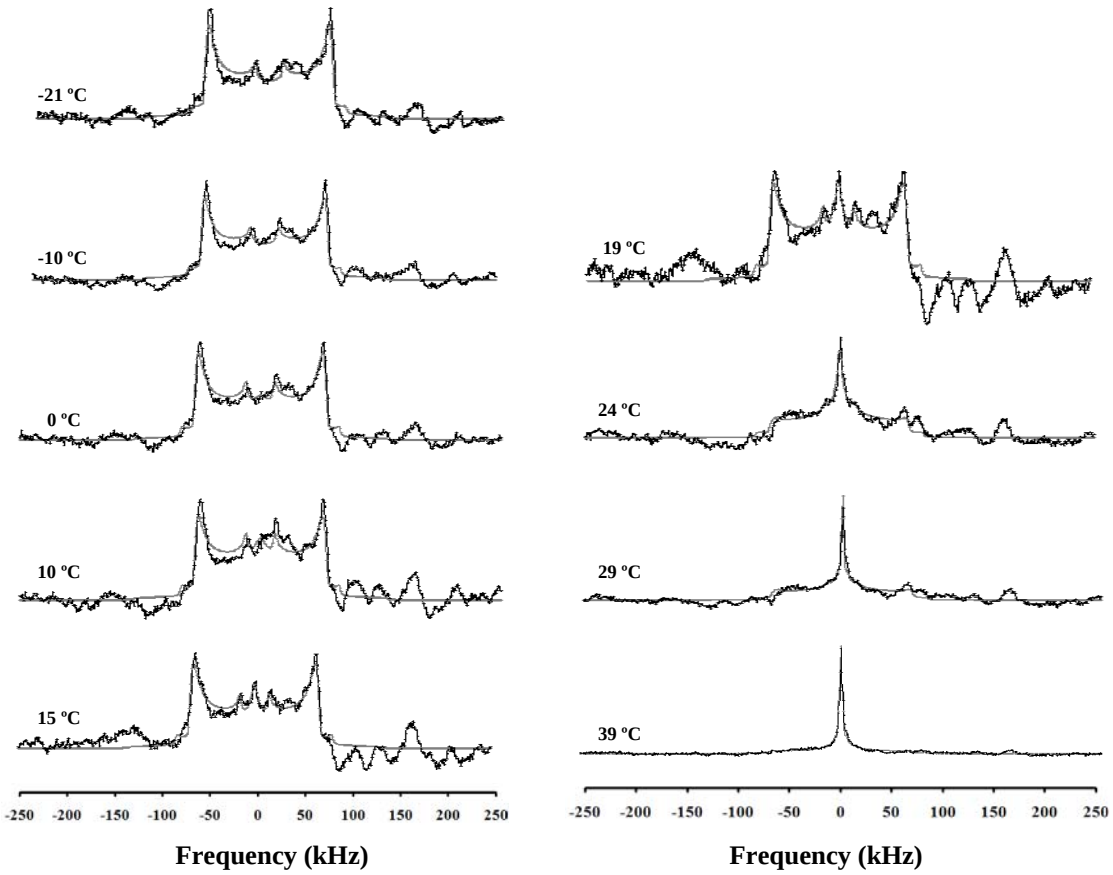

Figure 5. Experimental (black) and simulated (grey) ^{2}H NMR spectra for 37% plasticizer (DPGDB-d_{10}) with PVAc for the larger adsorbed-amount (2.60 mg/m^2) sample.

The ^{2}H NMR spectra for the 37% plasticized-d_{10} in an adsorbed PVAc sample with smaller adsorbed amount of 0.76 mg/m^2, as a function of temperature are shown in Figure 6. The NMR glass transition took place roughly between -16 and 0 °C and was centered at plasticizer T_g (NMR) of about 10°C. As temperature increased, the narrow resonance of the central component also increased. As shown in Figure 6, at 0 ºC, only a slight residue of the Pake powder pattern remained and that became almost negligible at a higher temperature of about 24 ºC. A summary of the plasticizer T_gs for the pure plasticizer, 37% plasticized-bulk PVAc, 37% plasticized-adsorbed PVAc (including larger and smaller adsorbed-amount samples) as determined by NMR is shown in Table 1.

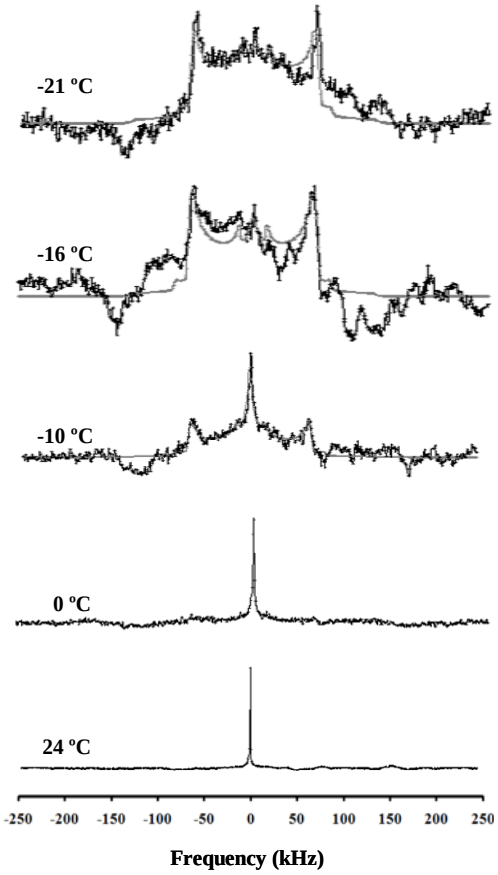

Figure 6. Experimental (black) and simulated (grey) ^{2}H NMR spectra for 37% plasticizer (DPGDB-d_{10}) with PVAc for the smaller adsorbed-amount (0.76 mg/m^2).

Table 1. NMR and TMDSC Glass Transition Temperature Ranges[a,b] for Pure Plasticizer and 37% Plasticized Samples

	NMR (from DPGDB-d_{10})			TMDSC	
sample	T_{onset}	T_{mid}	width	T_A	width
pure plasticizer	-30	-25	5	-53[c]	n/a
plasticized PVAc	5	15	10	-7	25
plasticized PVAc, larger adsorbed amount (2.60 mg/m^2)	0	24	24	15	30
plasticized PVAc, small adsorbed amount (0.76 mg/m^2)	< -21	-10	n/a	broad	n/a

[a] T_{onset} is where a narrowed component in the spectrum is first observed and T_{mid} is an estimate of the middle of the transition where the narrowed component is roughly about 3 times that of the height of the horns (rigid component).
[b] T_A is top of the peak from the derivative of the reversible heat flow component of the thermogram.
[c] Ref. 18

Comparisons of the ^{2}H NMR spectra of the pure plasticizer, 37% plasticized bulk polymer [44], and 37% plasticized-adsorbed samples were made at a temperature of about 24 ºC, as shown in Figure 7. While the spectrum of a sample containing a larger adsorbed amount, 2.60 mg/m^2, still showed a significant amount of the Pake powder pattern, the rest of the ^{2}H NMR spectra showed only a narrow resonance of the central component. However, the spectral width (the width at half-height) of the plasticized-bulk sample was broader than those of the pure plasticizer and the sample with a smaller adsorbed amount. Interestingly, the ^{2}H NMR spectrum of the sample containing the smaller adsorbed amount, 0.76 mg/m^2, was very similar to that of the pure plasticizer, as they both appeared as narrow sharp lines.

The simulations of the experimental ^{2}H NMR spectra are shown superimposed as the lighter lines in Figures 5 and 6. Although the spectra of adsorbed samples do not have a good signal to noise ratio, the fitting is quite reasonable. A series of simulated spectra with different jump rates, ranging from 1 to 1×10^9 Hz, was obtained using the MXQET program.

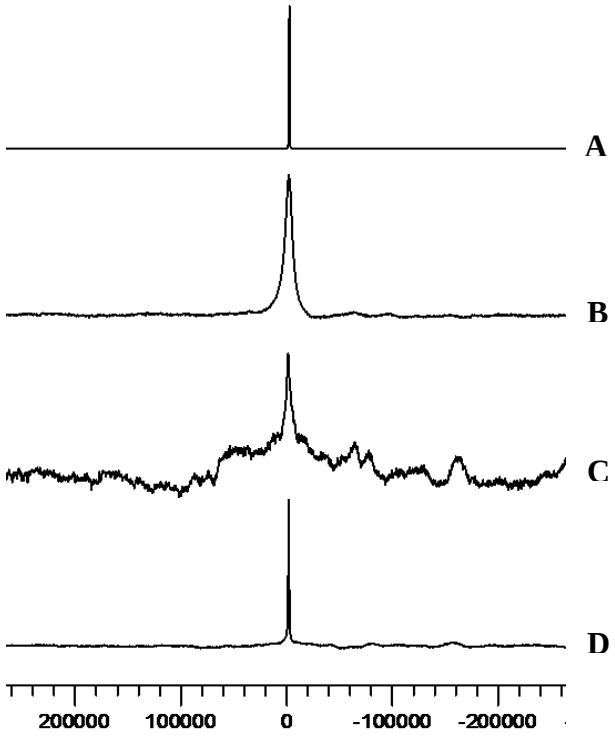

Figure 7. A comparison of the ^2H NMR spectra of the plasticizer DPGDB-d_{10} at a temperature of 24 ºC: A) pure plasticizer, B) 37% plasticizer in bulk sample, and 37% plasticizer in adsorbed samples with C) 2.60 mg/m^2 PVAc and D) 0.76 mg/m^2 PVAc.

A two-site jump model of a phenyl deuteron executing a 180º ring flip was used for the simulations. Fitting the simulations and experimental spectra was done using a MATLAB program. A broad distribution of spectra, with different jump rates was required for a good fit. The distributions of (log) jump rates as a function of temperature and plasticizer content are presented using bar graphs in the supporting information (appendix E). The fitted results represent the regimes of major motional components as slow, intermediate, and fast with respect to their jump rates. It is observed that, even with the fast exchange rate, $k > 10^8$ Hz, the 180º jumps about the C_2 symmetry axis does not result in isotropic motion. The isotropic motion, resulting in a narrow resonance, occurred at fast exchange rates when the spectrum was no longer sensitive to the jump rate. In a slow regime ($k < 10^4$ Hz), the phenyl ring flip motion was slow, resulting in Pake powder patterns with rigid components in which there was no significant loss of intensity during the quadrupole echo.

A loss in spectral intensity was observed as temperatures approached the glass transition. For the simulations, a significant intensity loss was found [45] as the exchange rate became faster, about 10^4-10^7 Hz (classified as the intermediate regime). This regime corresponds to the glass transition of a material where the collapse of a Pake pattern with rigid components and the rise of narrow resonance spectra of a liquid component are observed. Again, for the fast regime, k $>10^8$ Hz, there was little intensity loss of echo since liquid-like components are mostly found in this regime.

The log of the average jump rate (log <*k*>) as a function of temperature for the adsorbed samples with a larger adsorbed amount, 2.60 mg/m^2, is shown in Figure 8. The plot of log <k> values, as a function of inverse temperature for different plasticizer content, decreased with 1/T as expected. An apparent activation energy of the 180º ring flips (assuming linear behavior) was calculated to be 50 kJ/mol.

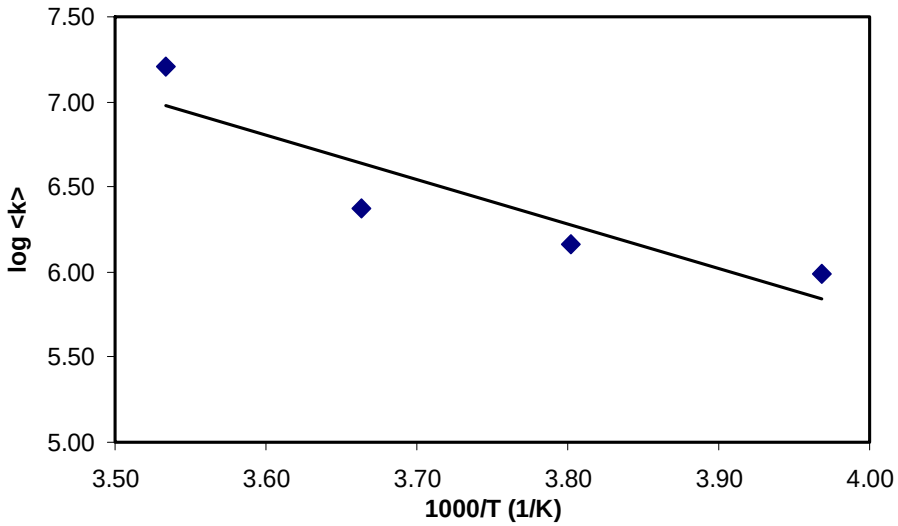

Figure 8. The log average jump rates values, log <*k*> for DPGDB-d_{10}, as a function of temperature for 37% plasticized-adsorbed sample, 2.60 mg/m^2.

However, with a broad distribution of jump rates (or correlation times), <k> was sometimes dominated by the larger rates. Therefore, the weight average of the logarithm of the jump rate, <log *k*> was also calculated for comparison, as shown in Figure 9. The

<log *k*> values, as a function of inverse temperature was quite linear and fitted well with the Arrhenius equation. The calculated activation energy from this <log k> was 18 kJ/mol. The k values used for both plots were obtained from the simulation of the rigid component with less than 10% of an isotropic motion was allowed. No plots were made for sample with small adsorbed amount, 0.76 mg/m^2, because the ^{2}H NMR spectra were composed of 25-30% of the narrowed component (isotropic motion).

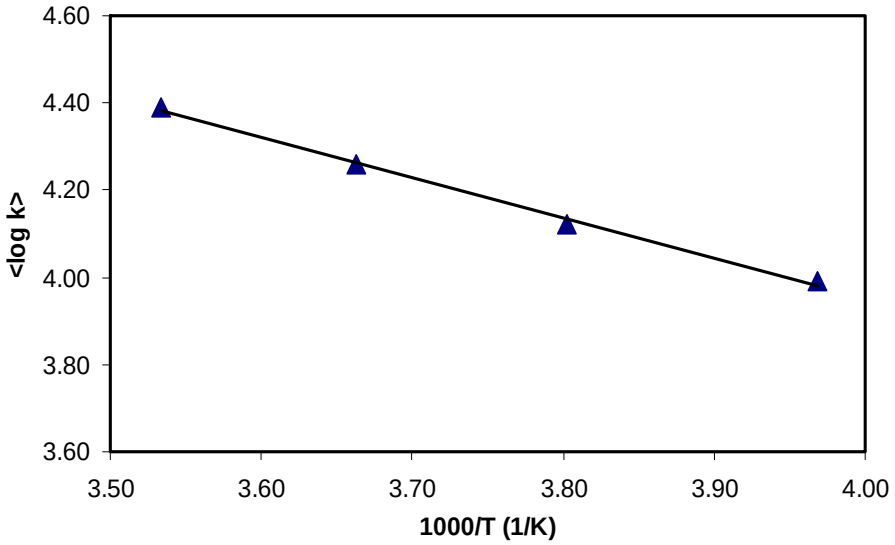

Figure 9. Average of the log jump rates values, <log *k*> for DPGDB-d$_{10}$, as a function of temperature for 37% plasticized-adsorbed sample, 2.60 mg/m^2.

Temperature modulated differential scanning calorimetry (TMDSC) was used to measure the T_gs of the adsorbed 37% plasticizer samples for the larger and the smaller adsorbed amounts. TMDSC thermograms of plasticized-adsorbed PVAc samples are shown in Figure 10. The derivative of the reversible heat flow rate was plotted as a function of temperature for the different adsorbed amount samples. The maximum of the derivative reversible heat flow rate curve was assigned as the T_g (TMDSC). For the 37% plasticized-bulk PVAc sample, only one transition was found with a T_g (TMDSC) of about -7 ºC and a transition width of about 25 ºC. On the other hand, the adsorbed sample with a larger adsorbed amount, 2.60 mg/m^2, showed two transitions described as loosely-

bound polymer (bulk-like), and tightly-bound polymer [7, 19, 46-47]. Although the two transitions found here were not as distinct as some in other reports [7, 46], the second transition appeared more like the shoulder of the first one. The T_g (TMDSC) observed for the loosely-bound transition of 37% plasticized-adsorbed PVAc, 2.60 mg/m^2, was about 15 ºC, with a transition width of about 30 ºC. Nevertheless, no transitions were observed for the sample with the smaller adsorbed amount, 0.76 mg/m^2. This is likely due to the broadened transition due to the plasticizer plus the small amount of polymer in the sample. For adsorbed PVAc on silica, the amount of tightly-bound polymer has been reported to be 0.78 mg/m^2 [47].

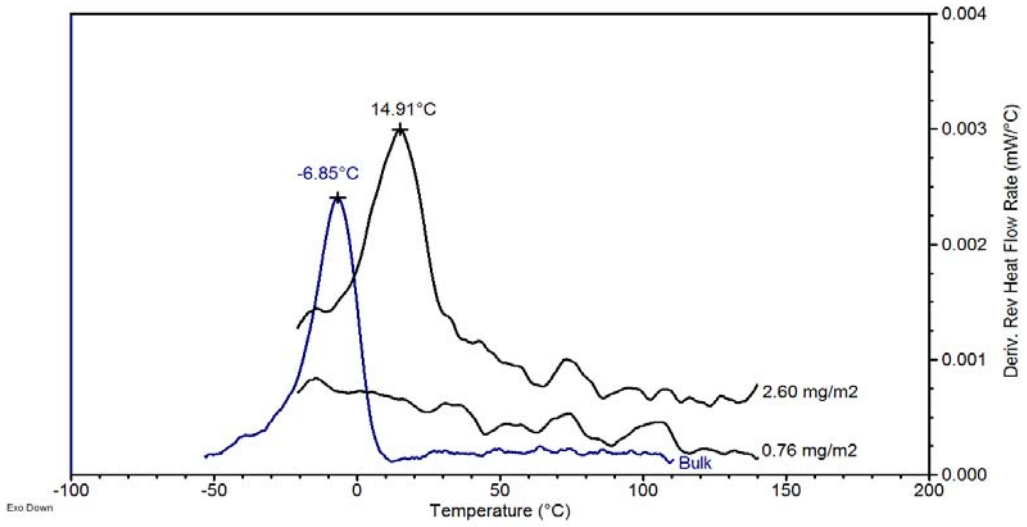

Figure 10. TMDSC derivative reversing heat flow rate curves of 37% plasticized-bulk PVAc (r.h. scale), 37% plasticized-adsorbed PVAc on silica for the larger (2.60 mg/m^2) and smaller (0.76 mg/m^2) adsorbed-amount samples. The bulk intensity has been normalized by arbitrary number to fit this overlay figure.

4. DISCUSSION

A Pake powder pattern was observed for a rigid component at low temperatures for the DPGDB-d_{10}. The quadrupolar splitting for a deuterium nucleus, $\Delta\nu_q$, is given by [18-19, 36, 44, 48-50].

$$\Delta\nu = \tfrac{3}{4} (e^2qQ/ h) (3\cos^2\theta (t) -1- \eta \sin^2 \theta (t) \cos^2 \varphi (t)) \quad (1)$$

where e^2qQ/h is the quadrupole coupling constant (qcc), θ and φ are the Euler angles from the principle-axis system. These angles define the relative orientation of the electric field tensor with respect to the applied magnetic field β_0, and η is the asymmetry parameter which defines the shape of the powder pattern. The asymmetry parameter is usually zero for aliphatic C-D bonds, indicating that the electric field gradient tensor is axially symmetric [17, 48-50]. However, for aromatic C-D bonds, the motionally averaged field gradient tensor is not axially symmetric [36].

Aromatic ring motions that included rigid, 180º ring flips, and isotropic motions were found for DPGDB-d_{10} corresponding to splittings of the two outer horns of 125 kHz, and the two inner horns of 29 kHz, and no splitting, respectively. The Pake powder patterns collapsed to a narrow resonance as the temperature increased. The changes in the line shapes for the adsorbed samples were similar to those of the bulk samples (PVAc/DPGDB-d_{10}), which have shown a certain degree of motional heterogeneity [44]. However, for the plasticized-adsorbed samples, the range of the temperatures where the two-component spectra existed was relatively larger than that of the plasticized-bulk samples (PVAc/DPGDB-d_{10}). In addition, the broader range of the plasticizer T_gs from both NMR and TMDSC was also observed for adsorbed samples, compared with those of the bulk samples (see Table 1). These results indicated a higher degree of motional heterogeneity in these adsorbed samples as compared with those of the bulk samples.

The activation energy of the 180º ring flips was calculated from the plot of log average jump rates, log <k> as a function of inverse temperature. The activation energy of the adsorbed sample was calculated to be 50 kJ/mol. The calculated activation energy from averages of the log of the jump rates plot, <log k>, was lower than those obtained from log <k>, about 18 kJ/mol. However, our results were not too far from other report with reported the apparent activation energy for pure 180 º ring flip motions of about 25 kJ/mol [51-53].

The objective of this study was to understand the reason for the ineffectiveness of plasticizer on a sample with the smaller adsorbed amount. The NMR results answer this quite well, based on the following evidence. First, there are significant differences in the dynamics of DPGDB-d_{10} in the two adsorbed samples, with the dynamics of the sample

with the smaller adsorbed amount being much faster than that in the larger adsorbed amount sample. Second, there is an unexpectedly large reduction in the T_g for the plasticizer in the adsorbed sample with a small adsorbed amount. Third, there was significant similarity in the pattern for the narrow resonance spectra of the adsorbed sample with the smaller adsorbed amount and that of a pure plasticizer.

The dynamics of plasticizer in bulk PVAc samples were previously reported [44]. Here, as shown in Figure 5, the dynamics of the adsorbed sample with the larger adsorbed amount seemed to be slower than that in bulk samples. Although, a rise in the central narrow resonance seemed to occur at about the same temperature (about 0-5 ºC) for both bulk and adsorbed (larger adsorbed amount) samples, the collapse of the powder pattern in bulk occurred at lower temperature than that in the larger adsorbed-amount sample. Several studies have also observed that the dynamics of bulk samples were faster than those of adsorbed samples [54-59]. On the other hand, as shown in Figure 6, the dynamics of DPGDB-d_{10} in the sample with the smaller adsorbed amount seems to be much faster than those found in the bulk plasticized PVAc samples and the sample with larger adsorbed amounts. The collapse of the powder pattern was seen at a lower temperature (-10 ºC) and only a small residual powder pattern was found at 0 ºC. Nevertheless, the dynamics of plasticizer on a smaller adsorbed-amount sample seemed to be somewhere between those of bulk and those of pure plasticizer, as seen in Figure 4.

It is known that the T_gs are good indicators and reflect the plasticization process. Hence, the effect of plasticizer can easily be observed through the T_gs. The reduction in T_g of thin polymeric films such as PVAc, poly(styrene), poly(methyl methacrylate) due to the presence of diluents such as water or plasticizers have been reported [60-62]. The effect of plasticizer on T_g reduction have also been found in supported PMMA films on silica. [63]

Several studies have compared the T_gs (NMR) of bulk and adsorbed polymers in the absence [4, 14, 17-19], and the presence of plasticizer [18, 19, 44]. Nambiar and Blum have reported a higher T_g of polymer for silica-adsorbed PVAc-d_3 than that of bulk PVAc-d_3 in both absence and presence of plasticizer. [18-19] In addition, they also observed that the weighted average of adsorbed PVAc-d_3 T_g's decreased with increased adsorbed amounts as determined by both NMR and TMDSC experiments [19]. In

contrast to the behavior monitored by the ^{2}H NMR spectra of adsorbed PVAc-d_3 [19], the collapse of the powder pattern for DPGDB-d_{10} in the smaller adsorbed-amount sample occurred at a temperature that was lower.

In our previous work [44], for polymer-plasticizer system, the T_g (NMR) of plasticizer and that of polymer were found to be similar. The plasticizer T_g of bulk PVAc containing 37% w/w plasticizer was reduced by 56 ºC while the sample with larger adsorbed amount has its plasticizer T_g reduced by 47 ºC compared with that of the pure polymer. On the other hand, an unexpectedly large decrease in the plasticizer T_g was observed in the smaller adsorbed-amount sample as shown in Table 1. However, this huge reduction in the plasticizer T_g has no effect on the polymer T_g as it has been previously reported [19].

As seen in Figure 7, the ^{2}H NMR spectra of a sample with a smaller adsorbed amount (0.78 mg/m^2) and those of a pure plasticizer are quite similar. Both spectra appeared as single narrow sharp lines representing the liquid-like component. This evidence has strongly suggested that, with a small amount of polymer adsorbed on the surfaces, plasticizer has very little or no involvement in the dynamics of the adsorbed polymer. Accordingly, it is clear that the plasticizer is not immobilized in the rigid polymer-silica interface. Instead, it is effectively excluded from the tightly-bound PVAc at the polymer-air interface where it can exist in a manner similar to that of pure plasticizer. Consequently, it has little or almost no effect on the dynamics of the adsorbed polymer.

5. CONCLUSIONS

^{2}H NMR has been used to probe the dynamics of the plasticizer, DPGDB-d_{10}, in conjunction with adsorbed PVAc on silica. The dynamics of plasticizer was in the adsorbed samples was found to be more heterogeneous than that observed in bulk samples. The DPGDB-d_{10} plasticizer has little or no effect on a small amount of adsorbed PVAc on silica. The ^{2}H NMR findings provided solid evidence that of the effect of

plasticizer in adsorbed polymers differs as a function of adsorbed amounts. An unexpectedly large decrease in the T_g as determined for the DPGDB-d_{10} occurs in the smaller adsorbed-amount samples. The narrow resonance spectra of samples with smaller adsorbed amounts of polymer were similar to those of the pure plasticizer. This evidence showed that, with a small amount of adsorbed polymer (i.e., tightly bound polymer), the DPGDB-d_{10} was excluded from penetrating the adsorbed PVAc at the polymer-air interface. Hence, it had very little or no effect on the dynamics of the adsorbed polymer.

6. ACKNOWLEDGEMENTS

The authors acknowledge the financial support of the National Science Foundation under grant DMR-1005606, the Missouri University of Science and Technology, and Oklahoma State University. The authors gratefully thank Raymond Kendrick for his technical support, Dr. Robert O'Connor for useful discussions, and Dr. Cyriac Kandoth and Waraporn Viyanon for their help on Fortran programming.

7. REFERENCES

1. Reading, M.; Hourston, D. J. *Modulated Temperature Differential Scanning Calorimetry, Theoretical and Practical Applications in Polymer Characterisation*. Springer: Dordrecht. The Netherlands, 2006.
2. Zou, H.; Wu, S.; Shen, J. *Chem. Rev.* **2008**, *108*, 3893.
3. Geppi, M.; Borsacchi, S.; Mollica, G.; Veracini, C. A. *Appl. Spec. Rev.* **2009**, *44*, 1.
4. Lin, W. Y.; Blum F. D. *Macromolecules* **1998**, *31*, 4135.
5. Fleer, G. J.; Cohen Stuart, M. A.; Scheutjens, J. M. H. M.; Cosgrove, T.; Vincent, B. *Polymers at Interfaces*; Chapman and Hall: London, U.K., 1993.
6. Blum, F. D. *Ann. Rep. NMR Spec.* **1994**, *28*, 277.
7. Blum, F. D.; Young, E. Y.; Smith, G.; Sitton O. C. *Langmuir* **2006**, 22, 4741.

8. Keddie, J. L.; Jones, R. A. L.; Cory, R. A. *Faraday Discuss.* **1994**, *98*, 219.
9. Reiter, G. *Europhys. Lett.* **1993**, *23*, 579.
10. Burak, M.; Blum, F. D. Langmuir **2010**, *26*, 5226.
11. Porter, C. E.; Blum, F. D. *Macromolecules* **2000**, *33*, 7016.
12. Porter, C. E.; Blum, F. D. *Macromolecules* **2002**, *35*, 7448.
13. Grohen, Y.; Brogly, M.; Labbe, C.; David, M. O.; Schultz, J. *Langmuir* **1998**, 14, 2929.
14. Blum, F. D.; Xu, G.; Liang, M.; Wade, C. G. *Macromolecules* **1996**, *29*, 8740.
15. Lin, W. Y.; Blum F. D. *Macromolecules* **1997**, *30*, 5331.
16. Lin, W. Y.; Blum F. D. *J. Am. Chem. Soc.* **2001**, *123*, 2032.
17. Metin, B.; Blum F. D. *J. Chem. Phys.* **2006**, *125*, 054707/1-054707/9.
18. Nambiar, R.; Blum, F. D. *Macromolecules* **2008**, *41*, 9837.
19. Nambiar, R.; Blum, F. D. *Macromolecules* **2009**, *42*, 8998.
20. Fortier-McGill, B.; Raven, L. *Macromolecules* **2009**, *42*, 247.
21. Robb, I. D.; Smith, R. *Polymer* **1977**, *18*, 500.
22. Afif, A.; Hommel, H.; Legrand, A. P. *Colloids Surf. A* **1996**, *111*, 177.
23. Painter, P. C.; Coleman, M. M. *Fundamentals of Polymer Science 2nd ed*; CRC Press: Boca Raton, 1997.
24. Billmeyer, F. W. *Textbook of Polymer Science*, *3rd ed.;* John Wiley and Sons: New York, 1984.
25. Gould, R. *Plasticization and Plasticizer Processes*, American Chemical Society, Washington, D.C, 1965.
26. Sears, J. K.; Darby, J. R. *The Technology of Plasticizers*; Wiley: New York, 1982.
27. Boyer, R. F. *Transitions and Relaxations in Amorphous and Semicrystalline Organic Polymers and Copolymers*; John Wiley and Sons: New York, 1977.
28. Pradhan, D. K.; Choudhary, R. N. P.; Samantaray, B. K.; Karan, N. K.; Katiyar, R. S. *Int. J. Electrochem. Sci.,* **2007,** *2*, 861.
29. Pradhan, D. K.; Samantaray, B. K.; Choudhary, R. N. P.; Thakur, A. K. *J. Pow. Sour.* **2005**, *139*, 384.
30. Wang, N.; Zhang, X.; Mab, X.; Fang, J. *Polymer Degradation and Stability* **2008**, *93* 1044.

31. Lirova, B. I.; Lyutikova, E. A.; Vasil'eva, N. V.; Berkuta, B. A.; Prusskii, M. I. *Russ. J. Appl. Chem.* **2008**, *81*, 298.
32. Vogel, A. I.; Tatchell, A. R.; Furnis, B. S.; Hannaford, A. J. *Vogel's Textbook of Practical Organic Chemistry 3rd ed.* Pearson Education Limited, England, 1956.
33. Metin, B. **2006**. *Segmental Dynamics in Poly(Methyl Acrylate) Through the Glass Transition Region.* Dissertation(Ph.D.). University of Missouri-Rolla.
34. Greenfield, M. S; Ronemus, A. D.; Vold, R. L.; Vold, R. R.; Ellis, P. D.; Raidy, T. E.; *J. Magn. Reson.* **1987***, 72,* 89.
35. Vold, R. R.; Vold, R. L. *Adv. Magn. Opt. Reson.* **1991***, 16,* 85.
36. Jelinski, L. W. *"Deuterium NMR of Solid Polymers", High-Resolution NMR*
37. Gall, C. M.; Diverdi, J. A.; Opella, S. J. *J. Am. Chem. Soc.* **1981**, *103*, 5039.
38. Hiraoki, T.; Kogame, A.; Nishi, N.; Tsutsumi, A. *J. Mol. Struct.* **1998**, *441*, 243.
39. Boden, N.; Clark, L. D.; Hanlon, S. M.; Mortimer, M. *Faraday Symp.* **1978**, *13*, 109.
40. Montgomery, C. R.; Bunce, N. J.; Jeffrey, K. R. *J. Phys, Chem.* **1988**, *92*, 3635.
41. Simpson, J. H.; Rice, D. M.; Karasz, F. E. *J. Polym. Sci. A*, **1992**, *30*, 11.
42. Silverstein, R. M.; Webster, F. X.; Kiemle, D. *Spectrometric Identification of Organic Compounds 7th ed*; John Wiley & Sons: New Jersey, 2005.
43. Navarro, R.; Perrino, M. P.; Tardajos, M. G.; Reinecke, H. *Macromolecules*, **2010**, *43*, 2377.
44. Hetayothin, B.; Blum F. D. "Dynamic of Plasticizer Di(propylene glycol) dibenzoate-d_{10} in Bulk Poly(Vinyl Acetate) by Solid-State ^{2}H NMR" *To be submitted*.
45. Abraham, A. *The principles of Nuclear Magnetism*; Clarendon Press: Oxford, U.K., 1961.
46. Hetayothin, B.; Blum F. D. "Thermal Analysis of Adsorbed Poly(Methyl methacrylate) on Silica: Effect of Molecular Mass" *To be submitted*.
47. Hetayothin, B.; Blum F. D. "Comparative Study of Adsorbed Poly(Methyl methacrylate), Poly(Vinyl Acetate), and Poly(Methyl Acrylate) on Silica using Temperature Modulated Differential Scanning Calorimetry (TMDSC)" *To be submitted*.
48. Higinbotham, J.; Marshall, I. in *Annual Reports on NMR Spectroscopy*, Webb, G. A., Ed.; Academic, San Diego, **2001**, vol. 43, p. 59.

49. Kemp, W. *NMR in Chemistry-A Multinuclear Introduction*, Macmillan, London, 1986.
50. Schmidt-Rohr, K.; Spiess, H. W. *Multidimensional Solid-State NMR and polymers*, Academic, San Diego, 1994.
51. Cholli, A. L.; Dumais, J. J.; Engel, A. K.; Jelinski, L. W. *Macromolecules* **1984**, *17*, 2399.
52. Hummel, J. P.; Flory, P. J. *Macromolecules* **1980**, *13*, 479
53. Tonelli, A. E. *J. Polym. Sci., Polym. Lett. Ed.* **1973**, *11*, 441.
54. Liang, T. M.; Dickson, P. N.; Miller, W. G. in *Polymerization Characterization by NMR and ESR*; Woodword, A. E., Bovey, F. A.; Eds.; ACS Symposium Series 142; American Chemical Society: Washington, DC, 1980; p 1.
55. Thambo, G.; Miller, W. G. *Macromolecules*, **1990**, *23*, 4397.
56. Neitering, K. E.; Miller, W. G. in *Molecular Characterization of Interfaces*; Ishida, H., Kumar, G., Eds.; Plenum: New York, 1985; p 145.
57. Mansfield, K. F.; Theodorou, D. N. *Macromolecules* **1989**, *22*, 3143.
58. Chakraborty, A. K.; Adriani, P. M. *Macromolecules* **1992**, *25*, 2470.
59. Shaffer, J. S.; Chakraborty, A. K. *Macromolecules* **1993**, *26*, 1120.
60. Kim, S.; Mundra, M. K.; Roth, C. B.; Torkelson, J. M. *Macromolecules* **2010**, *43*, 5158.
61. Ellison, C. J.; Ruszkowski, R. L.; Fredin, N. J.; Torkelson, J. M. *Phys. Rev. Lett.* **2004**, *92*, 095702.
62. Bingemann, D.; Wirth, N.; Gmeiner, J.; Rossler, E. A. *Macromolecules* **2007**, *40*, 5379.
63. Mundra, M. K.; Ellison, C. J.; Rittigstien, P.; Torkelson, J. M. *Eur. Phys. J. Spec. Top.* **2007**, *141*, 143.

5. QUANTITATIVE ANALYSIS OF THERMOGRAMS FOR ADSORBED POLYMERS ON SILICA

Boonta Hetayothin[1] and Frank D. Blum[1,2]

1. Departments of Chemistry, Missouri University of Science and Technology, Rolla, Missouri 65409-0010, USA

2. Departments of Chemistry, Oklahoma State University, Stillwater, Oklahoma 74078, USA

1. INTRODUCTION

Adsorbed polymers with thicknesses that range from a few to several hundred nanometers are of technological interest for development of electronic and optical devices. However, the physical properties of polymers at interfaces can be quite different from those in bulk due to the interactions between the absorbed polymers and the surface. In cases where polymer molecules are strongly adsorbed at the interface, polymer chains at the polymer-air interface will have more motional freedom than those at the polymer-substrate interface. When the chains are more restricted on the surface, a higher glass transition temperature (T_g) results, as compared with that of the bulk polymer.[1-2]

A study of adsorbed poly(methyl methacrylate) (PMMA) on silica using temperature-modulated differential scanning calorimetry (TMDSC) has recently been reported.[1] In that study, the thermograms of adsorbed PMMA on silica have been quantified. Here we report a comparison of two methods used to quantify the thermal transitions in adsorbed polymers on silica.

* Author to whom correspondence should be addressed: Frank D. Blum (fblum@okstate.edu)

2. EXPERIMENTAL

Poly(methyl methacrylate) (PMMA) (M_w = 450 kDa, Aldrich Chemical Co., Milwaukee, WI), poly(vinyl acetate) (PVAc) (Mw = 240 kDa, Scientific Polymer Products, Inc., Ontario, NY) were used as received. Poly(methyl acrylate) (Mw = 110 kDa) was prepared in our laboratory. The molecular masses were determined by using gel permeation chromatography with a Dawn EOS laser light scattering instrument and an Optilab refractive index detector (Wyatt Technology, Santa Barbara, CA). Sample preparation and thermal analysis procedures can be found elsewhere.[1,2]

One method for quantifying the glass transition of adsorbed polymers on silica is shown in Figure 1. A sigmoidal baseline was chosen for each separated transition.[1] In a second method (shown in Figure 2), a perpendicular drop method (TA Universal Analysis V4.2E software) was used to estimate the area under the transitions in the ($dQ_{reversing}/dT$) plots. In this method, a straight baseline was chosen over the range of two transition temperatures. The two overlapping transitions are separated by a vertical line that is perpendicular to the baseline at the temperature where the first transition (A) ends and the second transition (B) begins. The areas under those two transitions were integrated. The T_g of each transition was taken at the peak of the derivative curve.

2.1. Model

Recently, our research group described the thermal behavior of adsorbed polymers using a two-component model with the assumption that there are two distinct types of adsorbed polymer segments (A - loosely-bound and B - tightly-bound segments).[1] Starting with bare silica, one can envision adsorbing increasing amounts of polymer as tightly-bound polymer (B) until a certain amount, m'_{pB}, is reached, after which, additional polymer added becomes loosely bound.

A normalized polymer mass, m'_p, was defined as the total mass of adsorbed polymer (from thermogravimetric analysis) divided by the mass of silica used, which is also the sum of the masses for the two components, or

$$m'_p = m'_{pA} + m'_{pB} \quad (1)$$

The ratio of the heat flow changes of components A and B, given by r, is related to the ratios of the heat capacities of the components, or

$$r = \Delta Q_A / \Delta Q_B = m'_{pA} \Delta C_{pA} / (m'_{pB} \Delta C_{pB}) \quad (2)$$

In effect, the ratio, r, is the ratio of the intensities in the derivative mode thermograms. From eq. (2) and (3), a linear equation can be made, or

$$r = (m'_p - m'_{pB}) \Delta C_{pA} / (m'_{pB} \Delta C_{pB})$$

$$= [\Delta C_{pA} / (m'_{pB} \Delta C_{pB})] m'_p - \Delta C_{pA} / \Delta C_{pB} \quad (3)$$

This equation suggests that r should be a linear function m'_p as long as the amount of polymer adsorbed is greater than a minimum amount of tightly bound segments (m'_{pB}). One estimate of the behavior of the polymer at the interface is in terms of a bound fraction, f_B, which is the ratio of the mass of bound polymer at the interface to the total amount of adsorbed polymer.[1,3] This can be expressed as a function of the experimental observable, r, as

$$f_B = m'_{pB} / m'_p = m_{pB} / m_p = 1/(1 + r\Delta C_{pB} / \Delta C_{pA}) \quad (4)$$

The fraction of bound polymer, f_B, can be estimated from the model by using the value of m'_{pB} obtained from a linear regression.

3. RESULTS AND DISCUSSION

TMDSC thermograms show two distinct peaks for absorbed PMMA on silica which correspond to the loosely- and tightly-bound segments of polymer at the interface. The area under the two transitions must be carefully quantified to ensure the accuracy and reproducibility of the data. A comparison of the two aforementioned methods is discussed here using the thermograms of PMMA from a previous report.[1] The quantification of other adsorbed polymers on silica, PVAc, and PMA are also described.

In both methods, the determination of the baseline was estimated using the modification of T_g determination.[4] This method involves an extrapolation of the curves where the slope starts changing before and after each transition, as demonstrated in Figure 3. A tangential line (red dotted) is drawn to intersect with the extrapolation lines

(black dashed). The intercepts, before and after the transition, are taken as the starting and end points of the area under the transition in the derivative plot. The T_g is taken as the temperature at the inflection point of the transition.

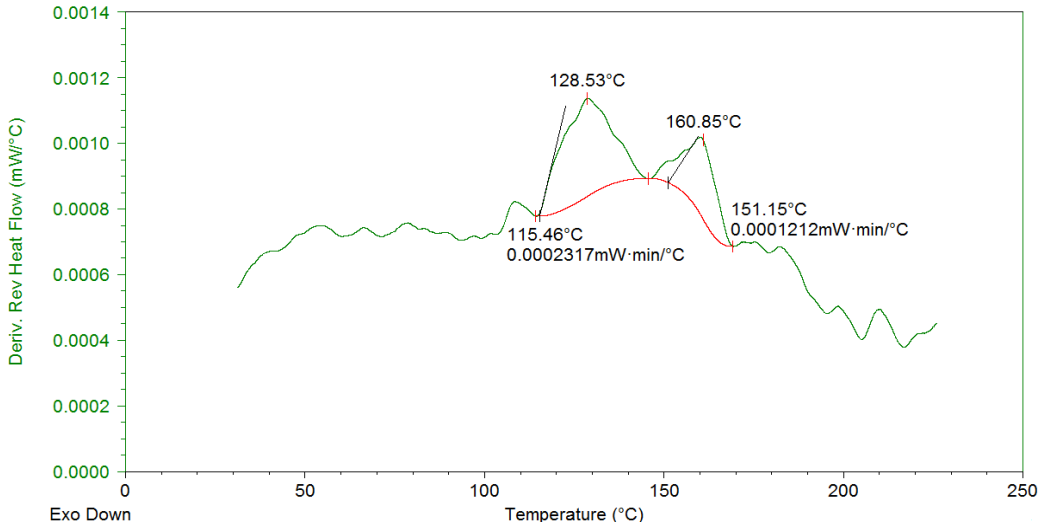

Figure 1. Derivative thermogram of adsorbed PMMA on silica showing the sigmoidal baseline applied for each transition in the earlier method.

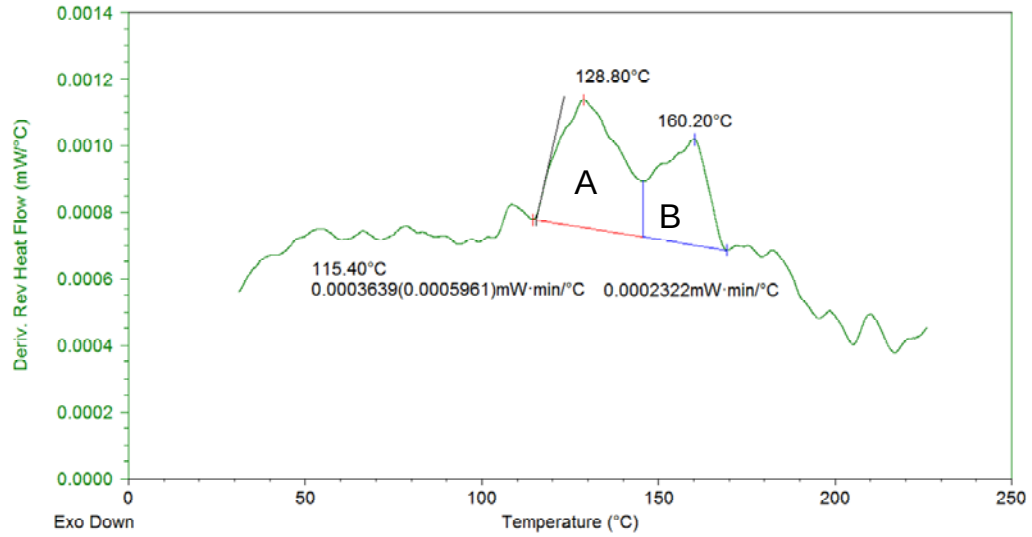

Figure 2. Derivative thermogram of adsorbed PMMA on silica showing the perpendicular drop method.

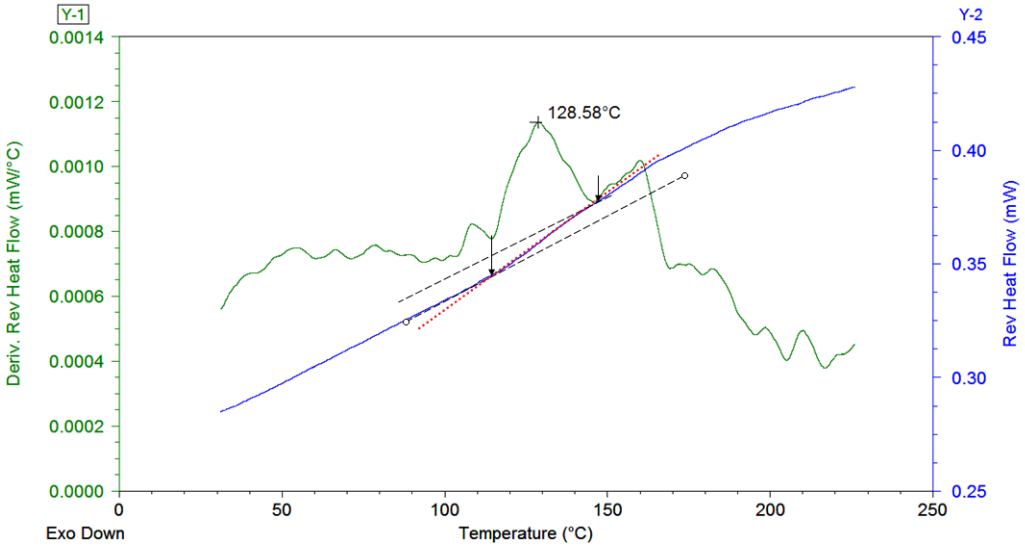

Figure 3. Derivative thermogram of adsorbed PMMA on silica showing the intercept of the tangent lines that determine the starting and end points for the area under the transition.

A plot of the ratio, r, for the areas of the A and B components in the thermograms is a linear function of the normalized mass of polymer (m'_p), as shown in Figure 4 (sigmoidal method) and Figure 5 (perpendicular drop method). The intercept of the line yields the ratio of the heat capacity changes, $\Delta C_{pA}/\Delta C_{pB}$, and the slope gives $\Delta C_{pA}/(m'_{pB}\ \Delta C_{pB})$. In previous work,[1] a sigmoidal baseline was used and the area under the transition was separately integrated, as shown in Figure 1. Integration using that method yielded a ratio of the heat capacities of about 6.1, as shown in Figure 4. The amount of tightly bound polymer, as calculated from equation 4 was 1.30 mg/m^2. On the other hand, a perpendicular drop method with linear baseline (shown in Figure 2), with the same set of thermograms, yielded a ratio of the heat capacities of about 3.6 (shown in Figure 5) with the amount of tightly bound polymer as 1.18 mg/m^2.

Instead of choosing a linear baseline over a range of two transition temperatures, the sigmoidal baseline can also be applied in the same manner with the perpendicular drop method; nevertheless, the choice of the baseline of the perpendicular drop method showed no significant difference in the results. When the sigmoidal baseline used with the perpendicular drop method, the ratio of the heat capacities was about 3.5 and the amount of tightly bound polymer was 1.17 mg/m^2.

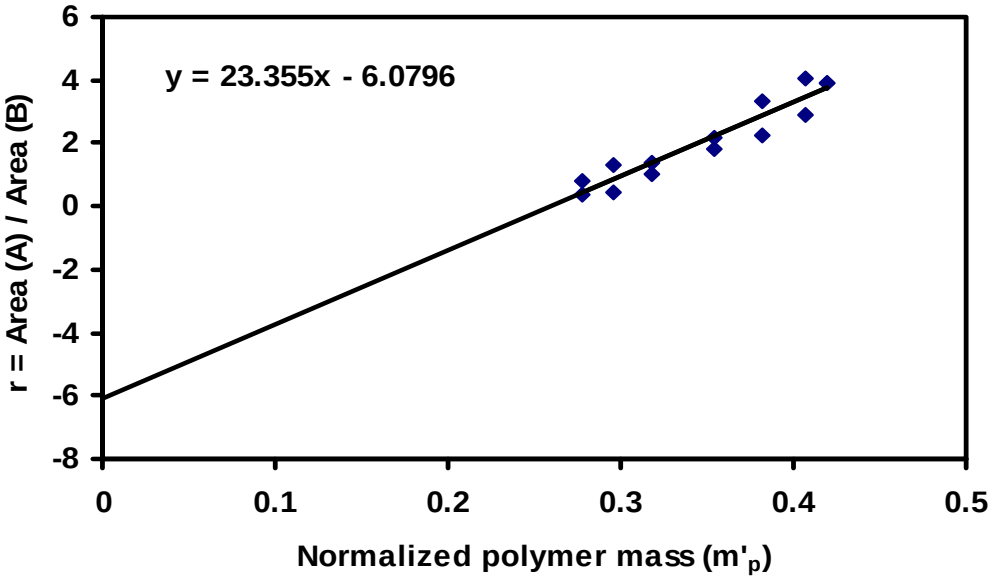

Figure 4. Ratio (r) of the areas of the A and B thermal transitions of adsorbed PMMA as a function of the relative amount of polymer (m'_p), using the sigmoidal baseline method for area integration.

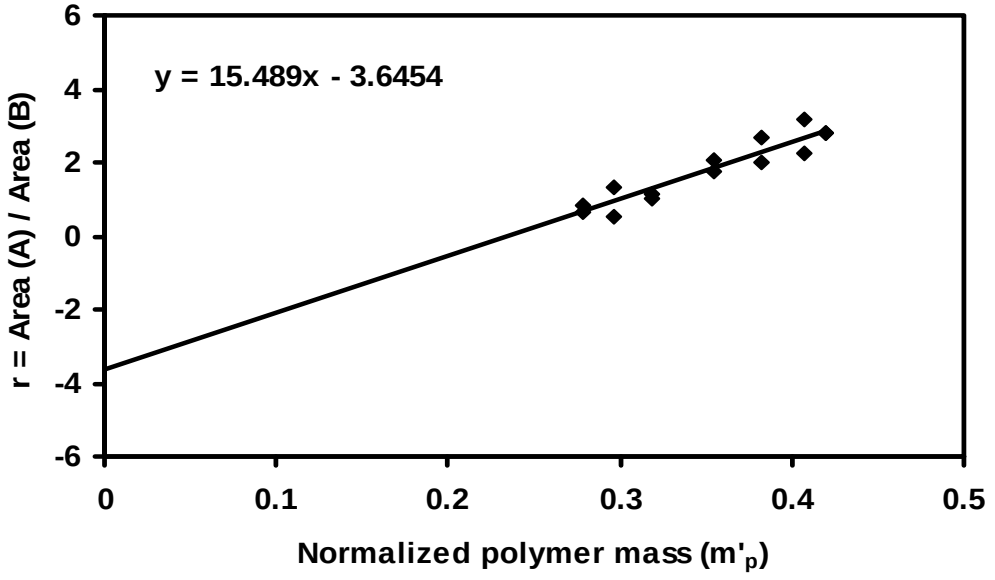

Figure 5. Ratio (r) of the areas of the A and B thermal transitions of adsorbed PMMA on silica as a function of the relative amount of polymer (m'_p), using the perpendicular drop method with linear baseline for area integration.

The major advantage of using the perpendicular drop method over the earlier method is that when the transition for the tightly-bound polymer becomes broader or shoulder-like (rather than a distinct peak) application of the sigmoidal baseline fails. Examples of these broader transitions can be found in other types of polymer adsorbed on silica, such as PVAc (Figure 6), and are even more pronounced in the broader PMA thermograms (Figure 7).

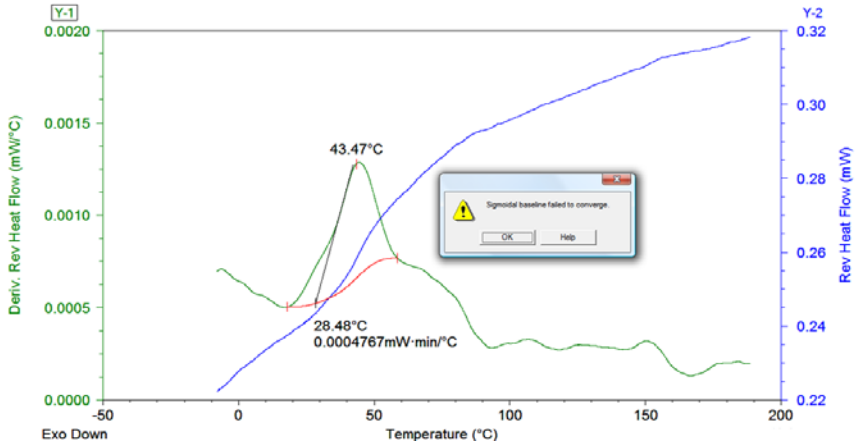

Figure 6. Failure of the sigmoidal baseline application in the second thermal transition (tightly-bound) of adsorbed PVAc on silica.

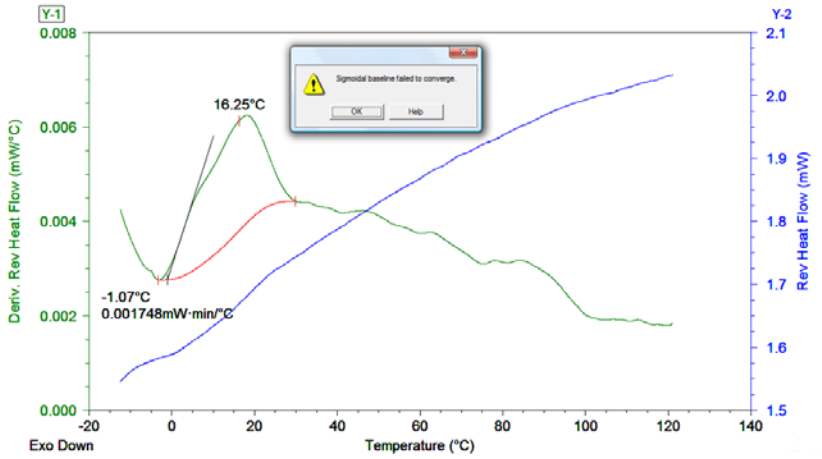

Figure 7. Failure of the sigmoidal baseline application in the second thermal transition (tightly-bound) of adsorbed PMA on silica.

4. CONCLUSIONS

A comparison was made of two methods for the integration of an area under the transition of adsorbed polymer on the silica. The integration of each separate transition using a sigmoidal baseline and a perpendicular drop. These two methods showed differences in both the ratio of heat capacity and the amount of tightly bound polymer. The sigmoidal one yielded a ratio of heat capacities that was about 1/3 higher than that of the perpendicular drop method, and approximately 10% more of the amount of tightly bound polymer. A major advantage of using a perpendicular method over the sigmoidal method is that the former is applicable to a wider range of systems, including those with broader or more shoulder-like transitions.

5. ACKNOWLEDGEMENTS

The authors thank the National Science Foundation under Grant No. DMR-0706197 and Missouri University of Science and Technology for financial support of this research. We also thank Mani Nair for providing the PMA.

6. REFERENCES

1. Blum, F.D.; Young, E.N.; Smith, G.; Oliver, S.C. *Langmuir* **2006**, *22*, 4741.
2. Kulkeratiyut, S.; Kulkeratiyut, S.; Blum F. D. *J. Polym. Sci, Part B.* **2006**, 44, 2071.
3. Fleer, G. J.; Cohen-Stuart, M. A.; Scheutjens, J. M. H. M.; Cosgrove, T.; Vincent, B. *Polymer at Interfaces*; Chapman & Hall: London, 1993.
4. Young, E.N. **2004**. *Thermal Characterization of the glass transition of adsorbed PMMA using modulated differential scanning calorimetry*. Thesis (Masters). University of Missouri-Rolla.

APPENDIX A.

TEMPERATURE-MODULATED DIFFERENTIAL SCANNING CALORIMETRY (TMDSC) THERMOGRAMS FOR ADSORBED POLYMERS ON SILICA

This appendix includes supporting figures for the work done on TMDSC experiments (paper 1 and 2). The area integrations of adsorbed PMMA on silica at various adsorbed amounts for three different molecular masses (32 kDa, 85 kDa, and 450 kDa) are shown in Figures A1-A15. While the area integrations of adsorbed PVAc and PMA on silica at various adsorbed amounts are shown in Figures A16-A24.

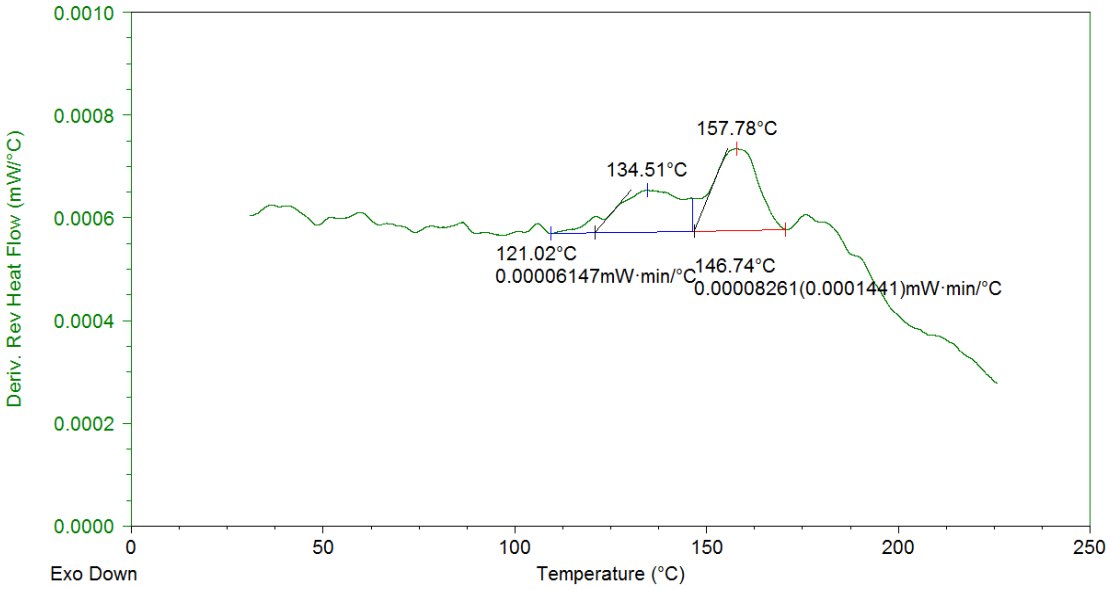

Figure A1. TMDSC thermogram of 32 kDa adsorbed PMMA on silica, 0.78 mg/m^2.

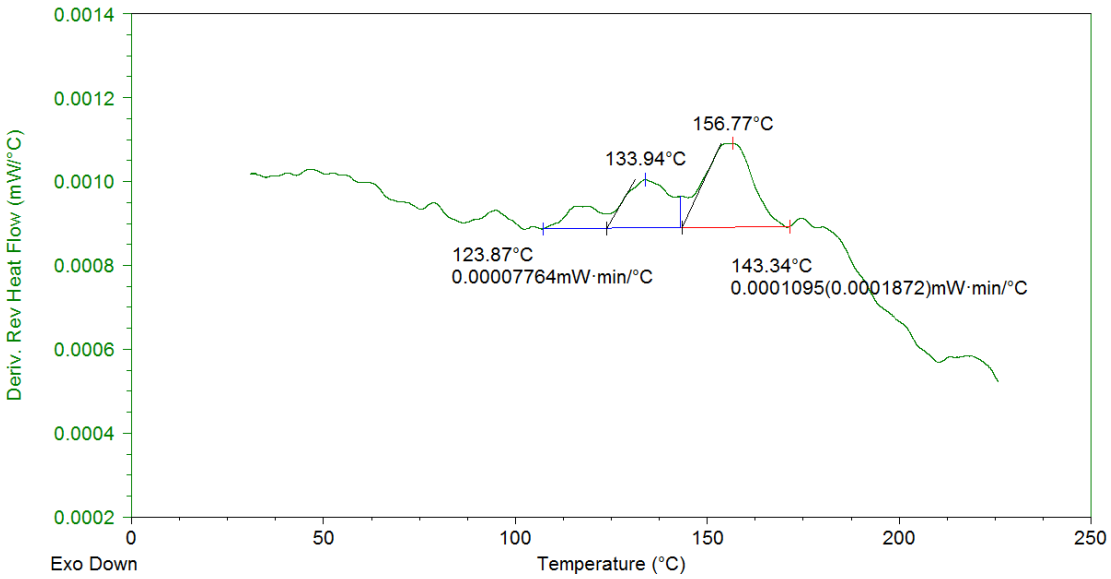

Figure A2. TMDSC thermogram of 32 kDa adsorbed PMMA on silica, 0.92 mg/m2.

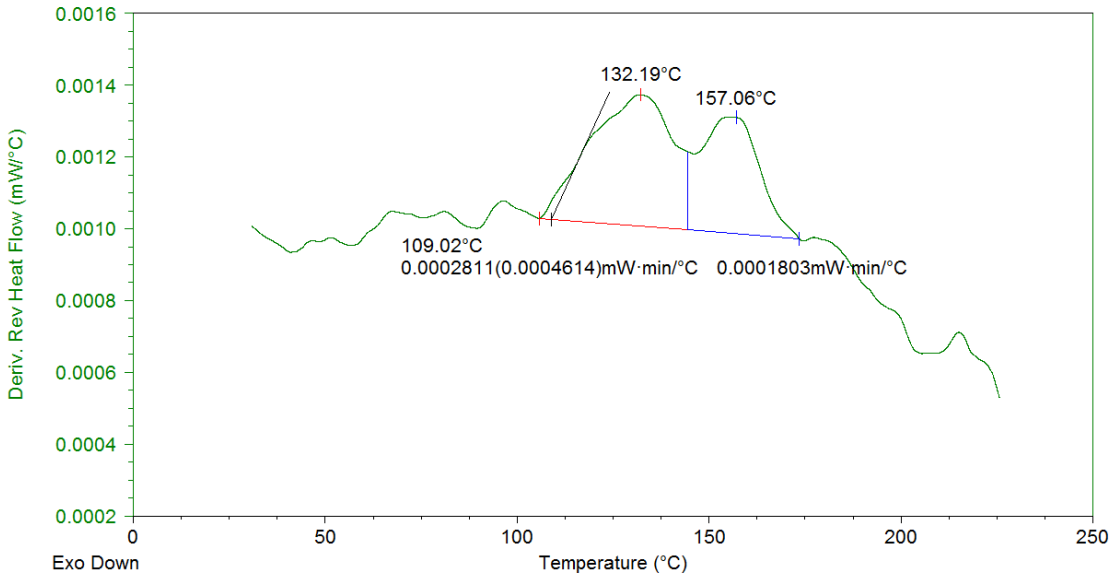

Figure A3. TMDSC thermogram of 32 kDa adsorbed PMMA on silica, 1.33 mg/m^2.

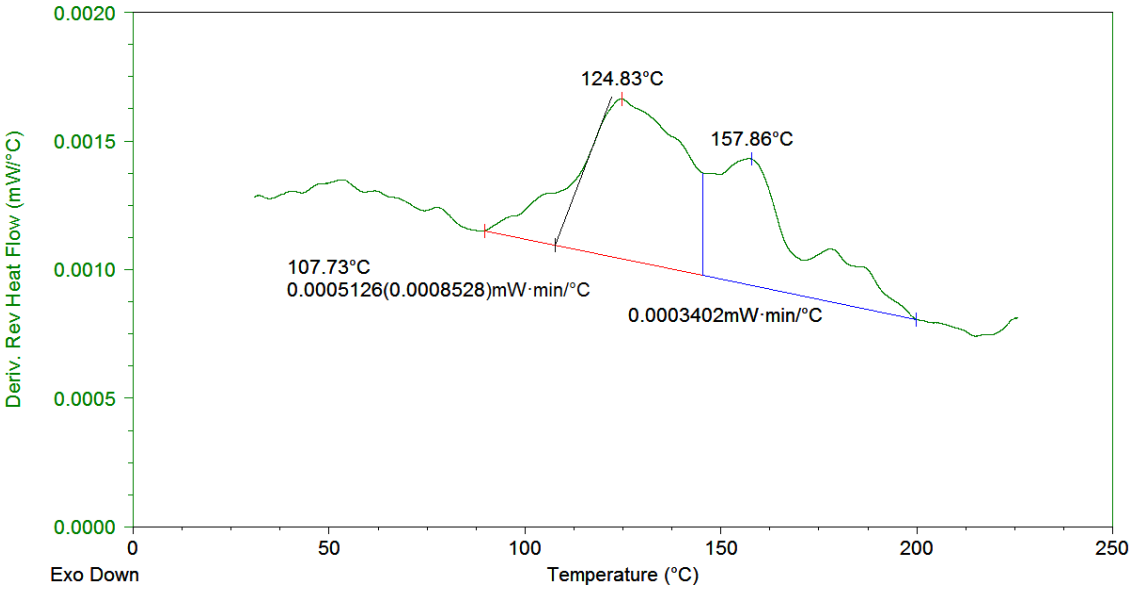

Figure A4. TMDSC thermogram of 32 kDa adsorbed PMMA on silica, 1.43 mg/m^2.

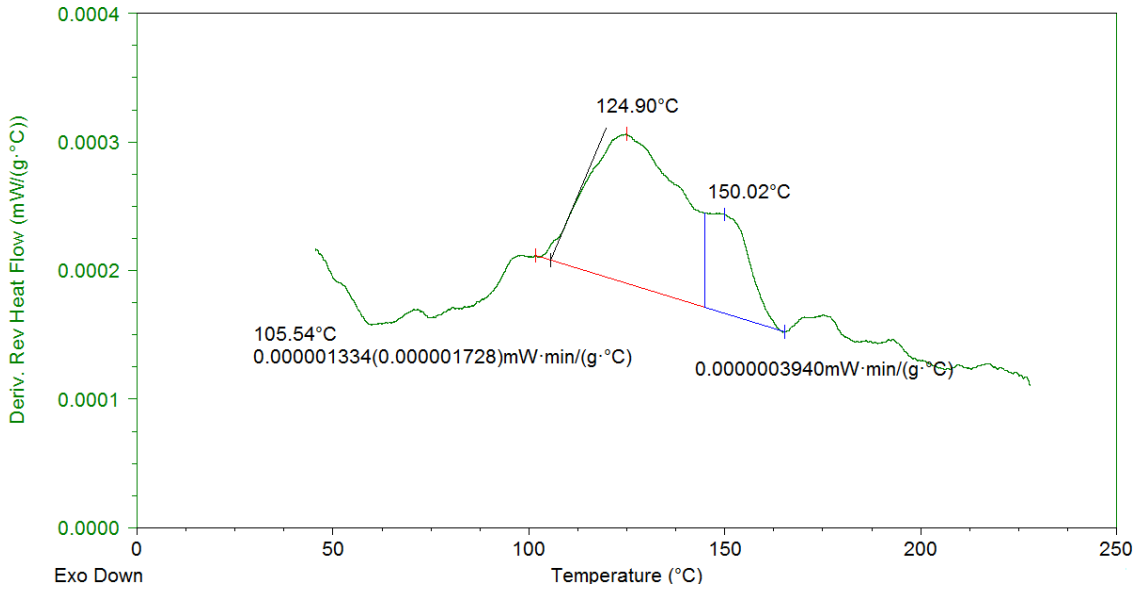

Figure A5. TMDSC thermogram of 32 kDa adsorbed PMMA on silica, 1.81 mg/m^2.

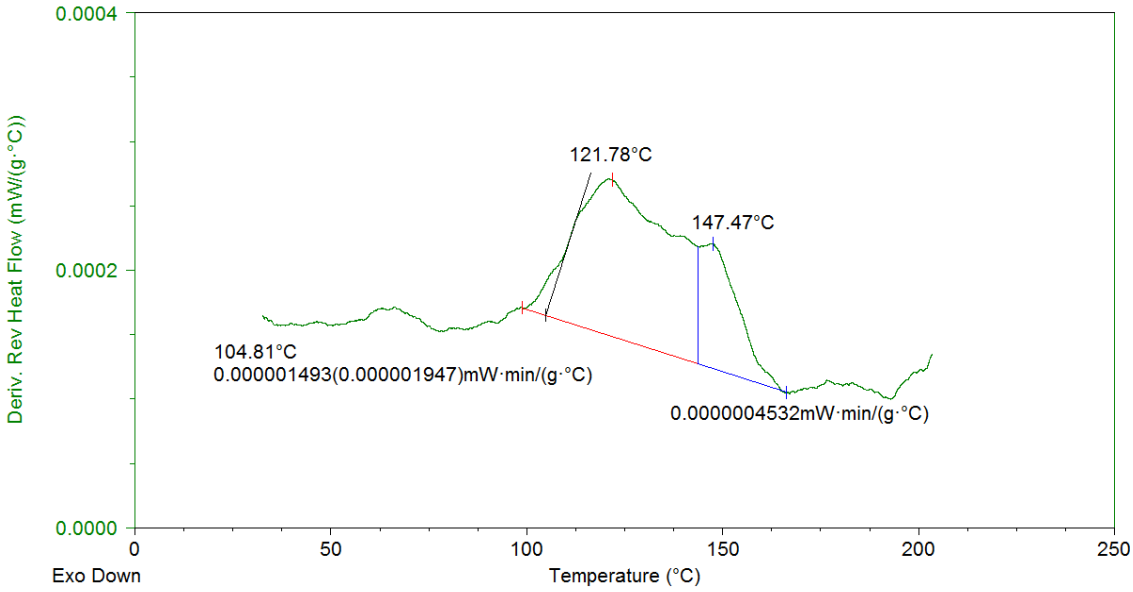

Figure A6. TMDSC thermogram of 32 kDa adsorbed PMMA on silica, 2.03 mg/m^2.

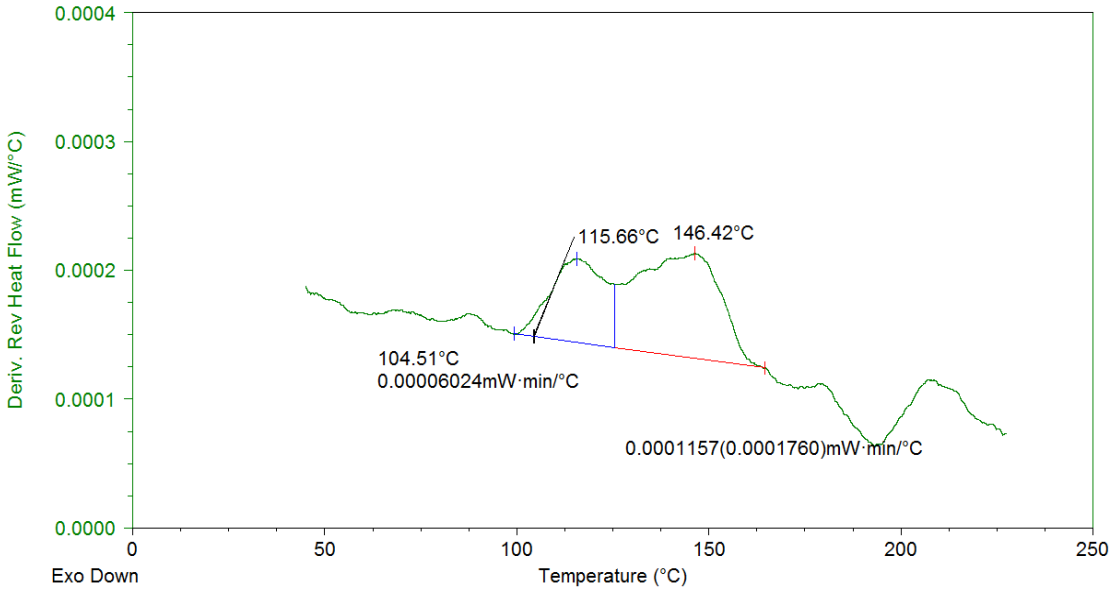

Figure A7. TMDSC thermogram of 85 kDa adsorbed PMMA on silica, 1.02 mg/m^2.

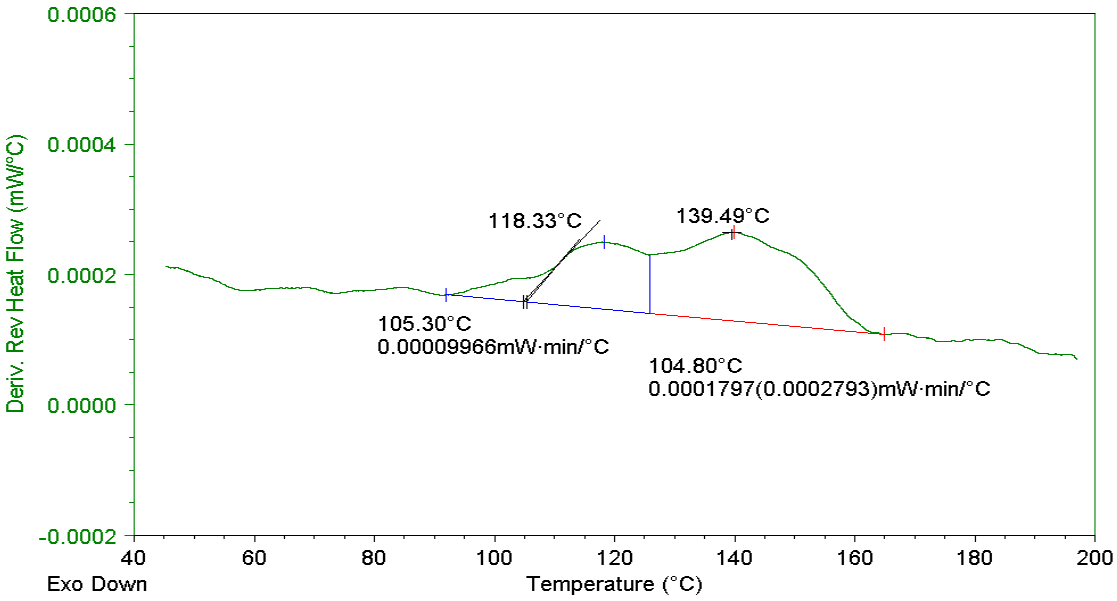

Figure A8. TMDSC thermogram of 85 kDa adsorbed PMMA on silica, 1.28 mg/m^2.

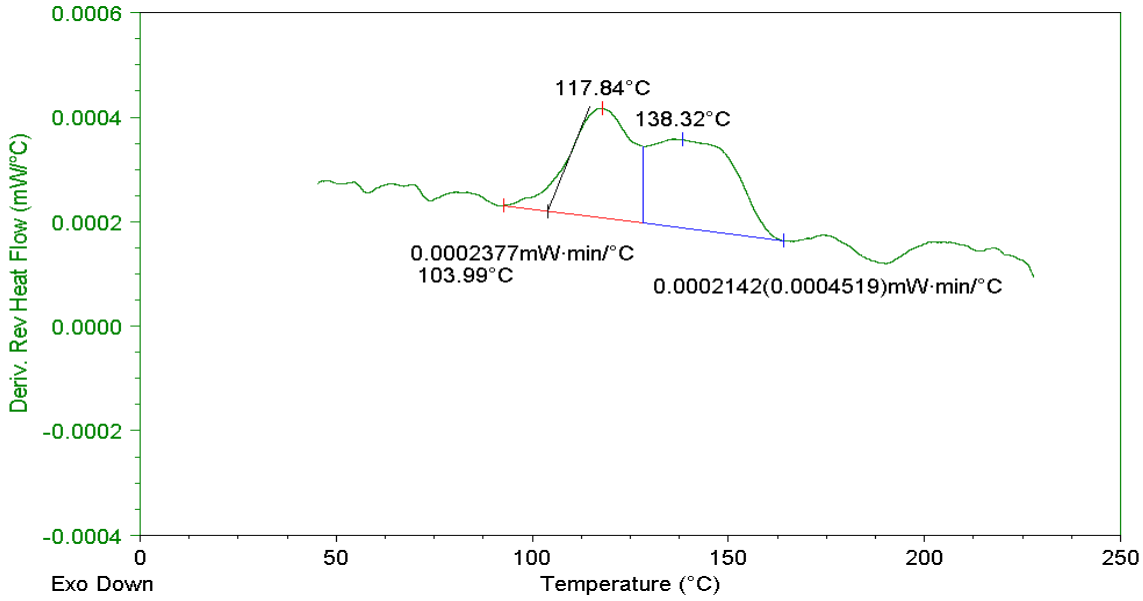

Figure A9. TMDSC thermogram of 85 kDa adsorbed PMMA on silica, 1.47 mg/m^2.

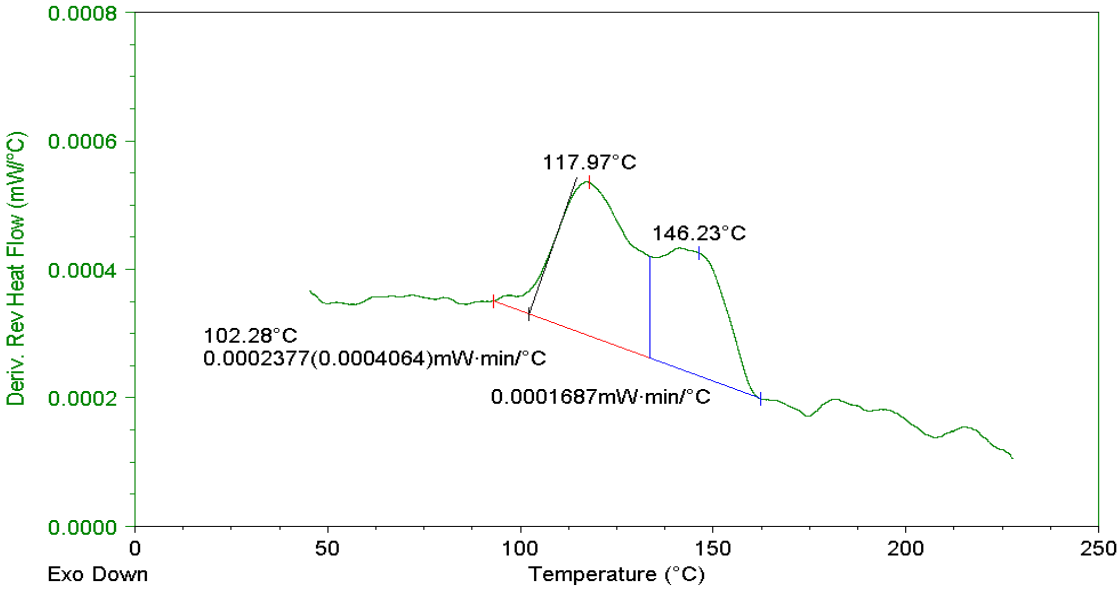

Figure A10. TMDSC thermogram of 85 kDa adsorbed PMMA on silica, 1.72 mg/m^2.

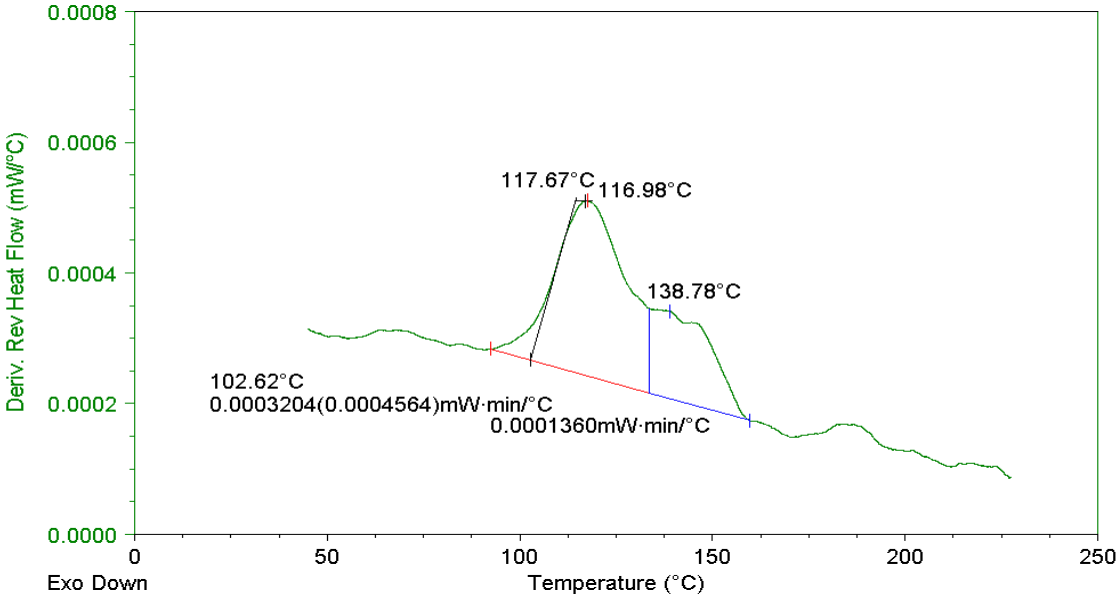

Figure A11. TMDSC thermogram of 85 kDa adsorbed PMMA on silica, 2.28 mg/m^2.

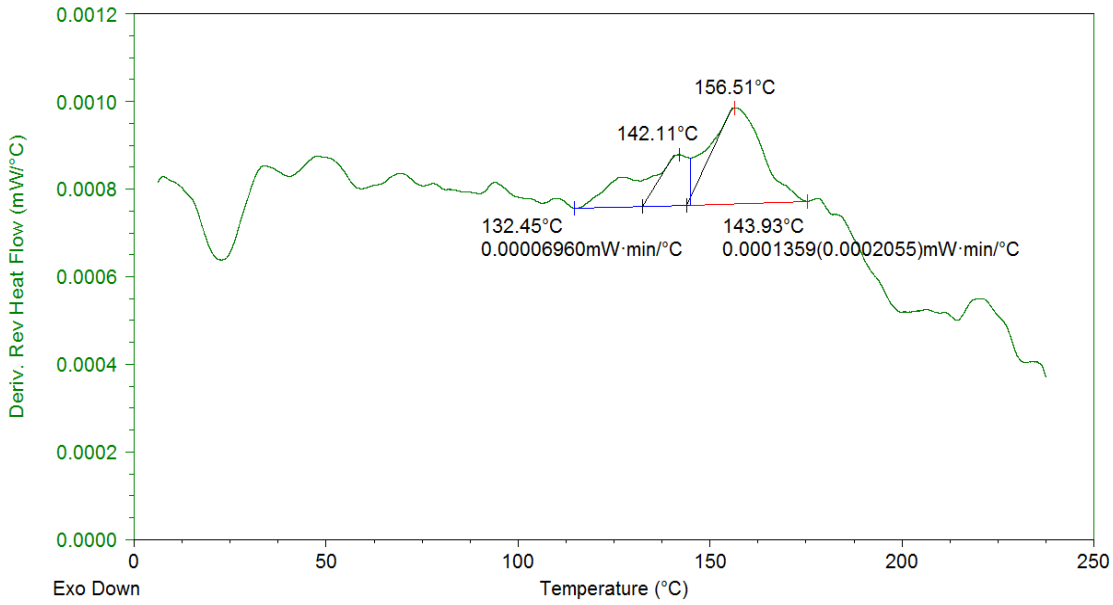

Figure A12. TMDSC thermogram of 450 kDa adsorbed PMMA on silica, 0.88 mg/m^2.

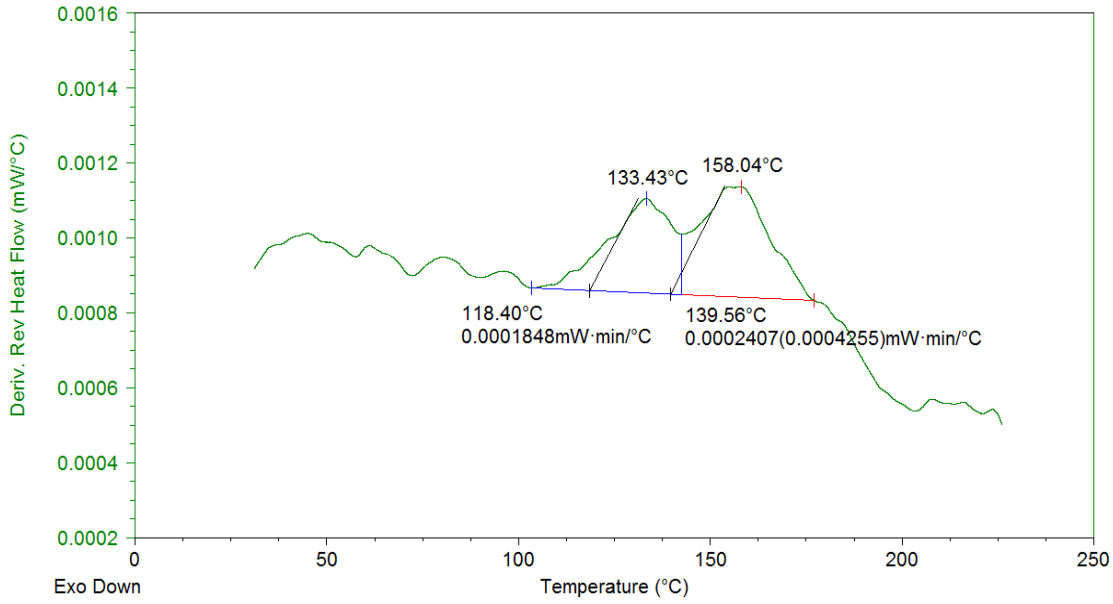

Figure A13. TMDSC thermogram of 450 kDa adsorbed PMMA on silica, 1.29 mg/m^2.

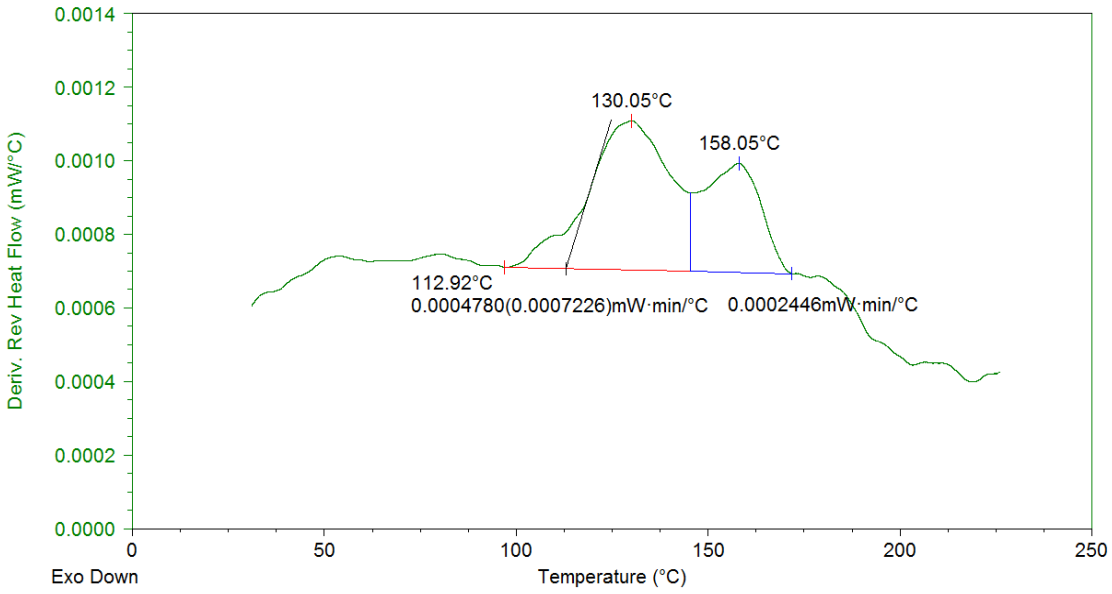

Figure A14. TMDSC thermogram of 450 kDa adsorbed PMMA on silica, 1.78 mg/m^2.

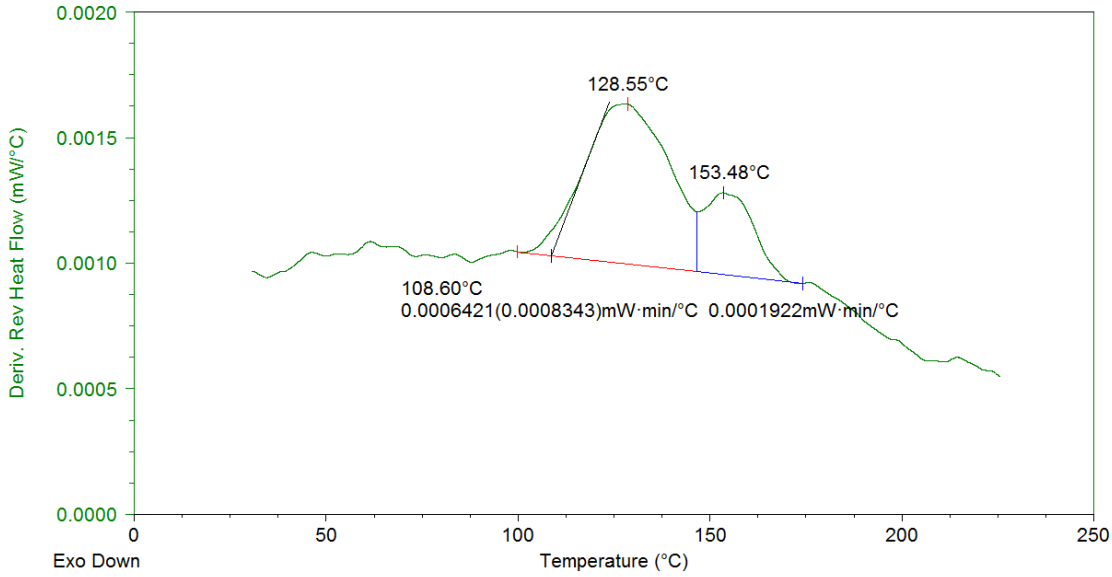

Figure A15. TMDSC thermogram of 450 kDa adsorbed PMMA on silica, 2.23 mg/m^2.

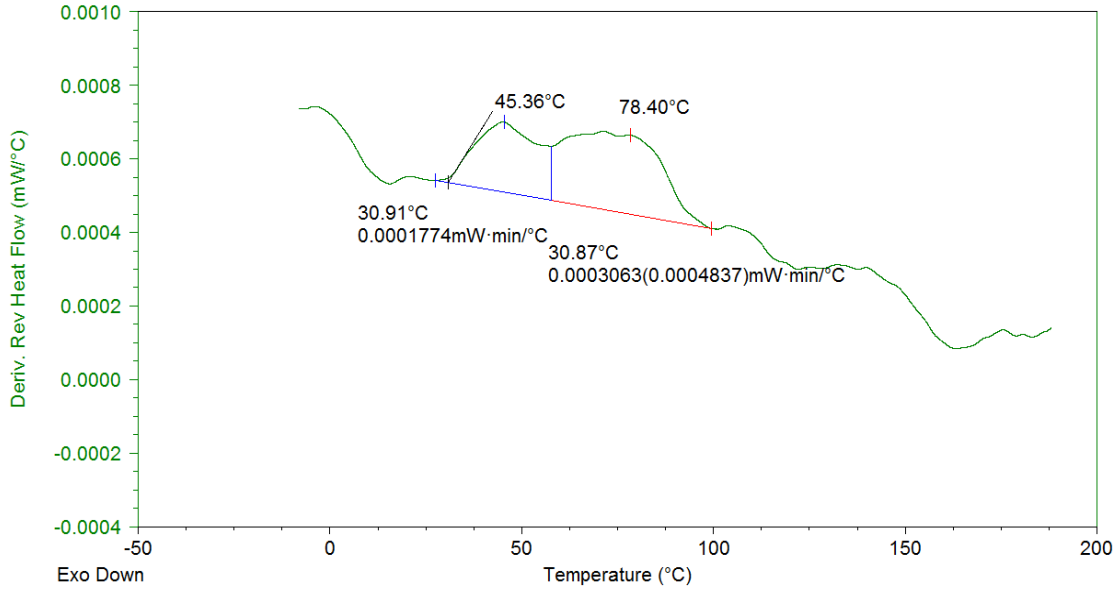

Figure A16. TMDSC thermogram of 240 kDa adsorbed PVAc on silica, 0.97 mg/m^2.

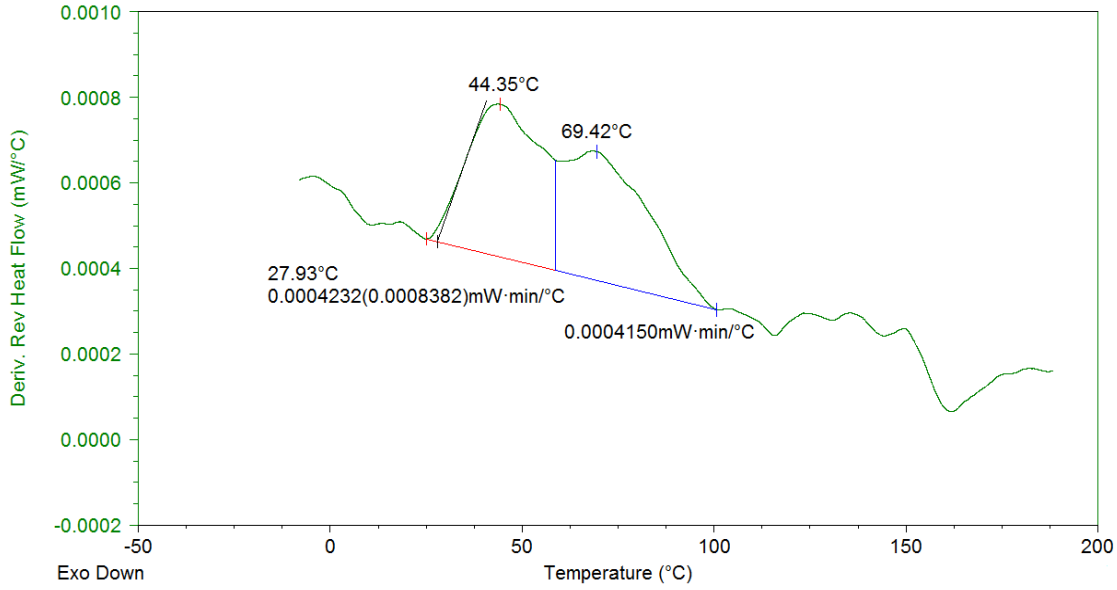

Figure A17. TMDSC thermogram of 240 kDa adsorbed PVAc on silica, 1.29 mg/m^2.

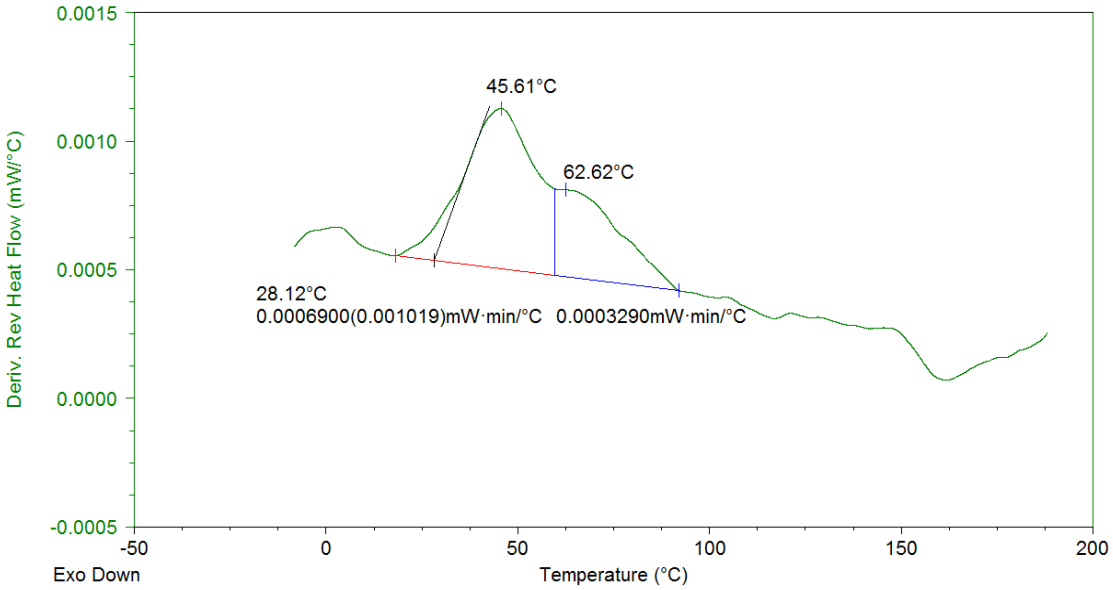

Figure A18. TMDSC thermogram of 240 kDa adsorbed PVAc on silica, 1.51 mg/m^2.

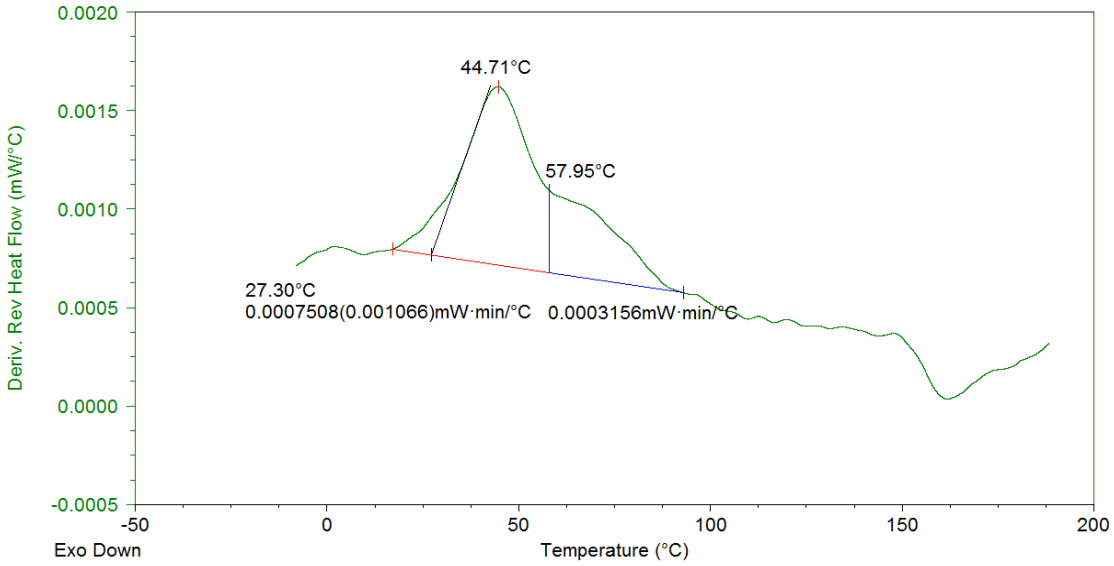

Figure A19. TMDSC thermogram of 240 kDa adsorbed PVAc on silica, 1.62 mg/m^2.

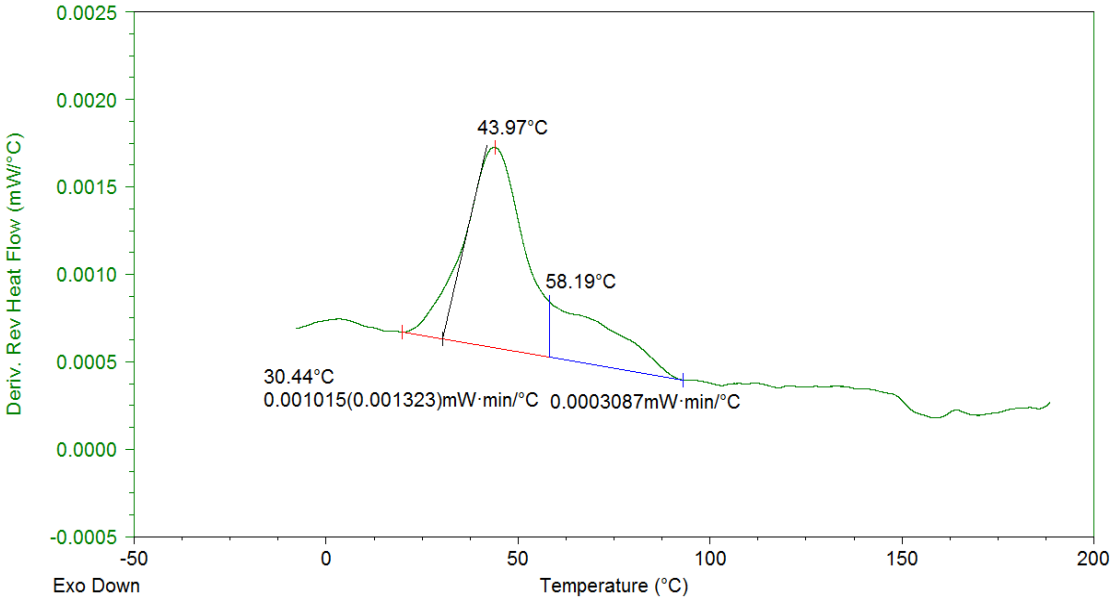

Figure A20. TMDSC thermogram of 240 kDa adsorbed PVAc on silica, 2.12 mg/m^2.

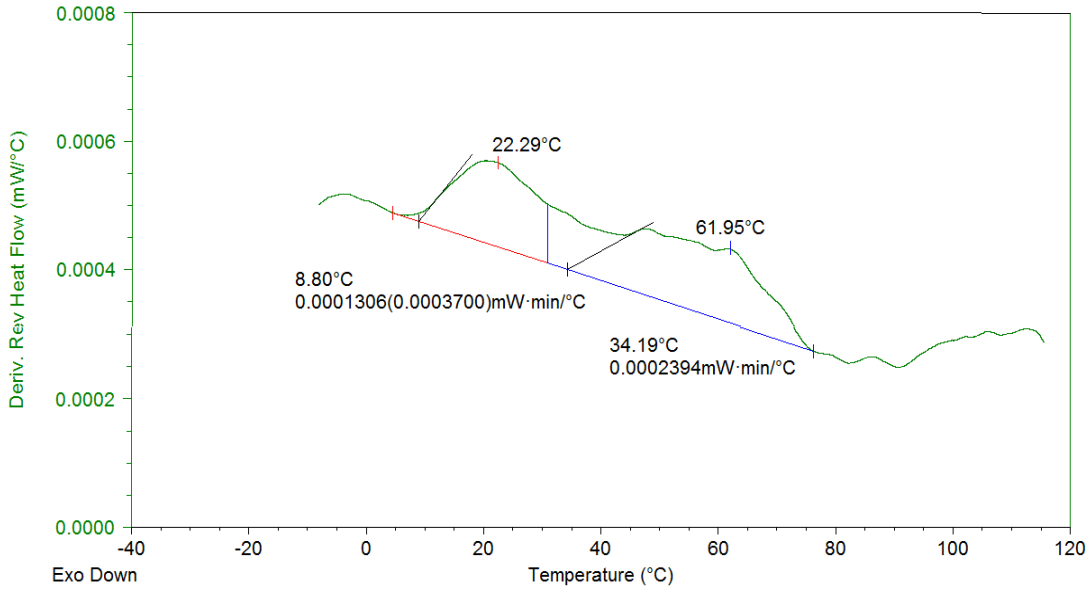

Figure A21. TMDSC thermogram of 130 kDa adsorbed PMA on silica, 0.93 mg/m^2.

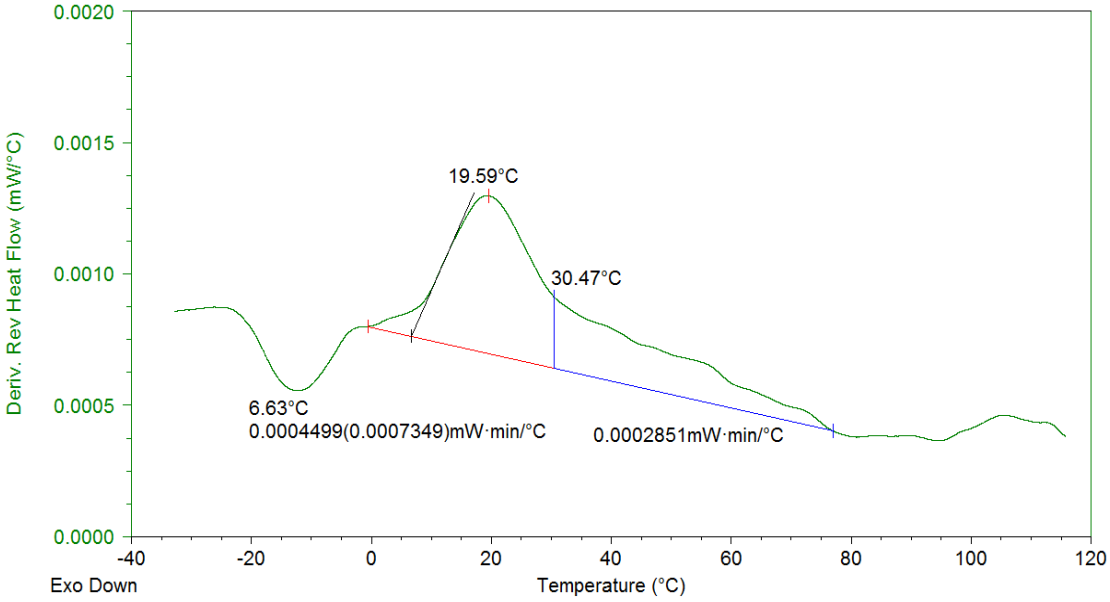

Figure A22. TMDSC thermogram of 130 kDa adsorbed PMA on silica, 1.49 mg/m^2.

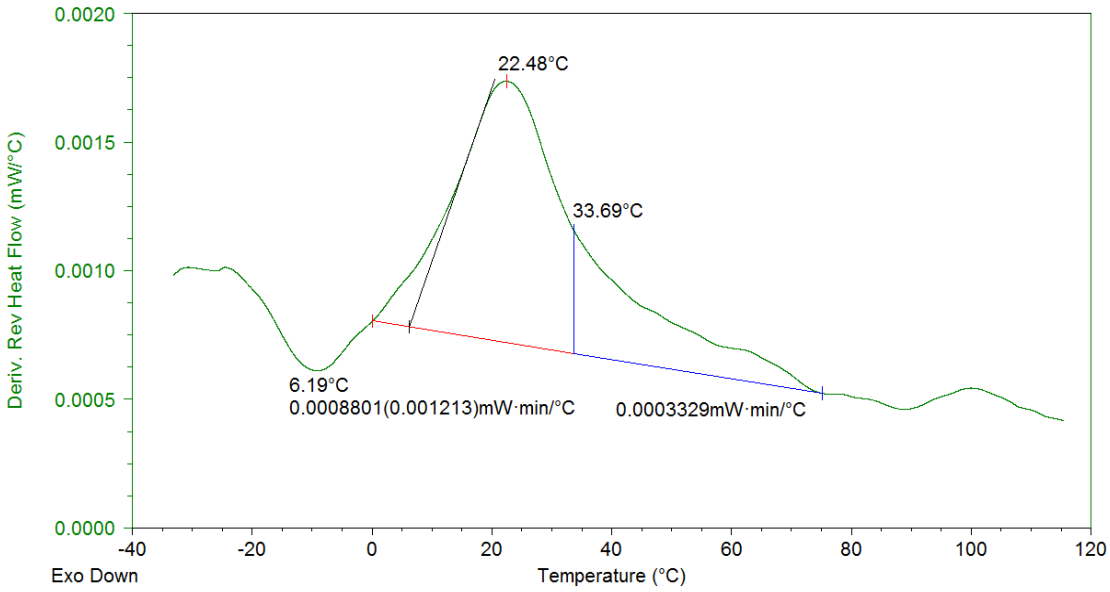

Figure A23. TMDSC thermogram of 130 kDa adsorbed PMA on silica, 1.78 mg/m^2.

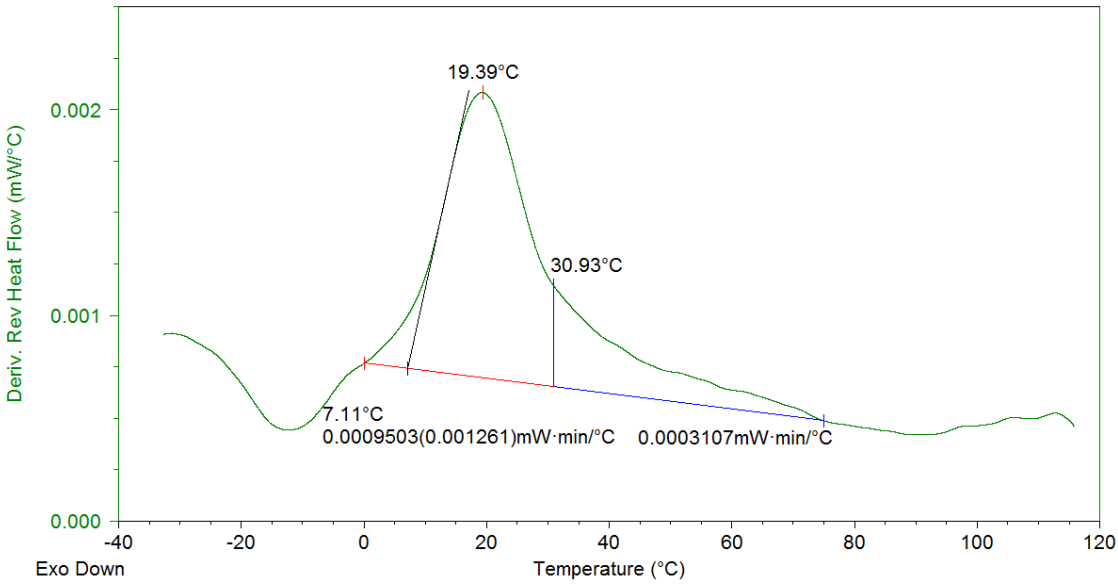

Figure A24. TMDSC thermogram of 130 kDa adsorbed PMA on silica, 2.04 mg/m^2.

APPENDIX B

THERMAL DEGRADATION OF ADSORBED PMMA ON AMORPHOUS FUMED SILICA (CAB-O-SIL M5)

FTIR spectra were used to observe the effect of the temperature on the stability of the adsorbed PMMA on silica. As shown in Figure B1, the spectrum *a* was as prepared, the sample was dried from solvent and heated to 75 °C, under vacuum. This sample was used as a reference. The spectra *b* and *c* were samples which were heated to 280 °C and held at that temperature for 3 min. in either the calorimeter or oven, respectively. The spectra *d-f* were taken for the samples that were heated in the oven at 280 °C and then held for 6, 15, and 25 min, respectively.

PMMA contains the carbonyl groups and silica has hydroxyl groups as part of surface silanols. Hence, the decrease or increase of the peak intensities of these functional groups could be related to changes in the interfacial structure. As seen from Figure B1, the spectra of the reference sample and samples underwent on heating at 280 °C for 3 min. were similar. High intensities of the carbonyl peak at 1729 cm^{-1} were found among those. It is therefore concluded that the 3 min. heating to 280°C had minimal effect on the structure of the interfacial species. After heating the adsorbed PMMA sample for 6 min or longer, the intensity of the carbonyl peak was gradually decreased upon time with the addition of a sharp peak at 3747 cm^{-1} which belongs to the free silanol groups (see peak assignment in Figure B2). The decrease in the carbonyl and the rise of the free silanol groups indicated the loss of polymer at the polymer-silica interface.

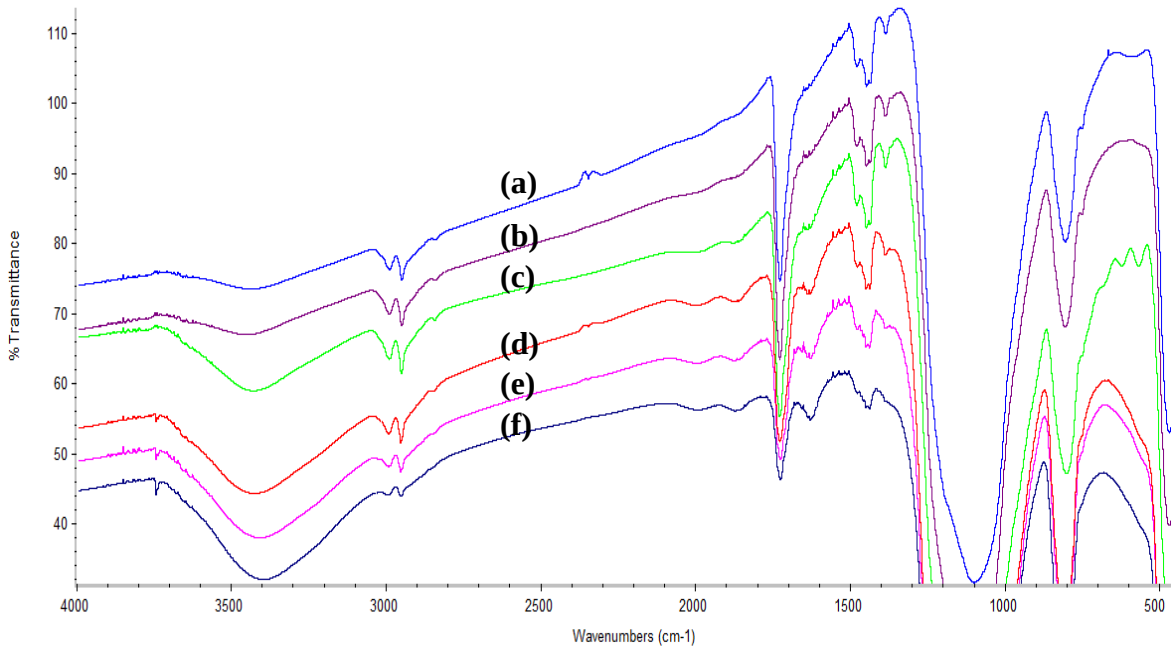

Figure B1. FTIR spectra of 85 kDa adsorbed PMMA (a) as prepared (dried from solvent and heated to 75 °C under vacuum, (b) after TMDSC run to at 280 °C (c) after 3 min in oven at 280 °C, (d) after 6 min in oven at 280 °C, (e) after 15 min in oven at 280 °C, (f) after 25 min in oven at 280 °C.

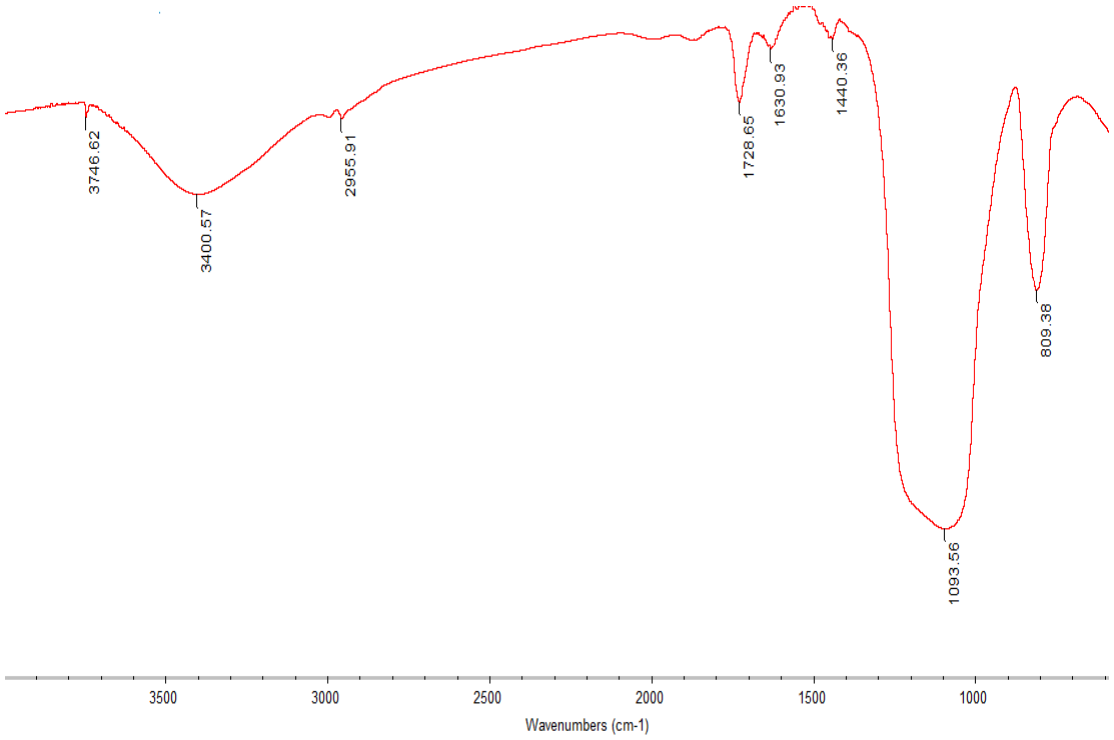

Figure B2. Resonance assignments of FTIR spectra of 85 kDa adsorbed PMMA after 25 min in oven at 280 °C.

Wave number (cm^{-1})	Functional group
3747	Free silanol[a]
3400	-OH stretch
2955	C-H alkane stretch
1729	C=O stretch
1093	Si-O stretch

[a] Azrak, G. R.; Angeli, C. L. *J. Phys. Chem.* **1973**, *77*, 3048.

The TMDSC thermograms, shown in Figure B3-B8, fairly correlated with the FTIR measurements. The first and second heating cycles of the adsorbed PMMA sample for low to medium adsorbed amounts (1.28-1.47 mg/m^2) looked similar while those of the larger adsorbed amount, 1.72 mg/m^2, were a little different. Nevertheless, for each sample, the ratios of the loosely- and tightly-bound polymer for the first and second heating cycles were comparable.

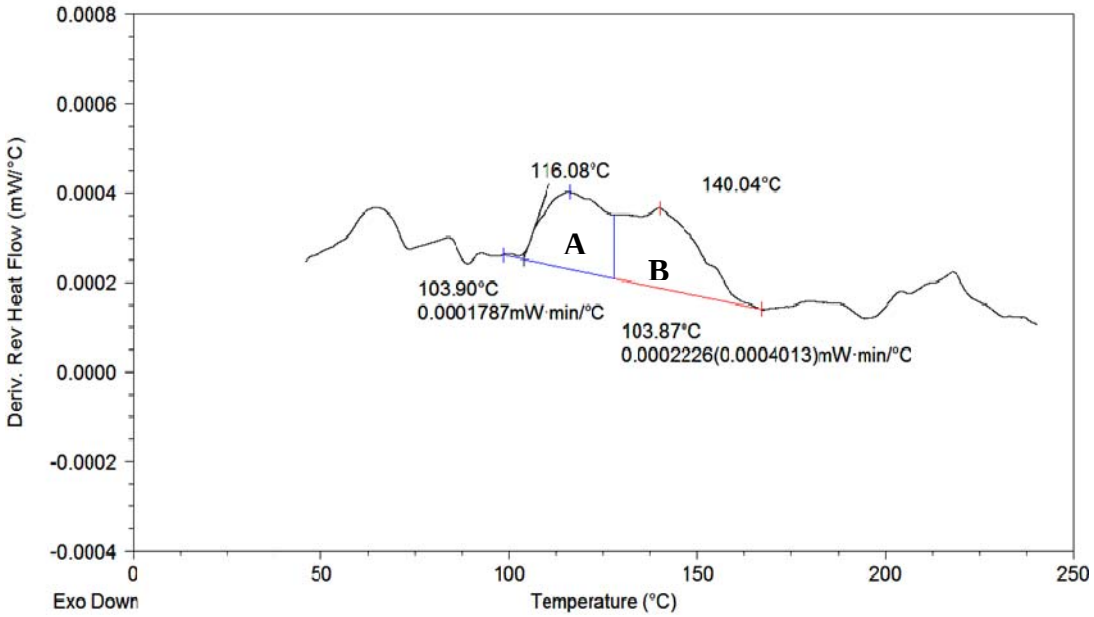

Figure B3. TMDSC of 85 kDa adsorbed 1.47 mg/m2 PMMA first heating cycle (A/B ratio = 0.80).

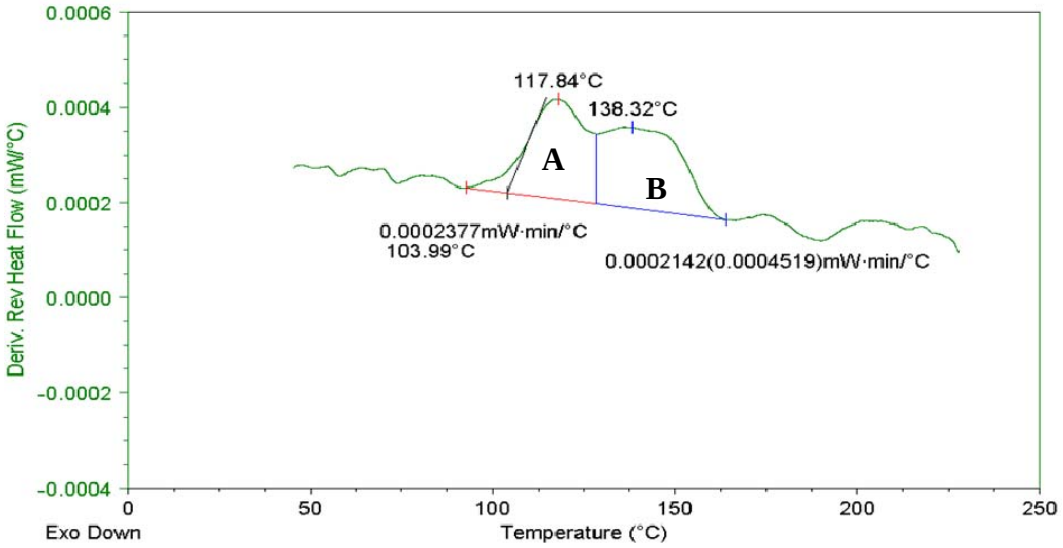

Figure B4. TMDSC of 85 kDa adsorbed 1.47 mg/m^2 PMMA second heating cycle (A/B ratio = 1.11).

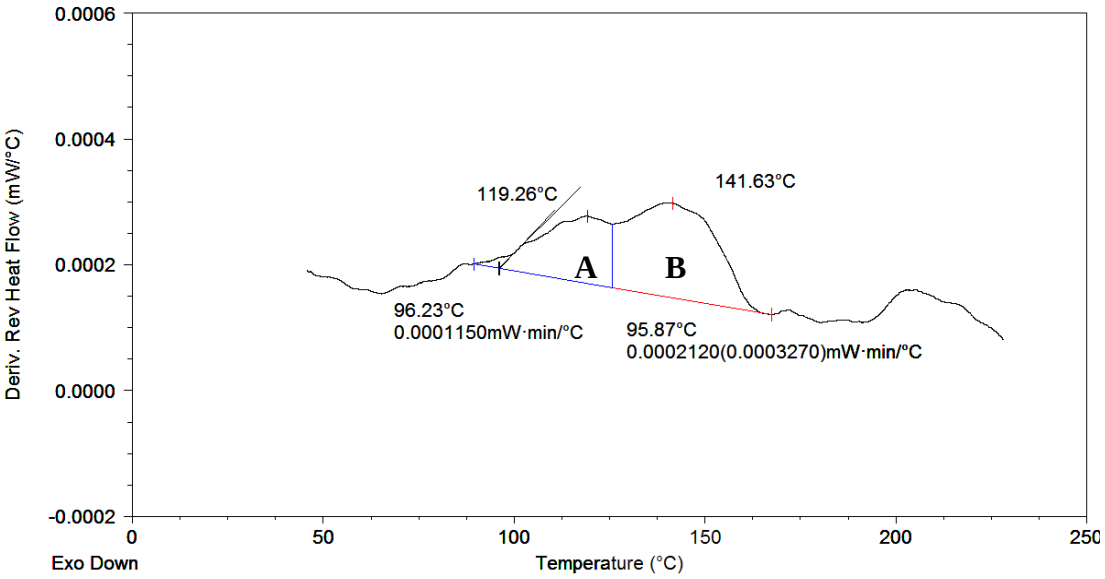

Figure B5. TMDSC of 85 kDa adsorbed 1.28 mg/m^2 PMMA first heating cycle (A/B ratio = 0.54).

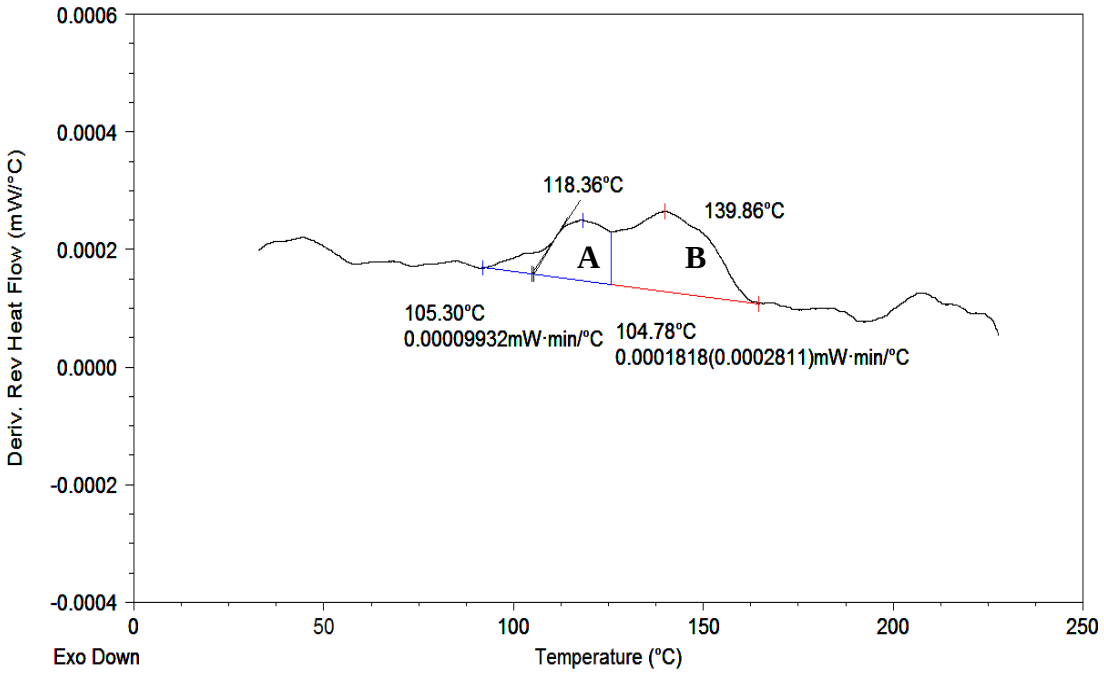

Figure B6. TMDSC of 85 kDa adsorbed 1.28 mg/m^2 PMMA second heating cycle (A/B ratio = 0.55).

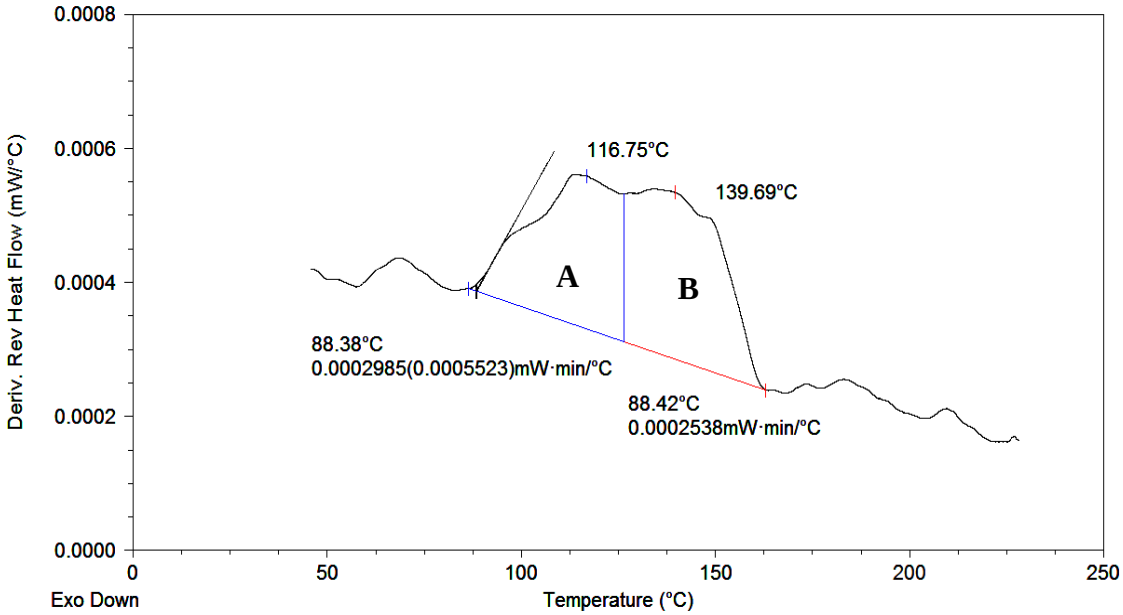

Figure B7. TMDSC of 85 kDa adsorbed 1.72 mg/m^2 PMMA first heating cycle (A/B ratio = 1.18).

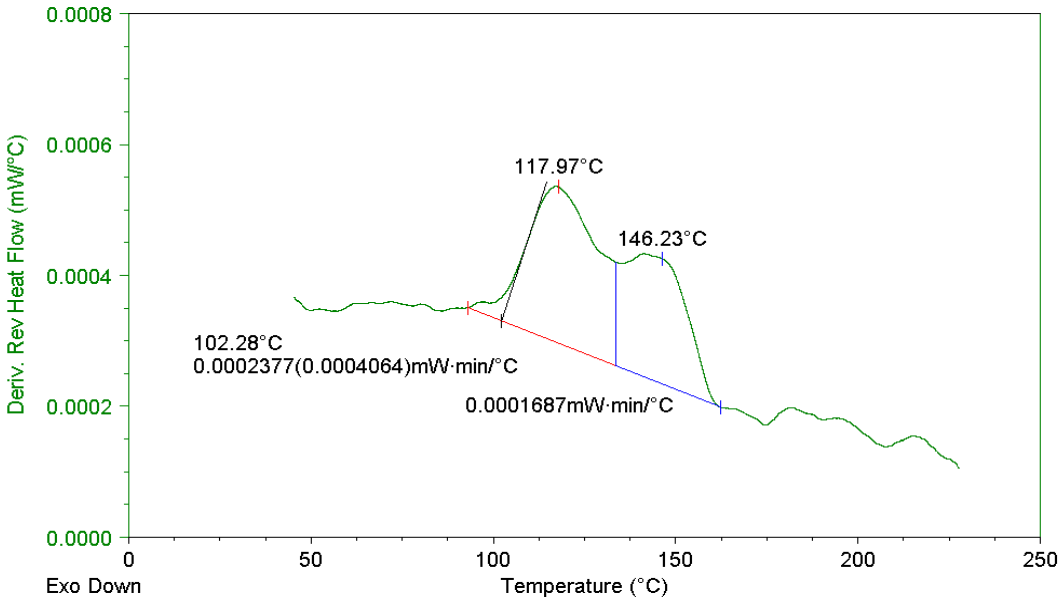

Figure B8. TMDSC of 85 kDa adsorbed 1.72 mg/m^2 PMMA second heating cycle (A/B ratio = 1.41).

The TGA thermogram for PMMA adsorbed on silica is shown in Figure B9. This thermogram showed about 0.5% mass loss at 110 °C, likely from a small amount of residual solvent or water. At 200 °C, by subtracting the solvent loss, a very small amount of further mass loss about 0.2% was observed. While at 280 °C, a small additional mass loss was found (0.7% decrease) from the mass at 200 °C. Larger mass losses for the sample occurred at temperatures over 300 °C.

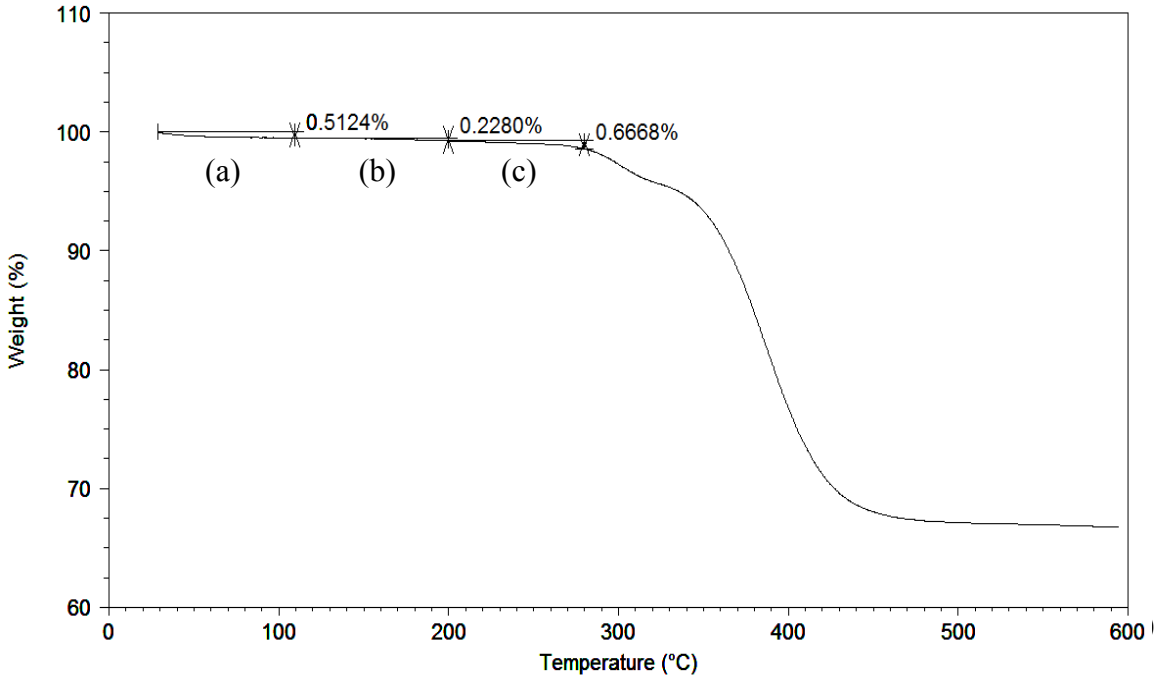

Figure B9. TGA thermogram of adsorbed PMMA on silica.

To summarize, the data from FTIR, TMDSC, and TGA showed that adsorbed PMMA on silica exhibited some thermally degradation at 280 °C. The amount of degradation depended upon the time period. From our observations, we estimated at times less than 3 min, the amount of thermal degradation was minimal. The TMDSC procedure reported in this thesis used a heating cycle to 280 °C, held for 3 min. for the adsorbed PMMA samples. At times longer than this, more degradation could occur. Although, isothermal time period of only 3 min was used here, the use of such high temperatures of about 280 °C is not recommended for future studies. An annealing temperature for the adsorbed PMMA sample of about 200-220 °C is recommended.

APPENDIX C

^{1}H NMR AND FTIR SPECTRA OF DEUTERATED PLASTICIZER, DI(PROPYLENE GLYCOL) DIBENZOATE (DPGDB-D_{10}).

The ^{1}H spectrum of deuterated plasticizer di(propylene glycol) dibenzoate (DPGDB-d_{10}) was shown in Figure C1 and its FTIR spectrum was shown in Figure C2 along with the assignments of the characteristic resonances.

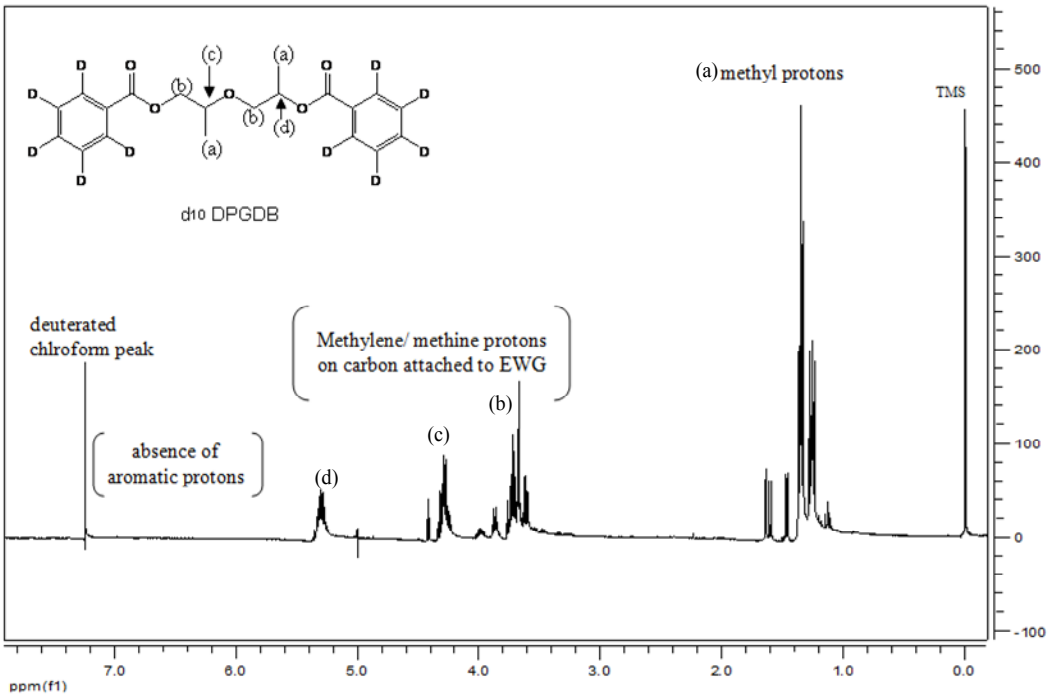

Figure C1. ^{1}H NMR spectrum of deuterated plasticizer di(propylene glycol) dibenzoate (DPGDB-d_{10}) in $CDCl_3$ δ a) 1.34 (m, 6H), b) 3.66 (m, 4H), c) 4.27 (m, 1H), d) 5.30 (m, 1H). There was no visible intensity of the aromatic protons even at very high magnification.

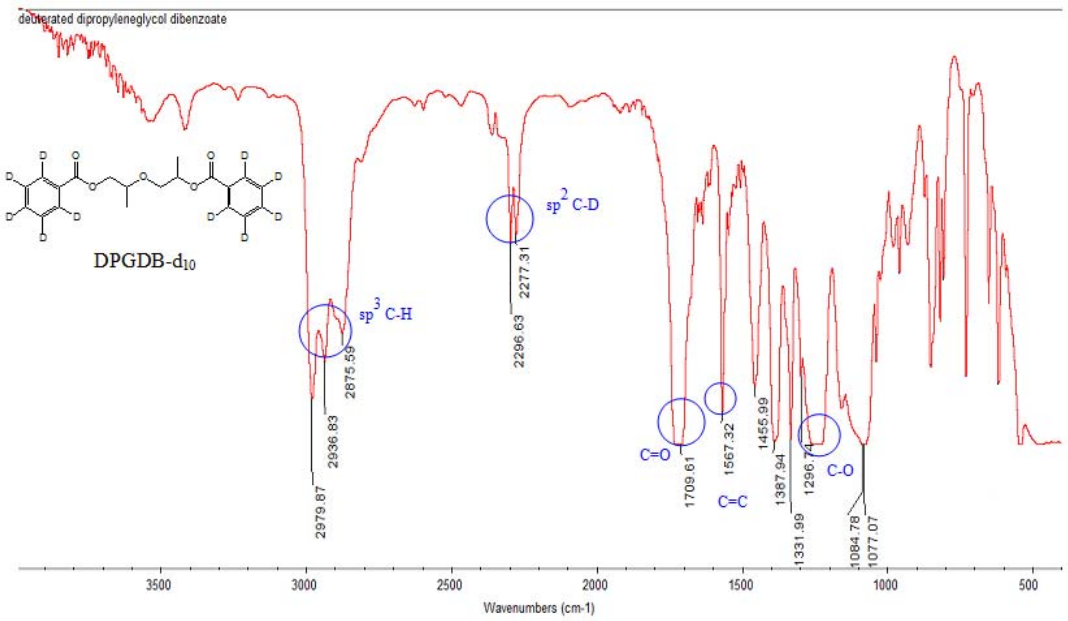

Figure C2. FT-IR spectrum of deuterated plasticizer di(propylene glycol) dibenzoate (DPGDB-d_{10}).

Wave number (cm-1)	Functional groups
2875-2979	C-H stretching of the methyl groups
2277-2296	C-D stretching
1709	C=O stretching
1567	C=C ring stretching
1296	C-O-C stretching

APPENDIX D

SOLID STATE ^{2}H NMR SPECTRA OF THE PLASTICIZER DI(PROPYLENE GLYCOL) DIBENZOATE-d_{10} IN BULK AND ADSORBED POLY(VINYL ACETATE)

A complete set of the ^{2}H NMR spectra of plasticized bulk PVAc at different plasticizer contents (37%, 27%, 22%, and 10%) were shown in Figure D1-D6. While those of 37% plasticized adsorbed PVAc with different adsorbed amounts of polymers on the silica surfaces (2.60 mg/m^2 and 0.76 mg/m^2) were shown in Figure D7-D8. (Not all of the spectra were used in the papers)

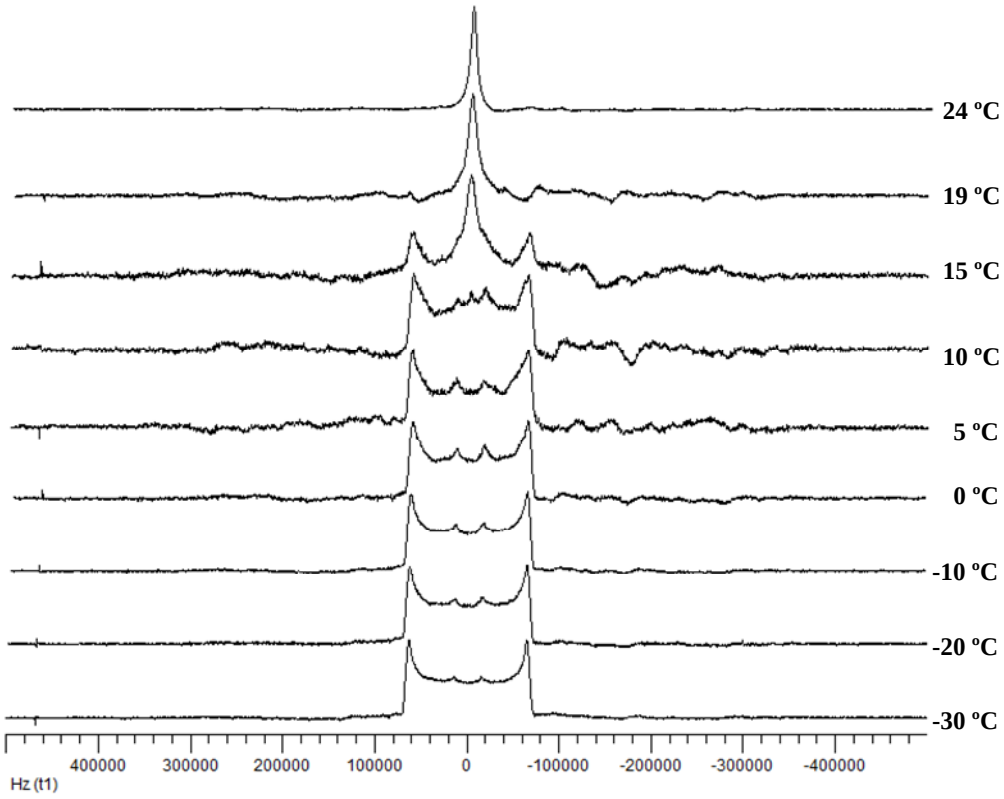

Figure D1. ^{2}H NMR of 37% plasticized-d_{10} in bulk poly(vinyl acetate).

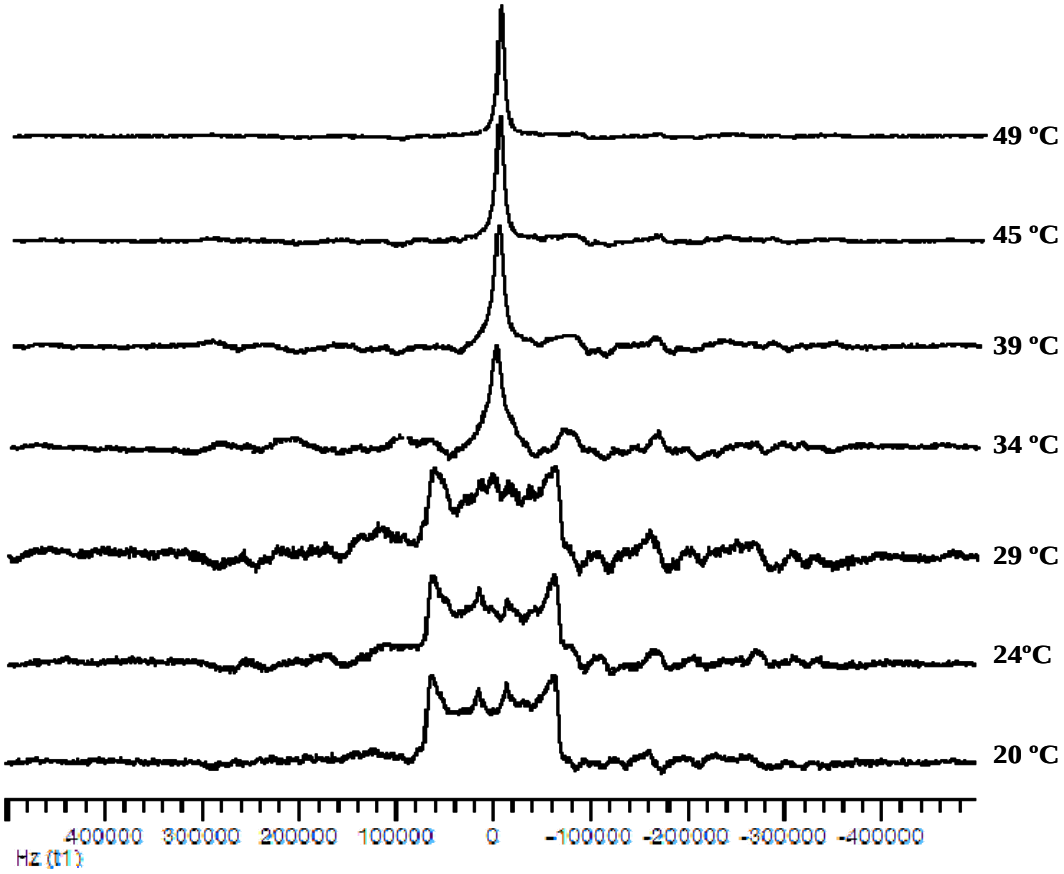

Figure D2. ^{2}H NMR of 27% plasticized-d_{10} in bulk poly(vinyl acetate) in the high temperature region.

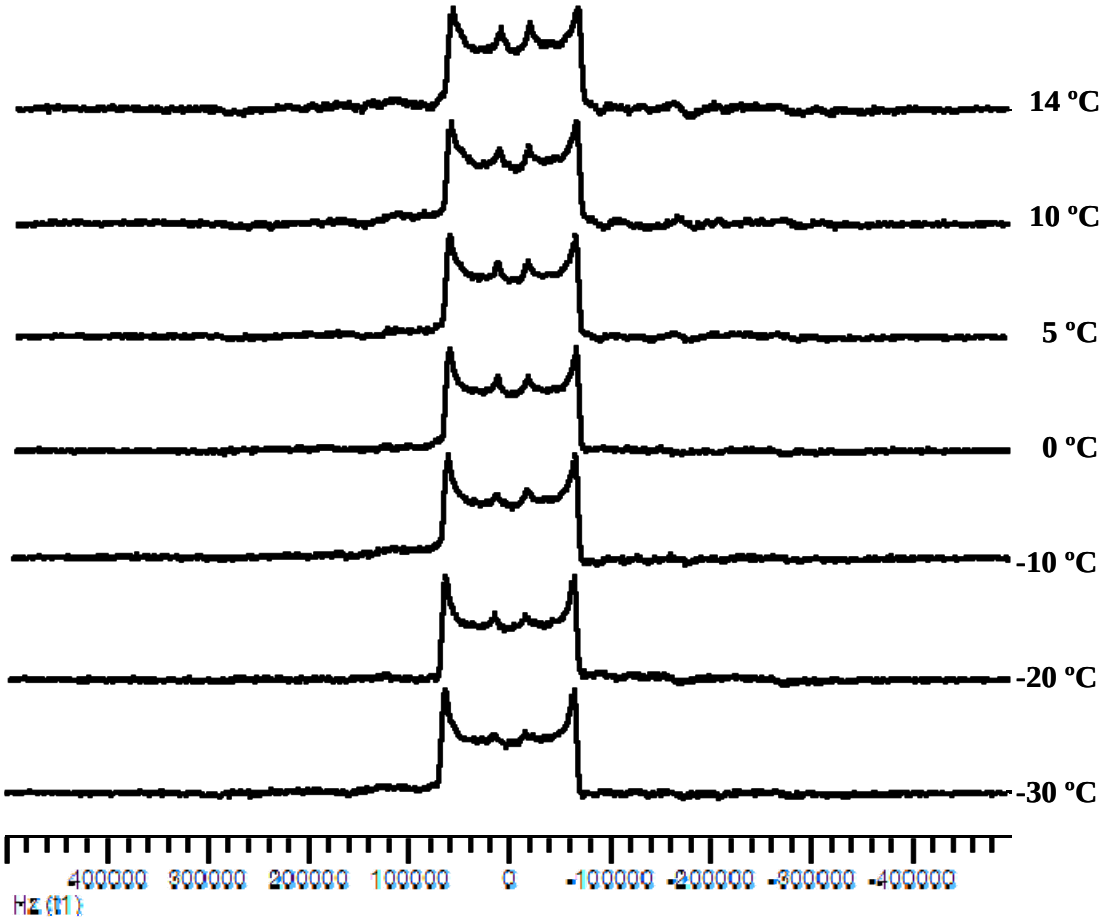

Figure D3. ^{2}H NMR of 27% plasticized-d_{10} in bulk poly(vinyl acetate) in the low temperature region.

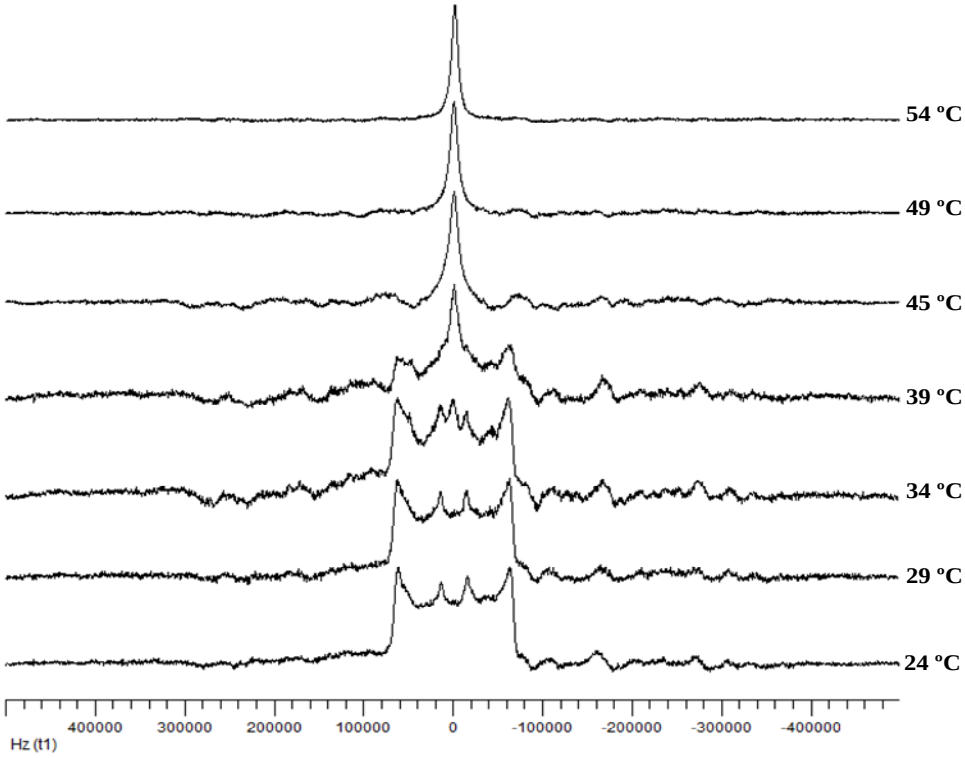

Figure D4. ^{2}H NMR of 22% plasticized-d_{10} in bulk poly(vinyl acetate) in the high temperature region.

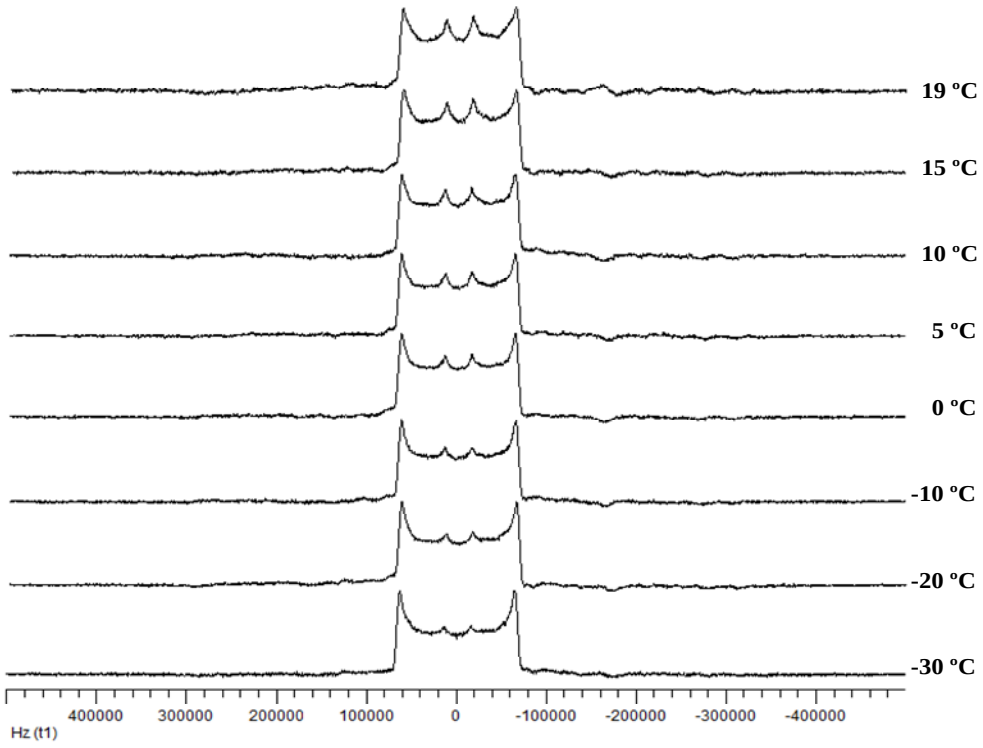

Figure D5. ^{2}H NMR of 22% plasticized-d_{10} in bulk poly(vinyl acetate) in the low temperature region.

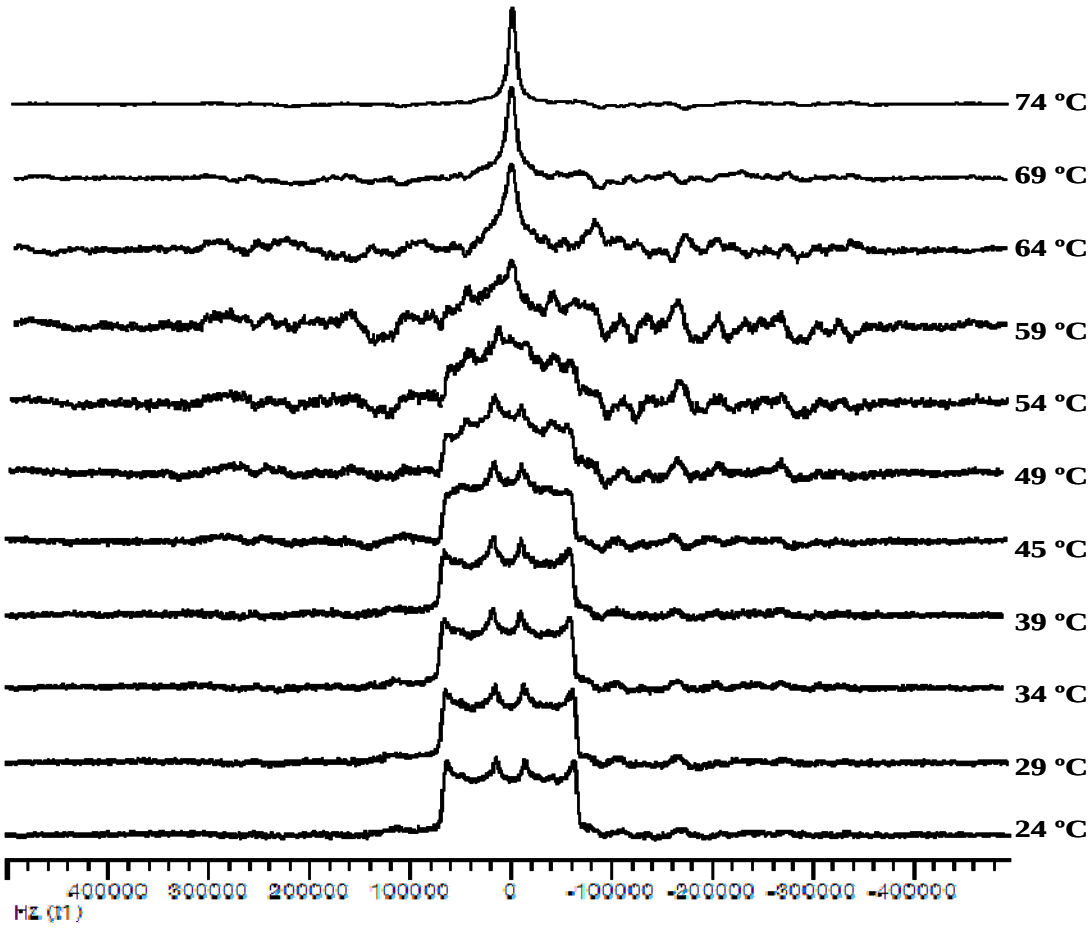

Figure D6. 2H NMR of 10% plasticized-d10 in bulk poly(vinyl acetate).

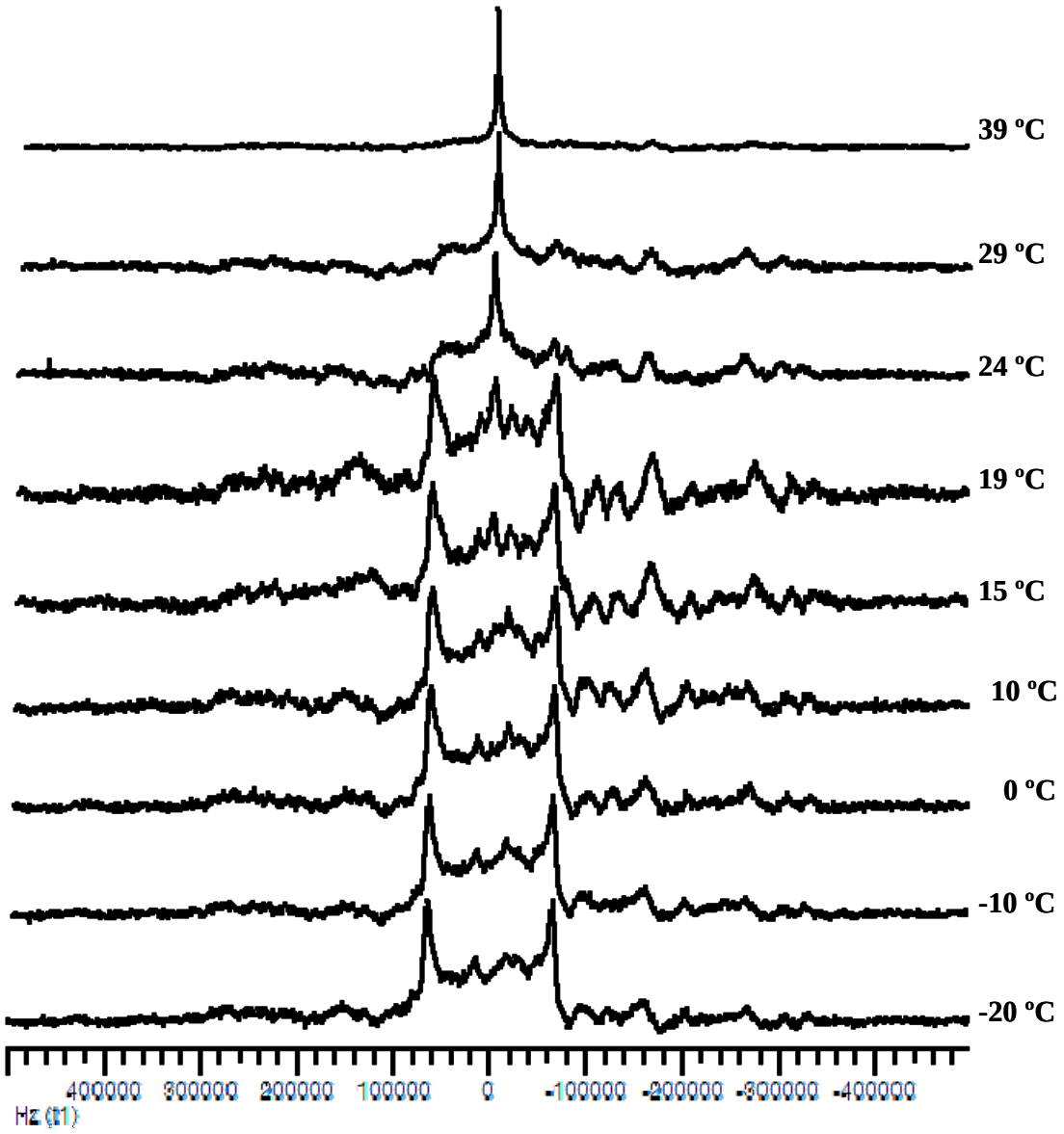

Figure D7. ^{2}H NMR of adsorbed poly(vinyl acetate) on silica, 2.60 mg/m^2, containing 37% plasticizer-d_{10}.

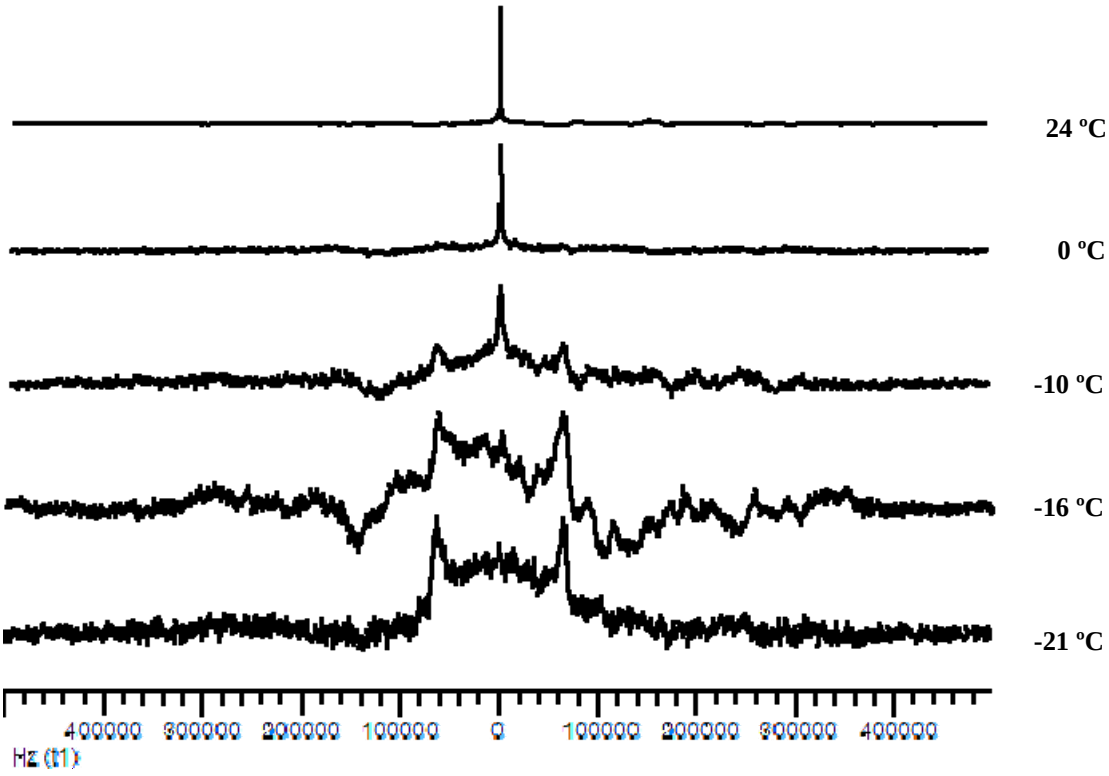

Figure D8. ^{2}H NMR of adsorbed poly(vinyl acetate) on silica, 0.76 mg/m^2, containing 37% plasticizer-d_{10}.

APPENDIX E

SIMULATIONS AND FITTINGS FOR SOLID STATE ^{2}H NMR SPECTRA

In the absence of motion, the ^2H NMR line shapes for aromatic rings can result in a rigid lattice with a splitting between the two horns of about D = 120-135 kHz. Continuous rotational diffusion (D/8 = 15-17 kHz) or a 180º jumps (D/4 = 30-34 kHz) reduce the quadrupole splitting and changes the line shapes. For our ^2H NMR spectra, the simulation was based on a two-site jump model for two different orientations of a phenyl deuteron that executes a 180º ring flip. There was little or no evidence for continuous rotation of the phenyl rings.

With respect to their jump rate (k), the phenyl ring motions were categorized into three groups or regimes as slow ($k < 1x10^4$ Hz), intermediate ($1x10^4 < k < 1x10^8$), and fast ($k > 1x10^8$) which have in different powder pattern intensities. As shown in scheme E1, slow motions yielded a rigid powder pattern. While the intermediate motions showed simultaneous changes in the ^2H NMR line shapes with a significant loss of intensity. In the fast motion regime, the quadrupole splitting was reduced and if the motion was fast enough, it was eliminated. The *para* deuterons are not affected by a 180º jump about the 1,4 phenylene flip axis because it does not change the orientation of that C-D bond; only a small amount of intensity loss occurred. A 180º jump about the C_2 symmetric axis would not yield an isotropic motion, even with the fast exchange rate, $k > 10^8$. The addition of an axial of motion was needed to further average the qcc to obtain an isotropic pattern (a narrow single peak). For this work, it was sufficient to add a mixed Gaussian/Lorentzian or a Lorentzian single central component.

The experimental line shapes were then fitted using a mathematical routine (MATLAB, the Mathworks, Inc., Natick, MA). The MATLAB codes for line shape fitting are included. The distributions of jump rates from the simulations for bulk PVAc samples with 10, 22, 27, and 37% w/w plasticizer/PVAc at various temperatures are shown in scheme E2 and those of adsorbed PVAc samples with 37% w/w plasticizer/PVAc were shown in scheme E3.

Scheme E1. Selected the experimental NMR line shapes at various jump rates (k) that were simulated using a FORTRAN program known as MXQET.

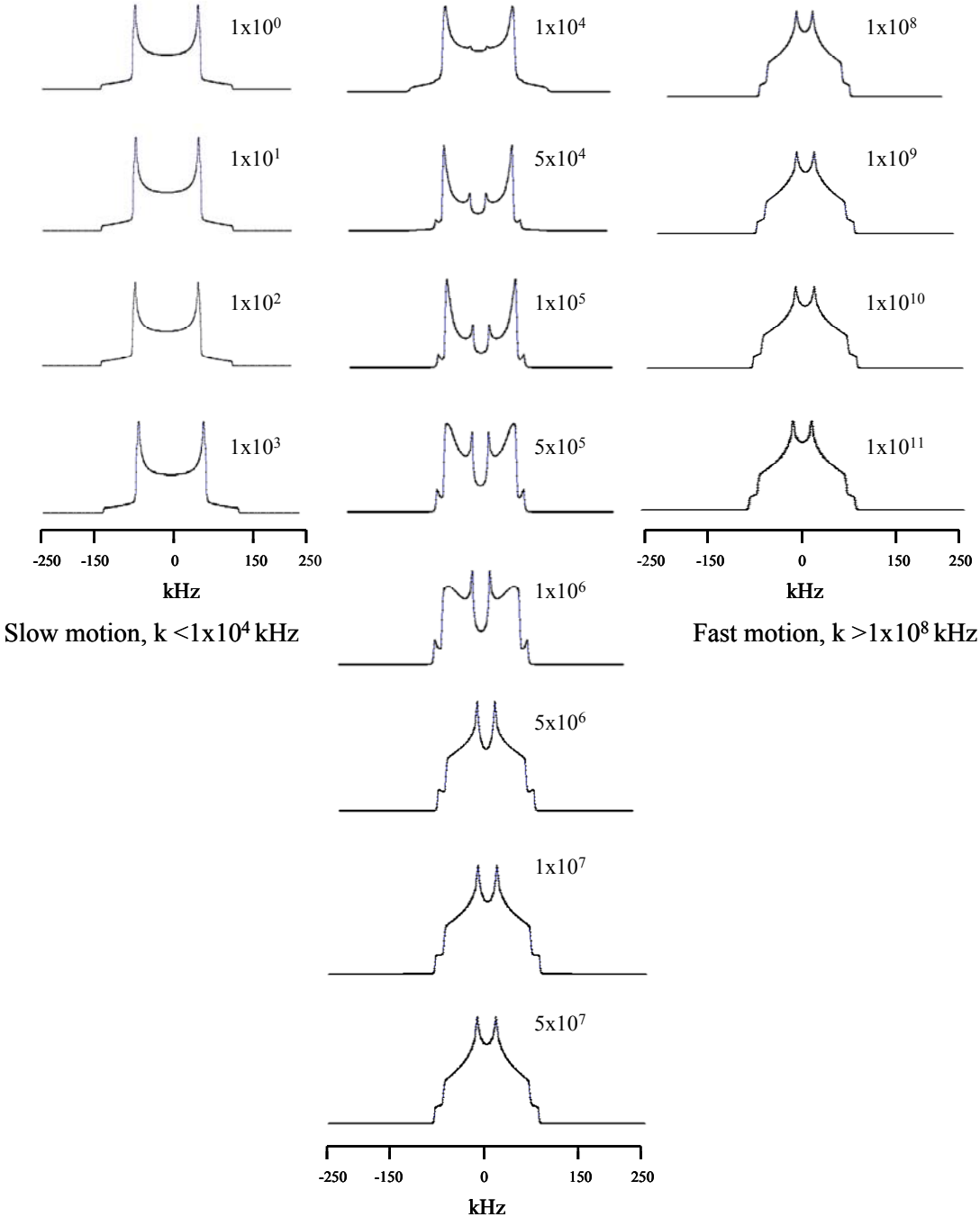

Slow motion, k <1x10^4 kHz

Fast motion, k >1x10^8 kHz

Intermediate motion,
1x10^4< k <1x10^8 kHz

MATLAB CODES FOR LINE SHAPE FITTINGS

The following MATLAB codes have been written by Roy A. Cabaniss (PhD Candidate), Department of Computer Science, Missouri University of Science and Technology.

```
function [ ] = main( expFile, outputFile )
clearvars -except expFile outputFile
clc

tmp=ls('data/*.txt');
tmp=strcat('./data/',tmp(:,:));

% Get a list of files in the data directory, and attempt to match them
to
% the experiment file provided. The result will be the best fit, a
value
% for the deviation of this fit, and a jpg file will be created which
% contains an image of the fit and the weights involved to get this
fit.

[hist, histDev] = getResult(cellstr(tmp), expFile, false, outputFile);
```

```
function [ hist, histDev ] = getResult( dataList, expFile, displayMe,
outputFile )

% First, collect the data from the input files in dataList. Use the
% my_interp function to interpolate the data over the data range,
ensuring
% there is a value for each element in the range (currently -250 to
250).
% At the end of this loop, data is an array of dat, each of which
contains
% the full range of data.
dataRange=-250:250;
```

```
data(1).dat=[];
[data(1:length(dataList)).dat]=deal([]);
for i=1:length(dataList)
    tmp=load(char(dataList(i)));
    data(i).dat=my_interp(tmp(:,1), tmp(:,2), dataRange);
end
dataNum=length(data);

% Load and normalize the Experimental data from expFile. We sort the
% dataset by the second column, and reduce the whole array to a range
of 0
% to 1. We then interpolate the data to get a full range of -250 to 250
% and nothing else.
expB=load(expFile);
[B,idx] = sort(expB(:,2));
expB=expB(idx, :);
expB=[expB(:,1)/max(expB(:,1)), expB(:,2)];
expB=my_interp(expB(:,1),expB(:,2),dataRange);
% Starting weights are set to normalize the data sets. The weight array
% contains a weight value for each dataset, plus an additional weight
which
% will apply to all of them (similar to normalization)
weight(1:dataNum+1)=1;
for i=1:dataNum
    data(i).dat=data(i).dat./(max(data(i).dat(:)-min(data(i).dat(:))));
end
weight(1:dataNum)=1;
weight(end+1)=1/dataNum;

% Find what the starting deviation is, and set the default values.
Other
% variables used later will be initialized.
summed(1:length(dataRange))=0;
for i=1:length(dataRange)
    for j=1:dataNum
        summed(i)=summed(i)+data(j).dat(i)/weight(j);
    end
end
```

```
summed(:)=summed(:)*weight(end);
histDev=sum((summed-expB).^2);
run=1;
changeby=8;
runCnt=1;
arch=weight;
upDown=0;
upDownHist=0;

while true
    % The variable weight will be applied to the dataset. It starts
from
    % the previous 'best' weight (contained in arch), then changes one
of
    % the weights (increasing or decreasing it.
    weight=arch;
    if run<=length(weight)
        weight(run) = weight(run)*(changeby);
    else
        weight(run-length(weight)) = weight(run-
length(weight))/(changeby);
    end

    % Calculate the sum of the various datasets times their weights...
    summed(1:length(dataRange))=0;
    for i=1:length(dataRange)
        for j=1:dataNum
            summed(i)=summed(i)+data(j).dat(i)*weight(j);
        end
    end
    summed(:)=summed(:)*weight(end);

    % Determine if the deviation can be improved by raising or lowering
the
    % dataset,
    dev=.0005;
    upDown=upDownHist;
```

```
    bestDev=sum((summed-(expB+upDown)).^2);
    upDev=sum((summed-(expB+upDown+dev)).^2);

    if upDev < bestDev
        while upDev < bestDev
            bestDev=upDev;
            upDown=upDown+dev;
            upDev = sum((summed-(expB+upDown+dev)).^2);
        end
    else
        downDev=sum((summed-(expB+(upDown-dev))).^2);
        if downDev < bestDev
            while downDev < bestDev
                bestDev=downDev;
                upDown=upDown-dev;
                downDev = sum((summed-(expB+upDown-dev)).^2);
            end
        end
    end

    % Compare the new Deviation value to the best of previous deviation
    % values.
    newDev = bestDev;
    if newDev < histDev && histDev/newDev>1.000001
        % If the new deviation is better (by more than .0001%), make
this
        % deviation the best, and change the archived weights to suit.
        hist=summed;
        arch=weight;
        upDownHist=upDown;
        histDev=newDev;
        % Some users prefer to watch the deviations change to closely
match
        % the experiments. If the displayMe parameter is on, display
the
        % new best (will slow the experiment down!)
        if displayMe
            figure(2);
```

```
            plot(dataRange, summed, dataRange, expB+upDown);
        end
        % Try to determine if changeing the next weight will improve
the
        % program.
        run=mod(run, 2*length(weight))+1;

        % runCnt is the number of iterations which have been performed
        % without showing an improvement. Reset this to 0 when there is
an
        % improvement.
        runCnt=0;
    elseif runCnt < 2*length(weight)+1
        % If there are no improvements and the program has not gone
through
        % tried to raise or lower all weights without improvement, then
        % just try to change the next weight and increment the number
of
        % null improvements.
        run=mod(run, 2*length(weight))+1;
        runCnt=runCnt+1;
    elseif changeby > 1.000002
        % If we have no improvements in a full sweep of possible
changes to
        % the program, try to change the weights by a smaller amount
(fine
        % tuning the result) to get a more exact answer. Continue this
        % until we are only changein the weights by .0002%.
        changeby=(changeby-1)*.8+1;
        runCnt=0;
    else
        % If there are no improvements and the weights are pretty
finely
        % tuned, time to quit the program.
        break
    end
end
```

```
% The following displays the results in two graphs. The top graph will
% compare the optimized fit, and the bottim will show the weights
attached
% to each dataset. The result is saved to a file specified by the user
% (preferably a .jpg file), and then closed.
clf;
figure('Visible','off');
subplot(2,1,1);
% First, plot the experimental results along with the resulting 'best
fit'
plot(dataRange, hist, dataRange, expB+upDownHist);
set(gca, 'YTickLabel','');
subplot(2,1,2);
arch(end)=[];
groupList=[];
agg=[];

% The following is dataset specific solution. The input files were a
list
% of files followed by the magnitude - fast3E+8.txt. To group the
results
% by their magnitude, the magnitude was found (based on the filename -
% fast3E+8 becomes 8), then the result was added to the aggregate data.
% This result was then plotted. Future users of this program will want
to
% modify or remove the following aggregation code.
for i=1:length(dataList)
    dataChar=char(dataList(i));

tmp=str2double(dataChar(find(dataChar=='+')+1:find(dataChar=='.',1,'las
t')-1))
    if ~ismember(tmp, groupList)
        groupList(end+1)=tmp;
        agg(end+1)=arch(i);
    else
        ix=find(groupList==tmp);
        agg(ix)=agg(ix)+arch(i);
    end
```

```
end
bar(groupList,agg/sum(agg));
set(gca, 'YTickLabel','');

% Save the figure, then close open figures.
saveas(gca, outputFile);
close all
end
```

```
function [ vals ] = my_interp( dataY, dataX, range )
%This function will fit dataY and dataX together to a range specified
by
%the input. The program will distribute dataY and dataX on a
scatterplot,
%then interpolate what the values of this scatterplot are at every
element
%in range. It does this by, for every element in range, finds the dataX
%elements immediatly before and after, then plots a straight line
between
%the dataY elements here to find what dataY is at the range position.
The
%goal is to simplify the datasets, ensuring that an element is
available
%for every position in the range, and extraneous data elements are
removed.

vals(1:length(range))=0;
[dataX, ix]=sort(dataX);
dataY=dataY(ix);
for i=1:length(vals)
    a=find(dataX<=range(i), 1, 'last' );
    b=find(dataX>range(i), 1);
    if(isempty(a))
        vals(i)=dataY(b);
    elseif isempty(b)
```

```
        vals(i)=dataY(a);
    else
        ratio=( range(i)-dataX(a) ) / ( dataX(b)-dataX(a) );
        vals(i)=dataY(a)+ratio*(dataY(b)-dataY(a));
    end
end
```

Scheme E2. Distributions of jump rates from the simulations for each of the experimental spectra for the DPGDB-d_{10} in bulk PVAc samples with 10, 22, 27, and 37% w/w plasticizer/PVAc at various temperatures. Slow, intermediate, and fast motions are represented by the log of jump rate (log k) from 0-9. The liquid like component is represented by the letters a-g indicating jump rate independent for a change in NMR line shapes. The line widths for the isotropic resonances are given in Table E1.

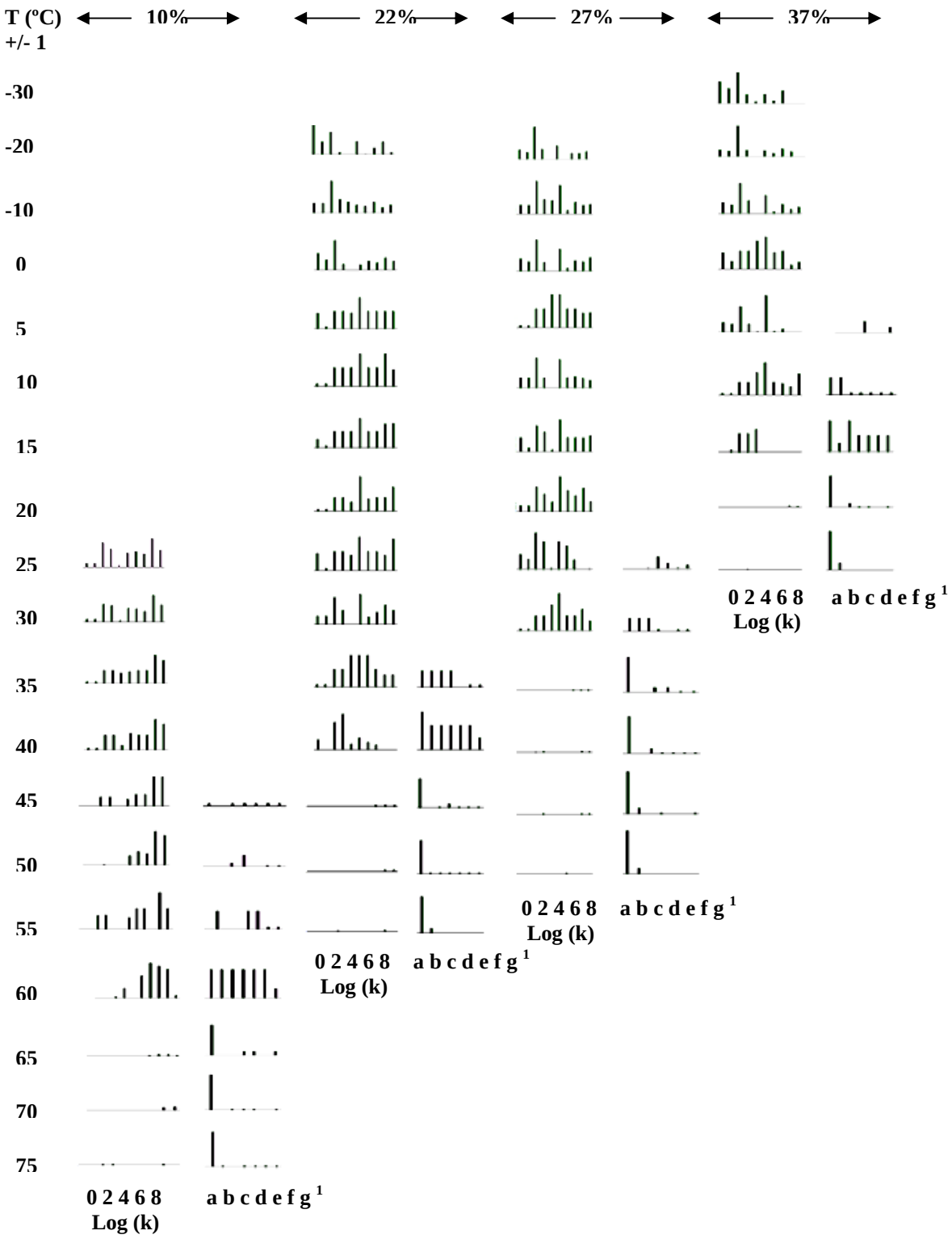
T (ºC)
+/- 1
10%
22%
27%
37%
-30
-20
-10
0
5
10
15
20
25
30
35
40
45
50
55
60
65
70
75
0 2 4 6 8
Log (k)
a b c d e f g 1

Scheme E3. Distributions of jump rates from the simulations for each of the experimental spectra for the DPGDB-d_{10} in adsorbed PVAc samples, 2.60 mg/m^2 and 0.76 mg/m^2, contains 37% w/w plasticizer/PVAc at various temperatures. Slow, intermediate, and fast motions are represented by the log of jump rate (log k) from 0-9. The liquid like component is represented by the letters a-i (or a-k) indicating jump rate independent for a change in NMR line shapes as shown in Table E1.

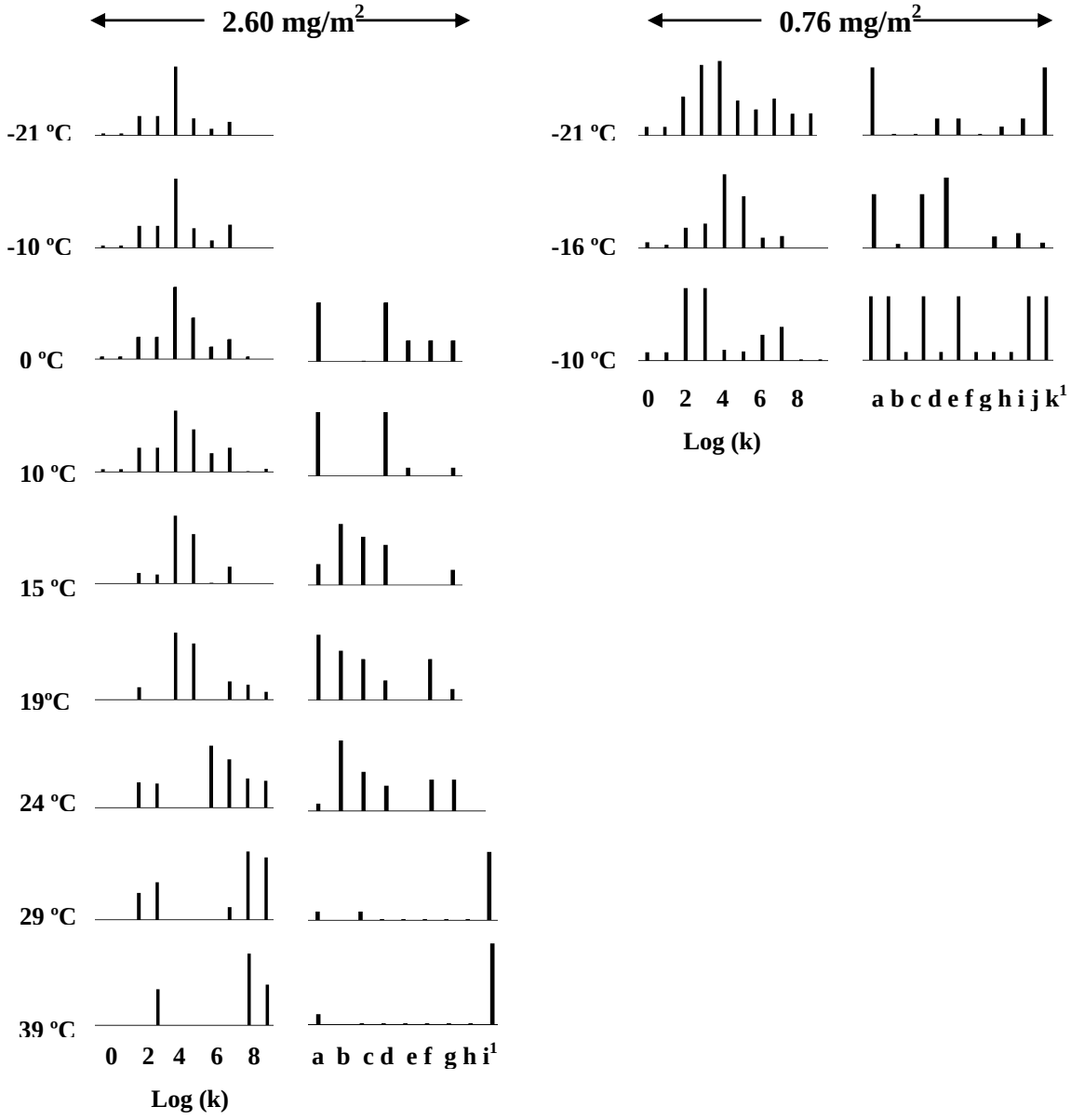

Table E1. The Liquid Like Component from Simulations

Assigned letter	Quadrupole coupling constant (QCC) (kHz)	Gaussian Broadenning (GB) (kHz)	Lorentzian Broadening (LB) (kHz)
a	1	5	5
b	5	1	1
c	5	5	5
d	5	10	10
e	5	20	20
f	5	0	5
g	5	0	10
h	5	0	20
i	1	1	1
j	1	0	1
k	1	0	5

VITA

Boonta Hetayothin was born in Bangkok, Thailand on July 4th 1974. She graduated with B.Sc. in chemistry from Chulalongkorn University, Bangkok, Thailand in 1997. She received MS degrees in Chemistry from Indiana University of Pennsylvania and University of California-Los Angeles in 2001 and 2005, respectively. She joined Missouri University of Science and Technology in July 2007 to continue her PhD degree in chemistry where she worked with Professor Frank D. Blum. Her work involved study of dynamics behavior of polymers at the interfaces using temperature-modulated scanning calorimetry (TMDSC) and the solid state deuterium NMR.

PUBLICATIONS

1. Hetayothin, B.; Kulkeratiyut, S.; Kulkeratiyut, S.; Blum, F. Thermal Analysis of Adsorbed Poly(Methyl methacrylate) (PMMA) on Silica: Effect of Molecular Mass. To be submitted.
2. Hetayothin, B.; Blum, F. Comparison of Hydrogen-Bonded Polymers on Silica using Temperature Modulated Scanning Calorimetry (TMDSC**).** To be submitted.
3. Hetayothin, B.; Blum, F. Dynamics of Di(propylene glycol) Dibenzoate-d_{10} in Poly(vinyl acetate) by Solid State ^{2}H NMR. To be submitted.
4. Hetayothin, B.; Blum, F. Dynamics of Di(propylene glycol) Dibenzoate-d_{10} in Adsorbed Poly(vinyl acetate) by Solid-State ^{2}H NMR. To be submitted.
5. Hetayothin, B.; Blum, F. Quantitative Analysis of Thermograms for Adsorbed Polymers on Silica. *Polymer Preprint,* **2010,** *51(1)*, 480.
6. Hetayothin, B.; Blum, F. Thermal Analysis of Adsorbed Poly(Vinyl Acetate) on Silica. *Polymer Preprint*, **2008**, *49(1)*, 632-2.
7. Zhang, T.; Xu, G.; Blum, F.; Hetayothin, B.; Li, Z.; Regev, O. Morphologies and Properties of Silica-Containing Emulsion-Gels and Their Composites. Manuscript in preparation.

8. Chatterjee, D.; Hetayothin, B.; Wheeler, A.; King, D.; Garrell, R. *Lab Chip*, **2006,** *6(2)*, 199-206.

POSTERS/PRESENTATIONS

1. Hetayothin, B.; Blum, F. Quantitative Analysis of Thermograms for Adsorbed Polymers on Silica. Poster presented at the 239th National ACS Meeting San Francisco, CA, March 21-25, 2010.
2. Hetayothin, B.; Blum, F. Thermal Analysis of Adsorbed Poly(Methyl methacrylate) (PMMA) on Silica: Effect of Molecular Mass. Poster presented at the 37th North American Thermal Analysis Society Conference, Lubbock, TX, September 20-23, 2009.
3. Hetayothin, B. Dynamics of Polymers at Interfaces using Temperature Modulated Differential Scanning Calorimetry (TMDSC) and NMR. Seminar at Department of Chemistry, Missouri University of Science and Technology, Rolla, MO, December 7, 2009.
4. Hetayothin, B.; Blum, F. Thermal Analysis of Adsorbed Polyvinyl Acetate on Silica. Poster presented at the 235th National ACS Meeting New Orleans, LA, April 6-10, 2008.
5. Hetayothin, B.; Klavetter, F. Tuning the Color of Luminescence by Introducing Nonconjugated Segments in a Series of Soluble Phenylene Vinylene Copolymers. Poster presented at the 227th National ACS Meeting, Anaheim, CA, March 28-April 1, 2004.
6. Hetayothin, B. RAFT (Reversible Addition-Fragmentation Chain Transfer) Polymerization. Seminar at Department of Chemistry, Indiana University of Pennsylvania, Indiana, PA, 2002.